LBL-13736

Lawrence Berkeley Laboratory

UNIVERSITY OF CALIFORNIA

Materials & Chemical Sciences Division

NMR Studies of Liquid Crystals and Molecules Dissolved in Liquid Crystal Solvents

G.P. Drobny
(Ph.D. Thesis)

November 1982

Prepared for the U.S. Department of Energy under Contract DE-AC03-76SF00098

DISCLAIMER

This document was prepared as an account of work sponsored by the United States Government. Neither the United States Government nor any agency thereof, nor The Regents of the University of California, nor any of their employees, makes any warranty, express or implied, or assumes any legal liability or responsibility for the accuracy, completeness, or usefulness of any information, apparatus, product, or process disclosed, or represents that its use would not infringe privately owned rights. Reference herein to any specific commercial products process, or service by its trade name, trademark, manufacturer, or otherwise, does not necessarily constitute or imply its endorsement, recommendation, or favoring by the United States Government or any agency thereof, or The Regents of the University of California. The views and opinions of authors expressed herein do not necessarily state or reflect those of the United States Government or any agency thereof or The Regents of the University of California and shall not be used for advertising or product endorsement purposes.

Lawrence Berkeley Laboratory is an equal opportunity employer.

LBL 13736

NMR STUDIES OF LIQUID CRYSTALS AND MOLECULES DISSOLVED IN LIQUID CRYSTAL SOLVENTS

By

Gary Peter Drobny

Ph.D. Thesis

November 1982

Materials and Molecular Research Division
Lawrence Berkeley Laboratory
University of California
Berkeley, CA 94720

This work was supported by the Director, Office of Energy Research, Office of Basic Energy Sciences, Materials Sciences Division of the U. S. Department of Energy under Contract Number DE-AC03-76SF00098.

This manuscript was printed from originals provided by the author.

ABSTRACT

This thesis describes several studies in which nuclear magnetic resonance (nmr) spectroscopy has been used to probe the structure, orientation and dynamics of liquid crystal mesogens and molecules dissolved in liquid crystalline phases. In addition, a modern high field nmr spectrometer is described which has been used to perform such nmr studies.

Chapter 1 introduces the quantum mechanical formalisms used throughout this thesis and briefly reviews the fundamentals of nuclear spin physics and pulsed nmr spectroscopy. First the density operator is described and a specific form for the canonical ensemble is derived. Then Clebsch-Gordon coefficients, Wigner rotation matrices, and irreducible tensor operators are reviewed. An expression for the equilibrium (Curie) magnetization is obtained and the linear response of a spin system to a strong pulsed r.f. irradiation is described. Finally, the spin interaction Hamiltonians relevant to this work are reviewed together with their truncated forms.

Chapter 2 is a deuterium magnetic resonance study of two "nom" liquid crystals which possess several low temperature mesomorphic phases. Specifically, deuterium quadrupolar echo spectroscopy is used to determine the orientation of the liquid crystal molecules in smectic phases, the changes in molecular orientation and motion that occur at smectic-smectic phase transitions, and the order of the phase transitions. For both compounds, the phase sequence is determined to be isotropic, nematic, smectic A, smectic C, smectic B_A,

smectic B_C, and crystalline. The structure of the smectic A phase is found to be consistent with the well-known model of a two dimensional liquid in which molecules are rapidly rotating about their long axes and oriented at right angles to the plane of the layers. Molecules in the smectic C phase are found to have their long axes tilted with respect to the layer normal, and the tilt angle is temperature dependent, increasing from zero at the smectic A - smectic C transition and reaching a maximum at 9° at the smectic C - smectic B_A transition. This finding contradicts the results of X-ray diffraction studies which indicate that the tilt angle is 18^{o} and temperature independent. The smectic B_A - smectic B_C phase transition is observed for the first time, and is found to be first order, a result that contradicts the prediction of a mean theory by McMillian.

Chapter 3 is a multiple quantum nmr study of n-hexane oriented in a nematic liquid crystal solvent. The basic three pulse multiple quantum experiment is discussed which enables the observation of transitions for which $|\Delta m|>1$, and then the technique of the separation of multiple quantum orders by phase incrementation in the multiple quantum evolution period is reviewed (TPPI). An explicit example of multiple quantum nmr is given by the calculation of the multiple quantum spectrum of an oriented methyl group.

Having introduced the fundamentals of multiple quantum nmr, the method is then used to study the configurational statistics of n-hexane-d_6 oriented in a nematic solvent. The symmetry group of a 4-methylene chain is derived (C_{2h}) and the energy level diagram is obtained. From the energy level diagram is determined that the six quantum spectrum contains 29 lines (14 pairs and a central line) and the seven quantum spectrum contains 4 lines (two pairs). A general expression for the dipolar coupling in a nonrigid alkyl chain molecule in a uniaxial phase is derived assuming a rotational isomeric model of motion. Six and seven quantum spectra of a 4-methylene chain are calculated assuming varying populations of isomeric states. The best fit is found to occur for the configurational probabilities:

$$P_{ttt} = .2$$

$$P_{ttg^{\pm}} = P^{\pm}_{tt} = P_{tg^{\pm}t} = .1$$

$$P_{g^{\pm}tg^{\pm}} = P_{g^{\pm}tg^{\pm}} = .05$$

$$P_{g^{\pm}g^{\pm}g^{\pm}} = P_{tg^{\pm}g^{\pm}} = P_{g^{\pm}g^{\pm}t} = 0$$

A refinement of the above values was attempted using the dipolar coupling constants as parameters in an iterative calculation of some five quantum lines and all the six and seven quantum lines. It was found that while there was a slight improvement in the 5 quantum fit, there is no improvement at all in the 6 and 7 quantum fits. In fact, the 6 and 7 quantum fits are not as close after iteration. It is concluded that convergence has occurred to a non-global minimum.

Acknowledgments

It has been my good fortune to be associated with the research group of Dr. Alexander Pines, and I now wish to acknowledge those people at Berkeley who have been my friends and colleagues. I am deeply grateful to Alex Pines for admitting me to his group and giving me the opportunity to participate in an exciting and rewarding research program. I also wish to thank Zeev Luz, Shimon Vega, and Melvin Klein for their advice and encouragement. And I would also like to extend my deepest thanks to the members of the research group: Dave Wemmer, Dave Ruben, Steven Sinton, Jim Murdoch, Dan Weitekamp, Yu Sze Yen, Jau Tang, Joel Garbow, Dick Eckman, Sid Wolfe, Herbert Zimmerman, Shan Hsi, and Homo Edzes. The technical support provided by the Electronics Shop staff and in particular Don Wilkinson has also been greatly appreciated as well as the efforts of Dione Carmichael who typed the first and second drafts of this thesis.

Finally, I would like to thank my wife, Franny, who has put up with me during some very trying times and is an endless source of understanding, advice, help and love.

To the memory of my parents,
George and Gertrude Drobny

CONTENTS

1. INTRODUCTORY TOPICS 1

1.1 Density Operator 1

1.1.1 Equation of Motion 1

1.1.2 Expectation Values 4

1.1.3 Equilibrium: Microcanonical Ensemble........... 5

1.1.4 Equilibrium: Canonical Ensemble................ 7

1.2 Transformation of Spherical Tensors.................... 8

1.2.1 The Rotation Operator 8

1.2.2 Wigner Rotation Matrices....................... 11

1.2.3 Clebsch-Gordon Coefficients.................... 13

1.2.4 Spherical Tensors.............................. 15

1.3 Nuclear Magnetic Resonance: Basic Theory.............. 16

1.3.1 Introduction 16

1.3.2 Equilibrium Magnetization...................... 17

1.3.3 Linear Response of a Spin System to a Pulsed R.F. Field.. 18

1.3.4 Spin Interaction Hamiltonians: General Forms.... 23

1.3.5 Spin Interaction Hamiltonians: Spherical Tensor Forms... 25

1.3.6 Truncation of Spin Hamiltonians................. 26

Appendix 1.1 Spherical Tensor Form......................... 29

Appendix 1.2 Cartesian vs. Spherical Forms................. 30

Appendix 1.3 Listings of $d^{(\ell)}_{mn}(\beta)$ for ℓ = 0, 1, 2........... 31

2. A DEUTERIUM MAGNETIC RESONANCE (DMR) STUDY OF THE SMECTIC PHASES OF A THERMOTROPIC LIQUID CRYSTAL

2.1 Introduction.. 32

2.2 Liquid Crystalline Mesophases........................ 33

  2.2.1 Nematic.. 36

  2.2.2 Smectic A...................................... 37

  2.2.3 Smectic C...................................... 37

  2.2.4 Smectic B 39

2.3 Quadrupolar Echo Spectroscopy........................ 39

2.4 Theory of the Orientational Dependence of the Quadrupolar Splitting in Smectic Phase Liquid Crystals............. 52

  2.4.1 Smectic A...................................... 52

  2.4.2 Smectic C...................................... 57

2.5 Experimental Results and Discussion.................. 66

  2.5.1 "nom" Liquid Crystals.......................... 66

  2.5.2 Chemical Synthesis............................. 68

  2.5.3 Experimental Methods........................... 69

  2.5.4 Phase Transitions.............................. 72

  2.5.5 DMR Spectra of Rotated Smectic Samples......... 79

Appendix 2.1 Ordering in the Smectic C Phase 97

Appendix 2.2 Calculation of the Magnetic Energy............ 102

Appendix 2.3 Spectral Simulation Programs 108

Appendix 2.4 Fictitious Spin $^{1}/2$ Operators 115

3. A MULTIPLE QUANTUM NMR STUDY OF A NONRIGID CHAIN MOLECULE ORIENTED IN A NEMATIC LIQUID CRYSTAL

3.1 Introduction.................................... 116

3.2 Basic Principles of Multiple Quantum NMR............ 120

    3.2.1 The Single Quantum Experiment: A Review...... 121
    3.2.2 The Multiple Quantum Experiment: General Scheme 127
    3.2.3 Basic Multiple Quantum Pulse Sequences......... 131
    3.2.4 Example: The Multiple Quantum Spectrum of an Oriented Methyl Group........................ 151
    3.2.5 Multiple Quantum NMR as a Method for Studying Molecules Oriented in Liquid Crystalline Phases. 160

3.3 Nonrigid Chain Molecules in Uniaxial Phases.......... 167

    3.3.1 The NMR Symmetry Group of a Polymethylene (PM) Chain.. 167
    3.3.2 The Orientational Dependence of Dipolar Couplings in a Nonrigid Molecule in a Uniaxial Phase...... 174

3.4 Experimental Methods, Results, and Discussion......... 184

    3.4.1 Chemical Synthesis: n-hexane-1,1,1,6,6,6-d_6... 184
    3.4.2 Experimental Methods......................... 187
    3.4.3 Single Quantum Experiment.................... 189
    3.4.4 Multiple Quantum Experiment.................. 192
    3.4.5 Calculations and Discussion.................. 197
    3.4.6 Conclusion................................... 210

Appendix 3.1 Matrix Form for $\exp(-i\mathcal{H}_{yy}\tau)$ 213

Appendix 3.2 Nuclear Coordinates: n-hexane-d_6............ 214

Appendix 3.3 Dipolar Couplings: n-hexane-d_6............ 220
Appendix 3.4 CPARAM............................... 227

4. A HIGH FIELD NMR SPECTROMETER

4.1 Introduction.................................... 230
4.2 Frequency and Phase Generation.................. 231
    4.2.1 LO Generation............................ 232
    4.2.2 IF Generation............................ 234
    4.2.3 Quadrature Phase Generation.............. 236
    4.2.4 R.F. Generation: proton and deuterium....... 240
4.3 R.F. Power Amplifiers............................ 241
    4.3.1 360 Mhz Amplifiers........................ 241
    4.3.2 Other High Power Amplifiers.............. 244
4.4 R.F. Receiver.................................... 244
    4.4.1 Preamplifier............................. 244
    4.4.2 I.F. Amplifiers.......................... 247
4.5 Phase Sensitive Detector......................... 247
    4.5.1 Dual Channel Detector.................... 247
    4.5.2 Audio Gain and D.C. Level-Control........... 249
    4.5.3 Audio Filters............................ 251
4.6 Data Acquisition................................. 251
    4.6.1 Sample and Hold Amplifiers................. 251
    4.6.2 Analog-Digital Converters.................. 253
    4.6.3 Fifo Memory Buffer and Data Channel Interface. 253

4.7 Digitally Controlled Analog Phase Shifter........... 256

4.8 Pulse Programmer: Hardware......................... 258

4.8.1 Introductory Remarks........................ 258

4.8.2 General Structure........................... 260

4.8.3 Pulse Programmer Operation: Buffer Memory Input....................................... 262

4.8.4 Pulse Programmer Operation: Buffer Memory Output 266

4.8.5 Front Panel Controls........................ 270

4.9 Pulse Programmer: Software 271

4.9.1 Program Outline............................. 271

4.9.2 Console Commands 273

4.9.3 Pulse Program Commands 277

4.9.4 Specification of Gate Masks 281

Appendix 4.1 Microprocessor Source Code.................. 284

References 319

Chapter 1: INTRODUCTORY TOPICS

In this chapter we introduce basic physical concepts and formalisms that will be used throughout this thesis. In section 1.1 we introduce the density operator which provides the connection between statistics and quantum mechanics. We will derive the equation of motion of the density operator, expressions for expectation values using the density operator, and finally, we will derive the explicit form of the canonical density operator.

In section 1.2 we discuss the transformation properties of spherical tensors. We begin by deriving an expression for the rotation operator and the elements of the Wigner rotation matrix. Finally, we will review Clebsch-Gordon coefficients and introduce equations governing the rotations of spherical tensors.

In section 1.3 we introduce the basic principles of nuclear magnetic resonance required to understand the material in this thesis. We begin by introducing the equilibrium magnetization of a diamagnetic substance in a magnetic field. Then we consider the displacement of the system from equilibrium by pulsed radio frequency field. Finally, we consider the general forms of the spin interaction Hamiltonians relevant to this work, and their truncated forms.

1. Introductory Topics

1.1 The Density Operator

1.1.1 Equation of Motion

We begin by introducing the basic tool of quantum mechanics, the density operator. Suppose we have an ensemble of N identical systems

The solution of the first order differential equation is $\rho(t) = e^{-i\mathcal{H}t}\rho(0)\rho^{i\mathcal{H}t}$ which can be easily verified:

$$\dot{\rho}(t) = -i\mathcal{H}(e^{-i\mathcal{H}t}\rho(0)e^{i\mathcal{H}t}) + (e^{-i\mathcal{H}t}\rho(0)e^{i\mathcal{H}t})(i\mathcal{H}) \tag{16}$$

$$= i\mathcal{H}\rho(t) + \rho(t)i\mathcal{H} \tag{17}$$

$$= i[\rho(t),\mathcal{H}] \tag{18}$$

1.1.2 Expectation Values

We are also interested in developing an expression for the ensemble average of the expectation value of a dynamical variable O, using the density operator formalism. We begin with the double average

$$<O> = {}^{1}/N \sum_{k=1}^{N} \int d\tau\psi^{k*}(r_i t)O\psi^{k}(r_i,t) \tag{19}$$

We now expand ψ^k in the $\phi(r_i)$ orthonormalized basis to get

$$<O> = {}^{1}/N \sum_{k=1}^{N} \int d\tau\,(\sum_n a_n^{k*}(t)\phi_n^*(r_i)O(\sum_m a_m^k(t)\phi_m(r_i) \tag{20}$$

$$= {}^{1}/N \sum_{k=i}^{N} \sum_{nm} a_n^{k*}(t)a_m^k(t)\int d\tau\phi_n^*(r_i)O\phi_m(r_i) \tag{21}$$

$$= {}^{1}/N \sum_{k=1}^{\nu} \sum_{nm} a_n^{k}(t)a_m^k(t)O_{nm} \tag{22}$$

where $O_{nm} = \int d\tau\phi_n^*(r_i)O\phi_m(r_i)$ (23)

We now use the definition of the density matrix, the principle of detailed balance, and the definition of the trace of a matrix to get

$$\langle O\rangle = {}^{1}/N \sum_{k=1}^{N} \sum_{nm} a_n^{k*}(t)a_m^{k}(t)O_{nm} \tag{24}$$

$$= \sum_{nm} \rho_{mn} O_{nm} \tag{25}$$

$$= \sum_{m} (\rho O)_{nm} \quad (\text{since } \sum_{n} |n\rangle\langle n| = 1) \tag{26}$$

$$= \mathrm{Tr}(\rho O) \tag{27}$$

1.1.3 Equilibrium: Microcanonical Ensemble

We now concern ourselves with the expression for the density operator of an ensemble of systems in equilibrium with a heat bath. Specifically we will obtain an expression for the canonical density operator corresponding to the classical canonical distribution function, which provides the connection between quantum mechanics and statistical mechanics.

Let us begin with the microcanonical ensemble. Such an ensemble is composed of systems characterized by a fixed volume V, particle number N, and energy lying within the interval $(E-\Delta/2, E+\Delta/2)$ and $\Delta \ll E$. Furthermore, the number of states accessible to a system is $\Gamma(N,V,E;\Delta)$. Evaluating matrix elements of the density operator in the eigenbasis of the Hamiltonian (i.e. an energy representation) and applying the postulate of equal a priori probabilities we obtain the following form for the microcanonical density matrix

$$\rho_{mn} = \delta_{mn}\rho_n \qquad \text{and} \tag{28}$$

$$\rho_n = \begin{cases} {}^{1}/\Gamma; & \text{accessible states} \\ 0\ ; & \text{otherwise} \end{cases}$$

and, corresponding to classical mechanics, the entropy is

$$S = k \ln \Gamma \tag{29}$$

Suppose now that the ensemble could be decoupled into components, so that the total wave function could be factored. Then we could associate with each system a definite wavefunction. This means that for any given system $\Gamma=1$, which is called the pure case. Then in any basis

$$\rho_{mn} = {}^{1}/N \sum_{k=1}^{N} a_m^k a_n^{k*} = a_m a_n^* \tag{30}$$

and then

$$\rho_{mn}^{2} = \sum_{\ell} \rho_{m\ell} \rho_{n\ell} \quad \sum_{\ell} \rho_{m\ell} \rho_{\ell n} \tag{31}$$

$$= \sum_{\ell} a_m a_{\ell}^* a_{\ell} a_n = a_m a_n^* = \rho_{mn} \tag{32}$$

This means that the density operator in a pure state is idempotent:

$$\rho^2 = \rho \quad . \tag{33}$$

If $\Gamma \gg 1$ we have a mixed case. Now to assure that equation 28 is fulfilled we must invoke an additional postulate, the postulate of random a priori phases. This postulate assures us that for all k, ψ^k in an incoherent superposition of the basis $\{\phi_n\}$. Now we have

$$\rho_{mn} = {}^{1}/N \sum_{k} a_m^k a_m^{k*} = {}^{1}/N \sum_{k} |a|^2 e^{i(\theta_m^k - \theta_n^k)} \tag{34}$$

$$= \frac{|a|^2}{N} \sum_{k} e^{i(\theta_m^k - \theta_n^k)} \tag{35}$$

$$= e\delta_{mn} \quad . \tag{36}$$

1.1.4 Equilibrium Canonical Ensemble

We now consider an ensemble in which each system is parametrized by N, V, and T, and the energy is variable. In such an ensemble, a system is at equilibrium if it does not evolve under its Hamiltonian which means that

$$[\mathcal{H},\rho] = 0 \qquad (37)$$

and so the density operator must be a function of the Hamiltonian

$$\rho = \rho(\mathcal{H}) \qquad (38)$$

The form of the density operator may be deduced from the following considerations. Suppose two separate systems are in contact with a heat bath and are in equilibrium with the heat bath. They may be imagined to form a composite system with a Hamiltonian $\mathcal{H} = \mathcal{H}_1 + \mathcal{H}_2$. On the other hand, the composite density operator is a product of the individual density operators. Thus it is reasonable to assume that the density operator is an exponential function of the Hamiltonian

$$\rho = ce^{\beta\mathcal{H}} \qquad (39)$$

and β is a function of the temperature. c is a normalizing constant and it can easily be shown that

$$c = [\,\mathrm{Tr}(e^{-\beta\mathcal{H}})]^{-1} \qquad (40)$$

which is the inverse of the partition function. Furthermore, it can be deduced, from the correspondence with classical mechanics that $\beta = {}^{1}/kT$.

Of interest is the expression for the canonical density operator for the limit $kT \gg \|\mathcal{H}\|$, which is termed the high temperature limit. This is usually the case for nmr. If $kT \gg \|\mathcal{H}\|$ then $\|\beta\mathcal{H}\| \ll 1$, and we can expand the exponent in equation 39 to get

$$\rho \sim c(1-\beta\mathcal{H}) \tag{41}$$

to first order. Also we note that

$$1/c \cong \mathrm{Tr}(1) \quad . \tag{42}$$

1.2 Transformations of Spherical Tensors

Throughout this thesis we will concern ourselves with the effect of coordinate transformations on tensor operators. The purpose of this section is to define the conventions to be used in this work. For a thorough discussion of the theory of angular momentum and tensor operators, the reader is referred to any of the standard texts by Rose (1), Edmunds (2), Tinkham (3), Brink (4), or especially Silver (5).

1.2.1 The Rotation Operator

By convention, a rotation of a function in real space is defined by a sequence of three rotations. The initial rotation is through an angle α about the z axis corresponding to an operation by $R_z(\alpha) = e^{i\alpha I_z}$. The second rotation is through an angle β about the y' axis corresponding to an operation by $R_{y'}(\beta) = e^{i\beta I_{y'}}$, and the final rotation is through an angle y about the z" axis corresponding to an operation by $R_{z''}(y) = e^{iyI_{z''}}$. For a sketch of the appropriate rotations, see figure 1. The angles α, β, and y are called Euler

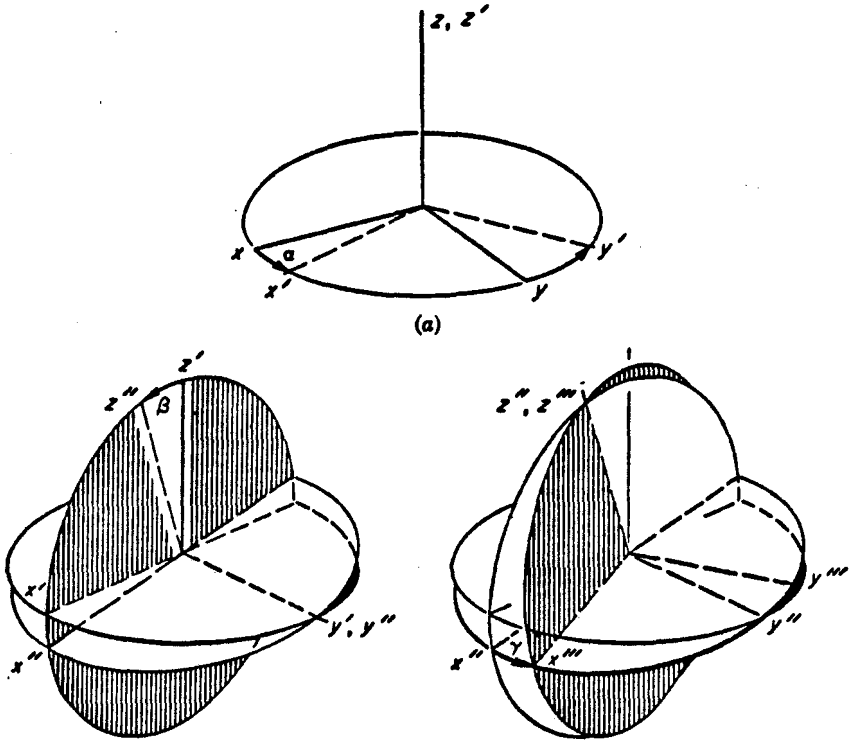

(a)

(b)

(c)

Figure 1. The Euler angles relate on initial coordinate system (x,y,z) to a final coordinate system (x''',y''',z'''). An initial rotation by an angle α about the z axis carries (x,y,z) into an intermediate system (x',y',z'). A second rotation by β about y' carries (x',y',z') into (x'',y'',z'') and a third rotation by γ about z'' carries (x'',y''z'') into (x''',y''',z''').

angles and I_x, I_y, and I_z are the familiar angular momentum operators related by the commutation relations

$$I_x = i[I_y, I_z] \tag{43a}$$

$$I_y = i[I_z, I_x] \quad . \tag{43b}$$

$$I_z = i[I_x, I_y] \quad . \tag{43c}$$

These commutation relations lead, in turn, to the equations

$$I_z|I,m> = m|I_m> \tag{44a}$$

$$I^2|I,m> = I(I+1)|I_m> \tag{44b}$$

$$I+|I,m> = [I(I+1) - m(m+1)]^{1/2}|I,m+1> \tag{44c}$$

$$I-|I,m> = [I(I+1) - m(m-1)]^{1/2}|I,m-1> \tag{44d}$$

where the phase terms $e^{\pm i\phi}$ have been set to 1 ($\phi = 0$).

Suppose we have a function f(r) and rotate it about z by α. The expression for $f_1(r)$, the function in the new coordinate system is

$$\begin{aligned} f_1(r) &= R_z(\alpha)f(r) \\ &= e^{i\alpha I_z}f(r) \quad . \end{aligned} \tag{45}$$

The next rotation is by β about y':

$$\begin{aligned} f_2(r') &= R_{y'}(\beta)R_{z'}(\alpha)f(r') \\ &= e^{i\beta I_{y'}}e^{i\alpha I_{z'}}f(r') \quad . \end{aligned} \tag{46}$$

The final rotation is by γ about z":

$$f_3(r'') = R_{z''}(\gamma)R_{y''}(\beta)R_{z''}(\alpha)f(r'') \tag{47}$$
$$= e^{i\gamma I_{z''}}e^{i\beta I_{y''}}e^{i\alpha I_{z''}}f(r'') \quad .$$

Dropping the primes we obtain an expression where all coordinates and operators are in the final frame:

$$f_3(r) = e^{i\gamma I_z}e^{i\beta I_y}e^{i\alpha I_z}f(r) \quad . \tag{48}$$

Finally we define the rotation operator as:

$$D(\alpha\beta\gamma) = e^{i\gamma I_z}e^{i\beta I_y}e^{i\alpha I_z} \quad . \tag{49}$$

1.2.2. Wigner Rotation Matrices

Having defined the rotation operator $D(\alpha,\beta,\gamma)$, we now consider the effect of a coordinate rotation upon the angular momentum eigenfunctions $|jm>$. We note that the $(2j+1)$ functions $|jm>$ span the irreducible representation $D^{(j)}$ of R_3 and so a rotation transforms $|jm>$ into a linear combination of the $(2j+1)$ functions

$$D(\alpha\beta\gamma)|jm> = \sum_{m'=-j}^{j} |jm'>D^{(j)}_{m'm}(\alpha\beta\gamma) \tag{50}$$

where the states $|jm'>$ are represented as a row vector. If we use a column vector then the equation is

$$D(\alpha\beta\gamma)|jm> = \sum_{m'=-j}^{j} {}^{t}D^{(j)}_{mm'}(\alpha\beta\gamma)|jm'> \tag{51}$$

and $(D^{(j)}_{mm'})^t$ is the transpose of $D^{(j)}_{m'm}$.

We get an explicit expression for $D^{(j)}_{mm'}(\alpha\beta\gamma)$ by premultiplying equation 50 by $<j'm'|$ and noting that,

$$<j'm'|jm> = \delta_{jj'}\delta_{mm'} \tag{52}$$

to get

$$D^{(j)}_{m'm}(\alpha\beta\gamma) = <jm'|D(\alpha\beta\gamma)|jm> \tag{53}$$

A final expression for the matrix element is obtained by expanding $D(\alpha\beta\gamma)$:

$$\begin{aligned} D^{(j)}_{m'm}(\alpha\beta\gamma) &= <jm'|D(\alpha\beta\gamma)|jm> \\ &= <jm'|e^{i\gamma I_z}e^{i\beta I_y}e^{i\alpha I_z}|jm> \\ &= e^{i\gamma m'}<jm'|e^{i\beta I_y}|jm>e^{i\alpha m} \\ &= e^{i\gamma m'}e^{i\alpha m}d^{(j)}_{m'm}(\beta) \quad . \end{aligned} \tag{54}$$

Several properties of Wigner rotation matrices will be utilized throughout this work and are now tabulated:

(i) $D(\alpha\beta\gamma)$ is a unitary operator and so $D^{(j)}_{m'm}(\alpha\beta\gamma)$ is a unitary matrix. As a consequence, the inverse of $D^{(j)}_{m'm}$ is equal to the adjoint. That is,

$$\begin{aligned} [D^{(j)}_{m'm}(\alpha\beta\gamma)]^{-1} &= D^{(j)}_{m'm}(-\gamma,-\beta,-\alpha) \\ &= (D^{(j)}_{m'm}(\alpha,\beta,\gamma))^{+} \\ &= (D^{(j)}_{mm'}(\alpha\beta\gamma))^{*} \end{aligned} \tag{55}$$

(ii) $D^{(j)}_{m'm}(\alpha\beta\gamma)$ is a unitary matrix so the rows and columns are orthogonal:

$$\sum_m D^{(j)}_{m'm}(\alpha\beta\gamma)D^{(j)}_{m''m}(\alpha\beta\gamma) = \delta_{m'm''} \tag{56a}$$

$$\sum_m D^{(j)}_{mm'}(\alpha\beta\gamma)D^{(j)}_{mm''}(\alpha\beta\gamma) = \delta_{m'm''} \tag{56b}$$

(iii) Elements of rotation matrices, considered as functions of α, β, and γ are orthogonal to each other within the domain covered by the Euler angles.

$$\int D^{(j_1)*}_{u_1m_1}(\alpha\beta\gamma)D^{(j_2)}_{u_2m_2}(\alpha\beta\gamma)d\Omega = (8\pi^2/2j_1+1)\delta_{u_1u_2}\delta_{m_1m_2}\delta_{j_1j_2} \tag{57}$$

where

$$\int d\Omega = \int_0^{2\pi} d \int_0^{\pi} d\beta \sin\beta \int_0^{2\pi} d\gamma \quad . \tag{58}$$

1.2.3 Clebsch-Gordon Coefficients

Given a representation $D^{(j_1)}$ spanned by the $2j_1+1$ eigenfunctions $|j_1m_1>$ and a representation $D^{(j_2)}$ spanned by the $2j_2+1$ eigenfunctions $|j_2m_2>$, what is the form of the $(2j_1+1)(2j_2+1)$ basis functions $|jm>$ which span $D^{(j_1)} X D^{(j_2)}$? Evidently $|jm>$ is obtained by a unitary transformation of the direct product states $|j_1m_1>|j_2m_2>$ and so we would expect

$$|jm> = \sum_{m_1m_2} C^{j_1j_2j}_{m_1m_2m}|j_1m_1>|j_2m_2> \quad . \tag{59}$$

To get an expression for the coefficients $C^{j_1j_2j}_{m_1m_2m}$, define

$$|jm> = |j_1j_2jm> \quad \text{and} \tag{60a}$$

$$|j_1j_2m_1m_2> = |j_1m_1>|j_2m_2> \quad . \tag{60b}$$

Now use the identity

$$\sum_{m_1m_2}|j_1j_2m_1m_2><j_1j_2m_1m_2| = 1 \tag{61}$$

to obtain the expression

$$|j_1j_2jm> = \sum_{m_1m_2} |j_1j_2m_1m_2><j_1j_2m_1m_2|j_1j_2m> \quad , \tag{62}$$

and we realize that

$$C^{j_1j_2j}_{m_1m_2m} = <j_1j_2m_1m_2|j_1j_2jm> \quad . \tag{63}$$

The geometric interpretation of equation 62 is that a given $|j_1j_2j>$ vector exists in a space spanned by $(2j_1+1)(2j_2+1)$ orthonormal direct product vectors $|j_1j_2m_1m_2>$ and can be expressed as a linear combination of those vectors. Therefore the projection of the vector $|j_1j_2m_1m_2>$ onto $|j_1j_2j>$ is the Clebsch-Gordon coefficient given by equation 63.

Clebsch-Gordon coefficients have several properties that we will find useful and are listed below without proof

(i) $C^{j_1j_2j}_{m_1m_2m} = <j_1j_2m_1m_2|j_1j_2j> = 0$ unless

$$m_1 + m_2 = m \text{ and} \tag{64a}$$

$$|j_1+j_2| \geq j \geq |j_1j_2| \qquad (\Delta(j_1j_2j)) \tag{64b}$$

(ii) The coefficients $C^{j_1j_2j}_{m_1m_2m}$ form a real, orthogonal matrix and so

$$<j_1j_2m_1m_2|j_1j_2jm> = <j_1j_2jm|j_1j_2m_1m_2> \tag{65a}$$

$$\sum_{m_1m_2} <j_1j_2m_1m_2|j_1j_2jm><j_1j_2m_1m_2|j_1j_2j'm'> = \delta_{jj'}\delta_{mm'}\Delta(j_1j_2j) \tag{65b}$$

$$\sum_j <j_1j_2m_1',m-m_1'|j_1j_2jm><j_1j_2jm|j\ ;j_2m_1,m-m_1> = \delta_{m_1m_1'} \tag{65c}$$

1.2.4 Spherical Tensors

Spherical tensor notation will be used extensively in this work. In this section we introduce the concept via Cartesian tensors, and then define irreducible spherical tensors. We will also consider the behavior of spherical tensors under rotations.

A Cartesian vector is a set of three elements that transform as the coordinates of a point. If R is a vector in some coordinate system and R' is the vector in a rotated system, R and R' are related by

$$R' = \bar{A}R \tag{66}$$

where $\bar{A}$ is a real, orthogonal matrix, and $R' = (x',y',z')$ and $R = (x,y,z)$. R is said to be a first rank Cartesian tensor.

Now consider the quadratic combinations of x, y, and z that span the direct product space (x, y, z) X (x, y, z), i.e. x^2, xy, yz etc. These 9 entities are related to the quadratic combinations of x', y', and z' (which span (x', y', z') X (x', y', z')) by a 9 X 9 matrix which is $\bar{A} \times \bar{A}$. The 9 elements are a second rank tensor. These relations are directly generalized to a higher rank. In fact, an n^{th} rank Cartesian tensor may be treated as a 1 X n vector, that is, its algebra is isomorphic to the algebra of a first rank Cartesian tensor.

What is the relationship between Cartesian rotations and rotations in R_3? We realize that $\bar{A}$ corresponds to $D^{(1)}$ and $\bar{A} \times \bar{A}$ corresponds to $D^{(1)} \times D^{(1)}$ which reduces to $D^{(2)} + D^{(1)} + D^{(0)}$. We define the set of 2k+1 entities that span $D^{(k)}$ a k^{th} rank irreducible speherical tensor, T_{kq}, since $D^{(k)}$ is an irreducible representation of R_3, the continuous group of all rotation operators

$D(\alpha\beta\gamma)$. Transformations of spherical tensors are governed by the equation:

$$D(\alpha\beta\gamma)T_{kq} = \sum_{q'} T_{kq'} D^{(k)}_{q'q}(\alpha\beta\gamma) \tag{67}$$

a relationship that will appear frequently in the following chapters of this thesis.

Another useful relationship allows us to express a spherical tensor as a sum of products of two other tensors.

$$T_{\ell m}(A_1,A_2) = \sum_{m_1} C(\ell_1\ell_2\ell,m_1,m-m_1)T_{\ell_1 m_1}(A_1)T_{\ell_2 m_2}(A_2) \ . \tag{68}$$

ℓ may vary from $|\ell_1+\ell_2|$ to $|\ell_1-\ell_2|$ and $m = m_1+m_2$. $C(\ell_1,\ell_2,\ell;m_1,m-m_1)$ is a Clebsch-Gordon coefficient.

In Appendix 1.1 we use equation 68 to give relationshps between tensors of zeroth, first, and second rank. In Appendix 1.2 we give the relationship between spherical tensor and Cartesian tensors. Finally, in Appendix 1.3 we compile values of $d^j_{mm'}(\beta)$ for $j = 0, 1,$ and 2.

1.3 Nuclear Magnetic Resonance

1.3.1 Introduction

The central phenomenon discussed in this thesis is nuclear magnetic resonance (nmr), the resonant absorption of radio frequency (r.f) energy by a diamagnetic substance in a magnetic field. The purpose of this section is to review the basic theory of nmr and to clarify the "jargon" of the field to the general reader. The reader is referred to the excellent texts by Abragam (6), Slichter (7), or Goldman (8).

1.3.2 Equilibrium Magnetization

We assume that a system of N nuclear spins I^j are equilibrated with a lattice which has a very large heat capacity compared to the spin system. Equilibration occurs via some relaxation phenomenon or combination of phenomena, and by equilibration is meant that the temperature of the nuclear spin system equals the lattice temperature. The Hamiltonian of the nuclear spin system has two parts:

$$\mathcal{H} = \mathcal{H}_0 + \mathcal{H}_1 \tag{69}$$

where

$$\hbar\mathcal{H}_0 = -\hbar y B \sum_{j=1}^{N} I_z^j = y\hbar I_z B_0 \tag{70}$$

is the Zeeman term and $\mathcal{H}_1$ is the spin interaction term, describing spin-spin couplings and the quadrupolar coupling.

Given an ensemble of such systems in contact with the lattice, the canonical density operator is given by equation 39:

$$\rho_{eq} = ce^{-\beta(\mathcal{H}_0+\mathcal{H}_1)} \tag{71}$$

where

$$1/_c = \mathrm{Tr}(e^{-\beta(\mathcal{H}_0+\mathcal{H}_1)}) \quad . \tag{72}$$

The equilibrium magnetization M_0 is the expection value of the magnetic moment $y\hbar I_z$ which is

$$M_0 = \mathrm{Tr}(y\hbar I_z \rho) \quad . \tag{73}$$

Since nmr is normally in the high temperature limit we can expand ρ as was indicated by equations 41 and 42:

$$M_0 \sim \frac{\mathrm{Tr}(yI_z(\mathcal{H}_0+\mathcal{H}_1)\rho)}{\mathrm{Tr}(1)} \tag{74}$$

where we have used the fact that I_z is a traceless operator. Now we use the fact that for spin-spin couplings and the quadrupolar coupling $\mathrm{Tr}(I_z\mathcal{H}_1) = 0$ with the result

$$M_0 \sim \frac{\mathrm{Tr}(y\beta I_z\mathcal{H}_0)}{\mathrm{Tr}(1)} \quad . \tag{75}$$

Now we substitute the expression for the $\mathcal{H}_0$ into equation 75 to get

$$M_0 \sim \frac{\mathrm{Tr}(y^2 B_0 I_z{}^2 \beta)}{\mathrm{Tr}(1)} \tag{76}$$

$$\sim \frac{Ny^2 I(I+1)B_0}{3}$$

where we have used the fact that

$$\mathrm{Tr}[(I_z{}^j)^2] = \frac{(2I+1)(I)(I+1)}{3} \tag{77}$$

and

$$\mathrm{Tr}(1) = 2I+1 \quad . \tag{78}$$

Finally, equation 76 may be written in the form $M_0 = \chi_0\mathcal{H}_0$ where

$$\chi_0 = \frac{y^2 I(I+1)}{3} \quad . \tag{79}$$

We call χ_0 the static magnetic susceptibility and M_0 is the Curie magnetization.

1.3.3 Linear Response of a Spin System to a Pulsed R.F. Field

In the last section we considered the nature of equilibrium in a system of nuclear spins in a strong magnetic field in the high temperature limit, in which the spin system is coupled through relaxation to some large heat bath. We now consider the linear response of the spin system to a pulsed r.f. field.

Suppose we have a spin system at equilibrium in a strong magnetic field. The density matrix is

$$\rho(0) \simeq e(1-\beta\mathcal{H}_0) \qquad (80)$$

where

$$\hbar\mathcal{H}_0 = \hbar y B_0 I_z$$

$$= \hbar\,\omega_0 I_z \qquad (81)$$

and

$$1/c \simeq \mathrm{Tr}(1) \qquad (82)$$

If we turn on an r.f. field, the complete Hamiltonian is, neglecting relaxation,

$$\mathcal{H} = -\omega_0 I_z - \omega_1 I_x \cos\omega t + \mathcal{H}_{int} \qquad (83)$$

where the first term is the Zeeman term, the second term is the r.f. field and the third term is an interaction Hamiltonian (see next section). We transform $\mathcal{H}$ into a frame rotating about the z-axis at ω by rewriting the Hamiltonian as

$$\mathcal{H} \sim \omega_0 I_z - \omega_1 e^{i\omega I_z t} I_x\, e^{-i\omega I_z t} + \mathcal{H}_{int} \quad , \qquad (84)$$

where we have introduced a counter-rotating component to the field. We now define the transformation operator

$$U = e^{i\omega I_z t} \qquad (85)$$

and the rotating frame Hamiltonian is defined as

$$\mathcal{H}_R = U^{-1}\ U - iU^{-1}\dot{U}$$

$$= U^{-1}(-\omega_0 I_z - \omega_1 e^{i\omega I_z t} I_x e^{-1\omega I_z t} + \mathcal{H}_{int})U$$

$$= ie^{-i\omega I_z t}(+i\omega I_z e^{+i\omega I_z t})$$

$$= -\omega_0 I_z - \omega_1 I_k + \mathcal{H}_{int} + \omega I_z \qquad (86)$$

where we have used the fact that $[I_z, \mathcal{H}_{int}] = 0^{(8)}$. We rewrite this expression as

$$\mathcal{H}_R = -\Delta\omega I_z - \omega_1 I_x + \mathcal{H}_{int} \quad . \qquad (87)$$

In all the work which follows we will use rotating frame Hamiltonians. Thus we drop the R subscript.

Now if the pulse is of very high power, $\omega_1 >> \Delta\omega, \|\mathcal{H}_{int}\|$, and the Hamiltonian is

$$\mathcal{H} \sim \omega_1 I_x \quad . \qquad (88)$$

So the density matrix immediately after the pulse is

$$\rho(tp) = -c\beta\omega_0\ e^{-i\omega_1 t_p I_x}\ I_z\ e^{i\omega_1 t_p I_x}$$

$$= -c\beta\omega_0(I_z \cos\omega_1 t_p + I_y \sin\omega_1 t_p) \quad , \qquad (89)$$

and we have neglected the scalar part of the density matrix.

Now the spin system evolves for a time t under the Hamiltonian

$$\mathcal{H} = -\Delta\omega I_z + \mathcal{H}_{int} \qquad (90)$$

and the density matrix is

$$\rho(t_p+t) = -\ c\beta\omega_0\ e^{i\mathcal{H}t}\rho(t_p)\ e^{-i\mathcal{H}t} \quad . \qquad (91)$$

We will neglect the I_z term in $\rho(t_p)$ since it commutes with $\mathcal{H}$. Therefore

$$\rho(t_p+t) = -c\beta\omega_0\sin\omega_1 t_p \, e^{i\mathcal{H}_{int}t} e^{-i\Delta\omega I_z} I_y \, e^{i\Delta\omega I_z} e^{-i\mathcal{H}_{int}t} \tag{92}$$

where we have used the fact that I_z and $\mathcal{H}_{int}$ commute. We obtain

$$\rho(t_p+t) = -c\beta\gamma_y B_0 \sin\omega_1 t_p \, e^{i\mathcal{H}_{int}t}(I_y\cos\Delta\omega t + I_x \sin\Delta\omega t)e^{-i\mathcal{H}_{int}}$$

$$= -c\beta\gamma_y B_0 \sin\omega_1 t_p (e^{i\mathcal{H}t} I_y e^{-i\mathcal{H}t}\cos\Delta\omega t + e^{i\mathcal{H}t} I_x e^{-i\mathcal{H}t}\sin\Delta\omega t)$$

$$= -c\beta\gamma_y B_0 \sin\omega_1 t_p (\rho_x(t_p+t) + \rho_y(t_p+t) \quad . \tag{93}$$

The x component of the transverse magnetization has the form

$$\langle I_x \rangle = \mathrm{Tr}(\rho I_x)$$

$$= \mathrm{Tr}(\rho_x I_x)$$

$$= \sum_{mn} (\rho_x)_{mn} (I_x)_{nm}$$

$$= -c\beta\omega_0 \sin\omega_1 t_p \sin\Delta\omega t \sum_{mn} e^{-i\omega_{nm}t} |(I_x)_{nm}|^2$$

$$= -\frac{1}{2}c\beta\omega_0 \sin(\omega_1 t_p) \sum_{mn} (e^{-i(\omega_{nm}+\Delta\omega)t} - e^{i(\omega_{nm}-\Delta\omega)t})|(I_x)_{nm}{}^2| \tag{94a}$$

Similarly,

$$\langle I_y \rangle = -\frac{1}{2}c\beta\omega_0 \sin(\omega_1 t_p) \sum_{mn} (e^{-i(\omega_{nm}+\Delta\omega)t} + e^{-i(\omega_{nm}-\Delta\omega)t})|(I_y)_{nm}|^2 \quad . \tag{94b}$$

We can add a decay term e^{-t/T_2} to obtain

$$\langle I_x\rangle = ic' \sum_{mn} (e^{(-i(\omega_{nm}+\Delta\omega)-{}^1/T_2)t} - e^{(i(\omega_{nm}-\Delta\omega)-{}^1/T_2)t} |(I_x)_{nm}|^2 \qquad (95a)$$

$$\langle I_y\rangle = c' \sum_{mn} (e^{(-i(\omega_{nm}+\Delta\omega)-{}^1/T_2)t} + e^{(-i(\omega_{nm}-\Delta\omega)-{}^1/T_2)t} |(I_y)_{nm}|^2 \qquad (95b)$$

where $c' = c\beta\omega_0 \sin\omega_1 t_p$.

To calculate the linear frequency response $F(\omega)$ we Fourier transform the complex function $\langle I_x\rangle + i\langle I_y\rangle$

$$F(\omega) = F_x(\omega) + iF_y(\omega) = \frac{1}{2\pi}\int dt\; e^{-i\omega t}(\langle I_x\rangle + i\langle I_y\rangle), \qquad (96a)$$

and we find that

$$F_x(\omega) = {}^{c'}/\pi \;_{mn} \frac{(T_2)^{-1}}{(T_2)^{-2} + (\omega_{nm} + \Delta\omega - \omega)^2} |(I_x)_{nm}|^2 \qquad (96b)$$

$$F_y(\omega) = {}^{c'}/\pi \sum_{mn} \frac{\omega_{nm} + \Delta\omega - \omega}{(T_2)^{-2} + (\omega_{nm} + \Delta\omega - \omega)^2} |(I_y)_{nm}|^2 \qquad (96c)$$

We notice that the quantities $F_x(\omega)$ and $F_y(\omega)$ defined in 96b and 96c are proportional to the components of the complex susceptibility

$$x(\omega) = x'(\omega) - ix''(\omega) \qquad (97)$$

obtained by solving the Bloch equations (10) in the limit of negligible saturation, that is,

$$\omega_1^2 T_1 T_2 >> 1 \quad . \tag{98}$$

Specifically,

$$F_x(\omega)\alpha x''(\omega) \text{ and } F_y(\omega)\alpha x'(\omega) \quad . \tag{99}$$

Therefore, the Fourier transform of the transient response of a spin system to a high power pulsed r.f. field, is proportional to the steady state response of a spin system to continuous irradiation by a weak r.f. field.

Finally, we notice that $F_x(\omega)$ and $F_y(\omega)$ are proportional to $|(I_x)_{nm}|^2$ and $|(I_y)_{nm}|^2$, respectively. It is evident that in the case of the linear response of a spin system to an r.f. field, the magnetic quantum number m can only change by 1:

$$|\Delta m| = 1 \tag{100}$$

In chapter 3 we will discuss nmr experiments in which this condition does not apply.

1.3.4. Spin Interaction Hamiltonians; General Expressions

We now introduce the Hamiltonians relevant to this work. For convenience, all Hamiltonians will be written in frequency units. Therefore:

$$\hbar\mathcal{H} = \hbar(\mathcal{H}_z + \mathcal{H}_{rf} + \mathcal{H}_{cs} + \mathcal{H}_Q + \mathcal{H}_J + \mathcal{H}_D) \tag{101}$$

a) Zeeman Hamiltonian: $\mathcal{H}_z$

This Hamiltonian has already been introduced. It describes the interaction between the dc magnetic field, taken to be in the z direction, and the magnetic dipole moments of the nuclei.

$$\hbar\mathcal{H}_z = -\hbar\sum_i \tilde{u}^i\cdot\tilde{B}_0 = -\hbar B_z \sum_i \gamma_i I_z^i = -\hbar\sum\omega_0^i I_z^i \tag{102}$$

γ_i is the magneto-gyric ratio of the i^{th} nucleus and $\tilde{B}_0 = (0,0,B_z\hat{k})$, and $\tilde{u}^i = \gamma_i(I_x^i, I_y^i, I_z^i)$.

b) Radio-Frequency (R.F.) Hamiltonian

This Hamiltonian describes the coupling of the spins with the magnetic components of an r.f. field. The field is assumed to be linearly polarized in the x direction

$$\hbar\mathcal{H}_{rf} = -\hbar\sum_i u^i\cdot\tilde{B}_1(t) = -\hbar B_1\cos(\omega t + \phi(t)) \sum_i y_i I_x^i \tag{103}$$

where $\tilde{B}_1(t) = (B_1\cos(\omega t + \phi t))\ \tilde{i},0,0)$.

c) Chemical Shielding Hamiltonian: $\mathcal{H}_{cs}$

This Hamiltonian describes the interaction of the nuclear spin with magnetic fields induced by electron currents. It has the form

$$\hbar\sum_i \tilde{u}^i\cdot\tilde{\tilde{\sigma}}^i\cdot B \tag{104}$$

where σ^i is a Cartesian tensor of rank 2 and $-\sigma^i\cdot B$ is the magnetic field induced by the electrons at the i^{th} nucleus.

d) Quadrupolar Hamiltonians: $\mathcal{H}_Q$

This Hamiltonian describes the interaction between the electric quadrupole moment of the nucleus and the surrounding electric field gradients. Nuclei with spin = $^1/2$ have no quadrupole moment.

$$\hbar\mathcal{H}_Q = \sum_i \frac{eQ^i}{6I^i(I^i-1)} \tilde{I}^i\cdot\tilde{\tilde{V}}^i\cdot\tilde{I}^i \tag{105}$$

eQ^i is the electric quadrupole moment of the i^{th} nucleus, V^i is the electric field gradient tensor at the i^{th} nucleus, i.e. the second derivative of the electric potential. V_i is a second rank Cartesian tensor.

e) Indirect Spin-Spin (J) Coupling Hamiltonian ($\mathcal{H}_J$)

This Hamiltonian describes the through-bond interaction of two nuclear spins. It has the form

$$\hbar\mathcal{H}_J = \sum_{ij} \tilde{I}_i\cdot\tilde{\tilde{J}}_{ij}\cdot\tilde{I} \tag{106}$$

where $\tilde{\tilde{J}}_{ij}$ is a second rank Cartesian tensor.

f) Direct Spin-Spin (Dipolar) Coupling Hamiltonian: $\mathcal{H}_D$

This Hamiltonian describes the through-space coupling of the magnetic dipole moments of the nuclei. It has the form

$$\hbar\mathcal{H}_D = -2\hbar^2 \sum_{i<j}\gamma_i\gamma_j \sum_{\alpha\beta}^{x,y,z}[I^i_\alpha\cdot D^{ij}_{\alpha\beta}\cdot I^j] \tag{107}$$

$D^{ij}_{\alpha\beta}$ is the $\alpha\beta$ component of $\tilde{\tilde{D}}^{ij}$, the second rank Cartesian tensor describing the coupling between the nuclear spins $i\neq j$.

1.3.5. Spherical Tensor Forms

We may refer to $\mathcal{H}_Q$, $\mathcal{H}_J$, $\mathcal{H}_{cs}$, and $\mathcal{H}_D$ as internal Hamiltonians since they describe interactions internal to the spin system as opposed to interactions with externally applied fields, described by $\mathcal{H}_{rf}$ and $\mathcal{H}_z$. We also notice that the internal Hamiltonians involve second rank Cartesian tensors. It is also possible to describe these Hamiltonians as scalar products of spherical tensors, (11, 12) given by the equation

$$\mathcal{H} = \sum_{\ell} \sum_{m=-\ell} (-)^{m} A_{\ell_1 -m} T_{\ell,m} \qquad (108)$$

where A is a tensor involving spin operators and T is a tensor involving interaction parameters.

Now the tensor A is written in the laboratory frame. Spin interaction parameters, however, are simply linked to some principal axis system (PAS) in which the interaction tensor is diagonal. Therefore we use equation 67 to relate T with the principal axis system tensor T^{PAS}

$$T_{\ell m} = \sum_{m'} T^{PAS}_{\ell m'} \cdot D^{(\ell)}_{m'm}(\Omega) \quad . \qquad (109)$$

Now the equation for the Hamiltonian is

$$\mathcal{H} = \sum_{\ell} \sum_{m=-\ell}^{\ell} (-)^{m} (\sum_{m'} T^{PAS}_{m'} \; D^{(\ell)}_{m'm}(\Omega)) A_{\ell,-m} \quad . \qquad (110)$$

1.3.6. Truncation of Spin Hamiltonian

The nuclear magnetic resonance experiment is usually carried out in very high magnetic fields. Typical field strengths reach tens of thousands of Gauss. However, nuclear spin interactions normally only involve fields of a few Gauss at best. The quadrupole interaction is an exception and may in some species like ^{79}Br exceed the Zeeman interaction for realistic magnetic fields, but we will not concern ourselves with such systems. The point to be realized is that for all spin systems discussed here, the spin interaction Hamiltonian may be considered a perturbation on the Zeeman Hamiltonian. Therefore, to first order, we need only concern ourselves with that portion of the interaction Hamiltonian which commutes with the Zeeman Hamiltonian. The commuting portion of the interaction Hamiltonian is called the secular Hamiltonisn, and only the secular Hamiltonian determines line positions to first order. Now by Racah's definition (13) of an irreducible tensor operator we have that

$$[I_z, A_{\ell m}] = mA_{\ell m} \tag{111}$$

and so only the $A_{\ell 0}$ components occur in the secular Hamiltonian. We now have, as an expression for the general interaction Hamiltonian

$$\mathcal{H}_{\text{secular}} = \sum_{\ell} (\sum_{m'} T^{\text{PAS}}_{\ell m'} D^{(\ell)}_{m'0}(\Omega) A_{\ell 0} \quad . \tag{112}$$

As an example let us consider the dipolar Hamiltonian. $T_{\ell m}$ is a second rank traceless tensor which is uniaxial in its PAS. Thus only $T^{\text{PAS}}_{20}(ij) = ({}^3/2)^{{}^1/2}\ r_{ij}{}^{-3}(-2)\hbar\gamma^i\gamma^j$ is nonzero. We obtain

$$\mathcal{H}_{d,\text{secular}} = -\ ({}^3/2)^{{}^1/2}\ \frac{2\hbar\gamma_i\gamma_j}{r_{ij}{}^3}\ D^{(2)}_{00}(\Omega)\ A_{20} \quad . \tag{113}$$

where $D^{(2)}_{00}(\Omega) = {}^1/2(3\cos^2\beta-1)$ and β is the angle between the internuclear vector and the z axis of the laboratory frame.

From equation 7 of appendix 1.2 we find that

$$\begin{aligned} A_{20} &= ({}^2/3)^{{}^1/2} I_{z1}I_{z2} - ({}^1/6)^{{}^1/2}(I_{x1}I_{x2} + I_{y1}I_{y2}) \\ &= 6^{-{}^1/2}(2I_{z1}I_{z2} - (I_{x1}I_{x2} + I_{y1}I_{y2})) \\ &= 6^{-{}^1/2}(3I_{z1}I_{z2} - I_1 \cdot I_2) \end{aligned} \tag{114}$$

and we finally get

$$\mathcal{H}_D^{\text{secular}} = -({}^3/2)^{{}^1/2}\,\frac{\hbar y_i y_j}{r_{ij}^3}(3\cos^2\beta-1)(3I_{z1}I_{z2}-I_1\cdot I_2) \qquad (115)$$

as the expression for the secular dipolar Hamiltonian in the laboratory frame. In all work that follows, only the secular part of the interaction Hamiltonian will be considered. Therefore the superscript "secular" will be dropped.

Truncated forms for the other Hamiltonians are (14):

(i) $\mathcal{H}_Q = {}^{\omega_Q}/3\ (3I_z^2 - I(I-1))$

where $\omega_Q = \frac{e^2qQ}{2I(2I-1)}\ ({}^1/2(3\cos^2\theta-1) + \eta\sin^2\theta\cos2\theta)$

(116)

(ii) Chemical Shift:

$$\mathcal{H}_{cs} = -\sum_i \sigma^i_{zz} I^i_z \qquad (117)$$

(iii) Scalar:

$$\mathcal{H}_J = J(I_1\cdot I_2) \qquad (118)$$

Appendix 1.1 Spherical Tensor Forms

Using equation 68 of section 1.2.4

$$T_{\ell m}(A_1,A_2) = \sum_{m_1} C(\ell_1,\ell_2,\ell;\ m_1,m-m_1)\ T_{\ell_1 m_1}(A_1).T_{\ell_2 m_2}(A_2) \qquad (1)$$

we obtain the following relationships:

$$T_{00}(A_1,A_2) = {}^1/\sqrt{3}\ (T_{1-1}(A_1)\ T_{11}(A_2) - T_{10}(A_1)\ T_{10}(A_2) + T_{11}(A_1)\ T_{1-1}(A_2) \qquad (2)$$

$$T_{1-1}(A_1A_2) = -{}^1/\sqrt{2}\ (T_{1-1}(A_1)T_{10}(A_2) - T_{10}(A_1)T_{1-1}(A_2) \qquad (3)$$

$$T_{10}(A_1,A_2) = -{}^1/\sqrt{2}\ (T_{1-1}(A_1)T_{11}(A_2) - T_{11}(A_1)T_{1-1}(A_2) \qquad (4)$$

$$T_{11}(A_1,A_2) = -{}^1/\sqrt{2}\ (T_{10}(A_1)T_{11}(A_2) - T_{11}(A_1)T_{10}(A_2) \qquad (5)$$

$$T_{2-2}(A_1,A_2) = T_{1-1}(A_1)T_{1-1}(A_2) \qquad (6)$$

$$T_{2-1}(A_1,A_2) = {}^1/\sqrt{2}\ (T_{1-1}(A_1)T_{11}(A_2) + 2T_{10}(A_1)T_{10}(A_2) + T_{11}(A_1)T_{1-1}(A_2) \qquad (7)$$

$$T_{20}(A_1,A_2) = {}^1/\sqrt{6}\ (T_{1-1}(A_1)T_{11}(A_2) + 2T_{10}(A_1)T_{10}(A_2) + T_{11}(A_1)T_{1-1}(A_2)) \qquad (8)$$

$$T_{21}(A_1,A_2) = {}^1/\sqrt{2}\ (T_{10}(A_1)T_{11}(A_2) + T_{11}(A_1)T_{10}(A_2)) \qquad (9)$$

$$T_{22}(A_1,A_2) = T_{11}(A_1)T_{11}(A_2) \qquad (10)$$

Appendix 1.2

The relationship between a second rank Cartesian tensor and the irreducible spherical tensor are:

$$T_{00} = - {}^{1}/\sqrt{3}\ (x_1x_2 + y_1y_2 + z_1z_2) \tag{1}$$

$$T_{11} = - {}^{1}/\sqrt{2}\ (x_1 + iy_1)z_2 - z_1(x_2 + iy_2)) \tag{2}$$

$$T_{1-1} = {}^{1}/\sqrt{2}\ ((x_1 - iy_1)z_2 - z_1(x_2 - iy_2)) \tag{3}$$

$$T_{10} = {}^{i}/\sqrt{2}\ (x_1y_2 - x_2y_1) \tag{4}$$

$$T_{22} = {}^{1}/2\ (x_1 + iy_1)(x_2 + iy_2) \tag{5}$$

$$T_{21} = - {}^{1}/2\ ((x_1 + iy_1)z_2 + z_1(x_2 + iy_2)) \tag{6}$$

$$T_{20} = \sqrt{{}^{2}/3}\ z_1z_2 - {}^{1}/\sqrt{6}\ (x_1x_2 + y_1y_2) \tag{7}$$

$$T_{2-1} = {}^{1}/2\ ((x_1 - iy_1)z_2 + z_1(x_2 - iy_2)) \tag{8}$$

$$T_{2-2} = {}^{1}/2(x_1 - iy_1)(x_2 - iy_2) \tag{9}$$

Appendix 1.3

The Wigner rotation matrix element is given by

$$D^{(\ell)}_{mn}(\alpha,\beta,\gamma) = e^{-i\ m}\ d^{(\ell)}_{mn}(\beta)\ e^{-i\ n}$$

$$d^{(0)}_{00}(\beta) = 1$$

$$d^{(1)}_{11}(\beta) = d^{(1)}_{{\sim}1{\sim}1}(\beta) = \frac{1}{2}(1 + \cos\beta)$$

$$d^{(1)}_{1{\sim}1}(\beta) = d^{(1)}_{{\sim}11}(\beta) = \frac{1}{2}(1 - \cos\beta)$$

$$d^{(1)}_{01}(\beta) = d^{(1)}_{{\sim}10}(\beta) = -d^{(1)}_{0{\sim}1}(\beta) = -d^{(1)}_{10}(\beta) = \frac{1}{\sqrt{2}}(\sin\beta)$$

$$d^{(1)}_{00}(\beta) = \cos\beta$$

$$d^{(2)}_{22}(\beta) = d^{(2)}_{-2-2}(\beta) = \cos^4(\frac{\beta}{2})$$

$$d^{(2)}_{21}(\beta) = d^{(2)}_{{\sim}1{\sim}2}(\beta) = -d^{(2)}_{12}(\beta) = -d^{(2)}_{{\sim}1{\sim}2}(\beta) = \frac{1}{2}\sin\beta(1 + \cos\beta)$$

$$d^{(2)}_{20}(\beta) = d^{(2)}_{02}(\beta) = d^{(2)}_{{\sim}20}(\beta) = d^{(2)}_{0{\sim}2}(\beta) = \sqrt{\frac{3}{8}}\ \sin^2\beta$$

$$d^{(2)}_{2{\sim}1}(\beta) = d^{(2)}_{1{\sim}2}(\beta) = -d^{(2)}_{-21}(\beta) = -d^{(2)}_{-12}(\beta) = \frac{1}{2}\sin\beta(\cos\beta-1)$$

$$d^{(2)}_{2-2}(\beta) = d^{(2)}_{-22}(\beta) = \sin^4(\frac{\beta}{2})$$

$$d^{(2)}_{11}(\beta) = d^{(2)}_{{\sim}1{\sim}1}(\beta) = \frac{1}{2}(2\cos\beta- 1)(1 + \cos\beta)$$

$$d^{(2)}_{1{\sim}1}(\beta) = d^{(2)}_{11}(\beta) = \frac{1}{2}(2\cos\beta + 1)(1 - \cos\beta)$$

$$d^{(2)}_{10}(\beta) = d^{(2)}_{0{\sim}1}(\beta) = -d^{(2)}_{01}(\beta) = -d^{(2)}_{10}(\beta) = -\sqrt{\frac{3}{2}}\sin\beta\cos\beta$$

$$d^{(2)}_{00}(\beta) = \frac{1}{2}(3\cos^2\beta - 1)$$

2. A DEUTERIUM MAGNETIC RESONANCE (DMR) STUDY OF THE SMECTIC PHASES OF A THERMOTROPIC LIQUID CRYSTAL

2.1 Introduction

In this chapter we will study the structure of some of the low temperature mesophases of a thermotropic liquid crystal, using deuterium magnetic resonance (DMR) as a probe of molecular order and orientation. In particular, we will concern ourselves with the changes that occur in molecular orientation at the smectic A-smectic C phase transition. We will also study two lower temperature smectic B phases.

In section 2.2, the study begins by briefly reviewing the structure of the various liquid crystalline mesophases as obtained via X-ray diffraction and conopscopic studies. In section 2.3 will be described the nmr method used as a probe of molecular orientation: deuterium magnetic resonance and in particular, quadrupolar echo spectroscopy. The quadrupolar echo experiment will be described by expanding the density matrix in a basis of fictitious spin $^1/2$ operators. We will consider the experiment in the limit in which the r.f. power (in frequency units) exceeds the quadrupolar splitting ($\omega_1 >> \omega_Q$). In section 2.4 we will introduce a single domain model of the smectic A mesophase and a multidomain model of the smectic C mesophase. Both models assume that the liquid crystal has been aligned in a strong magnetic field. These models will be used to simulate experimental DMR spectra. Finally, in section 2.5 we will use the models introduced in section 2.4 to interpret DMR spectra of a monodeuterated liquid crystal in its smectic A and C mesophases.

From the DMR spectra we will extract information on the changes in molecular orientation and order that occur at the smectic A-C phase transition. Comments will also be made on the order of the low temperature smectic B_A-B_C phase transition.

2.2 Liquid Crystalline Mesophases

Throughout this thesis we will study either compounds that possess, within certain temperature ranges, liquid crystalline phases, or molecules dissolved as solutes in such phases. In this section we will qualitatively describe various common liquid crystalline phases. The reader is referred to several general texts on liquid crystals: deGenne (15), Priestley et.al. (16), and Chandrasekhar (17), and Taylor (18).

It is well-known that certain organic compounds, rather than showing a single transition from liquid to crystal, pass instead through one or more phases that have mechanical and symmetry properties intermediate between isotopic liquids and ordered crystalline solids. Such compounds are called liquid crystals and their peculiar phases are called mesomorphic phases or simply mesophases. While the molecular structures of compounds with mesomorphic phases vary greatly, a broad class of liquid crystalline compounds have the general pattern shown in figure 2. R and R' are commonly alkyl or alkoxy groups while A=B may be a Schiff base linkage or an azoxy linkage. In figure 3 we show examples of several thermotropic liquid crystals. Empirically derived rules on the influence of R and R' on the stability of the various mesophases have been extensively reviewed in the literature (21), so we will not consider the subject here. Rather, we will turn to a descriptive review of the

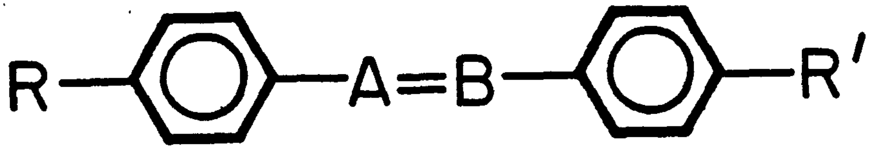

XBL 823-8600

Figure 2. Generalized structure of a molecule with mesomorphic phases. R and R' may be alkyl or alkoxy groups while A = B may be a Schiff base or an azoxy linkage. In a series of liquid crystals called cyanobiphenyls, R would be an alkyl or an alkoxy group, R' would be a CN group and A = B would be replaced by a single bond.

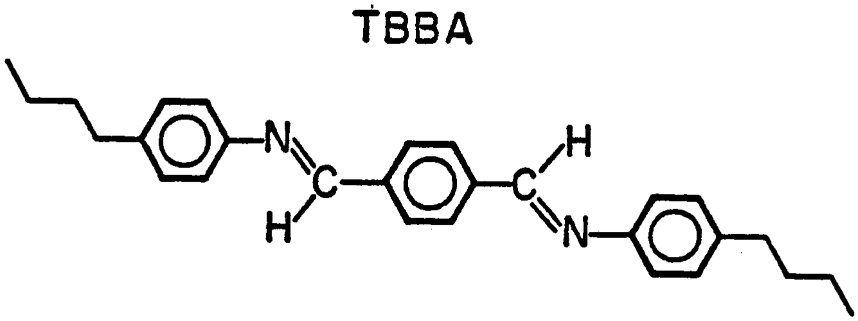
TBBA
N
C
H
C
H
N

XBL 751-5548 (a)

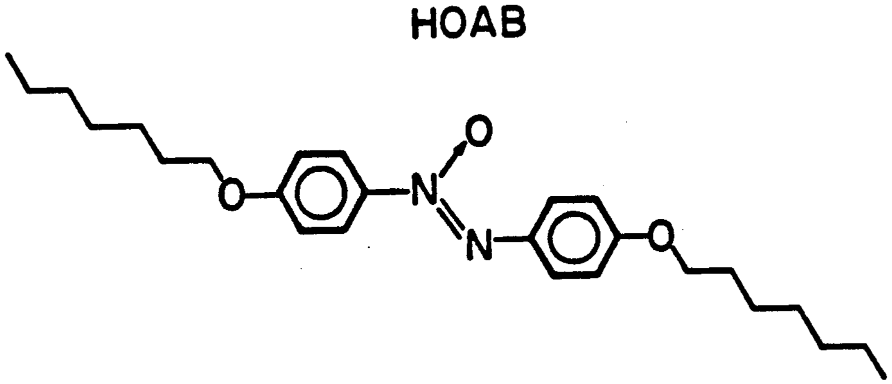

XBL 751-5547 (b)

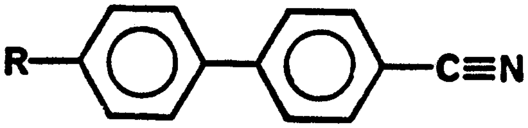

(c)

Figure 3. A. Teraphthalbisbutylaniline (TBBA)

B. Heptyloxyazoxybenzene (HOAB)

C. R-cyanobiphenyl. R is an alykl or an alkoxy group.

mesophases to be studied in this chapter.

2.2.1 Nematic

The first mesomorphic phase below the isotropic phase is usually the nematic. The main characteristics of the nematic phase are as follows:

a) There is no long-range translational order in a nematic liquid crystal, and so there is no Bragg peak in an x-ray diffraction pattern (23,24). The correlations between molecular centers of gravity are liquid-like. In fact, nematics flow, with typical viscosities of about .1 Poise.

b) Although there is no long-range translational order, there is long-range orientational order in the sense that the long axes of the individual molecules tend to align parallel to a common direction, labelled by a vector $\tilde{n}$. $\tilde{n}$ is called the director. This long-range orientational order causes macroscopic properties, such as the refractive index and the diamagnetic susceptibility, to be highly anisotropic. For instance, a nematic is optically uniaxial with the optical axis parallel to $\tilde{n}$ (25).

c) In the absence of external fields, the direction of $\tilde{n}$ is arbitrary, and can be influenced by wall conditions, for example. Static distortions of the director field can be described by an elastic continuum theory (18, 19, 22).

d) The states $\tilde{n}$ and $-\tilde{n}$ are equivalent. Thus, if the individual molecules have permanent electric dipole moments, $\tilde{n}$ and $-\tilde{n}$ are equally populated. Therefore the phase is not ferroelectric.

e) The component molecules of a nematic phase are either achiral or if chiral, the phase is a racemic mixture.

From the remarks above, we conclude that in a crystallographic sense, the nematic phase has $D_{\infty h}$ symmetry. A sketch of the nematic phase is shown in Figure 4b.

2.2.2 Smectic A

This phase is commonly the highest temperature smectic phase, if several smectic mesophases exist. Its characteristics are

a) A well-defined layer structure in which the layer thickness is about equal to the molecular strength. This thickness can be measured by x-ray diffraction (26,27).

b) Absence of long-range translational order within the layer structure.

c) Long-range orientational order within the layer structure described by the director $\tilde{n}$ as in nematics. The phase is optically uniaxial.

d) As in nematics, $\tilde{n}$ and $-\tilde{n}$ are equivalent.

Figure 4c shows the layer structure of the smectic A phase. Its crystallographic group is D_{∞}.

2.2.3 Smectic C

A smectic C phase is a two-dimensional liquid as is the smectic A. However the phase is observed to be optically biaxial (28). An interpretation of the phenomenon is that the molecules are tilted within the layer, an idea that has the support in the x-ray

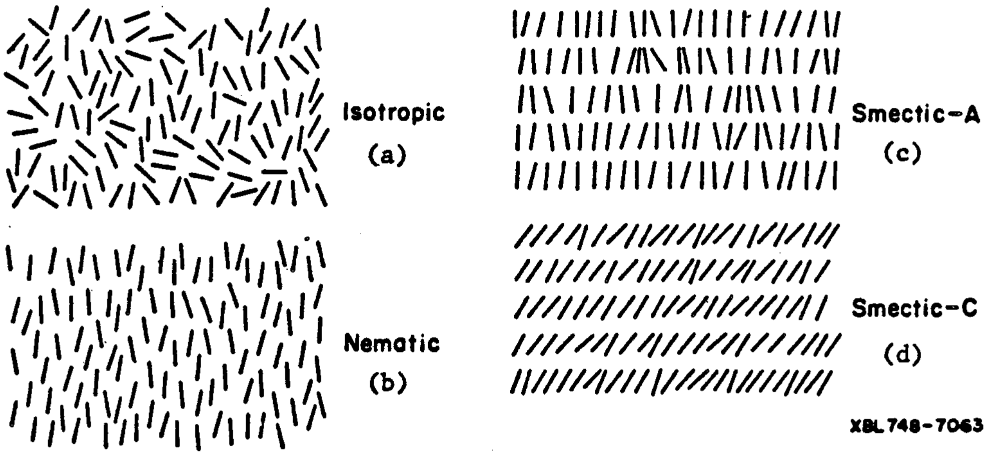

Figure 4. The common high temperature phases found in liquid crystaline systems.

(a) Isotropic: this phase is characterized by an absence of long range translational and orientational order.

(b) Nematic: this phase is characterized by an absence of long range translational order but orientational order occurs about a direction defined by a vector called the director.

(c) Smectic A: in this phase, orientational order is again described by the director, but molecules are confined to layers within which layer occurs isotropy of motion. The director is normal to the plane of each layer.

(d) Smectic C: this phase is similar to the smectic A except that the director is tilted relative to the normal vector of each plane.

literature since the layer thickness is found to be less than the molecular length (26,27,29). The tilt angle would also appear to be temperature dependent (30). Figure 4d shows the structure of the smectic C phase. There is a 2-fold axis parallel to the layer and a plane normal to it. Therefore, the smectic C phase has C_{2h} symmetry.

2.2.4 Smectic B Phases

There exist lower temperature uniaxial and biaxial smectic phases, and x-ray studies indicate that there is some order within each layer, although the exact type of packing is controversial (27,31,32,33,34). Uniaxial phases are called smectic B_A and biaxial phases are called smectic B_C. Smectic B_C phases are often called smectic H in the literature. Other more exotic phases have been reported, but they will not be discussed here.

2.3 Quadrupolar Echo Spectroscopy

In order to appreciate the utility of nmr as a method for studying the structure of liquid crystalline phases, we need only consider equation 110 of chapter 1:

$$\mathcal{H} = \sum_{\ell} \sum_{m=-\ell} (-)^m (\sum_{m'} T^{PAS}_{\ell m'} D^{(\ell)}_{m'm}(\Omega) A_{\ell m} \qquad (1)$$

Recall that A is a spherical tensor involving spin operators and T^{PAS} is a spherical tensor involving interaction parameters in some principal axis system. The $D^{(\ell)}_{m'm}(\Omega)$'s are elements of the Wigner rotation matrix that transform T into the laboratory frame. We assume throughout this thesis that the z axis of the laboratory frame is parallel to the magnetic field. Now the principal axis system is always related in some manner to molecular geometry. For example, the z axis of the principal axis system of the dipolar tensor is defined by the internuclear vector, and for deuterium bonded to trigonally hybridized carbon, the major axis of the electric field gradient tensor lies along the axis of the C-D sigma bond (see figure 5). Thus, by measuring the interaction in nmr, we effectively obtain the products $T^{PAS}_{m'} D^{(\ell)}_{m'm}(\Omega)$ which yield directly, information on the orientation of a molecular-fixed frame to the laboratory frame (we will develop these ideas thoroughly in the following section). Therefore nmr has come to be a popular tool in the study of liquid crystals. Since liquid crystals are organic compounds, natural abundance ^{13}C nmr has been used (35-37). Single quantum proton nmr spectroscopy has not been used extensively since oriented proton spectra are dominated by direct dipolar interactions. Since liquid crystal molecules contain large numbers of protons, the number of intramolecular dipolar couplings can be very large, resulting in very complex and often intractable spectra. In recent years multiple quantum proton nmr has been used to simplify such spectra, but we will reserve discussion of that technique for the next chapter.

Deuterium magnetic resonance has seen extensive use in the last fifteen years as a tool for liquid crystal study (38-51) as has the pure quadrupolar resonance spectroscopy (52-54) of ^{14}N and deuterium. THe NMR spectrum of selectively deuterated or perdeuterated liquid crystal molecules is dominated by the quadrupolar

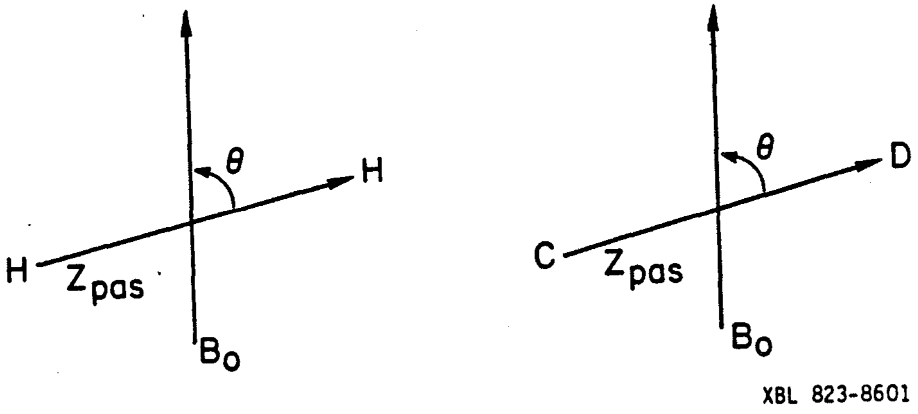

Figure 5. Principal axis systems of the dipolar and quadrupolar Hamiltonians. The dipolar Hamiltonian is uniaxial in its principal axis system (pas) and the z axis is parallel to the internuclear vector. In the case of the quadrupolar Hamiltonian, assuming the asymmetry parameter is small ($\eta \sim 0$) the Hamiltonian is approximately uniaxial in its pas. For deuterium bonded to carbon, the z axis is approximately parallel to the sigma bond axis.

interaction, the interaction of the nuclear electric quadrupolar moment with anisotropic electric fields which results in a first order splitting of the Zeeman resonance (see figure 6). The doublet splitting can vary from a few thousand hertz in very disordered nematic phases to almost 80 khz in very highly ordered smectic B phases.

The general form of the quadrupolar Hamiltonian was given by equation 105 of chapter 1:

$$\hbar\mathcal{H}_Q = \sum_i \frac{eQ^i}{6I(2I^i-1} \tilde{I}^i \cdot \tilde{\tilde{V}}^i \cdot \tilde{I}^i \qquad (2)$$

However, we will use the truncated version of the quadrupolar Hamiltonian, which is obtained from equaltion 2 above by the method described in section 1.3.6. The Hamiltonian for a single nucleus is:

$$\hbar\mathcal{H}_Q^{\text{secular}} = \frac{\omega_Q}{3}(3I_z^2 - I(I+1)) \qquad (3)$$

where

$$\omega_Q = \frac{e_q Q}{2I(2I-1)} \left(\frac{1}{2}(3\cos^2\theta - 1) + \eta\sin^2\theta\cos 2\phi\right) \quad .$$

We define $e_q = V_{zz}$ and $\eta = (V_{xx} - V_{yy})/V_{zz}$. q is called the field gradient and η is the asymmetry parameter.

When deuterium magnetic resonance is performed in the time domain, the free induction decay (fid) is detected after a high power "ninety degree" pulse. The free induction decay is the evolution of the single quantum coherence under the spin system's internal Hamiltonian, which includes the quadrupolar Hamiltonian.

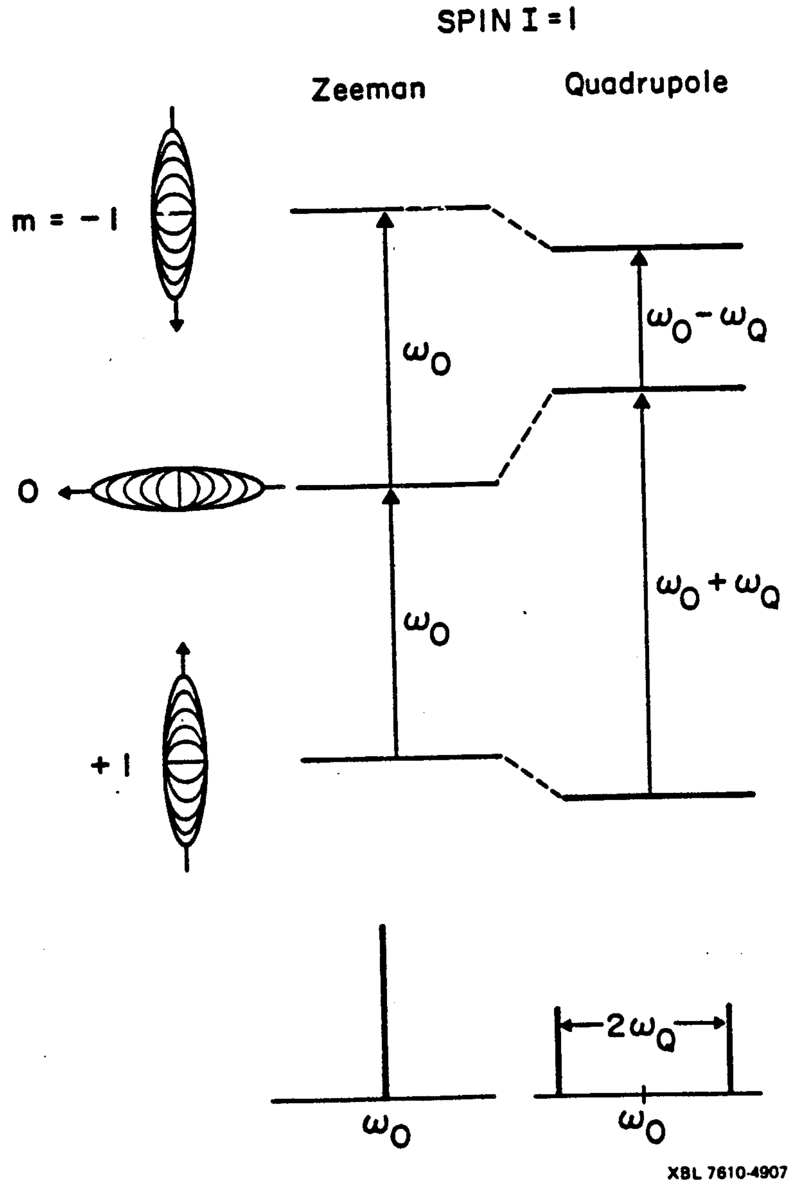
SPIN I = 1
Zeeman
Quadrupole
m = −1
0
+1
ω0
ω0
ω0 − ωQ
ω0 + ωQ
2ωQ
ω0
ω0
XBL 7610-4907

Figure 6. Energy level diagram of an oriented spin 1 nucleus. The interaction of a nuclear quadrupole moment with surrounding electric field gradients, results in a first order perturbation of the Zeeman Hamiltonian. The result is a splitting of the Zeeman resonance at ω_0 into a doublet.

However, the initial part of the fid may be unobservable since the preamplifier will be driven into saturation after the high power pulse and will require a finite time to recover.

An elegant solution to the problem is to produce a quadrupolar echo. Figure 7 is a schematic of the quadrupolar echo experiment. The spin system is first given a ninety degree pulse, and subsequently evolves under its internal Hamiltonian for a time τ. After the time τ a second ninety degree pulse is given where the phase of the of the irradiation is shifted ninety degrees relative to the first pulse. Further evolution occurs for a second period τ'. However, the evolution of the spin system during τ' is the reverse of the evolution during τ, and so at $\tau' = \tau$ the signal is without quadrupolar information. If the acquisition system is triggered at $\tau' = \tau$, and if after a time 2τ the preamplifier has recovered from saturation, the complete fid will be accurately recorded. Let us now describe the quadrupolar echo experiment quantitatively.

Suppose we have a system of noninteracting spin 1 particles. In general the density matrix may be expanded in as basis of $(2I + 1)^2$ operators. For $I = 1$ this is nine operators which includes the identity operator:

$$\rho(z) = \sum_{i=1}^{8} a_i(t) I_i + a_0 1 \qquad (4)$$

If the Hamiltonian is linear in spin operators, only three of these operators, I_x, I_y, and I_z, are relevant and are related by the commutation rules given by equation 43 of chapter 1. As a

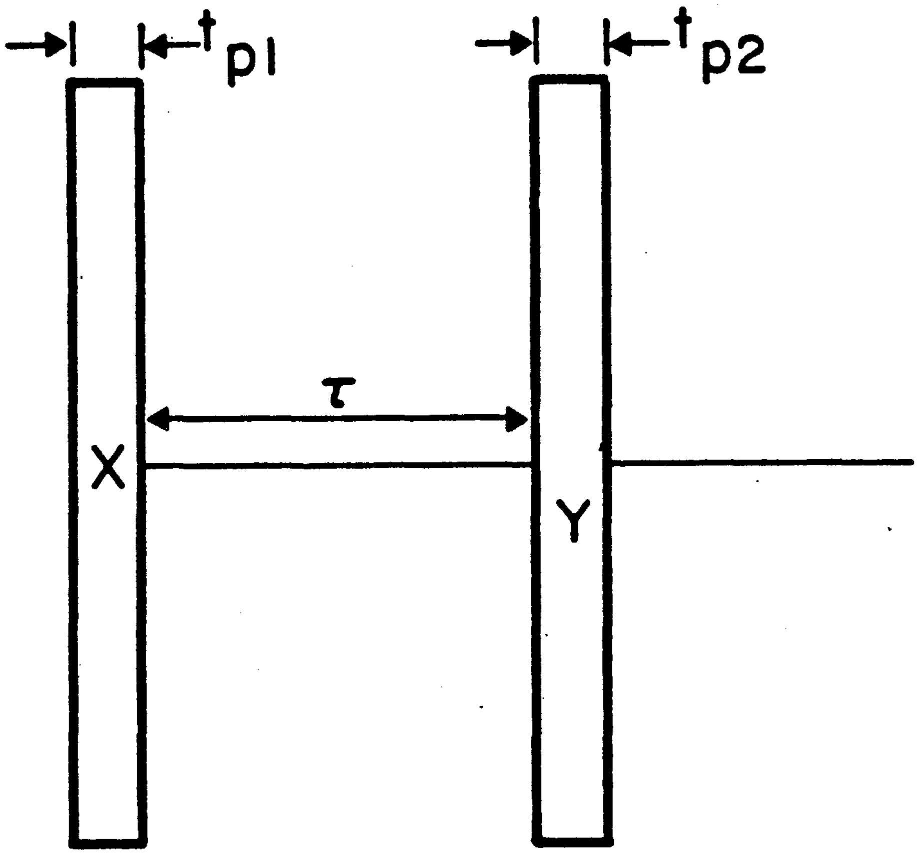

XBL 823-8597

Figure 7. A pulse sequence used to produce a quadrupolar echo. Assuming $\omega_1 >> \omega_Q$, the two pulses would be 90° pulses ($\omega_1 tp1$, $\omega_1 tp2 = \pi/2$). Then the density matrix after the x pulse is proportional to Iy1. Evolution under the quadrupolar Hamiltonian for a time T produces a coherent state described by a linear combination of Iy1 and Iy2. The second pulse is phase shifted relative to the first by 90° and echos Iy2 back to Iy1 at a time equal to 2τ.

result, the density matrix may be represented by a vector, and the effect of strong pulses irradiation may be represented as vector rotations. The effect of internal Hamiltonians in the absence of irradiation may also be represented as vector rotations, but only if those Hamiltonians are linear in spin operators. Once bilinear Hamiltonians are included, we require all $(2I+1)^2$ operators. Therefore, in a system of noninteracting spin 1 nuclei, 9 operators are required, including the identity operator. We are free to use any basis, but an especially convenient basis is related to I_x, I_y, and I_z by the relations:

$$\begin{array}{lll} I_{x,1} = \frac{1}{2}I_x & I_{y,1} = \frac{1}{2}I_y & I_{z,1} = \frac{1}{2}I_z \\ I_{x,2} = \frac{1}{2}(I_yI_z + I_zI_y) & I_{y,2} = \frac{1}{2}(I_zI_x + I_xI_z) & I_{z,2} = \frac{1}{2}(I_xI_y + I_yI_x) \\ I_{x,3} = \frac{1}{2}(I_z^2 - I_y^2) & I_{y,3} = \frac{1}{2}(I_x^2 - I_z^2) & I_{z,3} = \frac{1}{2}(I_y^2 - I_x^2) \end{array} \qquad (5)$$

Since there are nine operators, we must have the condition

$$I_{z,1} + I_{z,2} + I_{z,3} = 0 \quad . \qquad (6)$$

This set of operators was originally used to describe pure quadrupolar resonance (55), and has also been used to describe double quantum nmr in systems of noninteracting spin 1 nuclei (56, 51, 58). The convenience of this bases lies in the fact that $I_{p,1}$, $I_{p,2}$, and $I_{p,3}$ are related by the commutation rule

$$[I_{p,1}, I_{p,2}] = iI_{p,3} \text{ or cyclic permutation of } 1,2,3 \ . \qquad (7)$$

In other words the spin space has been divided into three subspaces, each spanned by a set of operators $I_{p,1}$, $I_{p,2}$, $I_{p,3}$. The operators of each set have transformation properties identical to spin $\frac{1}{2}$ operators due to the existence of the commutation relations given above. That is:

$$e^{-i\theta I_{p,1}} I_{p,2} \, e^{i\theta I_{p,1}} = I_{p,2}\cos\theta + I_{p,3}\sin\theta \quad . \qquad (8)$$

We are finally ready to describe the quadrupolar echo experiment. In Appendix 2.4 is listed the commutation relations and rotations that will be of use to us.

We begin by considering the form of the rotating frame Hamiltonian during the first pulse:

$$\mathcal{H} = -\Delta\omega I_z - \omega_1 I_x + \frac{1}{3}\omega_Q(3I_z^{\ 2} - I(I+1)) \quad . \qquad (9)$$

Converting to the new operator basis we get

$$\mathcal{H} = -2\Delta\omega I_{z,1} - 2\omega_1 I_{x,1} + \frac{2}{3}\omega_Q(I_{x,3} - I_{y,3}) \quad . \qquad (10)$$

For simplicity, let us assume that the irradiation is on resonance so $\Delta\omega = 0$. Then we get

$$\mathcal{H} = -2\omega_1, I_{x,1} + \frac{2}{3}\omega_Q(I_{x,3} + I_{y,3}) \quad . \qquad (11)$$

Now we make the assumption that during the pulse the Hamiltonian is $\mathcal{H} \sim -2\omega_1 I_{x,1}$ since $\omega_1 >> \omega_Q$. Since the initial density matrix is given by $\rho(0) \propto I_{z,1}$, the density matrix after the first pulse is given by:

$$\rho(t_{p1}+\tau) = e^{i(2\omega_1 I_{x,1})t_{\rho 1}} I_{z,1}\, e^{-i(2\omega_1 I_{x,1})t_{\rho 1}} \qquad (12)$$

$$= I_{z,1}\cos\omega_1 t_{\rho 1} + I_{y,1}\sin\omega_1 t_{\rho 1}$$

The spin system now is allowed to evolve under the Hamiltonian $\mathcal{H}_Q = \frac{2}{3}\omega_Q(I_{x,3} - I_{y,3})$ for a time τ. After a time τ the density matrix is given by

$$\rho(t_1+\tau) = e^{-i\frac{2}{3}\omega_Q(I_{x,3}-I_{y,3})} I_{z,1}\, e^{i\frac{2}{3}\omega_Q(I_{x,3}-I_{y,3})} \cos\omega_1 t_{\rho 1}$$

$$+ e^{-i\frac{2}{3}\omega_Q(I_{x,3}-I_{y,3})} I_{y,1}\, e^{i\frac{2}{3}\omega_Q(I_{x,3}-I_{y,3})} \sin\omega_1 t_{\rho 1} \quad .$$

(13)

The first term is unaffected since $[I_{z,1}, I_{x,3}-I_{y,3}] = 0$. To evaluate the second term we make the substitution

$$\frac{2}{3}\omega_Q(I_{x,3}-I_{y,3}) = \omega_Q I_{y,3} - \frac{\omega_Q}{3}(I_{z,3}-I_{x,3}) \qquad (14)$$

and realize that $[I_{y,1}, I_{z,3}-I_{x,3}] = 0$. We easily obtain the expression

$$e^{i\omega_Q I_{y,3}\tau} I_{y,1} e^{-i\omega_Q I_{y,3}\tau} = I_{y,1}\cos\omega_Q - I_{y,2}\sin\omega_Q\tau \quad .$$

(15)

So at the end of the first evolution time τ the density matrix is

$$\rho(t_{\rho 1}+\tau) = I_{z,1}\cos\omega_1 t_{\rho 1} + (I_{y,1}\cos\omega_Q\tau - I_{y,2}\sin\omega_Q\ )\sin\omega_1 t_{\rho 1} \quad . \qquad (16)$$

Now a second pulse is applied ninety degrees out of phase with the first pulse, and we must now evaluate the expression:

$$\rho(t_{\rho1} + \tau + t_{\rho2}) = e^{i2\omega_1 I_{y,1} t_{\rho2}} \rho(t_{\rho1} + \tau)\, e^{-i2\omega_1 I_{y,1} t_{\rho2}} \quad . \tag{17}$$

The first term becomes $(I_{z,1}\cos\omega_1 t_{\rho2} + I_{x,1}\sin\omega_1 t_{\rho2})\cos\omega_1 t_{\rho1}$. The second term contains $I_{y,1}$ so it is unaffected by the pulse. To obtain the third term we must evaluate the expression

$$e^{i2\omega_1 I_{y,1} t_{\rho2}}\, I_{y,2}\, e^{-i2\omega_1 I_{y,1} t_{\rho2}} = I_{y,2}\cos 2\omega_1 t_{\rho2} - I_{y,3}\sin 2\omega_1 t_{\rho2} \ . \tag{18}$$

The form of the density matrix at the conclusion of the second pulse is

$$\begin{aligned}\rho(t_{\rho1}+\tau+t_{\rho2}) = {} & (I_{z,1}\cos\omega_1 t_{\rho2} + I_{x,1}\sin\omega_1 t_{\rho2})\cos\omega_1 t_{\rho1} + I_{y,1}\cos\omega_Q\tau\sin\omega_1 t_{\rho1} \\ & + (I_{y,2}\cos 2\omega_1 t_{\rho2} - I_{y,3}\sin 2\omega_1 t_{\rho2})\sin\omega_Q\tau\ \sin\omega_1 t_{\rho1}) \quad .\end{aligned} \tag{19}$$

The spin system now evolves for a time τ' under the Hamiltonian

$$\begin{aligned}\mathcal{H} &= \frac{2}{3}\omega_Q(I_{x,3} - I_{y,3}) \qquad (20) \\ &= \omega_Q I_{x,3} - \frac{1}{3}\omega_Q(I_{y,3} - I_{z,3}) \\ &= \omega_Q I_{y,3} - \frac{1}{3}\omega_Q(I_{z,3} - I_{x,3}) \quad .\end{aligned}$$

The $I_{z,1}$ term is again unaffected since it commutes with the Hamiltonian, and the evolution of the $I_{x,1}$ term is obtained by evaluating

$$e^{-i\omega_Q I_{x,3}\tau'}\, I_{x,1}\, e^{i\omega_Q I_{x,3}\tau'} = I_{x,1}\cos\omega_Q\tau' + I_{x,2}\sin\omega_Q\tau' \quad . \tag{21}$$

The evolution of the $I_{y,1}$ and $I_{y,2}$ terms is given by the expressions

$$e^{i\omega_Q I_{y,3}\tau'} I_{y,1}\, e^{-i\omega_Q I_{y,3}\tau'} = I_{y,1}\cos\omega_Q\tau' + I_{y,2}\sin\omega_Q\tau' \qquad (22)$$

$$e^{i\omega_Q I_{y,3}\tau} I_{y,2}\, e^{-i\omega_Q I_{y,3}\tau'} = I_{y,2}\cos\omega_Q\tau' - I_{y,1}\sin\omega_Q\tau' \ . \qquad (23)$$

The $I_{y,3}$ term is unaffected since it commutes with $I_{x,3} - I_{z,3}$. So the final expression for the density matrix is

$$\begin{aligned}\rho(t_{\rho 1}+ \tau+t_{\rho 2}+ {}') = {} & I_{z,1}\cos\omega_1 t_{\rho 2}\cos\omega_1 t_{\rho 1} - I_{y,3}\sin 2\omega_1 t_{\rho 2}\sin\omega_Q\tau\sin\omega_1 t_{\rho 1} \\ & + (I_{x,1}\cos\omega_Q\tau' + I_{x,2}\sin\omega_Q\tau')\cos\omega_1 t_{\rho 1}\sin\omega_1 t_{\rho 2} \\ & + (I_{y,1}\cos\omega_Q\tau' + I_{y,2}\sin\omega_Q\tau')\cos\omega_Q\tau\sin\omega_1 t_{\rho 1} \\ & + (I_{y,2}\cos\omega_Q\tau' - I_{y,1}\sin\omega_Q\tau')\cos 2\omega_1 t_{\rho 2}\sin\omega_Q\tau\sin\omega_1 t_{\rho 1} \ .\end{aligned}$$

(24)

We consider the case of two ninety degree pulses, $\omega_1 t_{\rho 1} = \omega_1 t_{\rho 2} = \frac{\pi}{2}$,

$$\begin{aligned}\rho(t_{\rho 1}+\tau+t_{\rho 2}+\tau') = {} & I_{y,1}(\cos\omega_Q\tau'\cos\omega_Q\tau + \sin\omega_Q\tau'\sin\omega_Q\tau) \\ & + I_{y,2}(\cos\omega_Q\tau\sin\omega_Q\tau' - \cos\omega_Q\tau'\sin\omega_Q\tau) \qquad (25)\end{aligned}$$

and for $\tau = \tau'$ we get $\rho(t_{\rho 1} + t_{\rho 2} + 2\tau) = I_{y,1}$ (26)

We note that the density matrix $\rho(t_{\rho 1} + t_{\rho 2} + 2\tau)$ is identical to $\rho(t_{\rho 1})$ and subsequent evolution is identical to evolution after a single pulse.

We should also note that the phase shift is quite important for efficient echoing. Suppose the second pulse were in phase with

with the first pulse. The expression for the density matrix after the second pulse is

$$\rho(t_{\rho 1}+\tau+t_{\rho 2}) = e^{i2\omega_1, I_x t_{\rho 2}}(I_{y,1}\cos\omega_Q\tau - I_{y,2}\sin\omega_Q\tau)e^{-i2\omega_1, I_{x,1} t_{\rho 2}} \quad . \tag{27}$$

The $I_{y,1}$ term is

$$e^{i2\omega_1 I_{x,1} t_{\rho 2}} I_{y,1} e^{-i2\omega_1 I_{x,1} t_{\rho 2}} = I_{y,1}\cos\omega_1 t_{\rho 2} + I_{z,1}\sin\omega_1 t_{\rho 2} \quad . \tag{28}$$

and the $I_{y,2}$ term is

$$e^{i2\omega_1 I_{x,1} t_{\rho 2}} I_{y,2} e^{-i2\omega_1 I_{x,1} t_{\rho 2}} = I_{y,2}\cos\omega_1 t_{\rho 2} - I_{z,2}\sin\omega_1 t_{\rho 2} \quad . \tag{29}$$

If we assume that $\omega_1 t_{\rho 2} = \frac{\pi}{2}$ we get for the density matrix after the the second pulse

$$\rho(t_1+\tau+t_{\rho 2}) = I_{z,1}\cos\omega_Q\tau + I_{z,2}\sin\omega_Q\tau \tag{30}$$

We realize that there can be no echo since both terms commute with $I_{x,3}-I_{y,3}$. Thus, if the pulses are in phase the double quantum transition is pumped since $I_{z,2}$ is a double quantum operator.

2.4 Theory of the Orientational Dependence of the Quadrupolar Splitting in Smectic Phase Liquid Crystals

Having introduced the liquid crystalline mesophases of interest and having completed a study of quadrupolar echo spectroscopy, we are ready to develop a theory of the orientational dependence of the quadrupolar splitting in smectic phases. Of course, such a theory would apply equally to the chemical shift anisotropy or the dipolar interaction, so we will keep the notation quite general.

2.4.1 Smectic A

As we mentioned in chapter 1, spin interaction Hamiltonians may be written as scalar products of spherical tensors

$$\mathcal{H} = \sum_{\ell} \sum_{m=-\ell} (-)^m A_{\ell -m} T_{\ell, m} \tag{31}$$

where A is a tensor involving spin operators and T is a tensor involving interaction parameters.

Suppose T^p is the tensor in some principal axis system. We now obtain T in a molecular-fixed coordinate system by the expression

$$T^m_{\ell m} = \sum_{m'} T^p_{\ell m'} D^{(\ell)}_{m' m}(\Omega_0) \tag{32}$$

where $\Omega_0 = (\alpha_0, \beta_0, \gamma_0)$ are the Euler angles relating the principal axis system of T to a molecular-fixed coordinate system (see figure 8).

We now wish to transform T into a domain coordinate system in which the z axis is parallel to $\tilde{n}$, the director. However, this

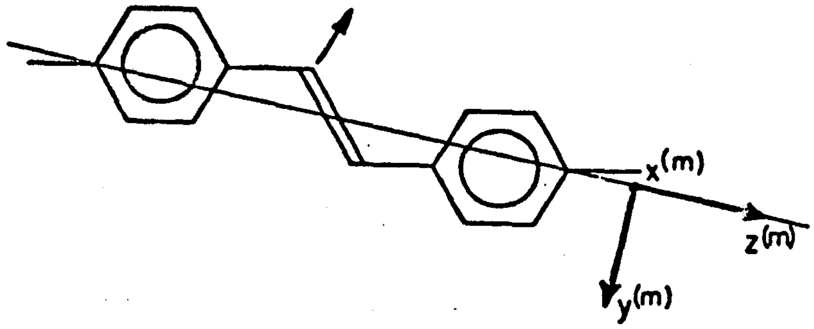

XBL757-6739

Figure 8. The molecular coordinate system of a liquid crystal (Xm,Ym,Zm). The arrow parallel to the C-D sigma bond axis indicates the z axis of the pas of the quadrupolar tensor. Zm is parallel to the "long axis" of the molecule. Xm is normal to the plane of the Schiff base linkage and Ym completes the right-handed coordinate system.

transformation must be averaged over all molecular orientations relative to $\tilde{n}$, since ordering is not perfect in a liquid crystalline phase. Therefore, we obtain

$$T^{d}_{\ell m} = \sum_{m'} \left(\sum_{q} T^{d}_{\ell q} D^{(\ell)}_{qm'}(\Omega_0)\right) \langle D^{(\ell)}_{m'm}(\Omega_1)\rangle \tag{33}$$

where $\langle D^{(\ell)}_{m'm}(\Omega_1)\rangle = \int d\Omega_1 P(\Omega_1) D^{(\ell)}_{m'm}(\Omega_1)$ (34)

and $P(\Omega_1)$ is the probability of a solid angle $\Omega_1 = (\alpha_1, \beta_1, \gamma_1)$ occuring between the molecular-fixed frame and the domain frame. Now $P(\Omega_1)$ may be expanded in terms of generalized spherical harmonics,

$$P(\Omega_1) = (8\pi^2)^{-1} \sum_{\ell kp} (2\ell+1)(-)^{k-p} C^{(\ell)}_{kp} D^{(\ell)}_{kp}(\Omega_1) \ . \tag{35}$$

If we substitute equations 34 and 35 into equation 33, and carry out the integration making use of the orthonormality property of Wigner rotation matrices and the relation

$$D^{(\ell)}_{kp}(\Omega) = (-)^{k-p} D^{(\ell)\,*}_{-k-p}(\Omega) \tag{36}$$

we obtain the result:

$$T^{d}_{\ell m} = \sum_{m'} \left(\sum_{q} T^{P}_{\ell q} D^{(\ell)}_{qm'}(\Omega_0)\right) (-)^{m} C^{(\ell)}_{-m'm}(\Omega_1) \quad . \tag{37}$$

The $C^{(\ell)}_{m'm}(\Omega_1)$'s are called complex motional constants or order parameters.

We will concern ourselves with second rank spherical tensors so $\ell = 2$. In general, we must have 25 motional constants since both m and m' vary integrally from -2 to 2. However, the smectic A phase is uniaxial and this requires that m = 0, since P must be independent of γ_1. Therefore we obtain

$$T^{d}_{20} = \sum_{m'} (\sum_{q} T^{p}_{2q} D^{(2)}_{qm'}(\Omega_0)) \; C^{(2)}_{-m'0}(\Omega_1) \quad . \qquad (38)$$

We conclude that in a uniaxial phase there are at most 5 order parameters. A further reduction in the number of order parameters may be achieved on the basis of molecular symmetry. If, for example, the molecule is linear, or rotates rapidly about its "long axis", P must be independent of α. Then $m' = 0$ and we get

$$T^{d}_{20} = \sum_{q} T^{p}_{2q} \; D^{(2)}_{q0}(\Omega_0) \; C^{(2)}_{0,0}(\Omega_1) \quad . \qquad (39)$$

If a smectic A or nematic liquid crystal is placed in a strong magnetic field, the molecules will align so that the director $\tilde{n}$ is parallel to the magnetic field. Then after truncation the Hamiltonian is

$$\mathcal{H} = A_{20}T^{d}_{20} = A_{20}(\sum_{q} T^{p}_{2q} \; D^{(2)}_{q0}(\Omega_0)) \; C^{(2)}_{0,0}(\Omega_1) \qquad (40)$$

where we have neglected the isotropic term $A_{00}T^{d}_{00}$.

If, however, the uniaxial liquid crystal is first aligned in a magnetic field and is then rotated through an angle β_2 (see figure 9) we obtain the expression

$$\mathcal{H} = A_{20}T^{L}_{20} = A_{20}T^{d}_{20}D^{(2)}_{00}(\Omega_2) \qquad (41)$$

$$= A_{20}(\sum_{q} T^{p}_{2q} \; D^{(2)}_{q0}(\Omega_0)) \; C^{(2)}_{00}(\Omega_1) \; D^{(2)}_{00}(\Omega_2)$$

where $(\Omega_2) = (0,\beta_2,0)$.

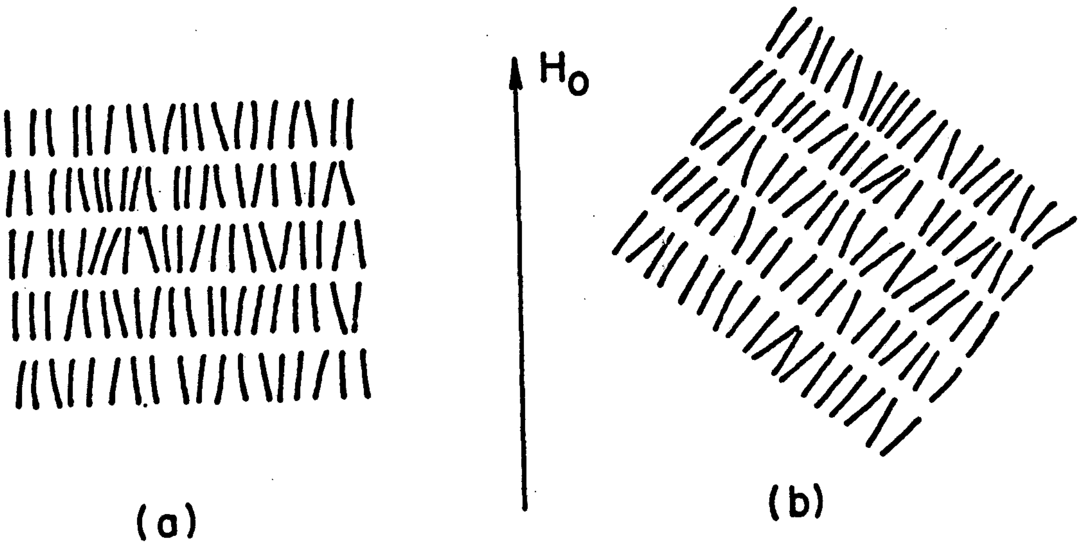

XBL 748-4010

Figure 9. Rotation of a smectic A liquid crystal. Given the uniaxial symmetry of the smectic A phase and assuming that the layer structure is preserved after the rotation, the quadrupolar splitting should be proportional to $3\cos^2\beta - 1$ where β is the angle between the z axis of the original laboratory frame (a) and the final laboratory frame (b).

2.4.2 Smectic C

We now describe a multidomain model of the smectic C phase in a strong magnetic field that will be used to simulate dmr spectra. Similar models were first proposed independently by Luz (41) and Wise (40), and later by Allison (59). The assumptions upon which multidomain models are based are:

(i) The molecules align with their long axes parallel to the magnetic field, but the smectic layers, rather than being normal to the magnetic field, are tilted.

(ii) The azimuthal distribution of molecular domains about the magnetic field direction is random (see figure 10).

(iii) If the sample is rotated, the domain structure is maintained, but molecules reorient in such a way as to minimize their magnetic energy ($-H.\chi.H$) while maintaining their tilt angle and orientation relative to one another. Since the subsequent angle between molecular long axes and the magnetic field is not the same for all domains, there will result a distribution of molecular orientations (see figure 11).

The maintenance of domain structure after sample rotation is supported by nmr (40,41) and esr (60) evidence while the reorientation of molecules on a cone is supported by magnetic torque studies (61).

The model involves six coordinate systems and five transformations. As in the last section, we will rotate from the principal axis system to the laboratory-fixed coordinate system. As before, the Hamiltonian is written as a scalar product of spherical tensor operators

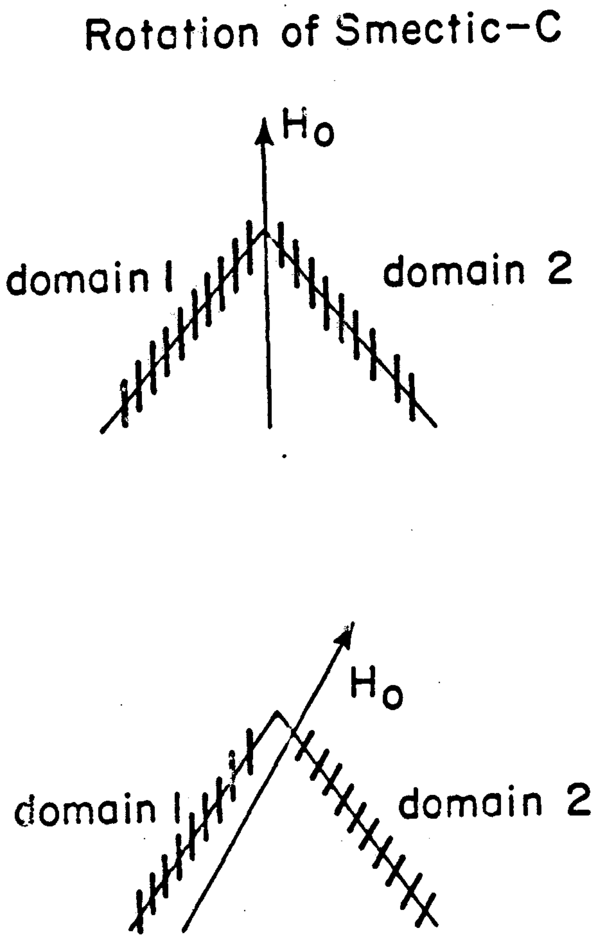
Rotation of Smectic-C
H_0
domain 1
domain 2
H_0
domain 1
domain 2

XBL 751-5494

Figure 10. Multidomain structure of a smectic C liquid crystal. The domains are oriented on a cone about the direction of H_0. The angle between the layer normal and the molecular long axis is the tilt angle. Rotation of smectic C phase preserves the domain structure, but molecular reorientation occurs within each domain in order to minimize magnetic energy while preserving the tilt angle.

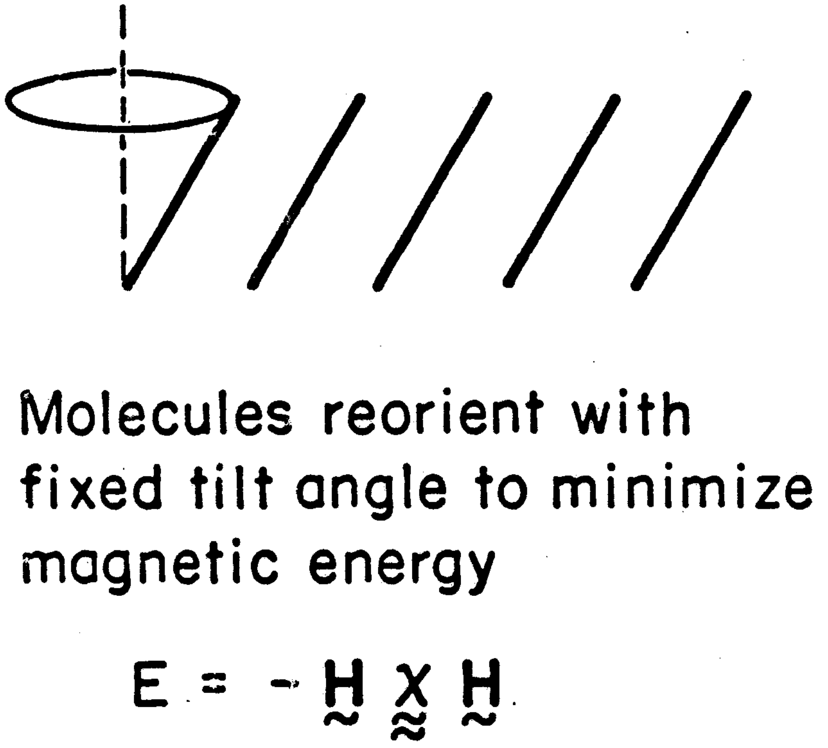
Molecules reorient with fixed tilt angle to minimize magnetic energy
$E = -\underset{\sim}{H}\,\underset{\approx}{\chi}\,\underset{\sim}{H}$

XBL 751-5493

Figure 11. Detail of molecular reorientation within a domain after rotation of a smectic c phase. Assuming preservation of the multidomain structure, molecules within a given domain will assume a position on a cone that minimizes the magnetic energy $E = -\underset{\sim}{H}\cdot\underset{\approx}{\chi}\cdot\underset{\sim}{H}$ while preserving the tilt angle.

$$\mathcal{H} = \sum_{\ell} \sum_{m=-\ell}^{\ell} (-)^m A_{\ell-m} T_{\ell m} \tag{42}$$

with A and T defined as before. We wish to rotate T from its principal axes system, through a molecular-fixed frame, into the director frame. The expression for T^d is identical to equation 7 of the preceding section:

$$T^{dir}_{m} = \sum_{n'} \left(\sum_{q} T^{pas}_{\ell q} D^{(\ell)}_{qn}(\Omega_0)\right) (-)^m C^{(\ell)}_{-nm}(\Omega_1) \quad . \tag{43}$$

We next rotate into the domain-fixed coordinate system or the domain frame. The z axis is normal to the plane of the layer while the y axis points radially away from the direction of axis of radial symmetry of the domain, and the direction of x defines a right-handed coordinate system

$$T^{dom}_{\ell p} = \sum_{m} T^{dir}_{\ell m} D^{(\ell)}_{mp}(\Omega_2) \tag{44}$$

$$= \sum_{mm'q} T^{pas}_{\ell q} D^{(\ell)}_{qn'}(\Omega_0)(-)^m C^{(\ell)}_{-n'm}(\Omega_1) D^{(\ell)}_{mp}(\Omega_2)$$

where $\Omega_2 = (0_2, \beta_2, \gamma_2)$. β_2 is the tilt angle and γ_2 specifies the position of the cone.

The next rotation is from the domain frame to the initial laboratory frame of the unrotated aligned sample (see figure 12). The expression is

$$T^{i\ell ab}_{\ell r} = \sum_{mnpq} (-)^m T^{pas}_{\ell q} D^{(\ell)}_{qn}(\Omega_0) C^{(\ell)}_{-nm}(\Omega_1) D^{(\ell)}_{mp}(\Omega_2) D^{(\ell)}_{pr}(\Omega_3) \tag{45}$$

where $\Omega_3 = (0, \beta_3, \gamma_3)$ and $\beta_3 = \beta_2$ and γ_3 specifies the domain.

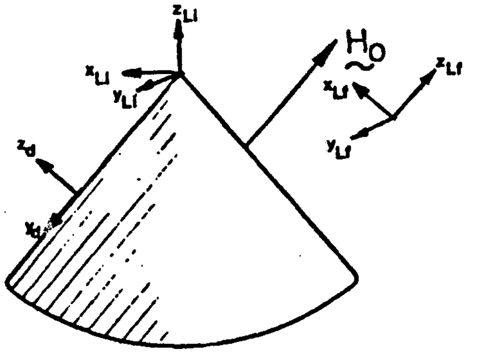

XBL 757-6747

Figure 12. Relationship between the domain coordinate system and the initial and final laboratory frames. The z axis of the domain frame is parallel to the layer normal, the y axis lies within a plane of symmetry of the cone and the x axis completes a right-handed coordinate system. The domain frame (x_d, y_d, z_d) is related to the initial lab frame (x_{Li}, y_{Li}, z_{Li}) by the Euler angles (0, β_3, γ_3) where β_3 is the tilt angle and γ_3 specifies the domain. The initial lab frame is related to the final lab frame (x_{Lf}, y_{Lf}, z_{Lf}) by the Euler angles (0, β_4, 0) where β_4 is the sample rotation. Z_{Lf} is parallel to H_0.

The final rotation is from the initial laboratory frame to the final laboratory frame. This frame has the magnetic field direction as the z axis (see figure 12). The expression is

$$T_{\ell s}^{\ell ab} = \sum_{mnpqr} (-)^{m} T_{\ell q}^{pas} D_{qn}^{(\ell)}(\Omega_0) C_{-nm}^{(\ell)}(\Omega_1) D_{mp}^{(\ell)}(\Omega_2) D_{pr}^{(\ell)}(\Omega_3) D_{rs}^{(\ell)}(\Omega_4) \tag{46}$$

where $(\Omega_4) = (0,\beta_4,0)$ and β_4 is the rotation angle. Again, we are only interested in a second rank tensor so $\ell = 2$. Truncation of the Hamiltonian leads us to consider only the $T_{20}^{\ell ab}$ component:

$$T_{20}^{\ell ab} = \sum_{mnpqr} (-)^{m} T_{2q}^{pas} D_{qn}^{(2)}(\Omega_0) C_{-nm}^{(2)}(\Omega_1) D_{mp}^{(2)}(\Omega_2) D_{pr}^{(2)}(\Omega_3) D_{ro}^{(2)}(\Omega_4) \quad . \tag{47}$$

Combining equation 47 with equation 42 we obtain the final expression for the Hamiltonian:

$$\mathcal{H} = A_{20} \sum_{mnpqr} (-)^{m} T_{2q}^{pas} D_{qn}^{(2)}(\Omega_0) C_{-nm}^{(2)}(\Omega_1) D_{mp}^{(2)}(\Omega_2) D_{pr}^{(2)}(\Omega_3) D_{ro}^{(2)}(\Omega_4) \quad . \tag{48}$$

In order for equation 48 to be of use to us in calculating nmr spectra, we need to determine the number of order parameters required by the symmetry of the smectic C phase. We also need to determine the position of a molecule on a cone (γ_2) as a function of the tilt angle (β_2), the domain (γ_3), and the rotation angle (γ_4).

In appendix 1 of this chapter we will rigorously derive the number of order parameters required by the symmetry of the smectic C phase. For our present purposes it is sufficient to make the following simplification. Let us assume that liquid crystal molecules are of low symmetry and so no simplification of the order tensor is possible. We rewrite equation 49 as:

$$\mathcal{H} = A_{20} \sum_{mpr} (-)^m Q_m^{(2)}(\Omega_0,\Omega_1) D_{mp}^{(2)}(\Omega_2) D_{pr}^{(2)}(\Omega_3) D_{ro}^{(2)}(\Omega_4) \qquad (50)$$

where

$$Q_m^{(2)}(\Omega_0,\Omega_1) = \sum_{qn} T_{2q}^{pas} D_{qn}^{(2)}(\Omega_0) C_{-nm}^{(2)}(\Omega_1) \ . \qquad (51)$$

The assumption that we wish to make is that the only term that we will retain in equation 50 is $Q_0^{(2)}(\Omega_0,\Omega_1)$. This simplification, which has been used in earlier studies (41, 47, 51), means that the biaxial order parameters are much smaller than the uniaxial order parameters and so the symmetry of the ordering may be approximated as cylindrical. Biaxial order parameters have not been extensively studied, however, Bos et.al. (45) report values better than an order of magnitude smaller than the uniaxial ordering. Therefore, we rewrite equation 50 as

$$\mathcal{H} = A_{20} \sum_{pr} Q_0^{(2)}(\Omega_0\Omega_1) D_{op}^{(2)}(\Omega_2) D_{pr}^{(2)}(\Omega_3) D_{ro}^{(2)}(\Omega_4) \ . \qquad (52)$$

It remains to determine the molecular orientation within a given domain (γ_2) as a function of the tilt angle (β_2), domain (γ_3), and rotation angle (β_4). It should be noted that reorientation in a liquid crystal is a cooperative effect, since it is done to minimize the magnetic energy

$$E = -H \cdot \chi \cdot H \ . \qquad (53)$$

Therefore the reorientation as specified by γ_2 is a domain reorientation. We emphasize that intermolecular orientations do not change (i.e. $\alpha_2 = 0$), since intermolecular interactions are much greater than magnetic interactions. We determine γ_2 in terms of β_2, γ_3, and β_4 by writing the magnetic energy in terms of γ_2, β_2, γ_3, and β_4

$$E = E(\beta_2, \gamma_2, \gamma_3, \beta_4) \tag{54}$$

and extremizing E with respect to γ_2,

$$\frac{\partial E}{\partial \gamma_2} = 0 \quad .$$

The value of γ_2 that yields the extreme magnetic for given β_2, γ_3, and β_4 is obtained by solving equation 55 for γ_2. E is a minimum if for the given β_2, γ_2, γ_3, and β_4.

$$\frac{\partial^2 E}{\partial \gamma^2} > 0 \quad . \tag{56}$$

We begin by assuming that the z axis of the magnetic susceptibility tensor is parallel to the z axis of the director frame. We write an expression for the magnetic energy with χ and H^2 in the spherical tensor form

$$E = -\sum_{\ell}\sum_{n}(-)^n (H^2)_{\ell n}\chi_{\ell -n} \quad . \tag{57}$$

It will be shown in appendix 2 of this chapter that in the director frame the magnetic energy is

$$E = - |H|^2 (\frac{1}{\sqrt{3}} \chi_{00} + \frac{1}{\sqrt{6}} \chi_{20} - \frac{1}{2}(\chi_{22} + \chi_{2-2})) -$$

$$(H_{10})^2 (\sqrt{\frac{3}{2}} \chi_{20} - \frac{1}{2}(\chi_{22} + \chi_{2-2})) -$$

$$(H_{11} + H_{1-1})^2 \; (\frac{1}{2}(\chi_{22} + \chi_{2-2})) \quad . \tag{58}$$

$H_{1,n}$ is the first rank magnetic field tensor in the director frame. If we again approximate the symmetry as cylindrical then we get

$$E \approx - \frac{1}{\sqrt{3}} |H|^2 \chi_{00} - \frac{1}{\sqrt{6}} (3(H_{10})^2 - |H|^2)\chi_{20} \quad . \tag{59}$$

The only term dependent on γ_2 is H_{10}. Therefore

$$\frac{\partial E}{\partial \gamma_2} = - \sqrt{6}\, H_{10} \frac{\partial H_{10}}{\partial \gamma_2} \chi_{20} \tag{60}$$

For an extremum the condition is

$$\frac{\partial E}{\partial \gamma_2} = 0 \text{ or } \frac{\partial H_{10}}{\partial \gamma_2} = 0 \quad . \tag{61}$$

Now H_{10} is related to H in the laboratory frame (H_{10}^{lab}) by the transformation

$$H_{10}^{dir} = \sum_{mn} H_{10}^{lab} D_{om}^{(1)}(-\Omega_4) D_{mn}^{(1)}(-\Omega_3) D_{no}^{(1)}(-\Omega_2) \tag{62}$$

where $-\Omega_2 = (-\gamma_2, -\beta_2, 0)$. $-\Omega_3 = (-\gamma_3, -\beta_2, 0)$, $-\Omega_4 = (0, -\beta_4, 0)$.

In appendix 2 it will also be shown that equation 62 leads to

$$H_{10}^{dir} = \sum_{mn} (in, H_{10}^{lab} d_{om}^{(1)}(-\beta_4) d_{mn}^{(1)}(-\beta_2) d_{no}^{(1)}(-\beta_2) e^{i(n\gamma_2+m\gamma_3)} \quad . \tag{63}$$

Equating equation 63 to zero and solving for γ_2 yields after some algebra (see appendix 2)

$$\gamma_2 = \tan^{-1}\left(-\left(\frac{\sin\beta_4 \sin\gamma_3}{\sin\beta_2\cos\beta_4 + \cos\beta_2\sin\beta_4\cos\gamma_3}\right)\right) \quad . \tag{64}$$

Therefore, assuming approximately cylindrical symmetry in the director frame, the dmr spectrum for a given domain, tilt angle, and sample rotation may be obtained from equation 52 and the condition given by equation 64. The value $Q_0^{(2)}(\Omega_0,\Omega_1)$ may be obtained by normalizing to the dmr spectrum at zero rotation.

2.5 Experimental Results and Discussion

2.5.1 "nom" Liquid Crystals

The liquid crystals that we chose to study were selected from a series called benzylidineanilines (figure 13). These compounds are of interest since they are known to possess several mesomorphic phases at reasonably low temperatures. The members of the series chosen were

N-(p-pentoxybenzylidine)-p-n-heptyaniline (507)

N-(p-heptyloxybenzylidine)-p-n-pentylaniline (705).

Each compound is known to possess 5 mesomorphic phases. The transition energies, entropies, and temperatures have been reported in the literature using differential scanning calorimetry, and some of the ranges for the various phases are given in table 1.

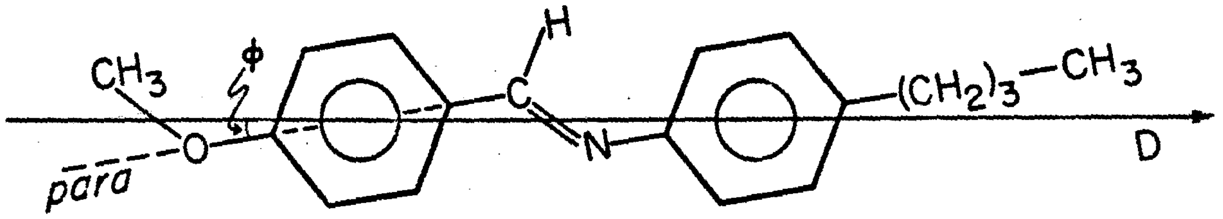
CH3
ϕ
H
C
N
(CH2)3—CH3
O
para
D

XRL 752-5832

Figure 13. MBBA. An example of a "nom" liquid crystal.

2.5.2 Chemical Synthesis

Each liquid crystal was deuterated at the methine position. The synthesis was accomplished in three steps. We will describe the synthesis of monodeuterated 705. The synthesis of 507 is analogous.

a) 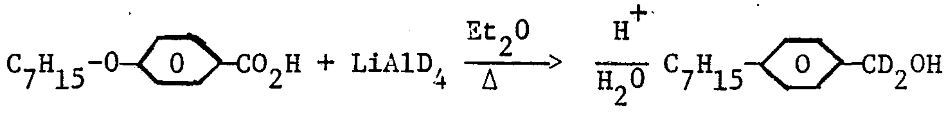

In a 500 ml flask, under nitrogen, 1.17 gm (28 mmoles) of lithium aluminum deuteride were added to 100 ml of dry ether. 4-heptyloxybenzoic acid in 150 ml dry ether was added dropwise with stirring. The mixture was refluxed for 2 hours. The reaction was quenched with dilute sulphuric acid and worked up in a standard manner. The deuterated alcohol was recrystallized in aqueous ethanol. The melting point was 45-46°C. The literature value is 48°C (63).

b) 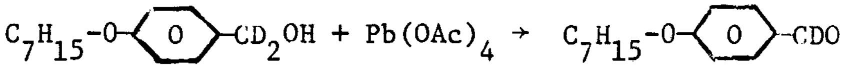

In a 300 ml flask, 2.80 gm (12.5 mmole) of 4-heptylaxybenzyl-d_2 alcohol were mixed with 65 ml of pyridine. 5.54 gm (12.5 mmole) of lead tetraacetate were added and the mixture was stirred overnight. Most of the pyridine was removed by rotary evaporation. The residue was stirred with 150 ml of ether and filtered, and the the mixture was distilled after removal of the ether by a bulb-to-bulb apparatus at approximately .1 mm from 115°-120°C. The yield was 2.01 gm (~76%).

c)

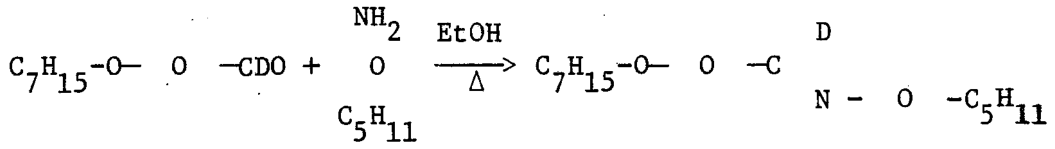

$$C_7H_{15}\text{-O-}\ \text{O}\ \text{-CDO} + \underset{C_5H_{11}}{\overset{NH_2}{\text{O}}} \xrightarrow[\Delta]{\text{EtOH}} C_7H_{15}\text{-O-}\ \text{O}\ \text{-C}\overset{\text{D}}{\underset{\text{N - O -}C_5H_{11}}{}}$$

1.00 gm (4.5 mmole) of 4-heptyloxybenzaldehyde-d_1 and .74 gm (4.5 mmole) of 4-pentylaniline (Kodak) were refluxed in 10 ml of absolute ethanol overnight and recrystallized in 95% ethanol. The yield was 1.00 gm (~60%). Measured transition temperatures are compared to literature values in table 1. A mass spectrum indicated 98% deuteration.

Table 2.1 Mesomorphic Transition Temperatures : 705

	S_4-S_3	S_3-S_2	S_2-S_1	S_1-N	N-I
Literature	58.0	64.4	68.3	79.6	83.2
Found	57.2	63.0	67.6	78.9	82.5

2.5.3 Experimental Methods

Approximately .7 gm of the liquid crystal were sealed under vacuum in pyrex tubes (00 = 8 mn) after three or four freeze-pump-thaw cycles. The pyrex tubes were cut to a length of about 12 mm.

The nmr probe was of the type shown in figure 14. The probe was of a double coil arrangement where the deuterium coil was of a solenoidal type and the proton decoupling coil was of the Helmholtz type, Tuning was performed with a high power series capacitor and matching to 50 ohms was done with low power capacitors to ground.

Sample orientation was controlled by a goniometer which consisted of a vertical shift passing through the base and

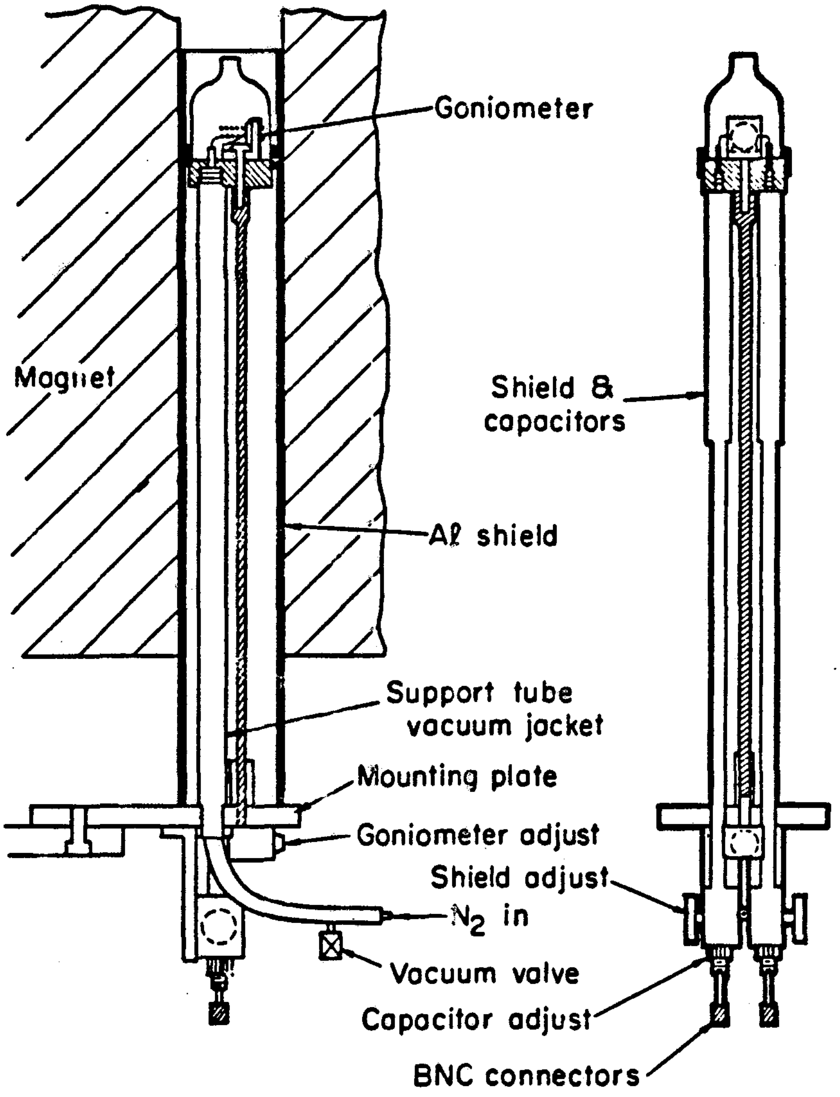
Goniometer
Magnet
Shield &
capacitors
Aℓ shield
Support tube
vacuum jacket
Mounting plate
Goniometer adjust
Shield adjust
N_2 in
Vacuum valve
Capacitor adjust
BNC connectors

XBL738-3691

Figure 14. A schematic of the nmr probe used in the study of two nom liquid crystals. Sample rotation was effected by turning a goniometer which rotated a worm screw through a miter gear set. The screw in turn rotated a worm wheel to which was attached the liquid crystal sample.

attached to a worm gear. The worm gear is rotated by two gears which turn the gear wheel mounting the sample. Rotation was precise to about 1°.

Temperature was controlled to within .1°C by a two stage heating system. Dry nitrogen was preheated and sent through an evacuated stainless steel transfer line. At the top of the transfer tube was a second auxiliary heater. Temperature was monitored by a copper-constantan thermocouple mounted near the sample, and the entire probe head was enclosed by a glass dewar. The thermocouple voltage was amplified and sent to a comparator amplifier which output a voltage proportional to the difference between the thermocouple voltage and a reference voltage.

DMR spectra were obtained on a homebuilt spectrometer which has been described in detail elsewhere (57,65). The magnet was a 24 kGauss superconducting system. The deuterium frequency was 16.33 Mhz and the proton frequency was 106 Mhz. The procedure for obtaining spectra was as follows. A liquid crystal sample was aligned in the magnetic field by being heated to its isotropic phase and then being very slowly cooled to the nematic phase where it was allowed to equilibrate for about 1 hour. The sample was then slowly cooled to the desired temperature, allowed to equilibrate for about another hour, and then rotated to the desired angle. Free induction decays were obtained using the quadrupolar echo pulse sequence described in section 2,3 with high power proton decoupling. The decay signals were digitized at a rate of 200 khz, and approximately 200 shots were averaged together to increase the signal to noise ratio. The 1024 point

FID was then Fourier transformed by a PDP 8E minicomputer and plotted.

2.5.4 Phase Transitions

The separation between quadrupolar satellites was observed versus temperature for both 507 and 705. The results are shown in figures 15 and 16. In both phase diagrams the transition temperatures are lower than measured by thermal microscopy by 1-2°C. This is not surprising since the thermocouple was separated from the sample by about 1 cm. We will make a few comments on the five phase transitions observed.

a) Isotropic-Nematic (I-N) Transition

For 507, the I-N transition occurred at about 74.8°C and for 705 occurred at about 80.9°C. The coexistence of two phases at the transition, indicated by an isotropic line at zero frequency, superimposed on a quadrupolar spectrum, established the transition as first order, an observation predicted by various mean field theories (66,67).

b) Nematic-S_1 (N-S_1) Transition

Texture studies (62) have established the S_1 as a smectic A phase. The first order phase transition occurred at about 63.6°C in 507 and 77.5°C in 705.

c) Smectic A-S_2 Transition

Texture studies (62) indicate that the S_2 phase is smectic C. We observed no discontinuity in the quadrupolar splitting between the smectic A and the smectic C phase. Discontinuities in the slope of ω_Q versus temperature were observed at 53°C for 507 and

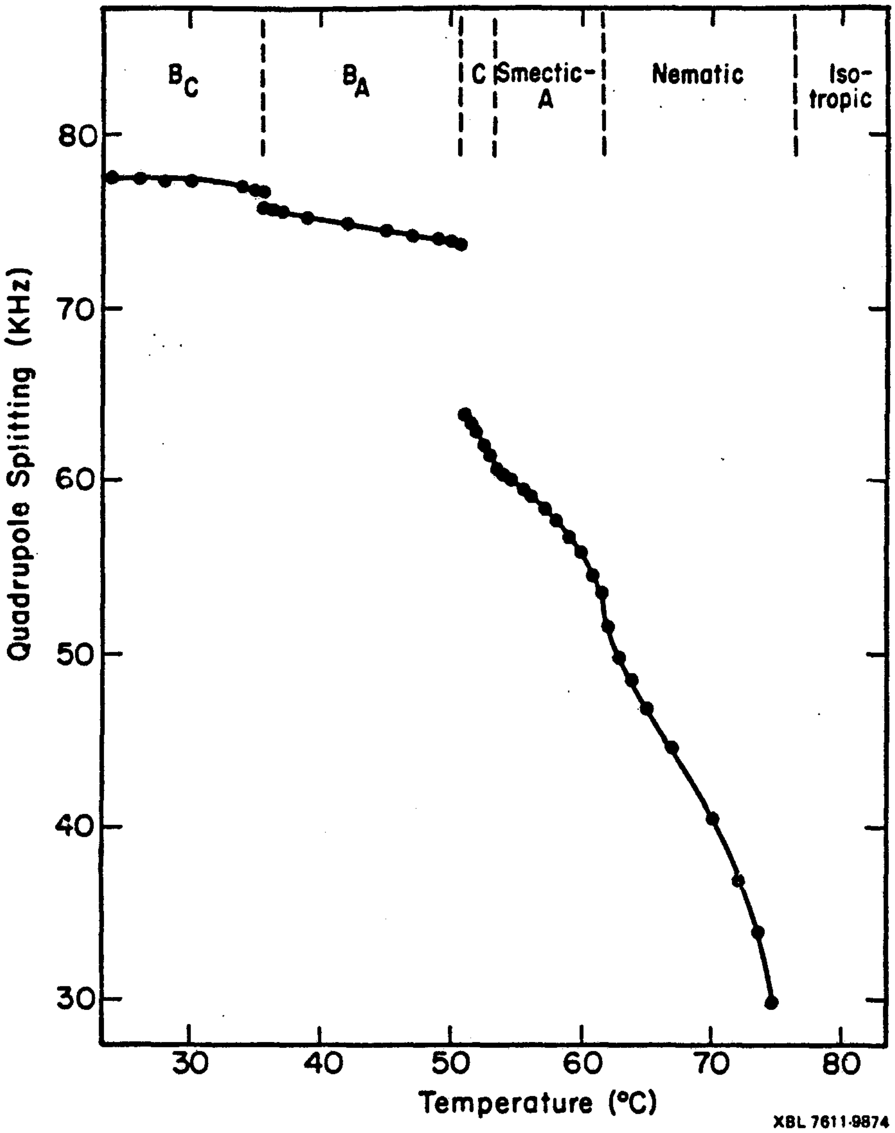

Figure 15. The quadrupolar splitting ($2\omega_Q$) vs. temperature for 507. The discontinuities in $2\omega_Q$ at about 76°C, 61°C, 51°C, and 37°C are first order phase transitions between the various mesomorphic phases. The discontinuity in the slope at about 53°C is the second order phase transition between the smectic A and the smectic C phases.

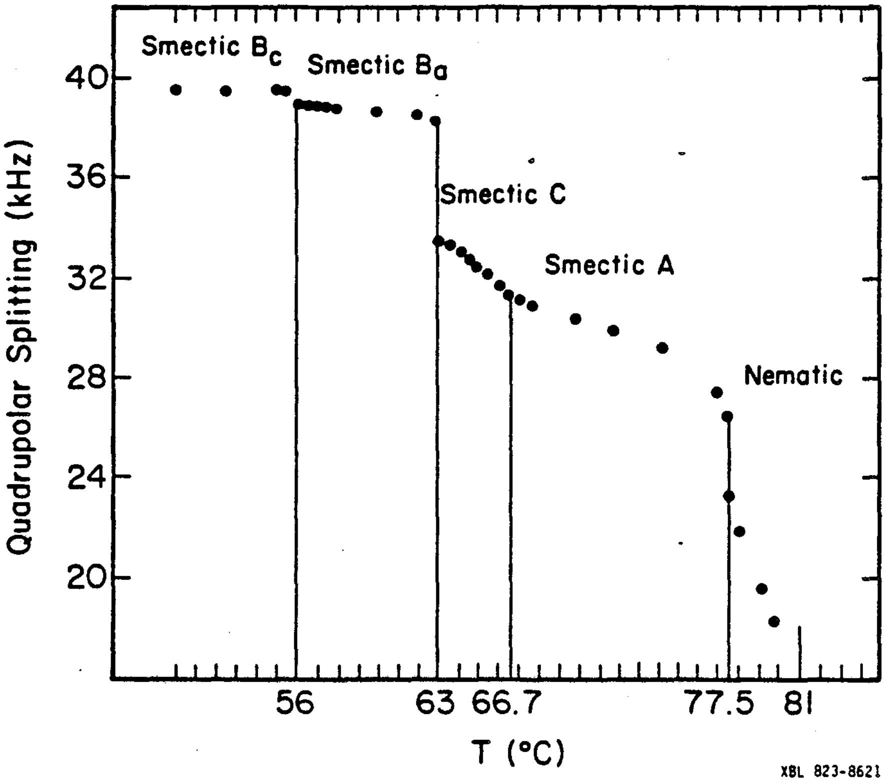

Figure 16. Same as Figure 15 except for the nom liquid crystal 705.

and 66.7°C for 705. The lack of discontinuity in the quadrupolar splitting indicates either a very small first order transition or a second order transition. A second order smectic A - smectic C (S_A - S_C) phase transition is predicted by a deGenne-Landau theory (68) and several mean field theories (68,69,70,71,72). We will study the nature of this phase transition in some detail in a later section.

d) Smectic C-S_3

This large first order transition occurred at 51°C for 507 and 63°C for 705. In a later section we will show that the S_3 phase is an untilted smectic phase, establishing it as smectic B_A. The order of the transition is predicted by a mean field theory (70).

e) Smectic B_A-S_4

In a later section we will show that the S_4 phase is a tilted smectic phase, which we identify as smectic B_C. At the time that this work was done, a study of the smectic B_A-B_C transition had not been reported in the literature. A texture study (62) did not establish the phase as tilted, but an x-ray diffraction study later appeared that supported our finding that S_4 is a B_C phase (74). From figures 18 and 19, we observe that the B_A-B_C transition is first order and appears at 32°C for 507 and at about 56°C for 705. The first order character of this transition is also supported by differential scanning calorimetry studies (62,74) and magnetic anisotropy studies (75).

The above observation is interesting for the following reasons.

The nature of the molecular interactions that stabilize the various mesomorphic phases has been of great interest to theoreticians and experimentalists. It is known that the high temperature uniaxial phases (nematic and smectic A) are stabilized by van der Waals interactions, but the nature of the interactions in the tilted, biaxial phases is less clear.

McMillian (69) has proposed a mean field theory for the smectic A to smectic C transition that assumes that molecules are free to rotate about their long axes in the smectic A phase. However, once smectic A order is established, there occurs a rotational freeze-out. The theory then states that once rotational motion begins to freeze out, the molecules will tilt relative to the smectic planes in order to minimize the energy of interaction of the "outboard" electric dipole moments (see figure 17). The model was specifically applied to TBBA, which has two antiparallel dipoles associated with the azoxy moieties. Later, the theory was extended to include the smectic B phases (70).

The latter theory yields three order parameters:

a) a translational order parameter α

b) a tilt order parameter β

c) a cross term γ, which correlates the two types of order.

The various smectic phases are described as follows:

a) smectic A $\alpha=\beta=\gamma=0$

b) smectic B_A $\beta=\gamma=0$, $\alpha\neq0$

c) smectic B_C $\alpha\neq0$, $\beta\neq0$, $\gamma\neq0$

d) smectic C $\alpha=\gamma=0$. $\beta\neq0$.

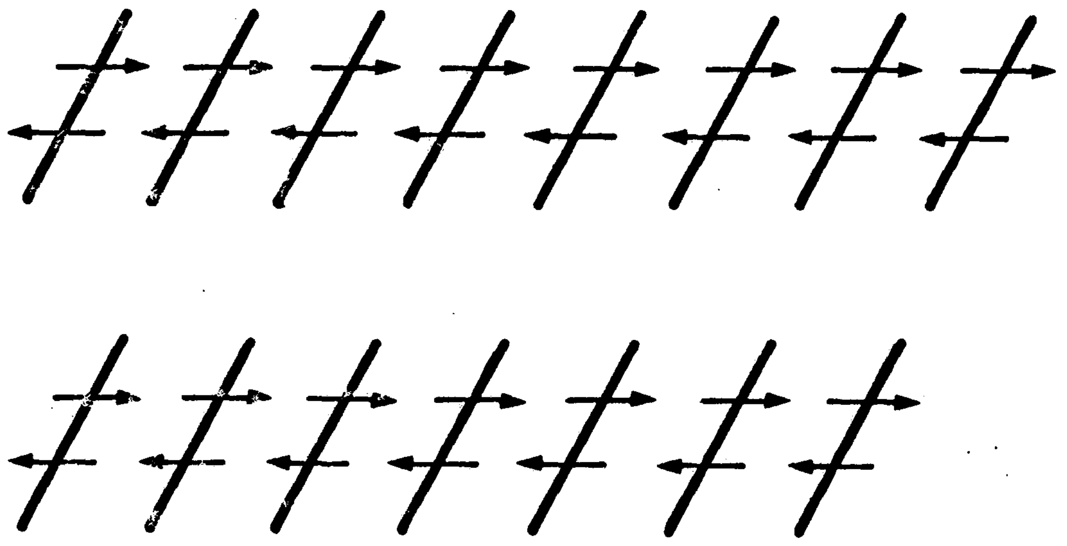

XBL 751-5436

Figure 17. Detail of McMillian's model for smectic C phase formation in TBBA. After the establishment of smectic A order, molecules tilt in the layer in order to minimize the energy of interaction between the outboard electric dipolar moments. This model assumes a rotational "freeze-out" in the smectic C phase.

The orders of the various phase transitions are unambiguously defined as

a) S_A-S_C second order

b) S_C-S_{BA} first order

c) S_C-S_{BC} first order

d) S_{BA}-S_{BC} second order .

Experimental studies of the smectic B_C phase in TBBA have not agreed as to the validity of McMillian's theory. Interpretations of x-ray diffraction data tend to support the idea of rotational freeze-out in the smectic B_C (32), while nmr data (42) and quasi-elastic neutron scattering studies (76,77) have indicated that molecular rotation is not "frozen out". It should be noted that TBBA has an S_A-S_C transition which appears to be second order and an S_C-S_{BC} transition which is first order, facts which agree with McMillian's theory. TBBA does not possess a smectic B_A phase.

Our studies indicate that McMillian's theory is inadequate in that it incorrectly assigns to the S_{BA}-S_{BC} transition, second order character. Our data clearly indicate that the transition is first order. There have appeared in the literature mean field theories that do not postulate a rotational freeze-out in the smectic C, and in particular, a theory due to Carib (73) develops a smectic C potential based upon the interaction of the axial components of the outboard dipoles. Therefore the molecules are free to rotate about their long axes in the smectic C phase. Carib concludes that the S_A-S_C transition may be first or second order depending upon the parameters of the theory. It would be interesting to see this theory extended to include translational ordering, but this has not appeared in the literature to out knowledge.

2.5.5 DMR Spectra of Rotated Smectic Samples

a) Smectic A

DMR spectra were obtained of the aligned smectic A phases of the 507 and 705 for sample rotations varying between 0 and 90°. Figure 18 shows a typical series of spectra taken of 507 at 55.2°C for rotations between 0° and 90°. (Half of the spectrum is shown). In figure 19 is shown a plot of the quadrupolar splitting (V_Q) vs. rotation angle. The solid line is $3\cos^2\theta-1$, the functional dependence predicted by the model. The qualitative features of the spectra are easily explained by the model. As the sample is rotated from 0°, the lines broaden due to imperefct alignment of the molecular long axes. At small rotation angles (<24°) the lines are asymmetric since $3\cos^2\theta-1$ is quite nonlinear for those angles. For angles between 30° and 80°, the lines are broad and symmetric since $3\cos^2\theta-1$ is almost linear and of maximum slope. At 54° the quadrupolar spliting is zero since the molecules are rotating rapidly at the "magic angle". From 80° to 90° the lines become narrower but more asymmetric. At 90°, the quadrupolar splitting is $\frac{1}{2}$ of its original value.

b) Smectic C

DMR spectra were also obtained of the aligned smectic C phases of 507 and 705 for sample rotations varying between 0° and 90°. Figures 21, 22, and 23 show smectic C spectra for small sample rotations at 52.8°C, 52.2°C, and 51.7°C. The behavior of smectic C behavior differs markedly from smectic A behavior shown in figure 20.

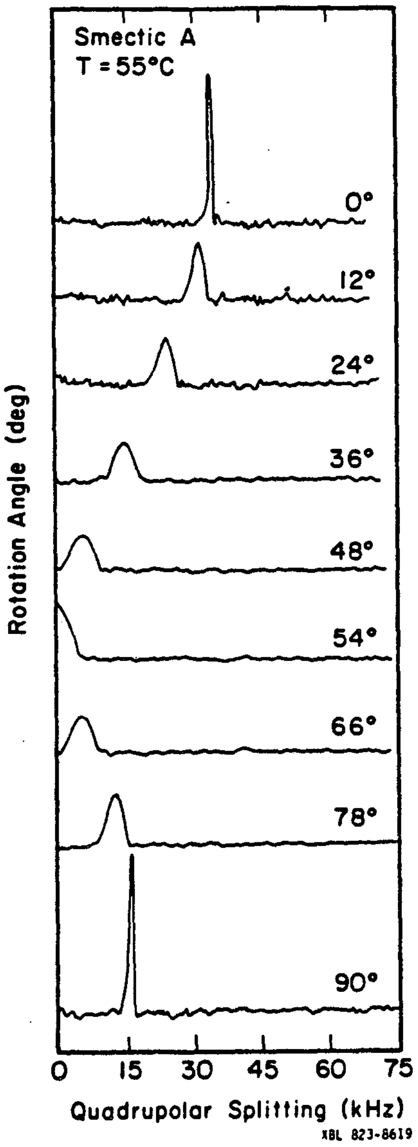

Figure 18. Behavior of the smectic A phase of 507 with sample rotation. Each spectrum was taken for a different sample rotation. The higher frequency half ($>\omega_0$) of the spectrum is shown. Note the asymmetry of the lineshape for small sample rotation. At about 54° the quadrupolar splitting has vanished and at 90° the splitting is one half ot is unrotated value.

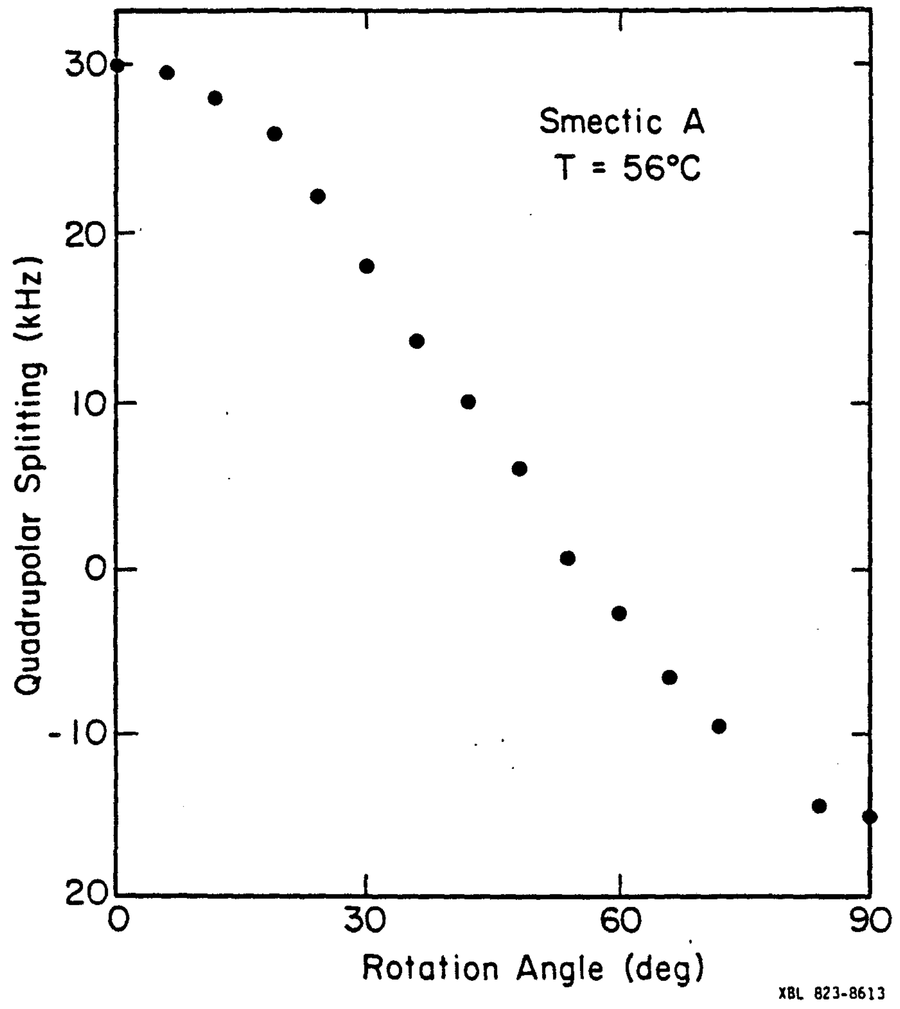

Figure 19. A plot of the quadrupolar splitting vs. sample rotation for 507. The experimental data are in excellent agreement with the expected functional dependence on $3\cos^2\beta -1$ where β is the sample rotation.

We will now attempt to explain the qualitative features of these smectic C spectra based on the model.

From figures 21, 22 and 23 it is seen that at small sample rotations the lines become highly asymmetric with an "edge" at the initial v_Q and a "tail" at lower values of v_Q. As the sample is rotated through larger angles, the signal intensity at the initial v_Q decreases to zero. It is also notcied that at lower temperatures, the signal persists at the initial v_Q through larger rotation angles. Figure 24 shows a rotation series for angles 0 to 90 taken at 53°C. It is noted that at 90° the line is boradened and virtually no signal is at one half the initial v_Q.

The smectic C model described in 2.4.2 explains the qualitative features of these spectra. If the rotation angle (β_4) is less than twice the smectic tilt angle (β_2), then in some domain or domains (sepcified by γ_3) the molecules will be able to assume a position on the cone (specified by γ_2) that will allow them to be parallel to the magnetic field. The spins of those molecules will resonate at the initial v_Q. But molecules in other domains will assume a variety of orientations and so a polycrystalline pattern will result. Once the sample rotation exceeds twice the tilt angle, the signal at the initial v_Q will decrease to zero. Therefore, the persistence of signal intensity at the initial v_Q for larger sample rotations at lower temperatures implies a temperature-dependent tilt angle, which increases as the temperature is lowered. We also note that for a given domain, when the angle between the axis of the cone and the magnetic field approaches 90°, the molecules jump from γ_2 to $\gamma_2-\pi$.

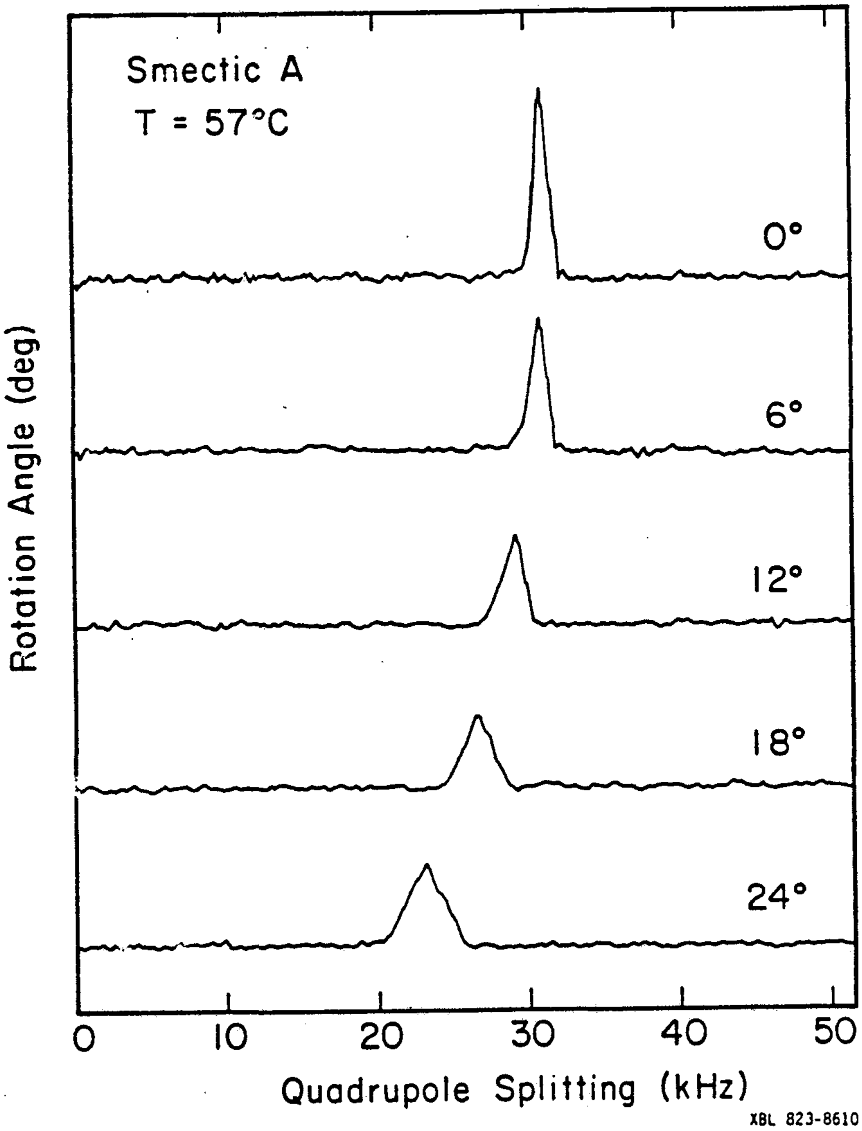

Figure 20. DMR spectra of 507 in its smectic A phase at 57°C for various small rotation angles. Note the slight asymmetry in lineshape due to the $3\cos^2\beta-1$ dependence.

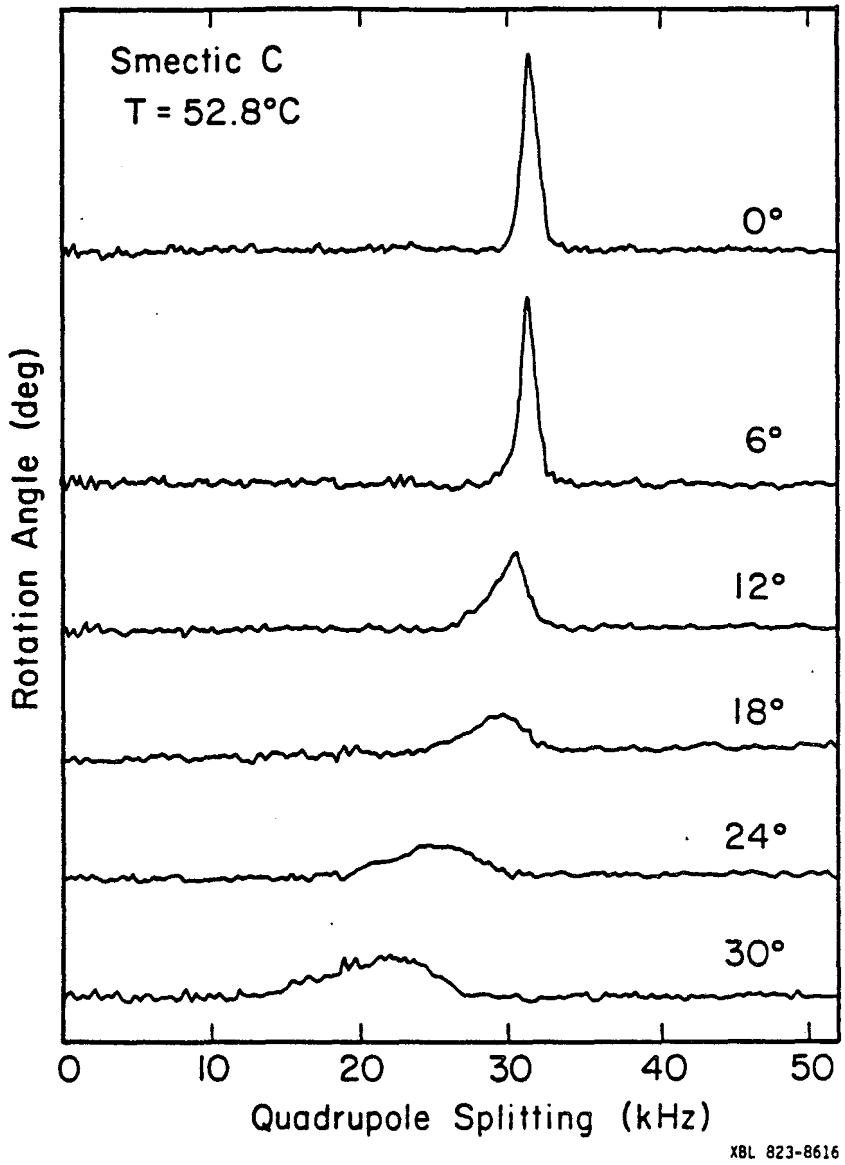

Figure 21. DMR spectra of 507 in its smectic C phase at 52.8°C for small rotation angles. Note the persistence of intensity at the initial ω_Q due to the reorientation of molecules in some domains such that their long axes are parallel to the magnetic field.

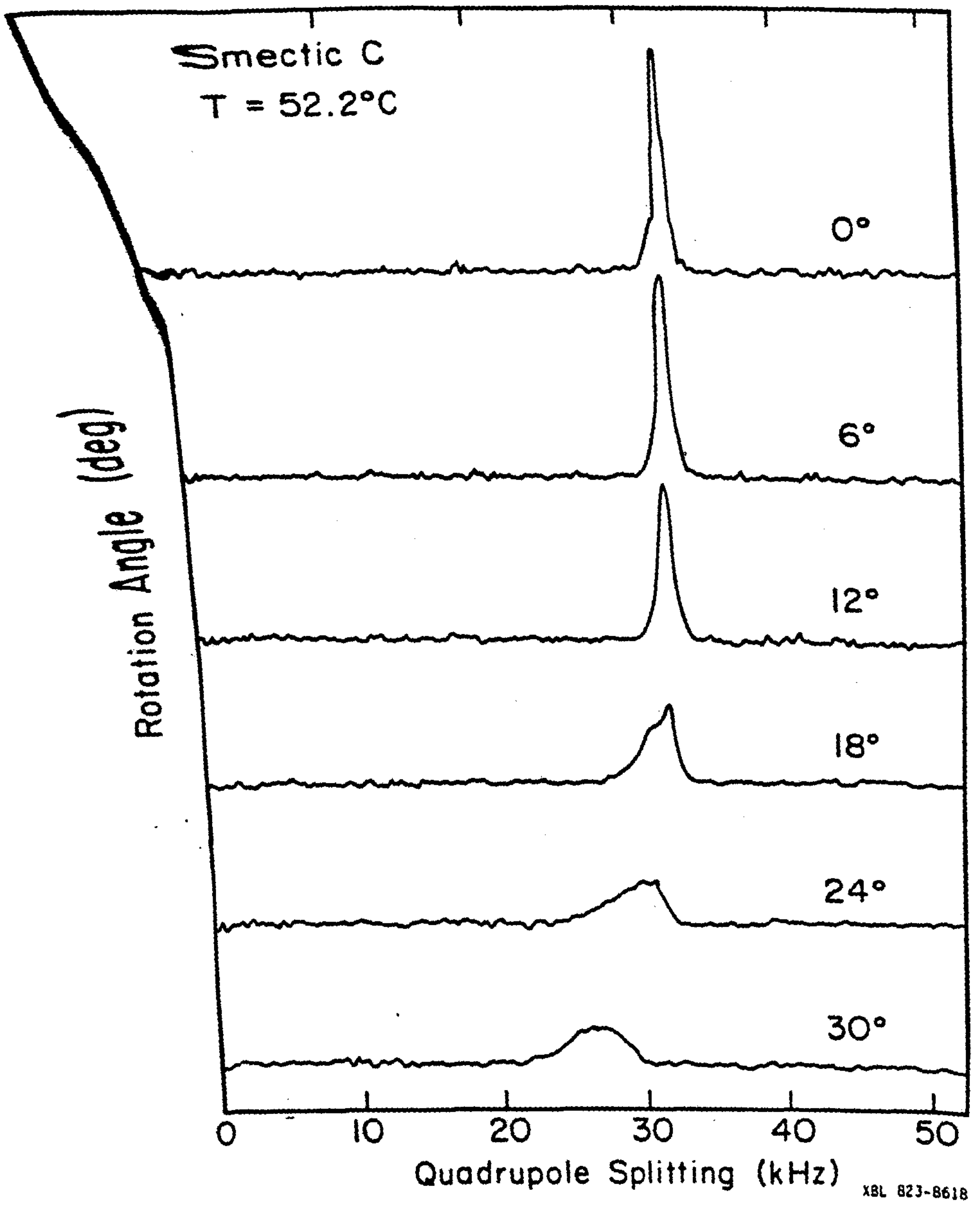

Figure 22. Same as Figure 21, only taken at 52.2°C. Note the persistence of intensity at the initial ω_Q at larger rotation angles.

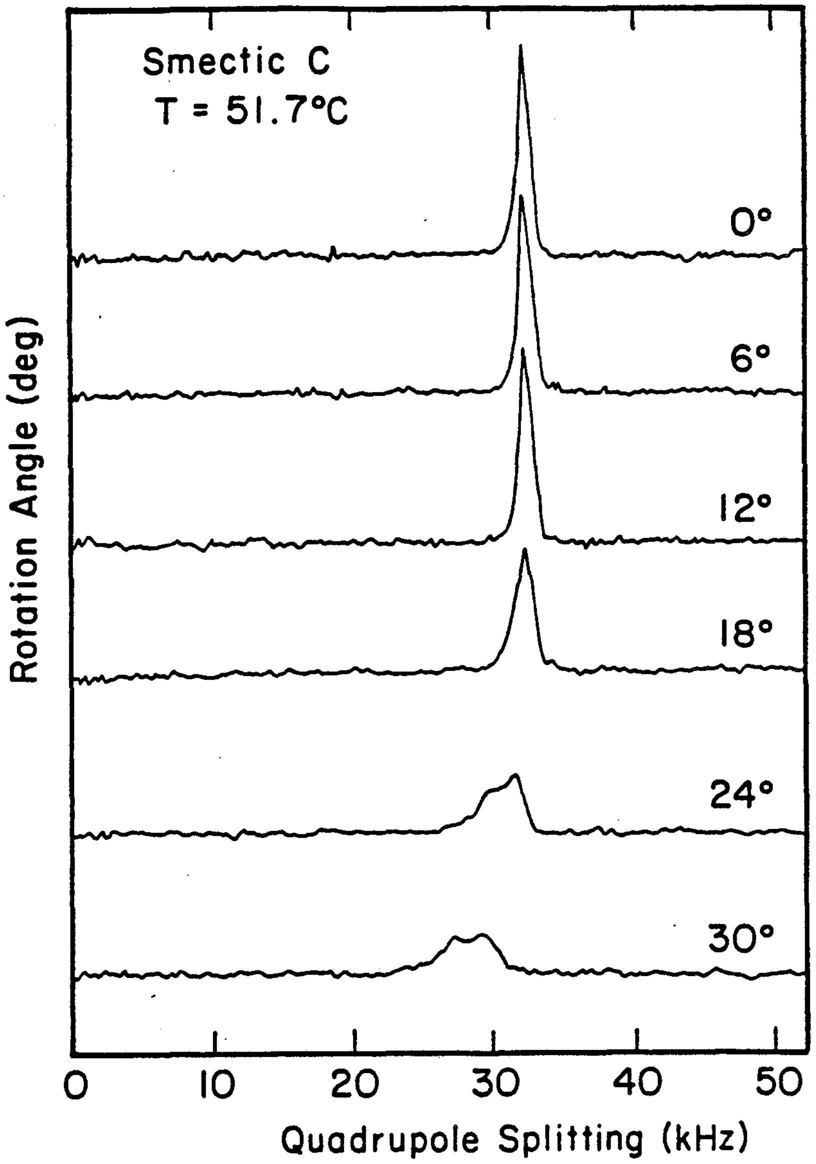

XBL 823-8615

Figure 23. Same as Figures 21 and 22, only taken at 51.7°C. Intensity persists at the initial ω_Q for sample rotations of up to 18° indicating that molecules in some domains can realign with their long axes parallel to the magnetic field. The trend in Figures 21-23 may be attributed to an increase in tilt angle as the temperature is lowered.

Therefore at large rotation angles, the lines are broad and at a sample rotation of 90^o, no signal is expected at one half the initial v_Q.

In figure 25 is shown a series of theoretical spectra generated by the program SMEC10 (see appendix 2.3) which uses the theory given in section 2.4.2 for smectic C phases. Specifically, the program uses equation 52 to calculate v_Q for a domain, given a tilt angle (β_2) and rotation angle (β_4). Four hundred domain angles (γ_2) were used and the molecular orientation angle (γ_2) was calculated for each domain using equation 64. Figure 25 is in good agreement with the experimental data of figure 24.

In figures 26 and 27 we plot v_Q at the half height of the high frequency edge of the polycrystalline pattern as a function of rotation angle for various temperatures for 507 and 705. Figure 28 is a theoretical plot assuming different tilt angles.The tilt angle is clearly temperature dependent in both compounds with a maximum at about $9\text{-}10^o$. This result contradicts the conclusions of an x-ray study of 705 by de Jeu and de Poorter in which it is stated that the tilt angle in the smectic C phase of 705 is 18^o and independent of temperature (27).

c) Smectic B Phases

DMR spectra were obtained of aligned sample of 507 and 705 in the two smectic phases below the smectic C phase. Spectra of rotated samples of the S_3 phase lying within the range $32^oC\text{-}51^oC$ for 507, and 56^oC to 63^oC for 705 showed the same qualitative features as rotated smectic A samples. The unrotated spectra of

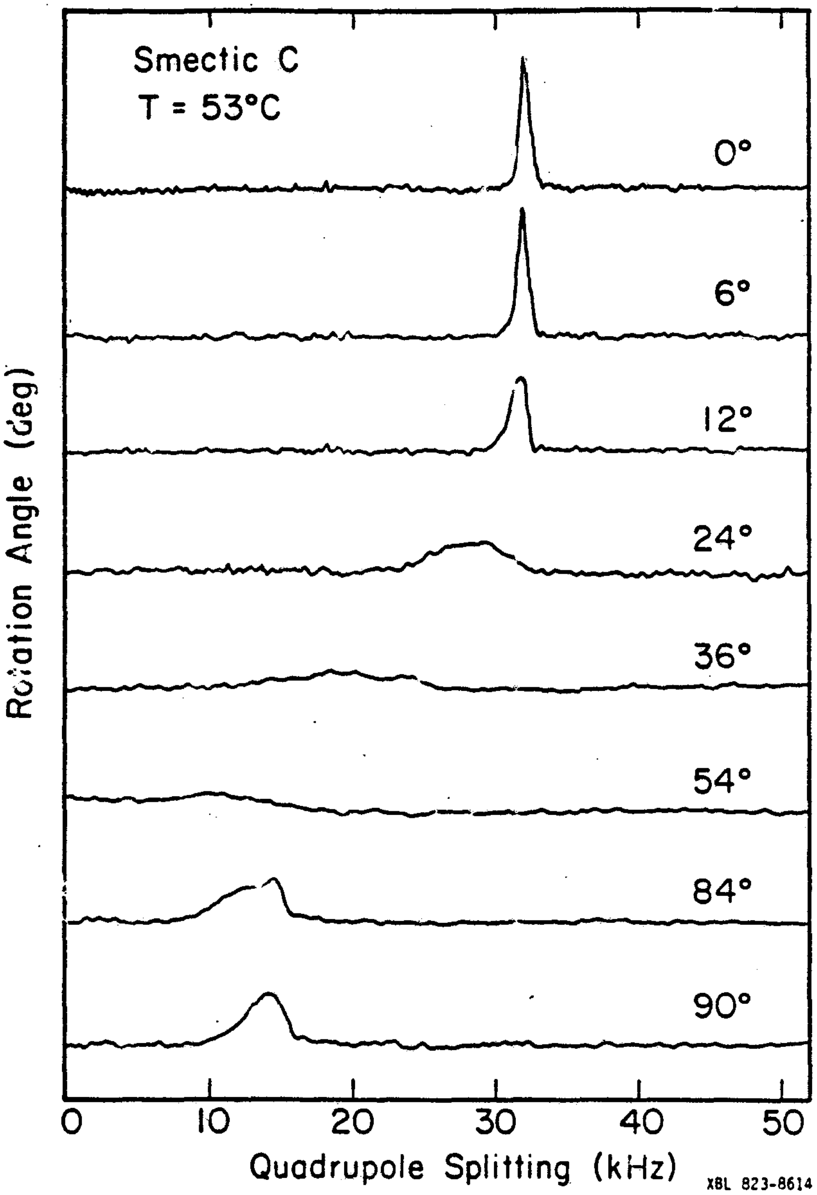

Figure 24. A complete rotation of 507 in its smectic C phase for rotation angles up to 90°.

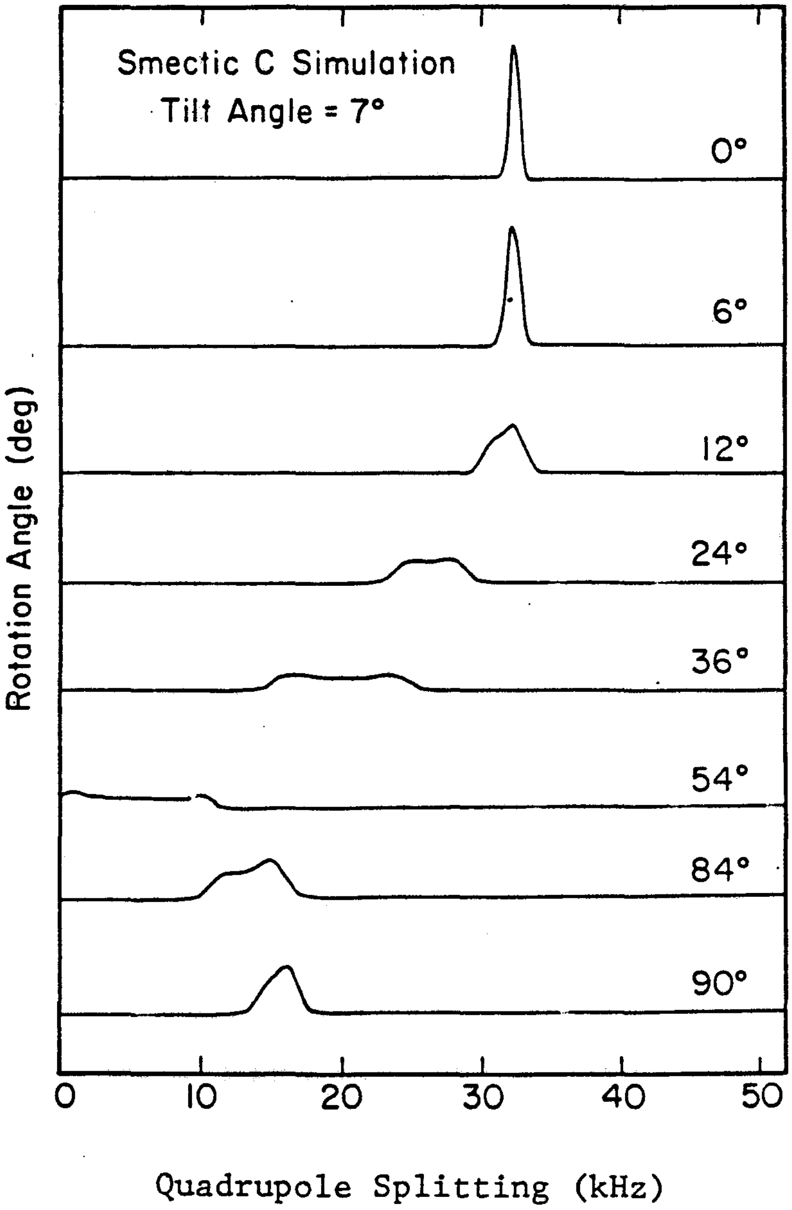

Figure 25. A series of spectra calculated with the program Smec 10 assuming a multidomain structure, molecular reorientation, and a tilt angle of 7°. Agreement with the experimental data in Figure 24 is quite good.

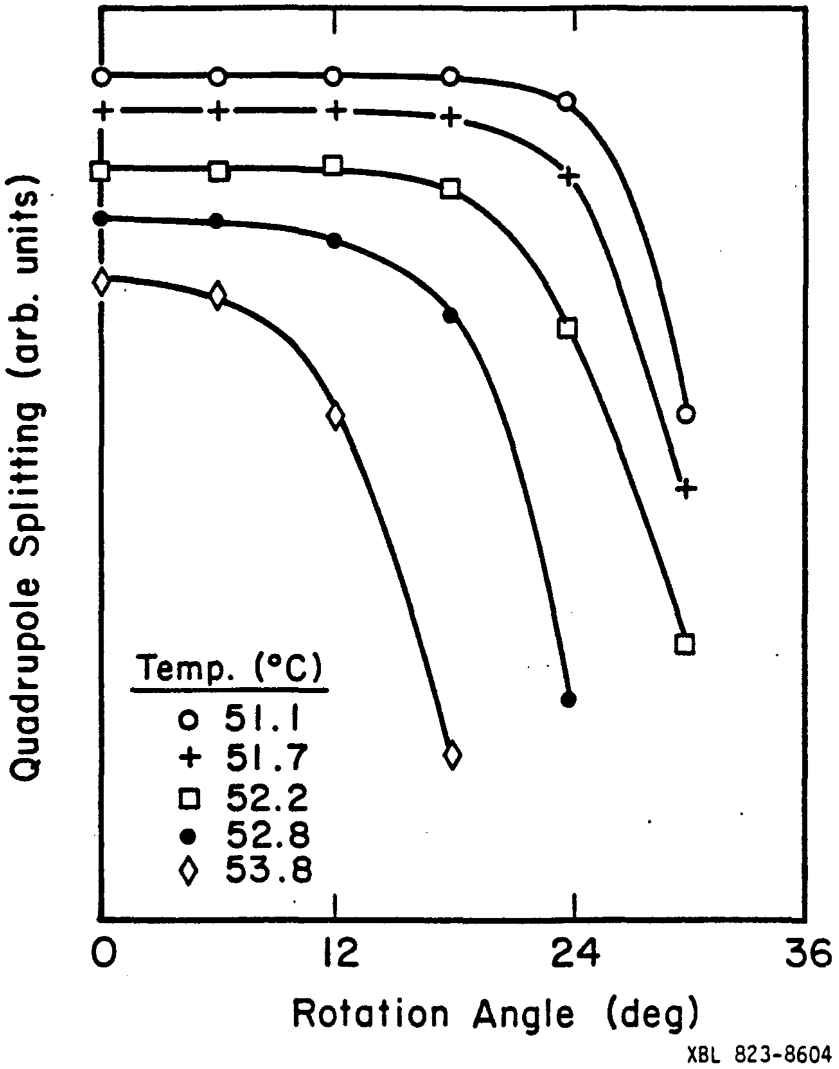

Figure 26. A plot of the frequency of the outer edge of the high frequency quadrupolar satellite at half maximum vs. rotation angle for 507. Data for several temperatures within the smectic C phase are shown.

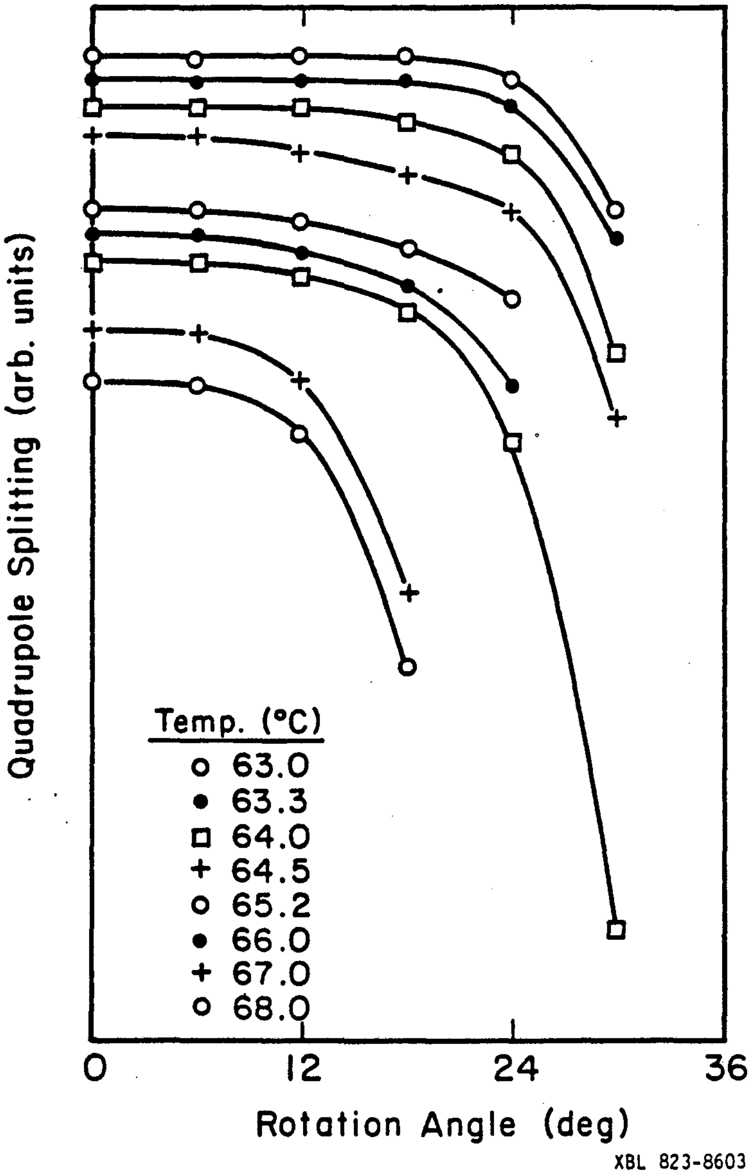

Figure 27. Same as Figure 26, only for the nom liquid crystal 705.

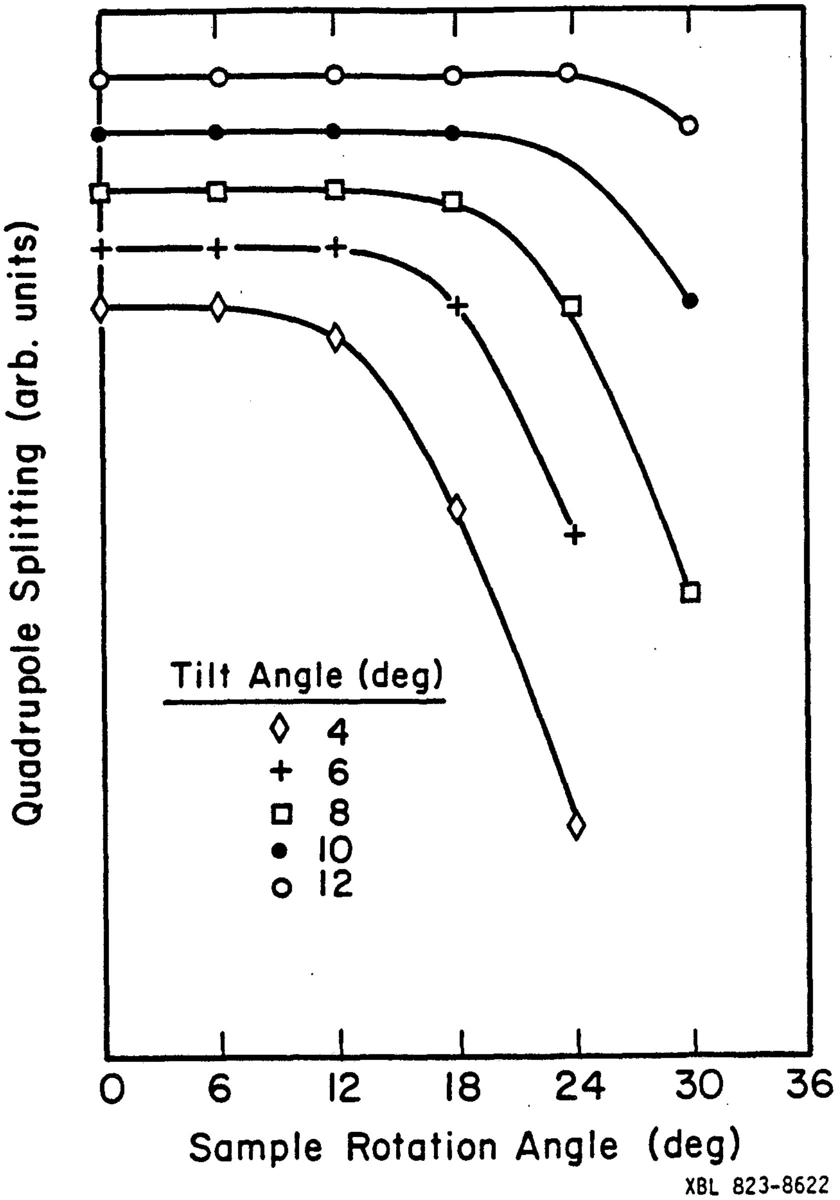

Figure 28. Computer generated plot produced by the program SMEC 10 showing the frequency of the outer edge of the high frequency quadrupolar satellite at half maximum vs. rotation angle for various tilt angles. The data in Figures 26 and 27 indicate a temperature dependent tilt angle reaching a maximum of 9° at the smectic C-B_A phase transition.

of 507 and 705 showed greater broadening in the S_3 phase than in the smectic A, indicating less uniform alignemnt in the former than in the latter phase. However, spectra of rotated S_3 samples are broadened asymmetrically at small angles and almost symmetrically at angles approaching 54°. At 54°, the spectrum is a single broadened line centered at resonance, and at 90° the satellites are narrowed and the splitting is $\frac{1}{2}$ the unrotated value. Figure 29 shows a plot of v_Q vs. rotation angle plotted against the function $\frac{1}{2}(3\cos\theta-1)$ for S_3. v_Q is measured from resonance to the peak of the satellite and θ is the rotation angle. These observations indicate that S_3 is an untilted uniaxial phase in which the molecules are either rotating rapidly around their long axes, or the orientational distribution around the molecular long axes is three-fold or higher.

Figure 30 shows a series of spectra of aligned samples of 507 in the S_4 phases for various rotation angles between 0° and 90°. For small rotation angles, the spectra display features typical of the spectra of a tilted smectic phase. For small rotation angles (18°) the satellites broaden asymmetrically with an edge persisting at the initial v_Q. At large rotation angles the satellites are asymmetrically broadened although agreement with theory is less perfect. The line at 90° is broadened with intensity persisting at one half the initial v_Q. No simple model based on realignment into absolute or local minima has succeeded in simulating the 90° spectrum. Although realignment into local minima (see appendix 2.2) can explain the persistence of intensity at one half

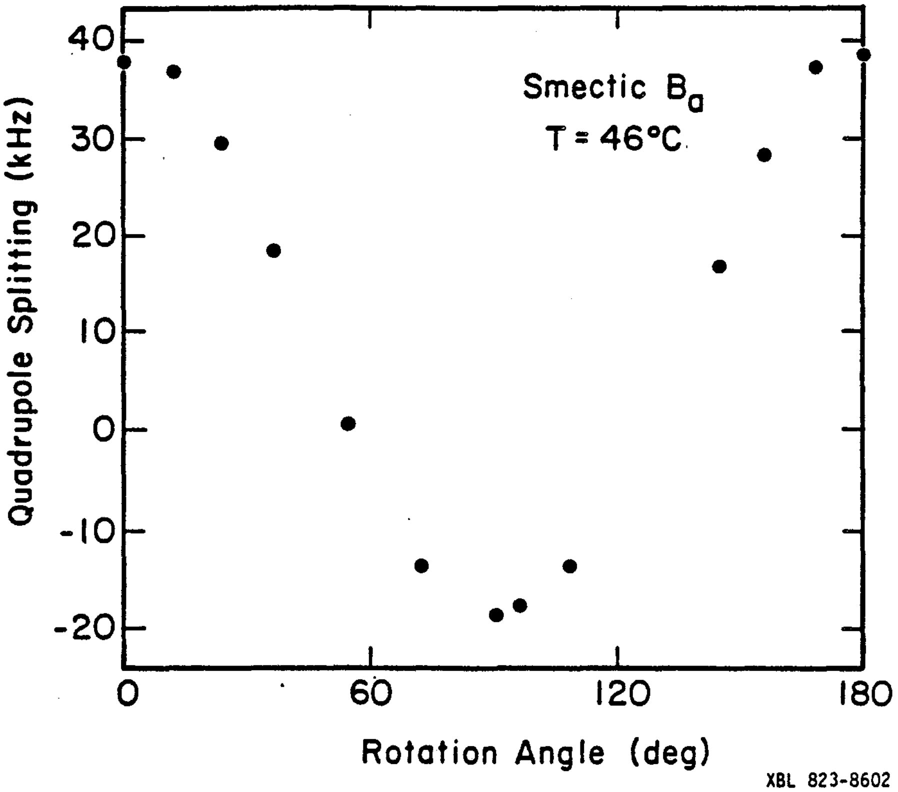

XBL 823-8602

Figure 29. A plot of ω_Q vs. rotation angle for 507 in its smectic B_A phase at 46°C. The data follows the expected dependence on the rotation angle, $3\cos^2\beta-1$.

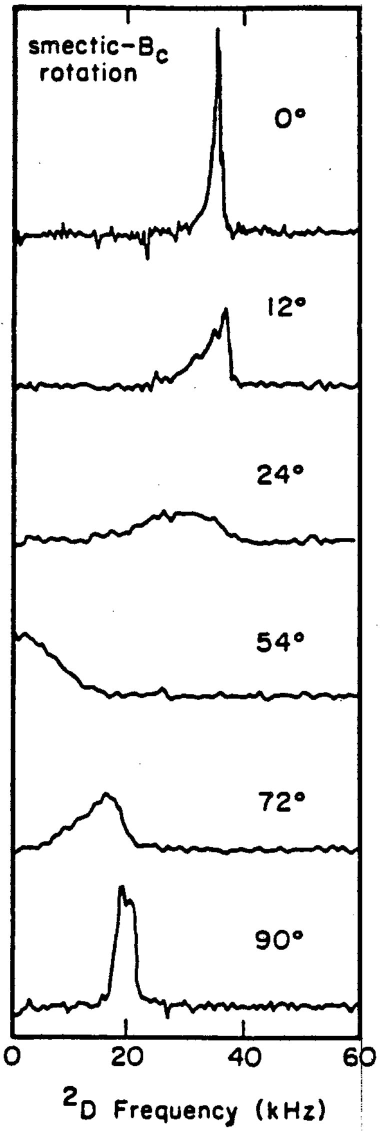

XBL 782-7142

Figure 30. DMR spectra of 50.7 in its smectic B_C phase for various rotation angles.

the initial v_Q, the satellites should be slightly broader than for the case of realignment to an absolute minimum since the distribution of alignment angles γ_2 is larger in the former case than in the latter case. However, the 90^o satellite appears narrower than expected.

Except for the 90^o spectrum, in which the satellites are narrower than expected, the spectra of rotated S_4 samples indicate that the phase is a tilted smectic, and are in fact similar to the spectra obtained by Luz (42) for the smectic B_C phase of TBBA.

Appendix 2.1 Ordering in the Smectic C Phase

In this appendix we will derive the number of unique order parameters required by the symmetry of the smectic C phase. The assumptions that we will use are:

(i) Molecules are of very low symmetry and so no reduction in the number of order parameters is possible via molecular symmetry arguments.

(ii) To a good approximation the ordering distribution is symmetric about the molecular frame.

(iii) Molecules are "invertible" within the smectic layer.

(iv) The degree of uniaxial ordering is high. That is, angular excursions from the director are small.

We define order parameter as a motionally averaged element of a Wigner rotation matrix:

$$\begin{aligned} <D^{(2)}_{mn}(\Omega) &= \int d\Omega P(\Omega) D^{(2)}_{mn}(\Omega) \\ &= \int d\Omega \sum_{k\ell} C^{(2)}_{k\ell} D^{(2)}_{k\ell}(\Omega)\ D^{(2)}_{mn}(\Omega) \qquad (1) \end{aligned}$$

Such a transformation is required since the molecular frame is not fixed relative to the director frame.

Linear combinations of these complex order parameters form purely real order parameters that express some geometric mode of ordering. A simple example is

$$<D^{(2)}_{00}(\Omega)> = <\tfrac{1}{2}(3\cos^2\beta - 1)> \quad . \qquad (2)$$

β is the angle between the molecular z axis and the z axis of the director frame. It measures the degree to which the molecular z axis aligns parallel to the director. We note that the function is maximum if $\beta = 0$.

In general the number of order parameters $\langle D^{(2)}_{mn}(\Omega)\rangle$ depends upon the symmetry of the molecule and the symmetry of the phase. For example, if the molecular z axis were an axis of three fold symmetry or higher, only order parameters of the form $\langle D^{(2)}_{0n}(\Omega)\rangle$ would be nonzero. On the other hand, if the phase were uniaxial, that is, if the director frame were to have cylindrical symmetry, then only order parameters of the form $D^{(2)}_{m0}(\Omega)$ would be nonzero. Therefore, to describe a molecule of any symmetry in a uniaxial phase, one requires five order parameters. If no symmetry were to exist in the phase, then the number of order parameters would be 25.

Assumption (i) states that we will not, in general, be able to reduce the number of order parameters based on the presence of molecular planes of symmetry, n-fold axes, inversion centers etc.

Assumption (ii) states that the distribution of molecular orientations to the director frame is symmetric, that

$$P(-\alpha,-\beta,\gamma) = P(\alpha,\beta,\gamma) \quad . \tag{3}$$

Let us consider first the α rotation:

$$P(-\alpha,0,0) = P(\alpha,0,0) \quad . \tag{4}$$

Substituting equation 1 into equation 3 we get

$$\sum_{mn} C^{(2)}_{mn} D^{(2)}_{mn}(\alpha,0,0) = \Sigma C_{mn} D_{mn}(-\alpha,0,0) \quad . \tag{5}$$

We substitute the identity

$$D_{mn}^{(2)}(-\alpha,0,0) = D_{mn}^{(2)*}(\alpha,0,0) = (-)^{m-n}D_{-m-n}^{(2)}(\alpha,0,0) \qquad (6)$$

in equation 5 to get

$$\sum_{mn} C_{mn}^{(2)}D_{mn}^{(2)}(\alpha,0,0) = \sum_{mn} (-)^{m-n}C_{mn}^{(2)}D_{-m-n}^{(2)}(\alpha,0,0)$$

$$= \Sigma(-)^{-m+n}C_{-m-n}^{(2)}D_{mn}^{(2)}(\alpha,0,0) \quad . \qquad (7)$$

Equating coefficients on the left and right hand sides of equation 7 we get

$$C_{mn}^{(2)} = (-)^{-m+n}C_{-m-n} \quad . \qquad (8)$$

The second condition is that

$$P(0,\beta,0) = P(0,-\beta,0) \quad . \qquad (9)$$

We substitute equation 1 into equation 9 to get

$$\sum_{mn} C_{mn}^{(2)}D_{mn}^{(2)}(0,\beta,0) = \Sigma\, C_{mn}D_{mn}^{(2)}(0,-\beta,0) \qquad (10a)$$

or

$$\sum_{mn} C_{mn}^{(2)}d_{mn}^{(2)}(\beta) = \Sigma\, C_{mn}^{(2)}d_{mn}^{(2)}(-\beta) \quad . \qquad (10b)$$

If we substitute the identity

$$d_{mn}^{(2)}(-\beta) = (-)^{m-n}d_{mn}^{(2)}(\beta) \qquad (11)$$

into equation 10 we get

$$\sum_{mn} C_{mn}^{(2)}d_{mn}^{(2)}(\beta) = \Sigma(-)^{m-n}C_{mn}^{(2)}d_{mn}^{(2)}(\beta) \quad . \qquad (12)$$

If we now equate the left and right hand sides of equation 12 the result is:

$$C^{(2)}_{mn} = (-)^{m-n} C^{(2)}_{mn} \quad . \tag{13}$$

Equation 13 is valid only if m-n is zero or an even integer.

Assumption (iii) implies that

$$P(\alpha,\beta,0) = P(-\alpha,\beta+\pi,0) \quad . \tag{14}$$

If we again substitute equation 1 into equation 14 we get

$$\begin{aligned}\sum_{mn} C^{(2)}_{mn} D^{(2)}_{mn}(\alpha,\beta,\gamma) &= \sum_{mn} C^{(2)}_{mn} D^{(2)}_{mn}(-\alpha,\beta+\pi,\gamma) \\ &= \sum_{mn} C^{(2)}_{mn} e^{i\alpha m} d^{(2)}_{mn}(\beta+\pi)\ e^{-i\gamma n} \quad . \end{aligned}\tag{15}$$

We now substitute the identity

$$d^{(2)}_{mn}(\ +\ ) = (-)^m d_{-mn}(\ ) \tag{16}$$

into equation 15 to obtain

$$\begin{aligned}\sum_{mn} C^{(2)}_{mn} D^{(2)}_{mn}(\alpha,\beta,\gamma) &= \sum_{mn} (-)^m C^{(2)}_{mn} D^{(2)}_{-mn}(\alpha,\beta,\gamma) \\ &= \Sigma(-)^m C^{(2)}_{-mn} D^{(2)}_{mn}(\alpha,\beta,\gamma)\end{aligned}\tag{17}$$

which implies the final condition

$$C^{(2)}_{mn} = (-)^m C^{(2)}_{-mn} \quad . \tag{18}$$

Equations 8, 13, and 18 indicate that there are four unique order parameters:

$$<D^{(2)}_{00}(\Omega)>$$

$$<D^{(2)}_{11}(\Omega)> = <D^{(2)}_{-1-1}(\Omega)> = -<D^{(2)}_{-11}(\Omega)> = -<D^{(2)}_{1-1}(\Omega)>$$

$$<D^{(2)}_{20}(\Omega)> = <D^{(2)}_{-20}(\Omega)>$$

$$<D^{(2)}_{22}(\Omega)> = <D^{(2)}_{-2,-2}(\Omega)> = <D^{(2)}_{2,-2}(\Omega)> = <D^{(2)}_{-2,2}(\Omega)>$$

In the limit that the ordering is very high, $<D_{20}^{(2)}(\Omega)>$ will be small. The meaning of our approximation in section 2.4.2 is also clear. By retaining only the term $Q_0^{(2)}(\Omega_0,\Omega_1)$, we are discarding the biaxial order parameters $<D_{11}^{(2)}(\Omega_1)>$ and $<D_{22}^{(2)}(\Omega_1)>$.

Appendix 2.2 Calculation of the Magnetic Energy

In this appendix we will derive an expression for the magnetic energy

$$E = -H\cdot\chi\cdot H$$

in terms of the parameters of the model; the tilt angle (β_2), the position of the molecules of a domain on the cone (γ_2), the domain (γ_3), and the rotation angle (β_4).

χ is the magnetic susceptibility tensor of a given domain. When the sample is rotated, the magnetic field exerts a torque on the molecules of a given domain, and these molecules then reorient in order to minimize the magnetic energy, keeping the tilt angle and relative orientations constant. By minimizing equation 1, we obtain an expression for γ_2, in terms of β_2, γ_2, and β_4.

We begin by expressing equation 1 in spherical tensor form, in the director frame:

$$-E = \sum_{\ell m}(-)^m (H^2)_{\ell m}(\chi)_{\ell -m} \tag{2}$$

Expanding equation 2 we obtain

$$-E = (H^2)_{00}\chi_{00} + (H^2)_{20}\chi_{20} + (H^2)_{21}\chi_{2-1} + (H^2)_{2-1}\chi_{21}$$
$$+ (H^2)_{22}\chi_{2-2} + (H^2)_{2-2}\chi_{22} \quad . \tag{3}$$

Equation 3 could be simplified by symmetry arguments. For example, we can write the transformation of χ from the molecular frame into the director frame:

$$\chi_{20} \sim \chi'_{20} \, \langle D^{(2)}_{00}(\Omega) \rangle$$

$$\chi_{21} = -\chi_{2-1} \sim (\chi'_{21} - \chi'_{2-1}) \, \langle D^{(2)}_{11}(\Omega) \rangle$$

$$\chi_{22} = \overset{*}{\chi}{}'_{2-2} \sim (\chi'_{22} + \chi_{2-2}) \, \langle D^{(2)}_{22}(\Omega) \rangle \quad . \qquad (4)$$

Now if the principal axis system of χ coincides with the molecular frame, then

$$\chi'_{21} = \chi'_{2-1} = 0 \quad . \qquad (5)$$

Our assumption, though, will again be to approximate the symmetry of the director frame as cylindrical. Therefore equation 3 becomes:

$$-E \sim (H^2)_{00}\chi_{00} + (H^2)_{20}\chi_{20} \quad . \qquad (6)$$

Equation 6 may be rewritten as

$$-E \sim \chi_{00}|H|^2 + \chi_{20}/\sqrt{3} \, (3(H_{10})^2 - |H|^2) \qquad (7)$$

where we have used the expression

$$T_{\ell m}(A_1,A_2) = \sum_{m'} C(\ell_1\ell_2\ell,m_1,m-m_1)T_{\ell_1 m_1}(A_1)T_{\ell_2 m-m_1}(A_2) \qquad (8)$$

to write $(H^2)_{20}$ in terms of products of first rank tensors.

Now H_{10} is a component of the first rank magnetic field tensor in the director frame. We can write the relation between H_{10} in the director frame and the magnetic field tensor in the lab frame as

$$H_{10} = \sum_{mn} H_{10}^{lab} D_{0m}^{(1)}(-\Omega_4) D_{mn}^{(1)}(-\Omega_3) D_{n0}^{(1)}(-\Omega_2) \tag{9}$$

where $-\Omega_2 = (\gamma_2,-\beta_2,0)$; $-\Omega_3 = (-\gamma_3,-\beta_2,0)$; and $-\Omega_4 = (0,-\beta_4,0)$.

Equation 9 can be rewritten as

$$H_{10} = \sum_{mn} H_{10}^{lab} d_{0m}^{(1)}(-\beta_4) d_{mn}^{(1)}(-\beta_2) d_{n0}^{(1)}(-\beta_2) e^{i(m\gamma_3+n\gamma_2)} \quad . \tag{10}$$

To minimize E with respect to γ_2 we must calculate $\frac{\partial E}{\partial \gamma_2}$, and set it to zero. The dependence of E on γ_2 is through H_{10} in the director frame. Therefore we differentiate both sides of equation 7 to obtain

$$-\frac{\partial E}{\partial \gamma_2} = 2\sqrt{3}\chi_{20} H_{10} \frac{\partial H_{10}}{\partial \gamma_2} = 0 \tag{11a}$$

or simply

$$\frac{\partial H_{10}}{\partial \gamma_2} = 0 \quad . \tag{11b}$$

From equation 10,

$$\frac{\partial H_{10}}{\partial \gamma_2} = \sum_{mn} (in) H_{10}^{lab} d_{0m}^{(1)}(-\beta_4) d_{mn}^{(1)}(-\beta_2) d_{n0}^{(1)}(-\beta_2)\; e^{i(m\gamma_3+n\gamma_2)} \quad . \tag{12}$$

We now expand the right hand side of equation 12 and set it to zero:

$$d_{0-1}^{(1)}(-\beta_4) d_{-11}^{(1)}(-\beta_2) d_{10}^{(1)}(-\beta_2) e^{i(\gamma_2-\gamma_3)} \quad +$$

$$d_{00}^{(1)}(-\beta_4) d_{01}^{(1)}(-\beta_2) d_{10}^{(1)}(-\beta_2) e^{i\gamma_2} \quad +$$

$$d_{01}^{(1)}(-\beta_4) d_{11}^{(1)}(-\beta_2) d_{10}^{(1)}(\beta_2) e^{i(\gamma_2+\gamma_3)} \quad -$$

$$d^{(1)}_{0-1}(-\beta_4)d^{(1)}_{-1-1}(-\beta_2)d^{(1)}_{-10}(-\beta_2)e^{-i(\gamma_2+\gamma_3)} \quad -$$

$$d^{(1)}_{00}(-\beta_4)d^{(1)}_{0-1}(-\beta_2)d_{-10}(-\beta_2)e^{-i\gamma_2} \quad -$$

$$d_{01}(-\beta_4)d_{1-1}(-\beta_2)d_{-10}(-\beta_2)e^{-i(\gamma_2-\gamma_3)} \quad = \quad 0 \quad . \qquad (13)$$

We now substitute the definitions

$$d^{(1)}_{11}(\beta) = d^{(1)}_{-1-1}(\beta) = \frac{1}{2}(1+\cos\beta) \qquad (14a)$$

$$d^{(1)}_{1-1}(\beta) = d^{(1)}_{-11}(\beta) = \frac{1}{2}(1-\cos\beta) \qquad (14b)$$

$$d^{(1)}_{01}(\beta) = d^{(1)}_{10}(\beta) = -d^{(1)}_{-10}(\beta) = -d^{(1)}_{0-1}(\beta) = \frac{1}{\sqrt{2}}\sin\beta \qquad (14c)$$

$$d^{(1)}_{00}(\beta) = \cos\beta \qquad (14d)$$

into equation 13 and after some algebra we obtain

$$\sin\gamma_2(\sin\beta_2\cos\beta_4 + \cos\gamma_3\cos\beta_2\sin\beta_4) + \cos\gamma_2\sin\gamma_3\sin\beta_4 = 0 \quad . \qquad (15)$$

Solving for γ_2 we obtain

$$\gamma_2 = \tan^{-1}\frac{-\sin\gamma_3\sin\beta_4}{\sin\beta_2\cos\beta_4 + \cos\gamma_3\cos\beta_2\sin\beta_4} \qquad (16)$$

In general, there are two solutions: γ_2 and $\gamma_2+\pi$. For a given set of parameters $(\beta_2,\gamma_3,\beta_4)$, the minimum energy E is given by the maximum H_{10}. Thus it is necessary to calculate a value for $H_{10}(\gamma_2)$, assuming a reorientation angle γ_2 and a second value $H_{10}(\gamma_2+\pi)$, assuming a reorientation angle $\gamma_2+\pi$.

In the preceding discussion, we have assumed that after a rotation, the sample will always reorient into an absolute minimum, given by one of the solutions of equation 15. Another possibility is that whenever the sample is rotated through an angle $\beta_4 + \beta_2 > \frac{\pi}{2}$, reorientation will occur into a local minimum, which is designated by the sign of the initial torque. This, of course, assumes that no reorientation occurs during the rotation, which is a good assumption for a very viscous sample. Now the expression for the magnetic torque is, as given before

$$E = -2H \frac{\partial H}{\partial \gamma_2} \tag{16}$$

where H is in the director frame. Our expressions for H and $\frac{\partial H}{\partial \gamma_2}$ in the director frame are

$$\begin{aligned} H \propto \cos\beta_4 - \cos\beta_4 \sin^2\beta_2 (1+\cos\gamma_2) - \sin\beta_4 \sin\beta_2 \cos\gamma_3 (1+\cos\gamma_2) \\ + \sin\beta_4 \sin\beta_2 \sin\gamma_3 \sin\gamma_2 \end{aligned} \tag{17}$$

and so

$$\begin{aligned} \frac{\partial H}{\partial \gamma_2} \propto \cos\beta_4 \sin^2\beta_2 \sin\gamma_2 + \sin\beta_4 \sin\beta_2 \cos\beta_2 \cos\gamma_3 \sin\gamma_2 \\ + \sin\beta_4 \sin\beta_2 \sin\gamma_3 \cos\gamma_2 \end{aligned}$$

Now we define our initial position on the cone as $\gamma_2^{\,o} = \pi$. Therefore, we obtain for H^o and $\frac{\partial H^o}{\partial \gamma_2}$

$$H^o = \cos\beta_4 \tag{18}$$

$$\frac{\partial H^o}{\partial \gamma_2} = -\sin\beta_4 \sin\beta_2 \sin\gamma_3 \tag{19}$$

and the initial torque is given by

$$\frac{\partial E_o}{\partial \gamma_2} \propto \sin\beta_4 \cos\beta_4 \sin\beta_2 \sin\gamma_3 \tag{20}$$

If we define the tilt angle to be within the range $-\frac{\pi}{2} < \beta_2 < \frac{\pi}{2}$ then $\sin\beta_2$ is always positive. In addition, if the rotation angle angle is less than $\frac{\pi}{2}$, then $\sin\beta_4\cos\beta_4$ is always positive. In that case, the sign of the initial torque is determined by the domain position γ_3. Therefore, suppose that the γ_2^m, corresponding to the absolute minimum, is obtained by solving equation 15. The γ_2 corresponding to the local minimum, $\gamma_2^{m'}$, is determined by the sign conditions, when γ_2^m is defined in the range $-\frac{\pi}{2} < \gamma_2^m < \frac{\pi}{2}$

$$\begin{array}{lll}
\gamma_2^m > 0 & \frac{\partial E}{\partial \gamma_2} > 0 & \gamma_2^{m'} = \gamma_2^m + \pi \\[2ex]
\gamma_2^m < 0 & \frac{\partial E}{\partial \gamma_2} \quad 0 & \gamma_2^{m'} = \gamma_2^m \\[2ex]
 & \frac{\partial E}{\partial \gamma} < 0 & \gamma_2^{m'} = \gamma_2^m + \pi \quad .
\end{array}$$

We assume also that the initial γ_2 is π, i.e. $\gamma_2^o = \pi$.

Appendix 2.3 : Spectral Simulation Programs

DP1:DROBNYBU:SMEC10.FR 7/31/81

```
C               PROGRAM SMEC10   JULY 30,1977   H.T.EDZES
C               THIS PROGRAM CALCULATES A STICK SPECTRUM FOR
C               QUADRUPOLAR SPLITTINGS OF DEUTERIUM IN ROTATED
C               SMECTIC PHASES.
C               THE AVERAGED QUADRUPOLAR INTERACTION CONSTANTS ARE
C               USED: ORDER PARAMETERS ARE NOT EXPLICITELY USED.
C               THE AVERAGED QUADRUPOLAR SPLITTING IS NORMALIZED
C               TO 1.
C               STICK SPECTRA ARE CALCULATED FOR THE FOLLOWING CASES*
C               1.  NO ROTATION OF THE DIRECTOR ALLOWED
C               2.  ROTATION OF DIRECTOR FREE ON CONE;
C                   ABSOLUTE MINIMUM MAGNETIC ENERGY IS REACHED
C               3.   SAME. BUT POSSIBLE ROTATION TO LOCAL
C                   MINIMUM IS ALLOWED.
C               CALCULATED DATA ARE DISPLAYED VIA THE PROGRAM SPEC
C               AND ARE STORED IN SCRATCH FILE CD 1.
        DIMENSION QQ(3.3),NSTICK(0:255),NNSTICK(512)
        DIMENSION RAL(3,3),RRH(3,3),RPH(3,3),RTH(3,3)
C               DATA FILE FOR DATA DISPOSITION MUST BE OPENED.
        CALL OPEN(1,"DPOF:RESERVED:SCRATCH",3,IERR)
        IF (IERR.EQ.1) GOTO 10
        TYPE "ERROR CODE OPEN = ". IERR
        GOTO 990
C               ASK FOR INPUT DATA
10      ACCEPT "TILT ANGLE THETA = ",TH1
        ACCEPT "NUMBER OF DOMAIN ANGLES ALPHA PER QUADRANT = ".NAL
        ACCEPT " ROTATION ANGLE RHO BETWEEN 0-90 = ",RH1
        ACCEPT "AVERAGED QUADRUPOLAR ASYMMETRY FACTOR = ".QA
        ACCEPT "MAXIMUM SPLITTING IN STICK SPECTRUM NSP SMALLER 256 = ",NSP
        ACCEPT "TYPE 1 IF NO ROTATION ON THE CONE IS ALLOWED
     F  2 IF ABSOLUTE MINIMUM IN ENERGY IS REACHED. 3 IF RELATIVE
     F  MINIMUM IS REACHED".NOPT
        TYPE "BEGIN OF CALCIULATION"
C               CALCULATE PI. THETA, AND STEPS DRH FOR RHO AND DAL FOR ALPHA
        PI=4.0*ATAN(1.0)
        DAL=PI/(NAL+NAL)
        RH=2.0*PI*RH1/360.0
        TH=2.0*PI*TH1/360.0
        TYPE "TH,DAL,DRH CALCULATED"
C       FILL AVERAGED QUADRUPOLAR TENSOR; NORMALIZED TO QQ(3,3)=1(3,3)=1.0
        QQ(3.3)=1.0
        QQ(2.2)=-0.5-QA
        QQ(1,1)=-.5+QA
        QQ(1,2)=0.0
        QQ(1,3)=0.0
        QQ(2.3)=0.0
        QQ(3,2)=0.0
        QQ(2,1)=0.0
        QQ(3,1)=0.0
C       FILL NONCHANGING ELEMENTS OF RAL AND RPH
        RAL(3,3)=1.0
        RAL(1.3)=0.0
        RAL(2,3)=0.0
        RAL(3,2)=0.0
        RAL(3,1)=0.0
        RPH(3.3)=1.0
        RPH(1,3)=0.0
        RPH(2,3)=0.0
        RPH(3,2)=0.0
        RPH(3,1)=0.0
C               CALCULATE SIN AND COS (THETA), AND ROTATION MATRIX RTH
        CTH=COS(TH)
        STH=SIN(TH)
        RTH(1,1)=CTH
        RTH(3,3)=CTH
        RTH(2,2)=1.0
        RTH(1,2)=0.0
        RTH(2,1)=0.0
        RTH(2,3)=0.0
        RTH(3,2)=0.0
        RTH(1,3)=-STH
        RTH(3,1)=STH
        CRH=COS(RH)
        SRH=SIN(RH)
        RRH(1.1)=CRH
        RRH(2,2)=1.0
        RRH(3,3)=CRH
        RRH(1.2)=0.0
        RRH(2,1)=0.0
        RRH(2,3)=0.0
        RRH(3,2)=0.0
        RRH(1,3)=-SRH
        RRH(3,1)=SRH
        TYPE"CRH,SRH,RRH CALCULATED"
C               ZERO NSTICK
        DO 300 I=0,255
        NSTICK(I)=0
300     CONTINUE
C               CALCULATE PRODUCTS INVOLVING RHO AND THETA
        S2C=STH*STH*CRH
        SCS=STH*CTH*SRH
        SS=STH*SRH
        TYPE "BEGIN LOOP 800"
C               LOOP 800 TO CALCULATE FOR DIFFERENT DOMAIN ANGLES ALPHA
        DO 800 NA=1.NAL
        AL=(NA-0.5)*DAL
        CAL=COS(AL)
        SAL=SIN(AL)
        SCSC=SCS*CAL
        SSS=SS*SAL
        TYPE"600 NA=  ".NA
C               CALCULATE SPLITTING FOR FOUR QUADRANTS IN ALPHA
C       QAUDRANT N DETERMINES SIGN OF SIN(AL)AND COS(ALPHA), NSA & NCA
        DO 600 N=1,4
        GOTO (501,502.503,504),N
501     NSA=1
        NCA=1
        GOTO 510
502     NSA=1
        NCA=-1
        GOTO 510
503     NSA=-1
        NCA=-1
        GOTO 510
504     NSA=-1
        NCA=1
510     SOM=S2C+NCA*SCSC
```

```
        PHM=ATAN(-SSS/SOM)
        CPM=COS(PHM)
        SPM=SIN(PHM)
        H1=CRH-(1.0+CPM)*SOM+SPM*SSS*NSA
        H2=CRH-(1.0-CPM)*SOM-SPM*SSS*NSA
        PMA=PHM
        IF (ABS(H1).GT.ABS(H2)) GOTO 550
        PMA=PHM+PI
550     CONTINUE
        PMO=PI
        STORQ=NSA*PHM
        PML=PHM
        IF (STORQ.LT.0.0) GOTO 561
        PML=PHM+PI
561     CONTINUE
C       WE NOW HAVE CALCULATED FOR ALPHA THE RELEVANT VALUES PHI
C       THAT GIVE MINIMUM ENERGY
        RAL(1,1)=CAL*NCA
        RAL(2,2)=RAL(1,1)
        RAL(1,2)=SAL*NSA
        RAL(2,1)=-RAL(1.2)
        GOTO (581,582,583),NOPT
581     CALL SPLIT(QQ.PMO.RPH,RTH,RAL,RRH,NSTICK.NSP)
        GOTO 590
582     CALL SPLIT(QQ,PMA,RPH,RTH,RAL,RRH,NSTICK,NSP)
        GOTO 590
583     CALL SPLIT(QQ,PML,RPH,RTH,RAL,RRH,NSTICK,NSP)
590     CONTINUE
600     CONTINUE
800     CONTINUE
C               CALCULATE THE PROPER ELEMENTS OF NSTICK
C                FOR DISPLAY WITH SPEC PROGRAM
        DO 850 N=0,255
        NNSTICK(N+N+1)=NSTICK(N)
850     CONTINUE
        CALL WRBLK(1,0,NNSTICK,4,IERR)
        IF (IERR.EQ.1) GOTO 890
        TYPE"ERROR CODE WRBLK = ",IERR
        GOTO 990
890     CONTINUE
        WRITE (10.900) (I, NSTICK(I), I=0,138)
        ACCEPT "TYPE ANY INTEGER TO CONTINUE", WX
        WRITE (10,900) (I, NSTICK(I), I=139,255)
900     FORMAT (6(I4,"-",I4,3X))
990     END
```

DP1:DROBNYBU:TRANSF.FR 7/31/81

```
      SUBROUTINE TRANSF(RI.RO.RR)
      DIMENSION RI(3.3),RO(3.3).RR(3.3)
C     THIS SUBROUTINE CALCULATESIN A CLUMSY WAY THE MATRIX TRANSFORMATION
     FOR RR = RO(-1)*RI*RO
C     THE ELEMENTS ARE CALCULATED WITH
C    -RR(I,J) = SUM(K).SUM(L) (RO-1(I,K) * RI(K,L) *RO(L.J) )
C             = SUM(K).SUM(L)  RO(K.I) * RI(K,L) * RO(L,J)
      DO 40 I=1,3
      DO 30 J=1.3
      EL=0.0
      DO 20 K=1.3
      DO 10 L=1,3
      EL=EL+RO(I,K)*RI(K,L)*RO(J.L)
10    CONTINUE
20    CONTINUE
      RR(I,J)=EL
30    CONTINUE
40    CONTINUE
      RETURN
      END
```

```
DP1:DROENYBU:SPLIT.FR  7/31/81
        SUBROUTINE SPLIT(Q.PHI.RPHI,RTHE,RALP,RRHO,NSTICK,NST)
        DIMENSION Q(3,3).RPHI(3,3).RTHE(3,3),RALP(3,3),RRHO(3,3)
        DIMENSION NSTICK(0:255)
        DIMENSION RM1(3.3).RM2(3,3)
C       THIS SUBROUTINE CALCULATES A STICK SPECTRUM FOR ROTATED SMECTIC
    PHASES.
C       Q IS THE MATRIX CONTAINING THE AVERAGED QUADRUPOLAR INTERACTION
C       TENSOR (CARTESIAN COORDINATES) IN THE L.C. DIRECTOR FRAME.
C       RPHI.RTHE(THA),RALP(HA) AND RRHO ARE THE MATRICES WHICH DESCRIBE
C       THE TRANSFORMATION OF Q INTO THE LAB FRAME.
C       RHO IS THE ROTATION ANGLE
C       ALPHA CHARACTERIZES THE DOMAIN
C       THETHA IS THE TILT ANGLE
C       PHI GIVES THE ORIENTATION OF THE LOCAL DIRECTORS ON THE CONE
C       NSTICK IS AN ARRAY WHICH COMPRISES THE CALCULATED STICK SPECTRUM
C       NST IS THE ELEMENT OF NSTICK FOR WHICH THE SPLITTING
C       IS MAXIMUM; NST CAN BE USED TO NORMALIZE THE CALCULATED SPECTRUM
C       WITH RESPECT TO THE OBSERVED SPECTRA.
C       TRANSF IS THE SUBROUTINE TO CALCULATE MATRIX TRANSFORMATIONS
        CPH=COS(PHI)
        SPH=SIN(PHI)
        RPHI(1,1)=CPH
        RPHI(2,2)=CPH
        RPHI(1,2)=SPH
        RPHI(2.1)=-SPH
        CALL TRANSF(Q,RTHE,RM1)
        CALL TRANSF(RM1,RPHI,RM2)
        CALL TRANSF(RM2,RTHE.RM1)
        CALL TRANSF(RM1,RALP.RM2)
        CALL TRANSF(RM2,RRHO,RM1)
        NSX=ABS(RM1(3,3)*NST)
        TYPE RM1(3.3), NSX
        NSTICK(NSX)=NSTICK(NSX)+1
        RETURN
        END
```

```
DP1:DROBNYBU:SMECT01.FR 7/31/81

        DIMENSION NAH(256),NHH(128),NHD(128)
        CALL OPEN(1,"DPOF:RESERVED:SCRATCH",3,IERR)
        TYPE "ERROR CODE OPEN = ",IERR
100     WRITE(10) "PROGRAM SMECT01, JUNE 28, 1977. "
        TYPE "CALCULATES THE DEPENDENCE OF THE MAGNETIC ENERGY "
        TYPE "AND THE MAGNETIC TORQUE ON THE ANGLE OF ROTATION."
        TYPE "REAL DISPLAY IS MAGNETIC ENERGY."
        TYPE "IMAGINARY DISPLAYIS MAGNETIC TORQUE."
        ACCEPT "GIVE THE TILT ANGLE THETA  ",TH1
        ACCEPT "GIVE THE ROTATION ANGLE RHO  ",RH1
        ACCEPT "GIVE THE DOMAIN ANGLE ALPHA  ",AL1
        WRITE(10) "128 VALUES OF THE CONE ANGLE PHI ARE CALCULATED."
        NPH=128
        PI=4.0*ATAN(1.0)
        TH=2.0*PI*TH1/360
        RH=2.0*PI*RH1/360
        CTH=COS(TH)
        STH=SIN(TH)
        CRH=COS(RH)
        SRH=SIN(RH)
        AL=2.0*PI*AL1/360
        CAL=COS(AL)
        SAL=SIN(AL)
        DO 700 NP= 1,NPH
        PH=(NP-1)*2.0*PI/NPH
        CPH=COS(PH)
        SPH=SIN(PH)
        HA=STH*(CTH*CAL*SRH+STH*CRH)
        HB=STH*SAL*SRH
        HO=CRH-(1.0+CPH)*HA+SPH*HB
        NHH(NP)=HO*HO*10000
        H1=SPH*HA+CPH*HB
        NHD(NP)=HO*H1*10000
        NAH(NP+NP-1)=(6.0*HO*HO-3.0)*10000
        NAH(NP+NP)=(9.0*HO*H1)*10000
700     CONTINUE
        WRITE (10,300),TH1,RH1,AL1
300     FORMAT (" MAGNETIC ENERGY AND TORQUE CALCULATED FOR",/,
     F  " THETA =",F5.1,"   RHO =",F5.1,"   ALPHA =",F5.1)
        WRITE(10,400),NHH,NHD
400     FORMAT (" MAGNETIC ENERGY HH",/,8(16I5,/),/,
     F  " MAGNETIC TORQUE HD",/,8(16I5,/))
        CALL WRBLK(1,0,NAH,2,IERR)
        IF (IERR.EQ.1) GOTO 900
        TYPE "ERROR CODE WRBLK =",IERR
900     CALL RESET
        END
```

Appendix 2.4:

In this appendix we present the commutators and rotations of use in section 2.3.

Commutators

$$[I_{p,i}, I_{p,j}] = iI_{p,k} \qquad [I_{p,2}, I_{q,2}] = -\frac{1}{2}I_{r,1}$$

$$[I_{p,1}, I_{q,2}] = -\frac{i}{2}I_{r,2} \qquad [I_{p.1}, I_{q,3} - I_{r,3}] = 0$$

$$[I_{p,2}, I_{q,1}] = -\frac{i}{2}I_{r,2}$$

Rotations

$$e^{-i\theta I_{p,i}} I_{p,j} e^{i\theta I_{p,1}} = I_{p,j}\cos\theta + I_{p,k}\sin\theta$$

$$e^{-i\theta I_{p,1}} I_{q,1} e^{i\theta I_{p,1}} = I_{q,1} \cos{}^{\theta}/2 + I_{r,1}\sin{}^{\theta}/2$$

$$e^{-i\theta P_{p,1}} I_{q,2} e^{i\theta I_{p,1}} = I_{q,2}\cos{}^{\theta}/2 - I_{r,2}\sin{}^{\theta}/2$$

$$e^{-i\theta I_{p,2}} I_{q,1} e^{i\theta I_{p,2}} = I_{q,1}\cos{}^{\theta}/2 - I_{r,2}\sin{}^{\theta}/2$$

$$e^{-i\theta I_{p,2}} I_{q,2} e^{i\theta I_{p,2}} = I_{q,2}\cos{}^{\theta}/2 - I_{r,1}\sin{}^{\theta}/2$$

where p, q, r = x, y, z or cyclic permutation

and i, j, k = 1, 2, 3 or cyclic permutation .

Chapter 3: A MULTIPLE QUANTUM PROTON NMR STUDY OF AN ALKANE ORIENTED IN A NEMATIC LIQUID CRYSTAL

3.1 Introduction

In this chapter we will use the method of multiple quantum nmr (mqnmr) spectroscopy to study a nonrigid chain molecule oriented in a nematic liquid crystal solvent. In section 3.2 some general aspects of multiple quantum nmr will be discussed. We will first review the conventional pulsed nmr experiment in order to understand why only single quantum transitions are allowed. We will then discuss pulse sequences that will enable us to observe the multiple quantum transitions that are normally forbidden in conventional nmr. It will be useful to think of the mqnmr experiment as being composed of four parts:

a) the preparation period in which multiple quantum coherent states are produced;

b) the evolution period during which the multiple quantum coherences evolve under some internal Hamiltonian $\mathcal{H}_1$;

c) the mixing period in which multiple quantum coherences are converted back to observable single quantum coherences;

d) the detection period during which the resulting single quantum coherent states are observed as they evolve under some internal Hamiltonian $\mathcal{H}_2$.

As an example, we will calculate the multiple quantum proton spectrum of a methyl group in which the protons are coupled to each other through the direct dipole-dipole interaction.

Finally, we will consider the utility of mqnmr in the study of oriented systems and specifically of molecules dissolved in liquid crystal solvents. We will discuss the spectral simplification expected for coupled spin $\frac{1}{2}$ systems without symmetry, and the multiple quantum orders that will yield sufficient information to allow us to calculate the independent coupling constants characterizing the system.

In section 3.3 we will first discuss the symmetry operations that exist on the nmr time scale for an alkyl chain undergoing rapid gauche-trans interconversions. As a specific example we will consider n-hexane-1,1,1,6,6,6-d_6 (n-hexane-d_6). Having found the symmetry group, the energy level diagram of the nuclear spin system will be obtained, and from the energy level diagram, we will predict the number of transitions that will be observed in each multiple quantum spectral order. Then we will develop a theory of the orientational dependence of dipolar couplings in a nonrigid chain, using a rotational isomeric model to describe chain interconversions on the nmr time scale. We will consider several models in which the configurational states are populated to varying extents, and we will describe the general form of the order tensor required for each conformational symmetry.

In section 3.4 we will review the results of a mqnmr study of n-hexane-d_6, oriented in a nematic liquid crystal solvent. In particular, we will concern ourselves with the analyses of the 6 and 7 quantum spectral orders, since those orders yield sufficient information to allow a determination of the ten independent proton-

proton coupling constants of the system. Using the rotational isomeric approach mentioned above, a set of average coupling constants will be calculated for each conformational model, and will be used to generate theoretical 6 and 7 quantum spectra. The theoretical spectra for each model will be compared to the experimental data. Finally, iterative improvements of the theoretical spectra will be discussed.

Before proceeding, a few comments on notation are in order. In describing time domain nmr experiments, we will find it convenient to expand the density matrix in some type of operator basis

$$\rho(t) = \sum_i a_i(t) O_i + 1 \quad . \tag{1}$$

In section 2.3 such a "fictitious spin $\frac{1}{2}$" basis was introduced which has the advantage of dividing the 9-dimensional spin space into three 3-dimensional subspaces. The three operators spanning each subspace ($I_{p,i}$: p = x,y,z; i = 1,2,3) are related by the commutation rules:

$$[I_{p,i}, I_{p,j}] = iI_{p,k} \qquad p = x,y,z \quad i,j,k = 1,2,3 \tag{2}$$

or a cyclic permutation.

There is an additional condition that

$$I_{x,3} + I_{y,3} + I_{z,3} = 0 \tag{3}$$

which is necessary since the entire spin space must be spanned by the identity operator and eight other linearly independent operators. This is an especially convenient basis for describing transitions in systems of interacting and noninteracting spin 1 nuclei, since evolution of p operators can be confined to p space.

Another "fictitious spin $\frac{1}{2}$" operator basis has been introduced (78,79) which is convenient for describing single and multiple-quantum transitions. Three operators are associated with a transition r → s and are defined as follows;

$$<\psi_i|I_x^{(rs)}|\psi_j> = \frac{1}{2}(\delta_{ir}\delta_{js} + \delta_{is}\delta_{jr}) \tag{4a}$$

$$<\psi_i|I_y^{(rs)}|\psi_j> = \frac{i}{2}(-\delta_{ir}\delta_{js} + \delta_{is}\delta_{jr}) \tag{4b}$$

$$<\psi_i|I_z^{(rs)}|\psi_j> = \frac{1}{2}(\delta_{ir}\delta_{jr} - \delta_{is}\delta_{js}) \tag{4c}$$

The three operators are related by the familiar commutation rules

$$[\, I_\alpha^{(rs)}, I_\beta^{(rs)}] = iI_\gamma^{(rs)} \tag{5}$$

where (α,β,γ) is a cyclic permutation of (x,y,z). Also, given three states r, s, and t, the z components of the 3 operator sets are related by

$$I_z^{(rs)} + I_z^{st} + I_z^{rt} = 0 \quad . \tag{6}$$

Like the earlier "fictitious spin $\frac{1}{2}$" basis, this basis has the advantage that evolution of rs operators occurs entirely within an rs subspace.

In the treatment of multiple quantum nmr that follows, we will be primarily concerned with the general symmetry properties of multiple quantum coherent states as they evolve under a secular internal Hamiltonian, rather than explicitly calculating the set $\{a_i(t)\}$. Therefore, an expansion of the density matrix of a system of N spins $\frac{1}{2}$ in terms of a spherical tensor operator basis will suffice:

$$(t) = \sum_{L=-N}^{N} \sum_{M=-L}^{L} A_{LM}(t)\, A_{LM} \tag{7}$$

This is an especially convenient basis since, as will be presently shown, for a given tensor operator A_{LM}, M corresponds to the change in the magnetic quantum number. Therefore $A_{L\pm 1}$ is a one quantum operator, $A_{M\pm 2}$ is a two quantum operator, etc. Also, the operators I_x, I_y, and I_z are related to the complex angular momentum operators in the following ways.

$$I_0 = I_z \tag{8a}$$

$$I_\pm = I_x \pm iI_y \quad , \tag{8b}$$

and the complex angular momentum operators have the following commutation rules with spherical tensors:

$$\left[I_0, A_{LM}\right] = M \quad {}_{LM} \tag{9a}$$

$$\left[I_\pm\ , A_{LM}\right] + (L\pm M\pm 1)(L\pm M)\ \tfrac{1}{2} A_{LM}{\pm 1} \tag{9b}$$

3.2 Basic Principles of Multiple Quantum NMR

3.2.1 Single Quantum NMR

In section 1.3.3 we studied the linear response of a spin system to a pulsed r.f. field and found that the components of the resulting transverse magnetization are given by the expressions:

$$<I_x> \propto \sum_{mn}(e^{(-i(\omega_{nm}+\Delta\omega)-\frac{1}{T_2})t} - e^{(i(\omega_{nm}-\Delta\omega)-\frac{1}{T_2})t}|(I_x)_{nm}|^2 \tag{10}$$

$$<I_y> \propto \sum_{mn}(e^{(-i(\omega_{nm}+\Delta\omega)-\frac{1}{T_2})t} + e^{(-i(\omega_{nm}-\Delta\omega)-\frac{1}{T_2})t}|(I_y)_{nm}|^2 \quad . \tag{11}$$

We note that the x component of the magnetization is proportional to $|<n|I_x|m>^2$ and the y component is proportional to $|<n|I_y|m>|^2$. I_x and I_y are related to components of the first rank spherical tensor by the expressions:

$$I+ = -\frac{1}{\sqrt{2}}(I_x + iI_y) \tag{12}$$

$$I- = +\frac{1}{\sqrt{2}}(I_x - iI_y) \tag{12b}$$

$$I_0 = I_z \tag{12c}$$

In addition, matrix elements of I_0 and I± are governed by the expressions

$$<jm'|I_0|mj> = m\delta m,m' \tag{12d}$$

$$<jm'|I\pm|mj> = [(j\pm m\pm 1)(j\pm m)]^{1/2}\delta m', m\pm 1 \tag{12e}$$

Therefore, the operators I± can only connect spin states that differ in their magnetic quantum numbers by one, as shown in figure 31. A more general statement is the Wigner-Eckart theorem which has the form:

$$<j'm'|\mathcal{A}_{LM}|jm> = C(jLj';\, mMm')<j'\|\mathcal{A}_L\|j> \quad . \tag{13}$$

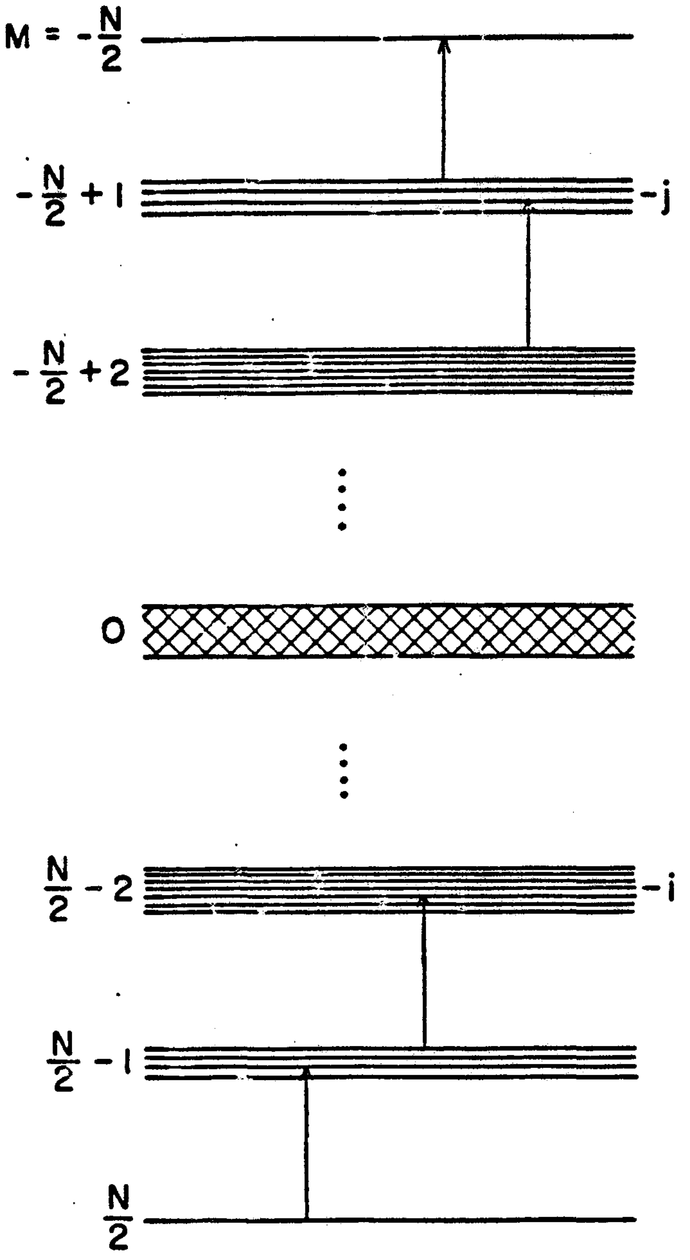

XBL 7710-10022

Figure 31. Generalized energy level diagram of a system of N coupled spin ½ nuclei. The single quantum nmr experiment only produces coherent states between energy levels differing in magnetic quantum number by ±1. Such allowed transitions are indicated by the arrows in the diagram.

$\langle j' \| A_L \| j \rangle$ is a reduced matrix element of the set of tensor operators A_{LM}, and for the Clebsch-Gordon coefficient $C(jLj';mMm')$ to be nonzero, angular momentum must be conserved:

$$\Delta(jLj') \text{ and } m' = M+m \quad . \tag{14}$$

Therefore, if $M = \pm 1$ we get the condition

$$m' = m\pm 1 \quad , \tag{15}$$

and we see that any operator of the form $A_{L}\pm 1$ can only connect states differing in magnetic quantum number by ±1. Evidently, if we expand the density matrix of a system of N spins in a spherical tensor operator basis, the conventional nmr experiment will only yield coherent states that correspond to operators of the form $A_L \pm 1$. Let us examine the reasons for this in detail.

Suppose a spin system at equilibrium is exposed to an r.f. field for a time t_p, and that the r.f. field is of sufficient intensity that

$$\omega_{rf} >> \|\mathcal{H}_{int}\| \quad . \tag{16}$$

Then as we have mentioned, the rotating frame Hamiltonian during the pulse is, assuming the field is linearly polarized along the y axis,

$$\mathcal{H} \sim -\omega_{rf} I_y \quad . \tag{17}$$

A single quantum coherent state must be produced due to the commutation relations between I_x, I_y, and I_z. That is, the density matrix after the pulse is

$$\rho(t_p) \propto e^{-i\omega_{rf}t_pI_y}\ I_z\ e^{i\omega_{rf}t_pI_y} \quad . \tag{18}$$

To evaluate equation 18 we differentiate twice with respect to t_p:

$$\dot{\rho}(t_p) = -\omega_1 i e^{-i\omega_{rf}t_pI_y}\,[I_z,I_y]\ e^{i\omega_{rf}t_pI_y}$$

$$= -\omega_1 e^{-i\omega_{rf}tI_y}\ I_x\ e^{i\omega_{rf}tI_y} \tag{19}$$

and

$$\ddot{\rho}(t_p) = -i\omega_1^{\,2}\ e^{-i\omega_{rf}t_pI_y}\,[I_x,I_y]\ e^{i\omega_{rf}t_pI_y}$$

$$= -\omega_1^{\,2}\ e^{-i\omega_{rf}t_pI_x}\ I_z\ e^{i\omega_{rf}t_pI_x} \quad . \tag{20}$$

Therefore

$$\ddot{\rho}(t_p) = -\omega_{rf}^{\,2}\rho(t_p) \text{ or } p''(t_p) = \omega_{rf}^{\,2}\rho(t_p) = 0 \quad . \tag{21}$$

Solving the differential equation we get

$$\rho(t_p) = A\cos\omega_{rf}t_p + \beta\sin\omega_{rf}t_p \tag{22}$$

and from the boundary conditions

$$\rho(0) = I_z \text{ and } \rho'(0) = \omega_1 I_x \tag{23}$$

we get that

$$\rho(t_p) = I_z\cos\omega_1 t_p + I_x\sin\omega_1 t_p \quad . \tag{24}$$

Therefore, if the field is intense enough to enable the Hamiltonian during the pulse to be represented in a form linear in spin operators, the irradiation will produce a simple rotation in spin space due to the commutation relations between I_x, I_y, and I_z. This fact can also be appreciated in the spherical tensor basis since

$$[I_0, I_{\pm 1}] = \pm I\pm \quad . \tag{25}$$

Of course, subsequent evolution under the internal Hamiltonian of the system will only produce operators that are single quantum since, as we found in section 1.3.5, the internal Hamiltonian must be secular. To find the form of coherent states produced by evolution under a secular Hamiltonian we write I_x in terms of spherical tensors:

$$I_x = \frac{1}{2}(I_+ + I_-) \tag{26}$$

and the internal Hamiltonian has the form

$$\mathcal{H}_{int} = \lambda A_{20} \quad . \tag{27}$$

To find the effect of evolution under $\mathcal{H}_{int}$ we must evaluate terms like

$$e^{-i\lambda A_{20}t} \, I\pm \, e^{i\lambda A_{20}t} \quad . \tag{28}$$

To do this we expand the exponential terms in equation 28 to obtain

$$e^{-i\lambda A_{20}t}\; I\pm 1\; e^{i\lambda A_{20}t} \approx I + \lambda t\; I_{,}A_{20} - \frac{(t)^2}{2!}[[I\pm, A_{20}], A_{20}] \ldots\ldots \quad (29)$$

From Rachah's definition of spherical tensor operators we have that

$$[I\pm, A_{LM}] = \pm[\tfrac{1}{2}(L\pm M)(L\pm M\pm 1)]^{1/2} A_{LM\pm 1} \quad (30)$$

and therefore

$$[I\pm A_{20}] \propto A_{2\pm 1} \quad (31)$$

Now $A_{2\pm 1}$ is obviously a single quantum operator. In addition, higher order terms will also be single quantum since they will always involve commutors of $A_{L\pm 1}$ and A_{20} .

In summary, if the density matrix for a system N spins is expanded in a spherical tensor basis

$$\rho(t) = \sum_{L=-N}^{N} \sum_{M=-L}^{L} a_{LM}(t) A_{LM} \quad (32)$$

the result of the conventional pulsed nmr experiment is that $a_{LM}(t) = 0$ unless

$$M = \pm 1 \text{ for } L\pm 1 \quad (33a)$$

$$M = 0, \pm 1 \text{ for } L = 1 \quad (33b)$$

Therefore, only single quantum coherent states can exist. In the next section we will discuss a type of nmr experiment in which multiple quantum coherent states can be produced.

3.2.2 Multiple Quantum Experiments: General Scheme

Multiple quantum nmr is an example of 2-dimensional spectroscopy. For that reason, we will describe the general scheme of the experiment using a convention introduced by Ernst and coworkers for 2-dimensional nmr experiments (80,81).

As shown in figure 32, the multiple quantum nmr experiment may be divided into four parts: preparation, evolution, mixing and detection.

(i) Preparation Period

During this period of length τ, multiple quantum coherent states are produced as a result of the action of the operator U on the density matrix ρ_0.

$$\rho(\tau) = U\rho_0 U^+ \quad . \tag{34}$$

Now U has the form

$$U = e^{-i\mathcal{H}_{MQ}\tau} \tag{35}$$

where $\mathcal{H}_{MQ}$ is a Hamiltonian with nonzero multiple quantum matrix elements. Furthermore, it can be shown (12) that for U to efficiently produce multiple quantum coherence $\mathcal{H}_{MQ}$ must satisfy the condition

$$\|\mathcal{H}_{MQ}\tau\| \sim 1 \tag{36}$$

(ii) Evolution Period

During this period, the multiple quantum coherent states evolve under some internal Hamiltonian $\mathcal{H}_1$ for a time t_1. Thus, the form

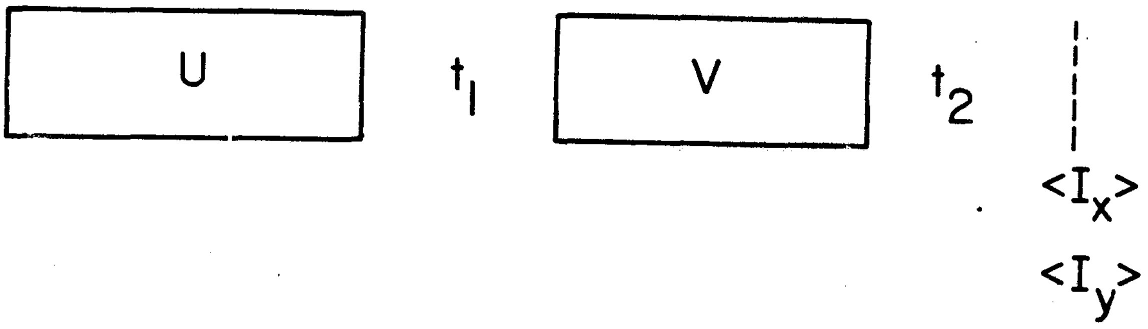

XBL 8010-12486

Figure 32. Multiple quantum nmr is an example of a two dimensional spectroscopy. The multiple quantum experiment may be thought of as being composed of four parts:

(i) A preparation time of length τ during which multiple quantum coherent states are produced by the action of a propagator U;

(ii) An evolution time of length t_1 during which the multiple quantum coherent states evolve under a Hamiltonian H_1;

(iii) A mixing time of length τ^1 during which multiple quantum coherent states are converted or mixed back to observable single quantum states by the action of a propagator V; and

(iv) A detection period, during which the single quantum singles are detected as they evolve under a Hamiltonian H_2.

of the density matrix is

$$\rho(\tau+t_1) = e^{-i\mathcal{H}_1 t_1} U \rho_0 U^+ e^{i\mathcal{H}_1 t_1} \qquad (37)$$

(iii) Mixing Period

Multiple quantum coherent states are not directly detectable since, in general, the trace of the product of a multiple quantum operator and I_x or I_y is zero. In nmr, detectable signal corresponds to coherent states that transform as components of first rank tensors. That is, transverse magnetization corresponds to coherent state operators I_x and I_y that are components of a vector operator $I = (I_x\hat{i}, I_y\hat{j}, I_z\hat{k})$. But multiple quantum coherence, as we have shown, corresponds to operators that are components of second rank tensors or higher. Therefore, we require that the multiple quantum coherence be converted, at least in part, back to detectable coherent states. This occurs during the mixing period τ' by the action of the operator V on the density matrix

$$\rho(\tau+t_1+\tau') = V e^{-i\mathcal{H}_1 t_1} U \rho_0 U^+ e^{i\mathcal{H}_1 t_1} V^+ \quad . \qquad (38)$$

It will be shown presently that V has the form

$$V = e^{-i\mathcal{H}'_{MQ}\tau'} \qquad (39)$$

where $\mathcal{H}_{MQ}$ is a Hamiltonian with nonzero multiple quantum matrix elements.

(iv) Detection Period

Through the action of V on the density matrix $\rho(\tau+t_1)$, at least some of the operators corresponding to multiple quantum coherent states are converted to single quantum operators. The evolution of these operators under the Hamiltonian $\mathcal{H}_2$ is observed during the detection period. The density matrix has the form

$$\rho(\tau+t_1+\tau_1'+t_2) = e^{-i\mathcal{H}_2 t_2} V e^{-\mathcal{H}_1 t_1} U \rho_0 U^+ e^{i\mathcal{H}_1 t_1} V^+ e^{i\mathcal{H}_2 t_2} \tag{40}$$

In general, the Hamiltonians $\mathcal{H}_1$ and $\mathcal{H}_2$ need not be the same and they need not commute.

If we assume that the initial density matrix ρ_0 is proportional to I_z, the expression for the x-component of the magnetization is

$$\begin{aligned} S_x(t_1,t_2) \propto \mathrm{Tr}(\rho(\tau+t_1+\tau'+t_2)I_x) &= \\ \mathrm{Tr}(e^{-i\mathcal{H}_2 t_2} V e^{-i\mathcal{H}_1 t_1} U I_z U^+ e^{i\mathcal{H}_1 t_1} V^+ e^{i\mathcal{H}_2 t_2} I_x) &= \\ \mathrm{Tr}(e^{-i\mathcal{H}_1 t_1} U I_z U^+ e^{i\mathcal{H}_1 t_1} V^+ e^{i\mathcal{H}_2 t_2} I_x e^{-i\mathcal{H}_2 t_2} V) & \end{aligned} \tag{41}$$

In this thesis, we will only concern ourselves with evolution under $\mathcal{H}_1$, and, as will be shown presently, only the signal at $t_2 = 0$ will be observed (with $\tau' = \tau$) as a function of t_1. Equation 41 may be rewritten:

$$S_x(t_1) \propto \mathrm{Tr}(e^{-i\mathcal{H}_1 t_1} U I_z U^+ e^{i\mathcal{H}_1 t_1} V^+ I_x V) \tag{42a}$$

and similarly

$$S_y(t_1) \propto \mathrm{Tr}(e^{-i\mathcal{H}_1 t_1} U I_z U^+ e^{i\mathcal{H}_1 t_1} V^+ I_y V) \qquad (42b)$$

Subsequent Fourier transformation of $S_x(t_1) + iS_y(t_1)$ yields the multiple quantum spectrum $F_x(\omega_1) + iF_y(\omega_2)$:

$$F_x(\omega_1) + iF_y(\omega_1) = \int dt_1 e^{-i\omega_1 t_1}(S_x(t_1) + iS_y(t_1)) \ . \qquad (42c)$$

3.2.3 Multiple Quantum Pulse Sequences

In the last section it was shown that in order to produce multiple quantum coherent states it is necessary to produce a non-secular Hamiltonian $\mathcal{H}_{MQ}$. Now it has been shown that in systems of noninteracting spin 1 nuclei, a weak pulse ($\omega_1 << \omega_Q$) applied near resonance will produce double quantum coherence (56,57,58). The pulse scheme of such an experiment is shown in figure 33. But as we found at the conclusion of section 2.3, double quantum coherences can also be produced in such a system by two high power 90^o pulses that are 180^o out of phase. We will pursue pulse sequences with the latter type of preparation.

In figure 34 is shown some basic multiple quantum pulse sequences that have been applied to systems of spin $\frac{1}{2}$ nuclei in anisotropic phases, where internuclear couplings are of the direct dipole-dipole type (58,83), and to systems of spin $\frac{1}{2}$ nuclei in isotropic phases, where internuclear couplings are of the indirect scalar type (80). We will concern ourselves with systems of the former kind.

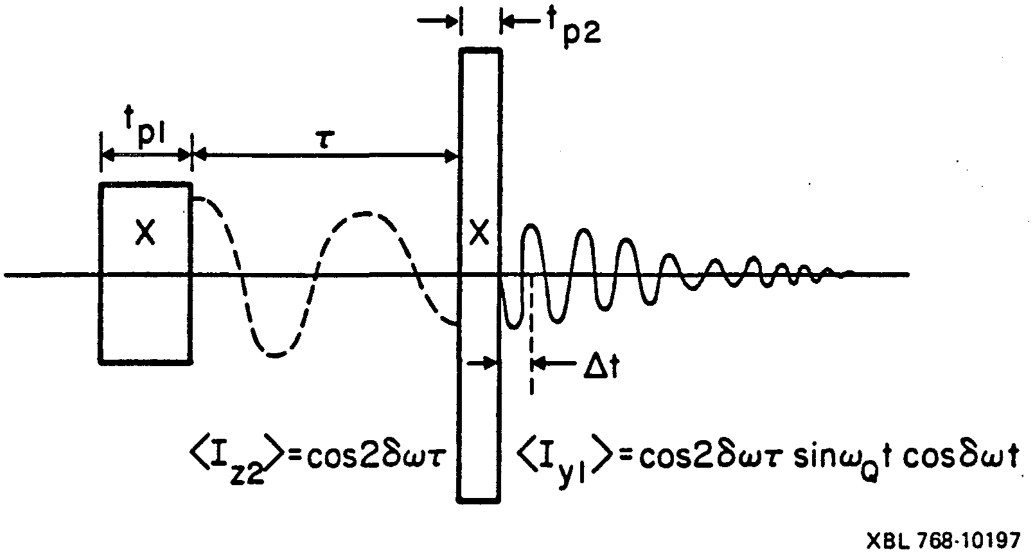
t_{p2}
t_{p1}
τ
X
X
Δt
$\langle I_{z2} \rangle = \cos 2\delta\omega\tau$
$\langle I_{y1} \rangle = \cos 2\delta\omega\tau \sin\omega_Q t \cos\delta\omega t$
XBL 768-10197

Figure 33. Multiple quantum nmr spectroscopy. A pulse sequence in which a weak pulse, applied on resonance, is used to prepare multiple quantum coherent states.

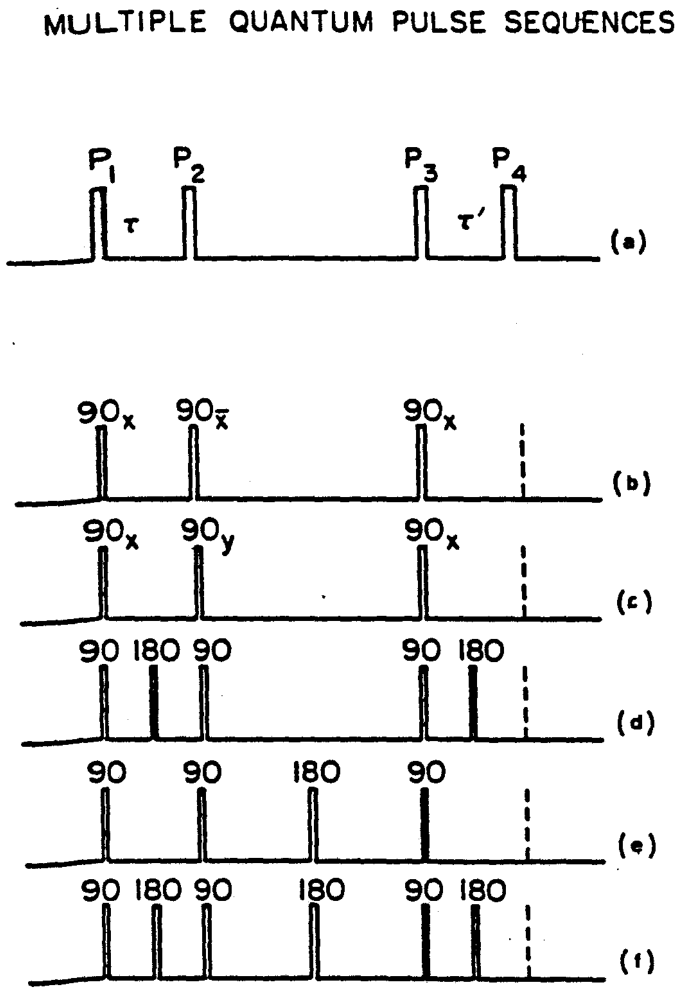
MULTIPLE QUANTUM PULSE SEQUENCES
P1
P2
P3
P4
τ
τ′
(a)
90x
90x̄
90x
(b)
90x
90y
90x
(c)
90 180 90
90 180
(d)
90
90
180
90
(e)
90 180 90
180
90 180
(f)

XBL 788-10105

(Figure 34)

Equation 46 may be rewritten in terms of spherical tensor operators

$$\mathcal{H}^{D}_{yy} = \sum_{i<j} D_{ij}(A_{20}(ij) + (\tfrac{3}{2})^{\frac{1}{2}} (A_{22}(ij) + A_{2-2}(ij)), \qquad (47)$$

and we see that $\mathcal{H}^{D}_{yy}$ contains zero quantum operators $A_{20}(ij)$ and double quantum operators $A_{2\pm2}(ij)$.

To evaluate equation 42 we first use the identities $I_z = I_0$ and $I_x = \frac{1}{2}(I_+ + I_-)$. Therefore we must evaluate

$$e^{-i\mathcal{H}^{D}_{yy}\tau} I_0 \, e^{i\mathcal{H}^{D}_{yy}\tau} \cos\Delta\omega\tau \qquad (48a)$$

and

$$e^{-i\mathcal{H}^{D}_{yy}\tau} I \, e^{i\mathcal{H}^{D}_{yy}\tau} \sin\Delta\omega\tau \, . \qquad (48b)$$

If $|D_{ij}'\tau| < 1$ we can evaluate 48a by expanding the exponentials as we did in the last section. We obtain

$$e^{-i\mathcal{H}^{D}_{yy}\tau} I_0 \, e^{i\mathcal{H}^{D}_{yy}\tau} = I_0 + i \sum_{i<j} D_{ij}\tau([I_0, A_{20}(ij)] + (\tfrac{3}{2})^{\frac{1}{2}}([I_0, A_{22}(ij)] + [I_0, A_{2-2}(ij)])) + \text{higher order terms.} \qquad (49)$$

From equation 9a we see that the first order terms will yield 2-quantum operators since

$$[I_0, A_{20}(ij)] = 0 \qquad (50a)$$

$$[I_0, A_{2\pm2}(ij)] = 2A_{2\pm2}(ij) \qquad (50b)$$

Second order terms will have the forms

$$\tau^2 D'_{ij} D'_{1m} [A_{2\pm 2}(ij),\ A_{20}(\ell m)] \tag{51a}$$

$$\tau^2 D'_{ij} D'_{1m} [A_{2\pm 2}(ij),\ A_{2\pm 2}(\ell m)] \tag{51b}$$

$$\tau^2 D'_{ij} D'_{1m} [A_{2\pm 2}(ij),\ A_{2\mp 2}(\ell m)] \tag{51c}$$

After summing over i, j, ℓ, and m such that $i < j$ and $\ell < m$, we find that terms like

$$[A_{2\pm 2}(ij),\ A_{20}(im)] \tag{52a}$$

form 2-quantum operators and terms like

$$[A_{2\pm 2}(ij),\ A_{2\mp 2}(im)] \tag{52b}$$

form zero-quantum operators. Terms like 51b are zero.

Higher-order terms produce higher quantum operators. For example, third order terms will appear of the form

$$\tau^3 D'_{ij} D'_{im} D'_{i\ell} [[A_{2\pm 2}(ij),\ A_{20}(im)],\ A_{2\pm 2}(i\ell)] \tag{53}$$

and will yield operators like

$$A_{4\pm 4}(ij,\ell m) \tag{54}$$

which are 4-quantum operators.

Equations 51 and 53 point out an important fact in multiple quantum nmr. We note that first order terms, which yield two quantum operators, are proportional to $\tau D'_{ij}$, second order terms are proportional to $\tau^2 D'_{ij} D'_{m}$, and in general the n^{th} order term is proportional to the product of n $\tau D'_{ij}$'s. Therefore, unless so $\rho(\tau) \neq \rho(\tau+t_1)$. We also note that for the three pulse sequence V has the form, assuming $\tau' = \tau$

$$V = e^{-i\mathcal{H}_{MQ}\tau} , \tag{60}$$

and therefore V is not the adjoint of U. To find the effect of this we write the expression for the signal at $t_2 = 0$:

$$\begin{aligned} S_y(t_1;\tau,\tau') &= \mathrm{Tr}(\rho(\tau+t_1+\tau')I_z) \\ &= \mathrm{Tr}(V\, e^{-i\mathcal{H}_1 t_1}\, U\, I_z U^+\, e^{i\mathcal{H}_1 t_1}\, V^+\, I_z) \\ &= \mathrm{Tr}(e^{-i\mathcal{H}_1 t_1}\, U\, I_z U^+\, e^{i\mathcal{H}_1 t_1}\, V^+\, I_z\, V) \end{aligned} \tag{61}$$

where we have used the fact that the trace is invariant to cyclic permutations. Now if we expand the trace in an eigenbasis of $\mathcal{H}_1$ we get

$$S_y(t_1;\tau,\tau') = \sum_{mn} e^{-i\omega_{mn}t_1}\, (U\, I_z\, U^+)_{mn}\, (V^+\, I_z\, V)_{nm} \tag{62}$$

If $U = V^+$ we would obtain

$$\begin{aligned} S_y(T_1;\tau,\tau') &= \sum_{mn} e^{-i\omega_{mn}t_1}\, (U\, I_z\, U^+)_{mn}(U\, I_z\, U^+)^*_{mn} \\ &= \sum_{mn} e^{-i\omega_{mn}t}\, (|U\, I_z\, U^+|^2)_{mn} \end{aligned} \tag{63}$$

But when $U \neq V^+$, as in the case in the 3-pulse experiment, phase terms will occur in $S_y(t_1;\tau,\tau')$. This means that the multiple quantum coherent states are out of phase, a condition which does not occur in single quantum nmr (see equations 10 and 11).

(ii) Four-Pulse Experiments: Echoes in t_1

The 3-pulse sequence is of limited utility for the following reason. Let us consider evolution of the density matrix

$$\rho(\tau) = \sum_M \rho_M(\tau) \tag{64}$$

under the Hamiltonian

$$\mathcal{H}_1 = -\Delta\omega(r) I_z + \mathcal{H}_{zz}^D \quad . \tag{65}$$

The first term implies that the offset is specially dependent, a situation that would occur in an inhomogeneous magnetic field. As before, we can consider evolution under the first term separately from evolution under the second tern since $\Delta\omega(r)I_z$ and $\mathcal{H}_{zz}$ commute. Evolution under the first term is identical to equation 55:

$$e^{i\Delta\omega(r)t_1 I_z} \rho_M(\tau)\, e^{-i\Delta\omega(r)t_1 I_z} = \rho_M(\tau)\, e^{-iM\Delta\omega(r)t_1} \tag{66}$$

Equation 66 implies that the inhomogeneous broadening is proportional to M, the order of the multiple quantum coherence. Therefore the inhomogeneous broadening in the M-quantum spectrum is M times the inhomogeneous broadening in the single quantum spectrum, a fact which would limit resolution and signal-to-noise in the high quantum orders.

A solution to the problem is to apply a 180° pulse in the center of the evolution time (see figure 35). This is the Hahn spin echo technique (85). The expression for the density matrix at the end of t_1 is:

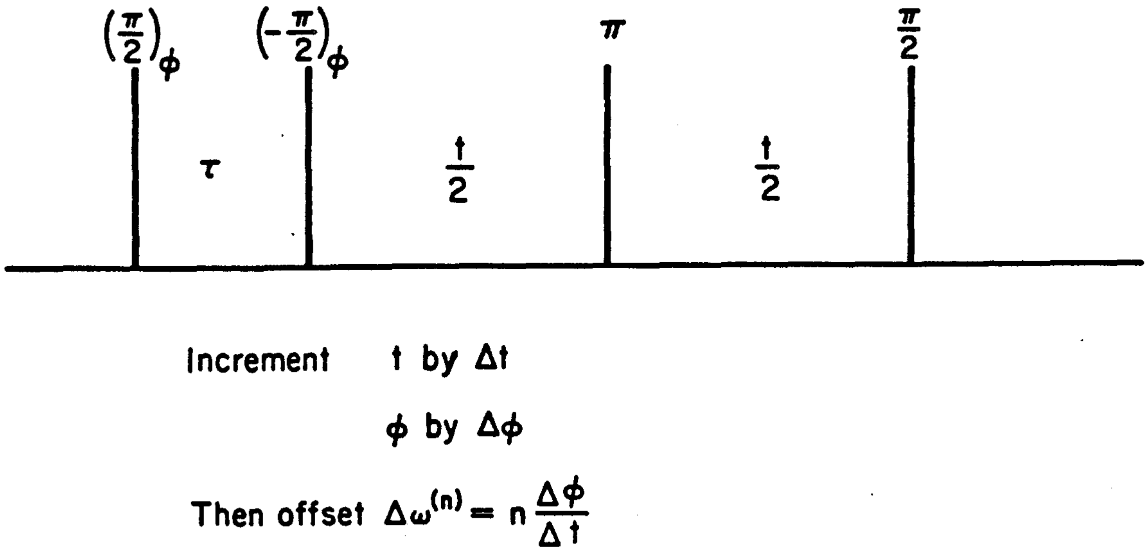
$(\frac{\pi}{2})_\phi$
$(-\frac{\pi}{2})_\phi$
π
$\frac{\pi}{2}$
τ
$\frac{t}{2}$
$\frac{t}{2}$
Increment t by Δt
ϕ by $\Delta\phi$
Then offset $\Delta\omega^{(n)} = n\frac{\Delta\phi}{\Delta t}$

XBL 796-10254

Figure 35. Time proportional phase incrementation (TPPI). Multiple quantum orders may be separated by off resonant irradiation unless a 180° pulse is included in the middle of the evolution time. But the multiple quantum orders may still be separated by an incrementation of the phases of the first two pulses (P_1 and P_2) relative to the third and fourth pulses. When the evolution time is incremented at Δt_1, the phase is incremented by $\Delta\phi$. The effective offset is then, for the n^{th} multiple quantum order $n\Delta\omega = \frac{\Delta\phi}{\Delta t_1}$.

$$\rho_M(\tau+t_1) = e^{-i\mathcal{H}_1 t_{1/2}}\, e^{i\pi I_x}\, e^{-i\mathcal{H}_1 t_{1/2}}\, \rho_M(\tau)\, e^{i\mathcal{H}_1 t_1}\, e^{-i\pi I_x}\, e^{i\mathcal{H}_1 t_{1/2}} \tag{67}$$

where $\mathcal{H}_1$ is given by equation 65. We now use the facts that $\mathcal{H}_{zz}$ and I_z commute, that $\mathcal{H}_{zz}$ is invariant to a 180° pulse, and the identity

$$e^{i\pi I_x}\, e^{i\Delta\omega(r) I_z t_{1/2}}\, e^{-i\pi I_x} = e^{-i\Delta\omega(r) I_z t_{1/2}} \tag{68}$$

to obtain the expression

$$\begin{aligned}\rho_M(\tau+t_1) &= e^{-i\mathcal{H}_1 t_{1/2}}\, e^{-i\Delta\omega(r) I_z t_{1/2}}\, e^{-i\mathcal{H}^D_{zz} t_{1/2}}\, \rho_M(\tau) \\ &\qquad e^{i\Delta\omega(r) I_z t_{1/2}}\, e^{i\mathcal{H}_1 t_{1/2}} \\ &= e^{-i\mathcal{H}^D_{zz} t_1}\, \rho'_M(\tau)\, e^{i\mathcal{H}^D_{zz} t_1}\end{aligned} \tag{69}$$

where $\rho'_M(\tau)$ is specified by

$$\rho_M(\tau), \text{ if } M \text{ is even} \tag{70a}$$

$$-\ \rho_M(\tau), \text{ if } M \text{ is odd.} \tag{70b}$$

Equation 69 means that the effect of magnetic field inhomogeneity has been removed during t_1 and only evolution under $\mathcal{H}^D_{zz}$ remains. However, we also notice that the echo removes the modulation term $e^{-iM\Delta\omega t_1}$ which allowed us to separate the different multiple quantum orders. Therefore, all multiple quantum transitions for all M will occur within $\pm\Delta\omega_{max}$ of resonance, where $2\Delta\omega_{max}$ is the bandwidth of the widest multiple quantum order. This may result in an intractable spectrum if the number of spins N is large.

We will discuss two solutions to the problem, phase Fourier transformation (PFT) and time proportional phase incrementation (TPPI).

PFT amounts to the selective detection of multiple quantum orders, and has been used in both isotropic systems (86) and anisotropic systems (58). Suppose we perform the 4-pulse multiple quantum experiment, and the resulting multiple quantum signal is

$$\begin{aligned} S_y(t_1;\tau,\tau') &= \sum_M \mathrm{Tr}(e^{-i\mathcal{H}_{yy}\tau} e^{-i\mathcal{H}_1 t_1} \rho_M(\tau) \times e^{i\mathcal{H}_1 t_1} e^{i\mathcal{H}_{yy}\tau} I_z) \\ &= \sum_M S_M(t_1;\tau,\tau') \quad . \end{aligned} \tag{71}$$

Now the experiment is repeated, but the phases of the first two pulses are shifted by ψ relative to the phase of the third and fourth pulses. By a phase shift is meant a rotation about the z axis. Therefore the density matrix at the end of the preparation time is

$$\rho(\tau,Q) = e^{+i\pi/2 I_\psi} e^{-i\mathcal{H}_{zz}\tau} e^{-i\pi/2 I_\psi}\,{}_0\, e^{i\pi/2 I_\psi} e^{i\mathcal{H}_{zz}\tau} e^{-i\pi/2 I_\psi} \tag{72}$$

where

$$I_\psi = e^{-i\psi I_z} I_x e^{i\psi I_z} \tag{73}$$

Using the fact that I_z commutes with $\mathcal{H}^D_{zz}$ and the definition of ρ_0 we can rewrite equation 72 as

$$\begin{aligned} \rho(\tau,\psi) &= e^{-i\psi I_z} \sum_M \rho_M(\tau)\, e^{i\psi I_z} \\ &= \sum_M \rho_M(\tau)\, e^{-iM\psi} \quad . \end{aligned} \tag{74}$$

Our expressions for $S_y(t_1;\tau,\tau',\psi)$ would now be

$$S_y(t_1;\tau,\tau',\psi) = \sum_M e^{-i\psi M}\ \mathrm{Tr}(e^{-i\mathcal{H}^D_{zz}\tau'}\ e^{-i\mathcal{H}_1 t_1}\ \rho_M(\tau)\ e^{i\mathcal{H}_1 t_1}\ e^{i\mathcal{H}^D_{yy}\tau'}\ I_z)$$

$$= \sum_M e^{-i\psi M}\ S_M(t_1;\tau,\tau') \quad . \tag{75}$$

Suppose the system has N nuclei with spin $\frac{1}{2}$, so M varies from -N to N. Let the experiment be repeated 2N times and let the phase of the first two pulses be shifted each time by $^{2\pi}/|M'|$ where M' lies between -N and N inclusively. Summing the resulting signals we obtain a Fourier expansion in phase

$$S_y(t_1;\tau,\tau') = \sum_{M=-N}^{N}\ \sum_{n=0}^{2N-1}\ e^{-iM(\frac{2\pi n}{M'})}\ S_M(t_1;\tau,\tau') \quad . \tag{76}$$

The only orders to add constructively are those for which $|M| = 2k|M'|$ and k = 0, 1, ...

The disadvantage of this type of detection is that the selectivity is limited in the sense that several orders will still be superimposed within the region $\pm\Delta\omega_{max}$. For example, if the phase increment is $\frac{\pi}{2}$, the multiple quantum coherences of order 0, 4, 8 etc. would add constructively. But as we will find in section 3.4, the zero quantum spectrum may be very complicated especially if N is large and the symmetry of the spin system is low, so an intractable spectrum may still result. The zero quantum coherent states may be eliminated by using the expansion

$$S_y(t_1;\tau,\tau') = \sum_{M=-N}^{N}\ \sum_{n=0}^{2N-1}\ (-)^n\ e^{-iM(\frac{2\pi n}{M'})}\ S_M(t_1;\tau,\tau') \quad . \tag{77}$$

Suppose we again increment the phase by $\frac{\pi}{2}$, but use the expansion given by equation 77. Then the coherences of order 2, 6, 10 etc. will add constructively. In any case, if the multiple quantum spectra are simple enough, the limited selectivity provided by PFT suffices. However, if the number of spins is large ($N \geq 8$) even the lower order multiple quantum spectra may be complicated enough so that PFT is not useful.

Time proportional phase incrementation (TPPI) has been applied primarily in anisotropic systems of spin $\frac{1}{2}$ and 1 nuclei (84, 87). TPPI enables complete separation of multiple quantum orders independent of evolution during t_1, by shifting the phases of the first 2 pulses relative to the third and fourth by an amount proportional to t_1 (see figure 37). Equation 75 may be rewritten as

$$S_y(t_1;\tau,\tau') = \sum_M e^{-i\psi(t_1)M} S_M(t_1,\tau,\tau') \quad . \tag{78}$$

Now if the timing increment in t_1 is Δt_1, and the phase increment is $\Delta\psi$, the effective modulation frequency is given by

$$\Delta\omega = \frac{\Delta\psi}{\Delta t_1}$$

or

$$\psi(t_1) = t_1\Delta\omega \quad . \tag{79}$$

Substituting 79 into 78 we get

$$S_y(t_1;\tau,\tau') = \sum_M e^{-iM\Delta\omega t_1} S_M(t_1;\tau,\tau') \quad , \tag{80}$$

and the order dependent modulation has been restored.

In figures 36, 37a and 37b are shown multiple quantum nmr spectra of benzene dissolved in a nematic liquid crystal solvent. Figure 36 shows the multiple quantum spectrum of benzene obtained from a 3 pulse experiment. In figures 37a and 37b the four pulse sequence was used and separation of the multiple quantum orders was accomplished by using the TPPI technique. In figure 37a the resolution is limited by truncation of the multiple quantum free induction decay. In figure 37b the multiple quantum signal was allowed to decay for several time constants, and subsequent Fourier transformation yielded a high resolution spectrum. Below the experimental spectrum in 37b is a stick spectrum generated by the program MQITER (88). The single quantum and multiple quantum nmr spectra of benzene have been extensively discussed in the literature (58, 83, 84, 89, 90, 91, 92), and so we will make only a few brief comments. As a consequence of the D_{6h} symmetry of benzene, all single and multiple quantum transitions may be calculated from a single independent dipole-dipole coupling constant and three scalar coupling constants.

From the single quantum spectrum these were determined to be:

$$2D_{12} = 3\sqrt{3}\,D_{13} = 8D_{14} = -867.5 \text{ hz} \tag{81a}$$

$$J_{12} = 8.0 \text{ hz} \tag{81b}$$

$$J_{13} = 2.0 \text{ hz} \tag{81c}$$

$$J_{14} = 0.5 \text{ hz} \quad . \tag{81d}$$

The multiple quantum spectra shown in figures 36, 37a, and 37b were the result of the coaddition of multiple quantum power spectra. Each power spectrum was obtained for a different value

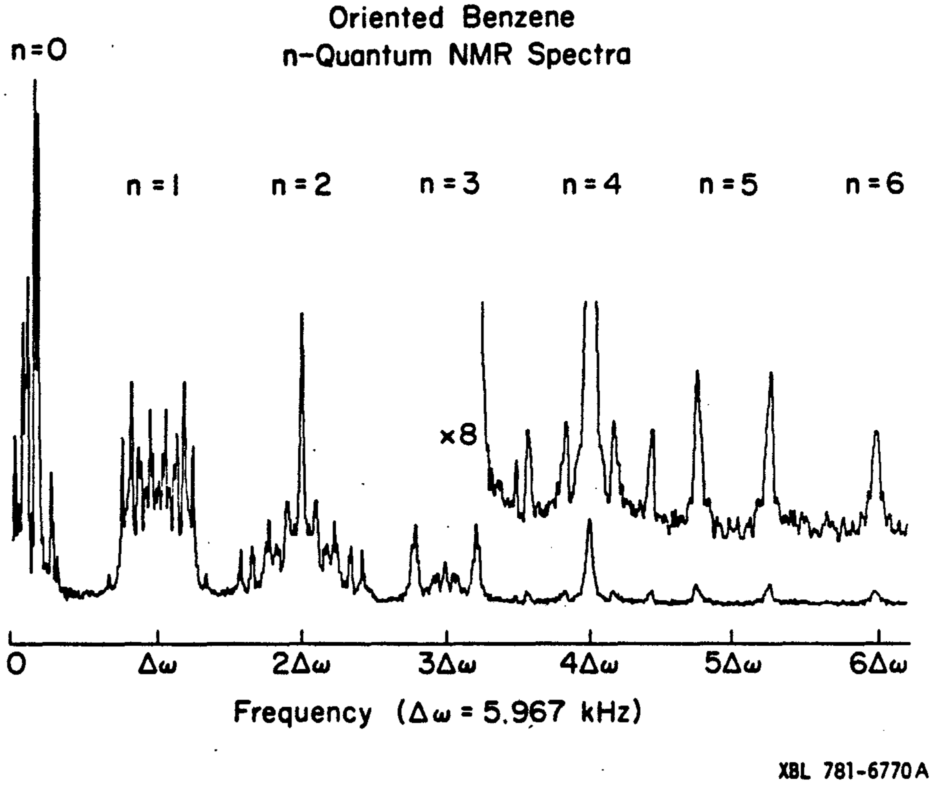

Figure 36. The multiple quantum spectrum of oriented benzene obtained by the three pulse sequence (see figure 34(b)). The irradiation was applied 5.967 khz off resonance and so all orders are observed.

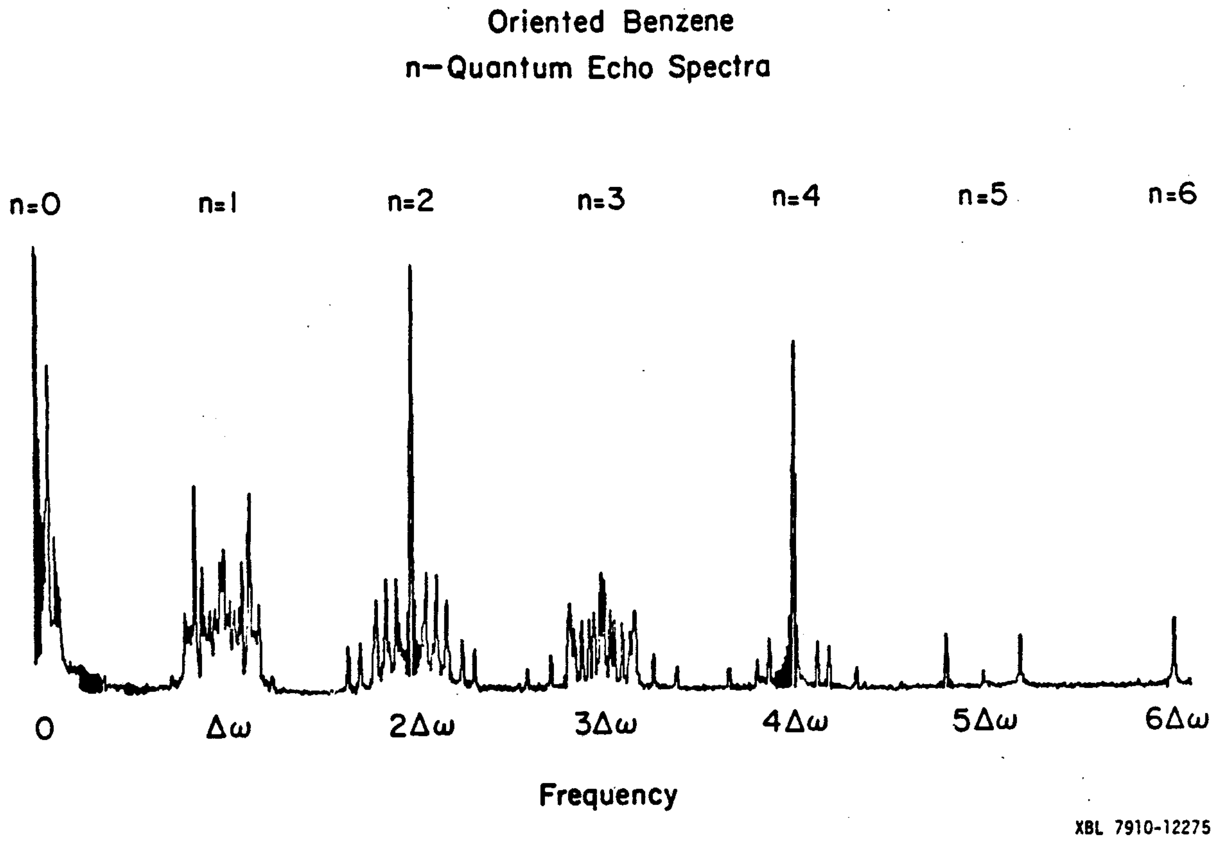

Figure 37(a). The multiple quantum spectrum of oriented benzene obtained by the TPPI pulse sequence (see figure 35). The phases of P_1 and P_2 were incremented by 29.5° each time t_1 was incremented by Δt_1 = 10 usec. Note the increased resolution relative to figure 36. The transformed FID was truncated thus limiting resolution.

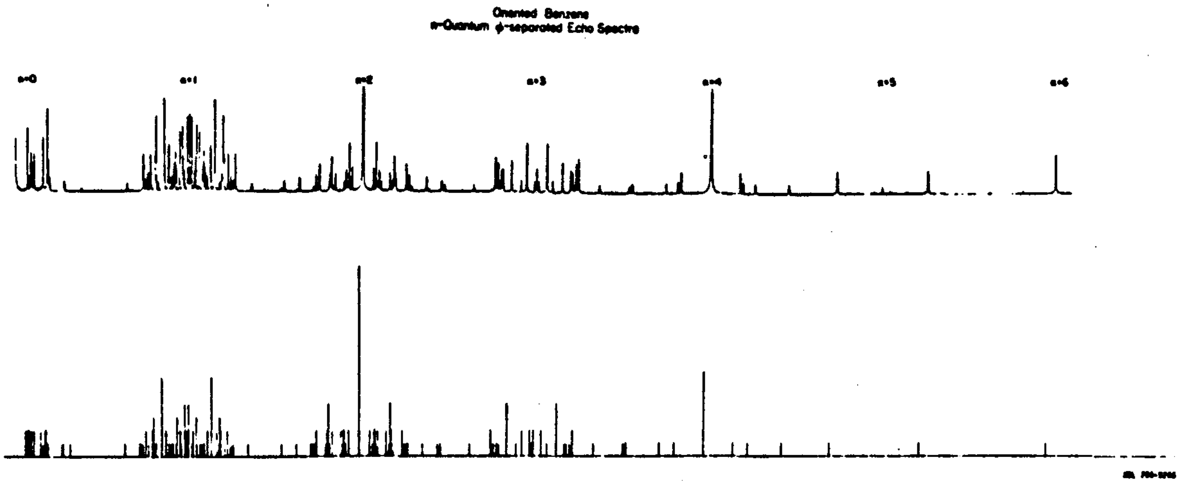

Figure 37(b). The multiple quantum spectrum of oriented benzene obtained by the TPPI pulse sequence. The multiple quantum FID was allowed to decay for at least one time constant. Below is shown the theoretical spectrum.

of the preparation time τ. Preparation times varied from 8 to 15 msec. The coaddition of several power spectra with different values of preparation time τ, is usually necessary in multiple quantum spectroscopy since multiple quantum transition intensities are a function of τ. Therefore, for a given value of τ, not all transitions may be observed. Power spectra are added since, as was shown by equation 62, multiple quantum transitions are out of phase unless $U^{+} = V$.

3.2.4 Example: Calculation of the multiple Quantum Spectrum of an Oriented Methyl Group

In sections 3.2.2 and 3.2.3 we discussed general aspects of the basic multiple quantum nmr experiment. A specific example will now be considered, that is, we will calculate the multiple quantum nmr spectrum of an oriented methyl group.

For the purposes of calculating the frequencies and intensities of multiple quantum transitions, it suffices to consider the symmetry group of an isolated, oriented methyl group as C_3. Accordingly the E representations have two states each and the A representation has four states (see table 3.1). In an oriented phase the protons are coupled through the direct dipole-dipole interaction, and the appropriate energy level diagram is given in figure 38. We see that we may treat the methyl group as 3 "pseudo-particles". Each of the "E" particles behaves as an isolated spin $\frac{1}{2}$ nucleus since the E transitions are independent of the dipole-dipole coupling, and so may only contribute to the central line of the single quantum

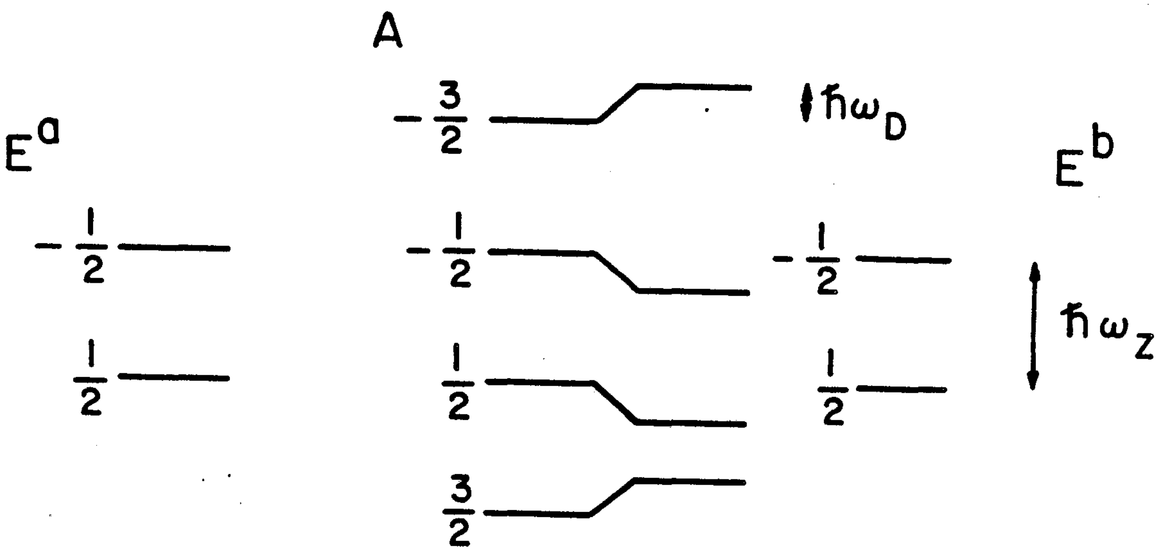
A
E^a
$-\frac{1}{2}$
$\frac{1}{2}$
$-\frac{3}{2}$
$-\frac{1}{2}$
$\frac{1}{2}$
$\frac{3}{2}$
$\hbar\omega_D$
E^b
$-\frac{1}{2}$
$\frac{1}{2}$
$\hbar\omega_z$

XBL 812-8118

Figure 38. The energy level diagram of an oriented methyl group. Multiple quantum transitions occur within the A manifold.

spectrum. The "A" particle behaves as an isolated spin $\frac{3}{2}$ particle with a "quadrupole", and we observe 3 single, 2 double, and a triple quantum transition within the A manifold (see figure 39)

Table 3.1 Symmetry-Adapted Basis Functions for an Oriented Methyl Group

(i) A representation

$$A(^3/2) = |\alpha\alpha\alpha\rangle$$
$$A(^1/2) = {}^1/\sqrt{3}\ (|\alpha\alpha\beta\rangle + |\alpha\beta\alpha\rangle + |\beta\alpha\alpha\rangle)$$
$$A(-^1/2) = {}^1/\sqrt{3}\ (|\beta\beta\alpha\rangle + |\beta\alpha\beta\rangle + |\alpha\beta\beta\rangle)$$
$$A(-^3/2) = |\beta\beta\beta\rangle$$

(ii) Ea representation

$$Ea(^1/2) = {}^1/\sqrt{3}\ (|\alpha\alpha\beta\rangle + \varepsilon|\alpha\beta\alpha\rangle + \varepsilon^*|\beta\alpha\alpha\rangle)$$
$$Ea(-^1/2) = {}^1/\sqrt{3}\ (|\beta\beta\alpha\rangle + \varepsilon|\beta\alpha\beta\rangle + \varepsilon^*|\alpha\beta\beta\rangle\ )$$

(iii) Eb representatiom

$$Eb(^1/2) = {}^1/\sqrt{3}\ (|\alpha\alpha\beta\rangle + \varepsilon^*|\alpha\beta\alpha\rangle + \varepsilon|\beta\alpha\alpha\rangle)$$
$$Eb(-^1/2) = {}^1/\sqrt{3}\ (|\beta\beta\alpha\rangle + \varepsilon^*|\beta\alpha\beta\rangle + \varepsilon|\alpha\beta\beta\rangle)$$

We will consider the 3-pulse sequence described in section 3.2.3 (see figure 34). In order to calculate the y component of the signal $S_y(t_1;\tau,\tau')$, we add a fictitious pulse P_4 at $t_2 = 0$ that is identical to P_2. Again, addition of the fictitious pulse P_4 means that we are really calaculating $\langle I_z(t)\rangle$. However, addition of a contiguous 90° pulse 180° out of phase with P_4 would transform I_z to I_y. If we wish to include the x component

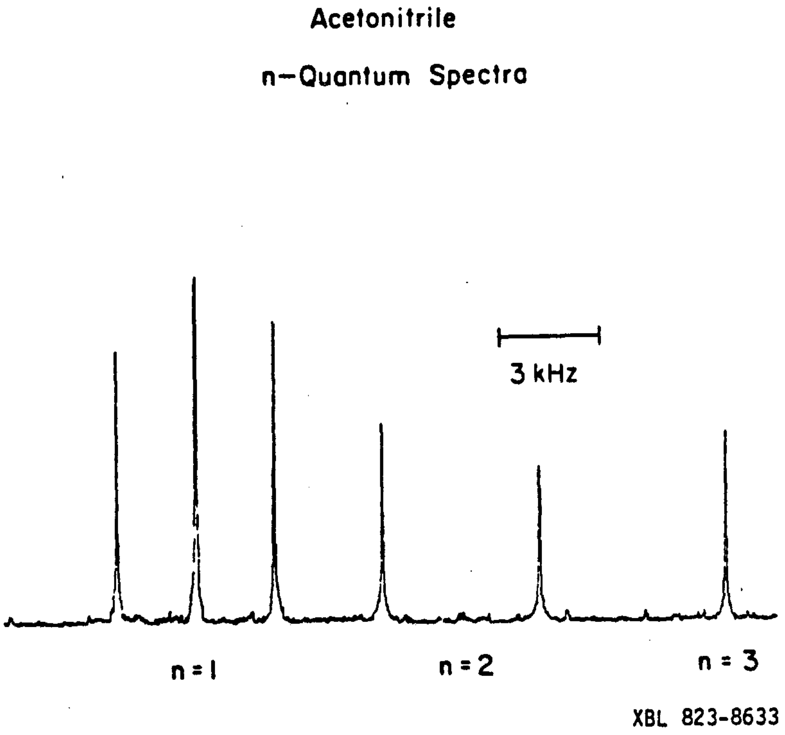

Figure 39. The multiple quantum spectrum of acetonitrile oriented in a nematic liquid crystal obtained by the TPPI pulse sequence.

of the signal $S_x(t_1;\tau,\tau')$ an analogous calculation is required in which P_4 is 90° out of phase with P_3. We will only consider the y component.

We begin by calculating the density matrix at $t_2 = 0$. We obtain, assuming $\tau = \tau'$

$$\rho(\tau+t_1+\tau) = e^{-i\frac{\pi}{2}I_x} e^{-i\mathcal{H}\tau} e^{i\frac{\pi}{2}I_x} e^{-i\mathcal{H}t_1} e^{-i\frac{\pi}{2}I_x} e^{-i\mathcal{H}\tau} e^{i\frac{\pi}{2}I_x} I_z \times$$
$$e^{-i\frac{\pi}{2}I_x} e^{i\mathcal{H}\tau} e^{i\frac{\pi}{2}I_x} e^{i\mathcal{H}t_1} e^{-i\frac{\pi}{2}I_x} e^{i\mathcal{H}\tau} e^{i\frac{\pi}{2}I_x} \qquad (82)$$

where the Hamiltonian $\mathcal{H}$ is

$$\mathcal{H} = -\Delta\omega I_z + \frac{d}{4}(3I_z^{\,2} - I^2) \qquad (83)$$

Equation 82 may be rewritten as

$$\rho(\tau+t_1+\tau) = e^{-i\mathcal{H}_{yy}\tau} e^{-i\mathcal{H}t_1} e^{-i\mathcal{H}_{yy}\tau} I_z e^{i\mathcal{H}_{yy}\tau} e^{i\mathcal{H}t_1} e^{i\mathcal{H}_{yy}\tau} \qquad (84)$$

where

$$e^{-i\mathcal{H}_{yy}\tau} = e^{-i\frac{\pi}{2}I_x} e^{-i\mathcal{H}_{zz}\tau} e^{i\frac{\pi}{2}I_x} \qquad (85)$$

and we have used the fact that I_z and $3I_z^{\,2} - I^2$ commute.

We are interested in calculating the quantity

$$<I_z(t)> = \mathrm{Tr}(\rho(t)I_z) \quad . \qquad (86)$$

Substituting equation 84 into 86 we obtain

$$<I_z(t)> = \mathrm{Tr}(e^{-i\mathcal{H}_{yy}\tau} e^{-i\mathcal{H}_{zz}t_1} e^{-i\mathcal{H}_{yy}\tau} I_z e^{i\mathcal{H}_{yy}\tau} e^{i\mathcal{H}_{zz}t_1} \times$$
$$e^{i\mathcal{H}_{yy}\tau} I_z)$$
$$= \mathrm{Tr}(e^{-i\mathcal{H}_{zz}t_1} e^{-i\mathcal{H}_{yy}\tau} I_z e^{i\mathcal{H}_{yy}\tau} e^{i\mathcal{H}_{zz}t_1} e^{i\mathcal{H}_{yy}\tau} I_z e^{-i\mathcal{H}_{yy}\tau})$$
$$(87)$$

where we have used the fact that the trace is invariant to cyclic permutations.

Now we expand the trace in an eigenbasis of $\mathcal{H}_{zz}$ to obtain

$$\langle I_z(t)\rangle = \sum_{\alpha\beta} \langle\alpha| e^{-i\mathcal{H}_{zz}t_1} e^{-i\mathcal{H}_{yy}\tau} I_z e^{i\mathcal{H}_{yy}\tau} e^{i\mathcal{H}_{zz}t_1} \quad \times$$

$$\langle\beta| e^{i\mathcal{H}_{yy}\tau} I_z e^{-i\mathcal{H}_{yy}\tau} |\alpha$$

$$= \sum_{\alpha\beta} e^{-i\omega_{\alpha\beta}t_1} \langle\alpha| e^{-i\mathcal{H}_{yy}\tau} I_z e^{i\mathcal{H}_{yy}\tau} |\beta\rangle \quad \times$$

$$\langle\beta| e^{i\mathcal{H}_{yy}\tau} I_z e^{i\mathcal{H}_{yy}\tau} |\alpha\rangle \quad . \tag{88}$$

In order to evaluate equation 88 we must obtain matrix elements of $e^{-i\mathcal{H}_{yy}\tau} I_z e^{i\mathcal{H}_{yy}\tau}$. We first rewrite $e^{-i\mathcal{H}_{yy}\tau}$ as

$$e^{-i\mathcal{H}_{yy}\tau} = e^{-i\frac{\pi}{2}I_x} e^{-i\mathcal{H}\tau} e^{i\frac{\pi}{2}I_x}$$

$$= e^{-i\frac{\pi}{2}I_x} e^{-i \quad \mathrm{DD}} e^{+i\frac{\pi}{2}I_x} e^{-i\frac{\pi}{2}I_x} e^{+\Delta\omega I_z} e^{+i\frac{\pi}{2}I_x}$$

$$= e^{-i\mathcal{H}^D_{yy}\tau} e^{i\Delta\omega I_y} \tag{89}$$

Therefore

$$e^{-i\mathcal{H}_{yy}\tau} I_z e^{i\mathcal{H}_{yy}\tau} = e^{-\mathcal{H}^D_{yy}\tau} e^{i\Delta\omega I_y\tau} I_z \quad \times \quad e^{i\mathcal{H}^D_{yy}\tau} e^{-i\Delta\omega I_y\tau}$$

$$= e^{-i\mathcal{H}^D_{yy}\tau} (I_z\cos\Delta\omega\tau + I_x \sin\Delta\omega\tau) \quad \times \quad e^{i\mathcal{H}^D_{yy}\tau} \quad . \tag{90}$$

and we must now calculate matrix elements of

$$e^{-i\mathcal{H}^D_{yy}\tau} I_z e^{i\mathcal{H}^D_{yy}\tau} \tag{91a}$$

and

$$e^{-i\mathcal{H}^D_{yy}\tau} I_x e^{i\mathcal{H}^D_{yy}\tau} \quad . \tag{91b}$$

To evaluate 91a and 91b we use the fact that

$$e^{-i\mathcal{H}^D_{yy}\tau} = \cos d'\tau - \frac{i}{2}M\sin d'\tau \qquad \text{(see appendix 3.1)} \tag{92}$$

to obtain

$$e^{-i\mathcal{H}^D_{yy}} = \begin{bmatrix} c(d'\tau)+\frac{i}{2}s(d'\tau) & 0 & \frac{i\sqrt{3}}{2}s(d'\tau) & 0 \\ 0 & c(d'\tau)-\frac{i}{2}s(d'\tau) & 0 & -\frac{i\sqrt{3}}{2}s(d'\tau) \\ \frac{i\sqrt{3}}{2}s(d'\tau) & 0 & c(d'\tau)-\frac{i}{2}s(d'\tau) & 0 \\ 0 & \frac{i\sqrt{3}}{2}s(d'\tau) & 0 & c(d'\tau)+\frac{i}{2}s(d'\tau) \end{bmatrix} \tag{93}$$

where

$$M = \begin{bmatrix} -1 & 0 & -\sqrt{3} & 0 \\ 0 & 1 & 0 & -\sqrt{3} \\ -\sqrt{3} & 0 & 1 & 0 \\ 0 & -\sqrt{3} & 0 & -1 \end{bmatrix} \tag{94}$$

and $c(x) = \cos x$, $s(x) = \sin x$, $2d' = \frac{3d}{2}$.

We can use the matrix elements of $e^{-i\mathcal{H}^D_{yy}}$ given in equation 93 together with the definitions of I_z and I_x,

$$I_z = \frac{1}{2}\begin{bmatrix} 3 & 0 & 0 & 0 \\ 0 & 1 & 0 & 0 \\ 0 & 0 & -1 & 0 \\ 0 & 0 & 0 & -3 \end{bmatrix}, \qquad I_x = \frac{i}{2}\begin{bmatrix} 0 & \sqrt{3} & 0 & 0 \\ \sqrt{3} & 0 & 2 & 0 \\ 0 & 2 & 0 & \sqrt{3} \\ 0 & 0 & \sqrt{3} & 0 \end{bmatrix} \qquad (95)$$

To evaluate the matrix elements of 91. The results are given in table 3.2.

To calculate the multiple quantum spectrum, equation 88 is Fourier transformed with respect to t_1:

$$\langle I_z(\omega_1)\rangle = \frac{1}{2}\pi \int at_1 e^{-i\omega t_1} \langle I_z(t_1)\rangle$$

$$= \sum_{\alpha<\beta} \delta(\omega_1 - \omega_{\alpha\beta}) \langle\alpha| e^{-i\mathcal{H}_{yy}\tau} I_z e^{i\mathcal{H}_{yy}\tau} |\beta\rangle$$

$$\langle\beta| e^{i\mathcal{H}_{yy}\tau} I_z e^{-i\mathcal{H}_{yy}\tau} |\alpha\rangle \qquad (96)$$

The eigenfrequencies are obtained by taking differences of matrix elements of the evolution Hamiltonian defined by equation 83:

$$\omega_{12} = -\Delta\omega + \frac{d}{2}$$

$$\omega_{23} = -\Delta\omega \qquad \text{Single Quantum} \qquad (97a)$$

$$\omega_{34} = -\Delta\omega - \frac{d}{2}$$

$$\omega_{13} = -2\Delta\omega + \frac{d}{2}$$

$$\omega_{24} = -2\Delta\omega - \frac{d}{2} \qquad \text{Double Quantum} \qquad (97b)$$

$$\omega_{14} = -3\Delta\omega \qquad \text{Triple Quantum} \qquad (97c)$$

Table 3.2 Matrix Elements of $e^{-i\mathcal{H}_{yy}\tau} I_z e^{i\mathcal{H}_{yy}\tau}$

$^{3}/2(c^{2}(d\tau) + {}^{1}/4s^{2}(d\tau)$	$\frac{\sqrt{3}}{2}(c^{2}(d\tau)+2is(d\tau)c(d\tau)s(\Delta\omega\tau)$	$-i\sqrt{3}(c(d\tau)s(d\tau)+{}^{1}/2s^{2}(d\tau)c(\Delta\omega\tau)$	$^{3}/2s^{2}(d\tau)s(\Delta\omega\tau)$
a^{*}_{12}	$^{1}/2(c^{2}(d\tau)-2s^{2}(d\tau))c(\Delta\omega\tau)$	$(c^{2}(d\tau)-{}^{1}/2s^{2}(d\tau))s(\Delta\omega\tau)$	$-i\sqrt{3}(c(d\tau)s(d\tau)-{}^{1}/_{2}s^{2}(d\tau)c(\Delta\omega\tau)$
a^{*}_{13}	a^{*}_{23}	$-{}^{1}/2(c^{2}(d\tau)-2s^{2}(d\tau))c(\Delta\omega\tau)$	$\frac{\sqrt{3}}{2}(c^{2}(d\tau)-2ic(d\tau)s(d\tau)s(\Delta\omega\tau)$
a^{*}_{14}	a^{*}_{24}	a^{*}_{34}	$-{}^{3}/2(c^{2}(d\tau)+{}^{1}/4s^{2}(d\tau)$

Note $c(x) = \cos x$

$s(x) = \sin x$

where the prime on the coupling constant has been dropped. In summary, the multiple quantum spectrum can be calculated using equation 96, obtaining intensities from matrix 95, and frequencies from equation 97. For example, the triple quantum line is at $\omega_{24} = -3\Delta\omega$ and has the intensity $\frac{3}{4}\sin^4(d\tau)\sin^2(\Delta\omega\tau)$.

It is also easily shown that the contribution to the single quantum transition at $\omega_{23} = -\Delta\omega$ from the E transitions is $\frac{1}{2}\sin^2\Delta\omega\tau$.

The matrix elements of $e^{-i\mathcal{H}_{yy}\tau} I_z e^{i\mathcal{H}_{yy}\tau}$, given in equation 91 explicitly demonstrate some features of multiple quantum nmr that we discussed in the preceding section. The single quantum and triple quantum transition intensities are proportional to $\sin^2\Delta\omega\tau$, while the double quantum transition intensities are proportional to $\cos^2\Delta\omega\tau$. So if the experiment is performed on resonance, only the double quantum transitions will be observed. We also note that while the single quantum transition intensities are proportional to $\cos^2 d\tau$, the double quantum intensities are proportional to $\sin^2 d\tau$ and the triple quantum intensity is proportional to $\sin^4 d\tau$. Therefore, unless $d\tau$ approaches $\frac{\pi}{2}$, the double and triple quantum transition intensities will be low.

3.2.5 Multiple Quantum NMR as a Method for Studying Molecules in Liquid Crystalline Mesophases

Thus far, we have considered in some detail, the basic multiple quantum experiment, through which we can observe transitions that are forbidden in conventional nmr. We will now discuss how this technique may be of use in the study of liquid crystals and nonrigid molecules dissolved in liquid crystal solvents.

As we have seen, transition frequencies in nmr are given by matrix elements of nuclear spin interaction Hamiltonians (see section 1.3.4). As we have also seen, such Hamiltonians are scalar products of tensors that involve spin operators (A) interaction parameters (T).

$$\mathcal{H} = \sum_{\ell} \sum_{m} (-)^{m} A_{\ell -m} T_{\ell m} \quad . \qquad (98)$$

It was also mentioned in the last chapter, that the principal axis system (pas) of the tensor T, is related in some straightforward way to the molecular geometry. For example, the dipolar tensor is uniaxial in its principal axis system and the unique axis is parallel to the internuclear vector. However, the spin operators are quantized along the magnetic field direction, and similarly, the z axis of the tensor T in equation 94 must be parallel to the magnetic field direction. If we then use the fact that interaction Hamiltonians are truncated, so that only the component A_{20} that commutes with the Zeeman Hamiltonian contributes to the static Hamiltonian, equation 98 may be rewritten as

$$\mathcal{H} = A_{20} \sum_{q} T_{2q}^{pas} D_{q0}^{(2)}(\Omega) \quad , \qquad (99)$$

where

$$T_{20}^{lab} = \sum_{q} T_{2q}^{pas} D_{q0}^{(2)}(\Omega) \quad , \qquad (100)$$

and we have neglected the isotropic component of the Hamiltonian.

Equations 99 and 100 assume that the principal axis system is fixed with respect to the laboratory frame. If, as occurs in liquid crystalline systems, the molecule moves in some anisotropic fashion, and if the rate of motion is fast on the nmr time scale, then the transformation from the pas to the laboratory frame may be motionally averaged (93). It is convenient to first transform from the pas to a fixed molecular coordinate system, and then carry out the motionally averaged transformation into the laboratory frame:

$$T_{20}^{lab} = \sum_{pq} T_{2q}^{pas} D_{qp}^{(2)}(\Omega_0) < D_{p0}^{(2)}(\Omega_1)> \quad . \tag{101}$$

Equation 101 assumes that the molecule is rigid and therefore any motion is "whole-molecular". However, if the molecule is not rigid, but interconverts rapidly between n geometric configurations, equation 101 must be rewritten as

$$T_{20}^{lab} = \sum_n P_n \Big(\sum_{pq} (T_q^{pas})^n D_{pq}^{(\ell)}(\Omega_0^n) < D_{p0}^{(\ell)}(\Omega_1^n)> \Big) \tag{102}$$

where P_n is the probability of the n^{th} configuration occurring. In equation 97 we have neglected vibrational and tortional effects. Given a knowledge of the tensors $(T_{\ell q}^{pas})^n$, the unknowns of the problem are the products

$$Q_{n,p} = F_n <D_{p0}^{(2)}(\Omega_1{}^n)> \tag{103}$$

of which there are, in general, 5n. Thus, in order to determine the problems, 5n independent tensors T must be measured.

As was mentioned in the last chapter, deuterium magnetic resonance has been a particularly popular method for studying liquid crystalline systems. What is required, then, is that 5n unique electric field gradient tensors exist in the molecule of interest.

Since the quadrupolar interaction is a "single particle" interaction, that is, the Hamiltonian only involves parameters of a single nucleus, there must exist 5n non-identical nuclei in the molecule. We will define the term 'non-identical nucleus" presently. But if the number of configurations n is large, the problem may be underdetermined. For example, suppose we wish to study an alkyl chain molecule with three internal bonds such as n-hexane. As we will learn in the next section, even if we only consider the all-trans and the single-gauche configurations there will be 10 products of the form given in equation 103. However, perdeuterated n-hexane has only 3 unique types of nuclei and therefore only 3 quadrupole splittings can be observed. So in many interesting molecular systems there is an insufficient number of quadrupolar splittings to determine the problem.

A solution to this difficulty is to observe the dipolar spectrum of the protonated molecule (93). Given N nonidentical spin $\frac{1}{2}$ nuclie, the number of dipole-dipole couplings is $N!/((N-2)!2!)$, and this is always larger than N for N > 3. Of course, the number of independent couplings decreases if there is molecular symmetry, but in general the number of couplings will exceed the number of nuclear types. For example, the number of independent dipole-dipole couplings in n-hexane is 16, a sufficient number to determine the problem if we consider only the all-trans and single-gauche configurations. In fact, if we were only to consider couplings between methylene protons we would still have a sufficient number of couplings (10) to determine the problem.

The main difficulty with observing proton dipolar spectra is

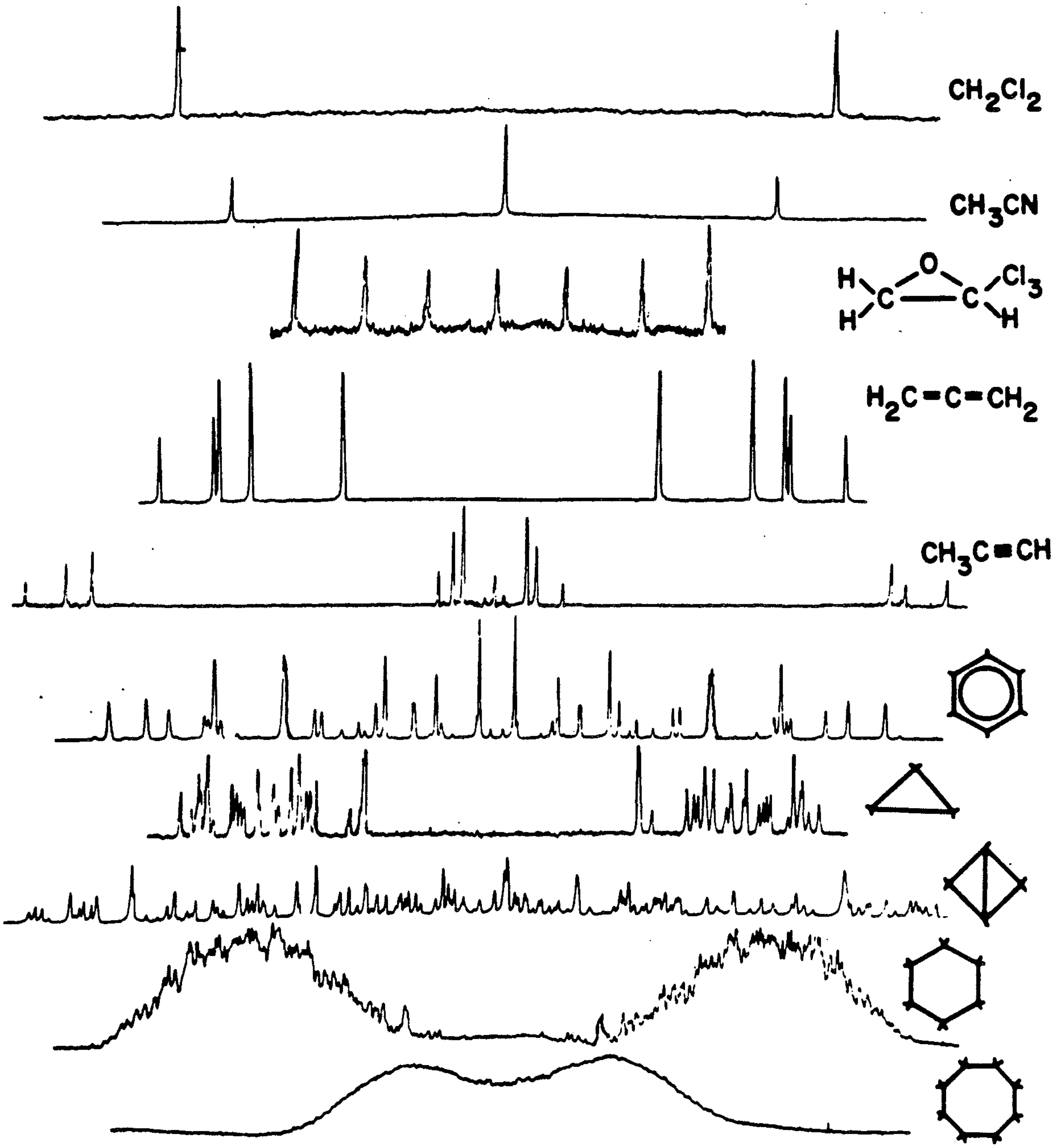

XBL 7910-12344

Figure 40. Proton nmr spectra of various molecules oriented in liquid crystal solvents.

that they tend to become very complex as the number of spins increases, as is shown for several molecules in figure 40. We note that even in a very symmetric molecule like cyclooctane, the number of transitions is so large that there is no resolution at all in the proton dipolar spectrum, and of course, the number of transitions increases for lower molecular symmetries.

A solution to the problem is to simplify the dipolar spectrum by selective isotopic labelling. One approach is to selectively deuterate the molecule, and observe the fine structure on the quadrupolar satellites due to dipole-dipole couplings between deuterium nuclei (with proton decoupling). This technique was used by Hsi and Luz (47) in a study of the alkoxy chain of an no.m liquid crystal. Another approach, used by Höhener et. al. (95) is to observe the natural abundance carbon-13 spectrum of selectively labelled liquid crystals. Natural abundance ^{13}C spectra of selectively deuterated MBBA and nitrogen-15 labelled 50.7 yielded carbon-deuterium and carbon-nitrogen couplings respectively. In addition, the ^{13}C local field spectrum of fully protonated MBBA yielded carbon-proton couplings free of complications due to proton-proton couplings.

At this point we wish to suggest an additional technique, multiple quantum nmr. The advantage of multiple quantum nmr lies in its ability to simplify dipolar spectra without loss of information and without the necessity of synthesizing series of selectively labelled compounds. The simplification occurs since the number of transitions in the high multiple quantum orders is far less than the number of single quantum transitions. From figure 41, it is evident

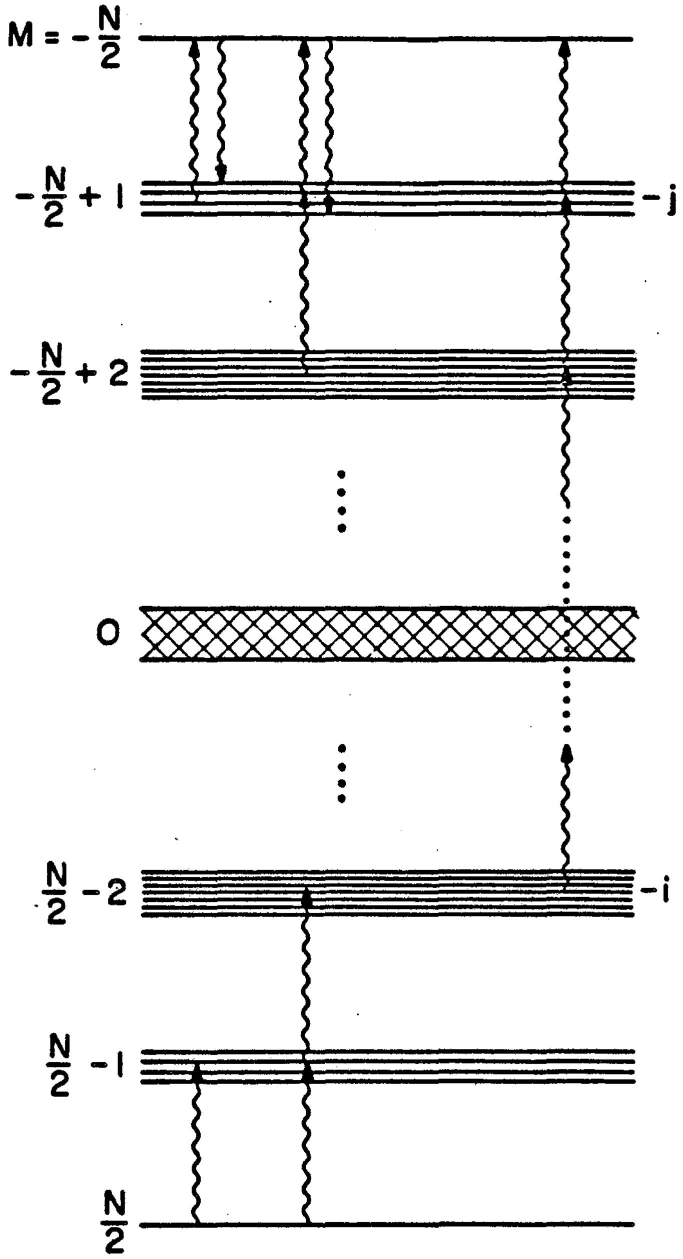
M = -N/2
-N/2 + 1
-N/2 + 2
O
N/2 -2
N/2 -1
N/2
-j
-i

XBL 7710-10021

Figure 41. Generalized enery level diagram of a system of N coupled spin ½ nuclei. Arrows indicate various multiple quantum transitions.

that while there are many transitions for which $\Delta m= 1$, there is only 1 transition for $\Delta m = N$, where N is the number of spin $\frac{1}{2}$ nuclei, the number of M-quantum transitions is, assuming no symmetry, $\binom{N}{M}2^{N-M}$. Therefore we expect 1 "N" quantum transition, 2N"N-1" transitions, 2N(N-1)"N-2" transitions etc. Since the number of single quantum transitions is $N2^{N-1}$, we realize that the higher multiple quantum orders are far simpler than the single quantum spectrum. We also realize that since there are N!(N-2)!2!) couplings, we will require at least N-2 quantum spectrum for the analysis.

In closing we wish to mention that multiple quantum nmr has already been used in several instances to study systems of strongly-coupled protons in liquid crystalline phases. In a study which is a classic example of the spectral simplification possible through multiple quantum nmr (88, 96), the average conformation of the biphenyl moiety of a cyanobiphenyl liquid crystal was studied. Also, multiple quantum nmr has been used to study the relaxation of an oriented methyl group (97), and the correlation bewteen two oriented methyl groups (98).

3.3 Nonrigid Chain Molecules in Uniaxial Phases

3.3.1 The NMR Symmetry Group of a Polymethylene (PM) Chain

In this section we will derive the symmetry group of a polymethylene chain. We wish to do this because once the symmetry group of the molecule is identified and the appropriate character table is available, the energy level diagram of the spin system can be determined. Once the energy level diagram ia available, we can calculate the number of transitions in each multiple quantum order.

We will derive the symmetry group of a chain composed of four methylene groups. The three internal bonds of such a chain are assumed to be undergoing rapid gauche-trans interconversions. By "rapid" is meant that the interconversion rates greatly exceed the proton dipole-dipole couplings in frequency units. Now for PM chains the gauche-trans interconversion rates are expected to exceed 10^9 $\sec^{-1}$ in liquid crystalline systems, whereas proton dipolar couplings are not expected to exceed 10^4 $\sec^{-1}$, so the term rapid is appropriate. Furthermore we assume that the probability of a trans to gauche$^{(+)}$ interconversion occurring equals the probability of a gauche$^{(-)}$ to trans-interconversion. Also we assume that the ends of the chain are indistinguishable, so we are interested in the proton nmr spectrum of say, deuterium-decoupled n-hexane-1,1,1,6,6,6-d_{6},0 or 1,4-dibromobutane.

To obtain the symmetry group of a nonrigid chain, we use the approach of Longuet-Higgins (99). By this method, the symmetry group is composed of all feasible permutations and permutation-inversions of identical nuclei. A feasible operation is defined as an operation that does not involve passage over an infinite energy barrier, and identical nuclei are defined as nuclei whose exchange leaves the nmr Hamiltonians invariant, where the nmr Hamiltonian is

$$\mathcal{H} = - \sum_i \Delta\omega_i I_z^i + \sum_{i<j} J_{ij} I^i \cdot I^j + \sum_{i<j} D_{ij} (3 I_z^i I_z^j - I^i \cdot I^j) \quad . \qquad (104)$$

If we use the numbering scheme shown in figure 42, given our assumptions on the nature of the chain motion, the symmetry group

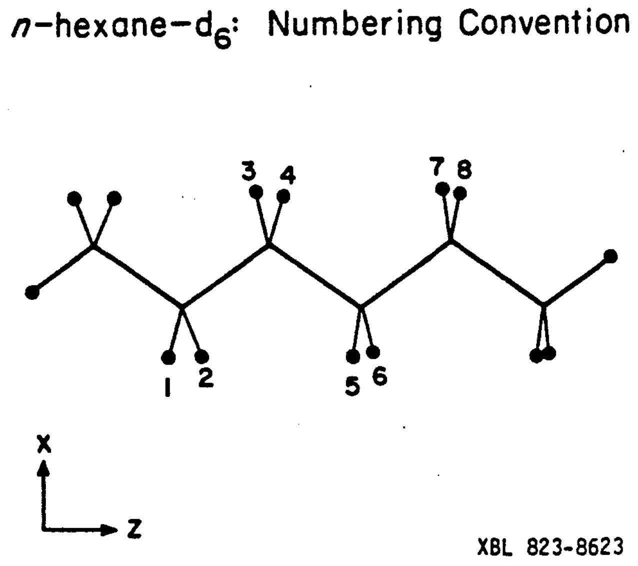
n-hexane-d_6: Numbering Convention
3
4
7
8
1
2
5
6
X
Z

XBL 823-8623

Figure 42. The nuclear labelling convention for n-hexane-d_6.

is of order 4 with the operations:

$$O_1 \equiv (12)(34)(56)(78) \equiv \sigma_n \qquad (105a)$$

$$O_2 \equiv (18)(27)(36)(45) \equiv i \qquad (105b)$$

$$O_3 \equiv (17)(28)(35)(46) \equiv C_2 \qquad (105c)$$

$$O_4 \equiv E \qquad (105d)$$

The symmetry group is therefore isomorphous to C_{2h} and has the character table:

	E	C_2	σ_h	i
Ag	1	1	1	1
Au	1	1	-1	-1
Bg	1	-1	-1	1
Bu	1	-1	1	-1

(106)

We now need to calculate the character table for the group using a set of reducible representations. Each reducible representation corresponds to a matrix representation of the operations of the group, in which the basis set of each representation is composed of the direct product functions of a given Zeeman manifold. The character table is:

	E	C_2	σ_h	i
$\Gamma(m=4)$	1	1	1	1
$\Gamma(m=3)$	8	0	0	0
$\Gamma(m=2)$	28	4	4	4
$\Gamma(m=1)$	56	0	0	0
$\Gamma(m=0)$	70	0	0	0

(107)

The energy level diagram may now be obtained if we decompose the reducible representations of 107 into irreducible representations. The number of times that a given irreducible representation occurs within a reducible representation is given by the equation;

$$a_j = h^{-1} \sum_k N_k \chi^{(j)}(C_k)^* \chi(C_k) \tag{108}$$

a_j is the number of times that the j^{th} irreducible representation occurs within a reducible representation. The summation is over classes and N_k is the number of operations within the k^{th} class. For C_{2h}, $h = 4$ and $N_k = 1$ for all k.

Using equation 108 we obtain the decompositions:

$$\Gamma(m=4) = Ag \tag{109a}$$

$$\Gamma(m=3) = 2Ag + 2Au + 2Bg + 2Bu \tag{109b}$$

$$\Gamma(m=2) = 10Ag + 6Au + 6Bg + 6Bu \tag{109c}$$

$$\Gamma(m=1) = 14Ag + 14Au + 14Bg + 14Bu \tag{109d}$$

$$\Gamma(m=0) = 22Ag + 16Au + 16Bg + 16Bu \tag{109e}$$

From equations 109 the energy level diagram may be easily deduced and is shown in figure 43. The number of lines in each multiple quantum order is as follows:

$M = \Delta m = 8$	1 line at $8\Delta\omega$
7	4 lines
6	28 lines and a central line at $6\Delta\omega$
5	140 lines
4	448 lines and a central line at $4\Delta\omega$
3	1092 lines
2	1988 lines and a central line at $2\Delta\omega$
1	2860 lines
0	2098 lines

(110)

n-Hexane-d_6
Energy Level Diagram

m	A_g	A_u	B_g	B_u
4	1			
3	2	2	2	2
2	10	6	6	6
1	14	14	14	14
0	22	16	16	16
-1	14	14	14	4
-2	10	6	6	6
-3	2	2	2	2
-4	1			

XBL 823-8629

Figure 43. The energy level diagram of a 4 methylene chain assuming equal population of the gauche (+) and gauche (-) states and rapid interconversion between configurations relative to the nmr time scale.

If the chemical shift difference of the protons on different methylene groups is negligible compared to the dipolar couplings, we expect the lines to occur in pairs about $M\Delta\omega$ in each order. Thus, there are two pairs in the seven quantum, 14 pairs in the six quantum with a central line at $6\Delta\omega$ etc. In general the number of lines in the seven quantum spectrum equals the number of "types" of nuclei that is, the number of nuclei connected by symmetry. This feature may be understood, in the case of n-hexane-1,1,1,6,6,6-d_6 as follows. Since the $m = \pm 4$ eigenfunctions are of Ag symmetry, 7-quantum transitions may only occur from Ag states in the $m = \pm 3$ manifolds. Let us consider the transitions from the $m = -3$ to the $m = 4$ manifolds. We know that for a given Zeeman manifold, the Ag basis functions can be projected out of the direct product basis by application of projection operators of the form

$$P^{Ag} = \frac{\ell_{Ag}}{h} \sum_R \chi^{Ag}(R) P_R \qquad (111)$$

where ℓ_{Ag} is the dimension of the irreducible representation Ag and equals 1, h is the order of the group and for C_{2h} equals 4, $\chi^{Ag}(R)$ is the character and equals 1 for all R, and P_R is a symmetry operator of the group. Equation 111 may be rewritten as

$$P^{Ag} = \frac{1}{4} (P_E + P_\sigma + P_i + P_{C_2}) \quad . \qquad (112)$$

Now there are eight direct product functions for the $m = -3$ manifold since the number of functions is the number of ways to permute a label among eight spins:

$|\beta\beta\beta\beta\beta\beta\beta\alpha>$ $|\beta\beta\beta\alpha\beta\beta\beta\beta>$

$|\beta\beta\beta\beta\beta\beta\alpha\beta>$ $|\beta\beta\alpha\beta\beta\beta\beta\beta>$

$|\beta\beta\beta\beta\beta\alpha\beta\beta>$ $|\beta\alpha\beta\beta\beta\beta\beta\beta>$

$|\beta\beta\beta\beta\alpha\beta\beta\beta>$ $|\alpha\beta\beta\beta\beta\beta\beta\beta>$

Also given the definitions of the group of P_R's (see equation 100), the single "α" label may only be permuted within the group of nuclei 1, 2, 7, and 8, or within the group 3, 4, 5, and 6. Thus from the form of the projection operator, we expect the number of Ag functions to equal the number of groups of nuclei connected by symmetry operations of the group C_{2h}. That number is two and the Ag functions are

$$\frac{1}{4}(|\alpha\beta\beta\beta\beta\beta\beta\beta> + |\beta\alpha\beta\beta\beta\beta\beta\beta> + |\beta\beta\beta\beta\beta\beta\alpha\beta> + |\beta\beta\beta\beta\beta\beta\beta\alpha>)$$

$$\frac{1}{4}(|\beta\beta\alpha\beta\beta\beta\beta\beta> + |\beta\beta\beta\alpha\beta\beta\beta\beta> + |\beta\beta\beta\beta\alpha\beta\beta\beta> + |\beta\beta\beta\beta\beta\alpha\beta\beta>) \quad .$$

So we expect two transitions from the m = −3 manifold to the m = 4 manifold. The other line in each pair comes from m = −4 to m = 3 transitions.

3.3.2 The Orientational Dependence of the Dipolar Couplings for a Nonrigid Chain Molecule in a Uniaxial Phase

In this section we will derive an expression for the orientational dependence of the dipolar coupling constant in a nonrigid molecule in a uniaxial phase.

We have already found that the components of a second rank tensor in the director frame may be related to the components of a second rank tensor in the principal axis system (pas) by the transformatiom

$$T_{2k}^{dir} = \sum_{pq} T_{2p}^{pas} D_{pq}^{(2)}(\Omega_o)\langle D_{qk}^{(2)}(\Omega_1)\rangle \qquad (113)$$

where $\Omega_o = (\alpha_o, \beta_o, \gamma_o)$ is the set of Euler angles relating the pas to the molecular-fixed frame and the second transformation is motionally averaged due to molecular reorientation. Equation 114 is valid for a rigid molecule.

The question arises, what effect does internal molecular motion have on equation 113? Let us first establish what we mean by "internal molecular motion". We will attempt to rewrite equation 113 to include large amplitude motions in which the molecule interconverts between discrete geometric configurations at a rate that is rapid on the nmr time scale. Thus we neglect vibrational and tortional motions, and we find, with reference to chain molecules, that our assumptions are equivalent to the rotational isomeric state approximation described by Flory (100). We rewrite equation 113 as

$$T_{2k}^{dir} = \sum_{n} P_n \sum_{pq} T_{2p}^{pas,n} D_{pq}^{(2)}(\Omega_o^n)\langle D_{qk}^{(2)}(\Omega_1^n)\rangle \quad . \qquad (114)$$

The summation over n is a summation over configurations, and P_n is the probability of the n^th configuration occurring. $T_{2p}^{pas,n}$ is the p component of the tensor in the pas, and the value of the component may vary with the configuration. We will abbreviate our notation to read

$$T_{2p}^{pas,n} = T_{2p}^{n} \quad . \qquad (115)$$

$(\Omega_o^n) = (\alpha_o^n, \beta_o^n, \gamma_o^n)$ is the set of Euler angles relating the pas to the molecular-fixed frame for the n^{th} configuration. We also note that the motionally averaged transformation is dependent on the configuration. Using the definition of $D_{pq}^{(\ell)}(\Omega)$ introduced in Chapter 2 and the identity given by equation 115, equation 114 may be rewritten as:

$$T_{2k}^{dir} = \sum_n F_n \sum_{pq} T_{2p}^n \, D_{pq}^{(2)}(\Omega_o^n) \, C_{-qk}^{(2)} \, (\Omega_1^n)(-)^{k-q} \tag{116}$$

where $C_{-qk}^{(2)}(\Omega_1^n)$ is an element of the complex ordering matrix for the n^{th} configuration.

Equation 116 is valid for any molecular symmetry, any phase symmetry, and assumes correlation between molecular reorientation and internal molecular motion. We wish to consider only the case of uniaxial phases such as nematic or smectic A phases, and so we only consider the component T_{20}^{dir} :

$$T_{20}^{dir} = \sum_n P_n \sum_{pq} T_{2p}^n \, D_{pq}^{(2)}(\Omega_o^n) C_{-qo}^{(2)}(\Omega_1^n)(-)^{-q} \quad . \tag{117}$$

Since q varies from 2 to -2 integrally, there are 5 order parameters per configuration. Furthermore, if the liquid crystal is well aligned, the director is parallel to the magnetic field and we get

$$T_{20}^{dir} = T_{20}^{lab} \quad . \tag{118}$$

Now we rewrite equation 117 for the case of direct dipole-dipole couplings. The dipolar tensor is uniaxial in its pas, as was mentioned in Chapter 1, and so the only nonzero component is T_{20}^n

which is defined as:

$$T_{20}^{n}(ij) = \frac{h\gamma^2}{2\pi^2}(r_{ijn})^{-3} \qquad (119)$$

where r_{ijn} is the distance between the nuclei i and j in the n^{th} configuration. Equation 117 may be rewritten as:

$$T_{20}^{dir}(ij) = -\frac{h\gamma^2}{2\pi^2}\sum_n (r_{ijn})^{-3}\ P_n \sum_q D_{oq}^{(2)}(\Omega_o^n)C_{-qo}^{(2)}(\Omega_1^n)(-)^{-q}$$

$$(120)$$

and $\Omega_o^n = (0,\ \beta_o^n,\ \gamma_o^n)$.

Now $T_{20}^{dir}(ij)$ is a real function and the terms on the right hand side of equation 120 are products of complex functions. We will now convert to a real ordering matrix. We use the definitions of $D_{oq}^{(2)}(\Omega_o^n)$ and $C_{-qo}^{(2)}(\Omega_1^n)$ to obtain

$$\begin{aligned}T_{20}^{dir}(ij) = -\frac{h\gamma^2}{2\pi^2}\sum_n (r_{ijn})^{-3}\ P_n\big(&d_{00}^{(2)}(\beta_0^n)\langle d_{00}^{(2)}(\beta_1^n)\rangle \\ &+ d_{0\pm2}^{(2)}(\beta_0^n)\ e^{\pm 2i\ {}_0^n}\langle e^{\pm 2i\alpha_1^n}\ d_{\pm20}^{(2)}\ (\beta_1^n)\rangle \\ &- d_{0\pm1}^{(2)}(\beta_0^n)\ e^{\pm i\gamma_0^n}\langle e^{\pm i\alpha_1^n}\ d\pm10(\beta_1^n)\rangle\ \big)\ . \qquad (121)\end{aligned}$$

Using the definitions of $d_{mn}^{(2)}(\beta)$ given in appendix 1.3 we obtain

$$\begin{aligned}T_{20}^{dir}(ij) = -\frac{h\gamma^2}{2\pi^2}\sum_n (r_{ijn})^{-3}\ P_n\Big(&\tfrac{1}{4}(3\cos^2\beta_0^n-1)\langle 3\cos^2\beta_1^n-1\rangle \\ &+ \tfrac{3}{4}\ (\sin^2\beta_0^n\cos2\gamma_0^n\langle\sin^2\beta_1^n\cos2\alpha_1^n\rangle \\ &+ \sin^2\beta_0^n\sin2\gamma_0^n\langle\sin^2\beta_1^n\sin2\alpha_1^n\rangle \\ &+ \sin\beta_0^n\cos\beta_0^n\cos\gamma_0^n\langle\sin\beta_1^n\cos\beta_1^n\cos\alpha_1^n\rangle \\ &+ \sin\beta_0^n\cos\beta_0^n\sin\gamma_0^n\langle\sin\beta_1^n\cos\beta_1^n\sin\alpha_1^n\rangle\ . \qquad (122)\end{aligned}$$

Using Saupe's notation for ordering parameters (67):

$$S_{zz} = \frac{1}{2}\langle\cos^2\beta - 1\rangle \tag{123a}$$

$$S_{xx} - S_{yy} = \frac{3}{2}\langle\sin^2\beta\cos 2\alpha\rangle \tag{123b}$$

$$S_{xy} = \frac{3}{2}\langle\sin^2\beta\sin 2\alpha\rangle \tag{123c}$$

$$S_{xz} = \frac{3}{2}\langle\sin\beta\cos\beta\cos\alpha\rangle \tag{123d}$$

$$S_{yz} = \frac{3}{2}\langle\sin\beta\cos\beta\sin\alpha\rangle \quad , \tag{123e}$$

equation 122 may be rewritten as:

$$\begin{aligned} T_{20}^{dir}(ij) = -\frac{h\gamma^2}{4\pi^2}\sum_n (r_{ijn})^{-3}\, P_n(S_{zz}(n)(3\cos^2\beta_n - 1) + (S_{xx}(n) - S_{yy}(n)\sin^2\beta_n\cos 2\gamma_n \\ + S_{xy}(n)\sin^2\beta_n\sin 2\gamma_n + S_{xz}(n)\sin\beta_n\cos\beta_n\cos\gamma_n + \\ + S_{yz}(n)\sin\beta_n\cos\beta_n\sin\gamma_n) \quad . \end{aligned} \tag{124}$$

Equation 124 is in the notation most often seen in the literature. We have dropped the 0 subscript on the Euler angles and so $\Omega_0^n = (0, \beta_n, \alpha_n)$. The S(n) matrix is a real, symmetric matrix, and since S = 0 in an isotropic phase, the matrix is traceless

$$Tr(S(n)) = S_{xx}(n) + S_{yy}(n) + S_{zz}(n) \quad . \tag{125}$$

Now admittedly, equation 124 is rather ominous. It states that, given a knowledge of the molecular geometry of each configuration, the unknowns of the problem are the products P_nS^n. Since each ordering matrix has five independent components we expect 5 x n

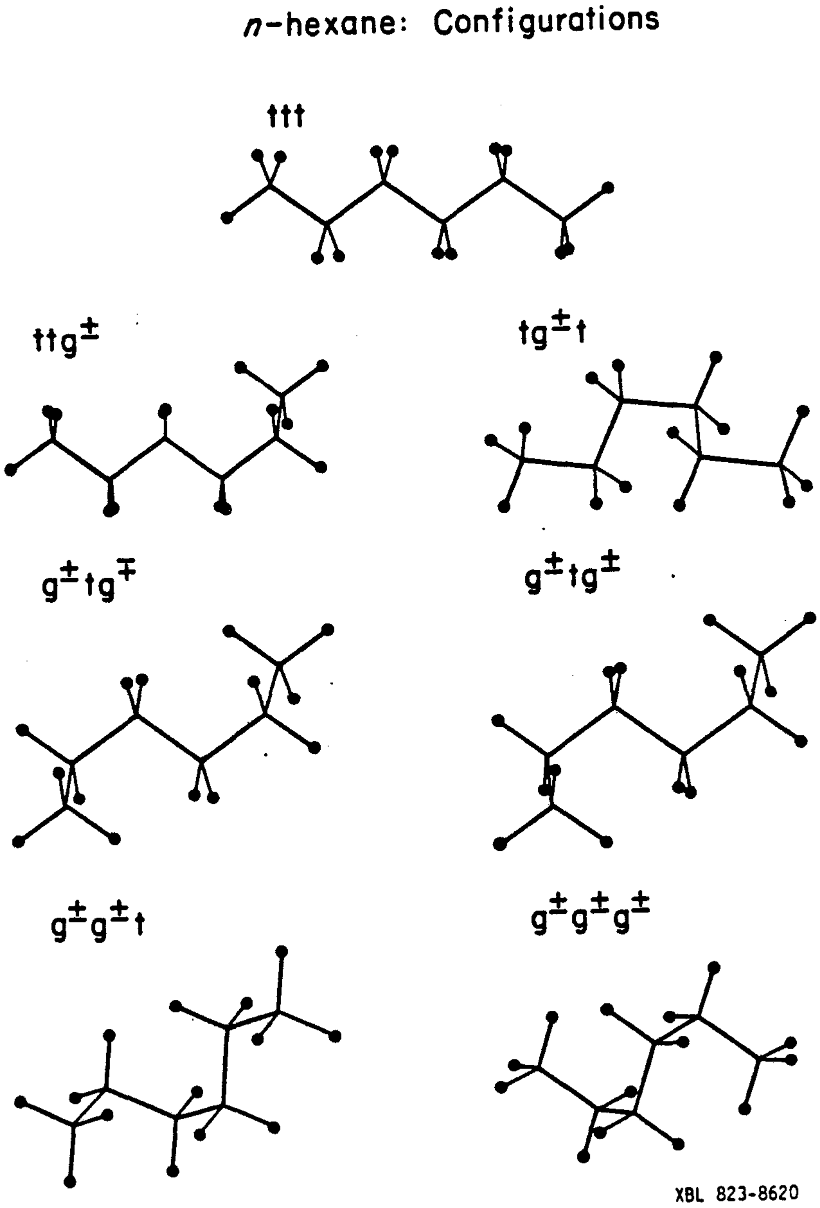
n-hexane: Configurations
ttt
ttg±
tg±t
g±tg∓
g±tg±
g±g±t
g±g±g±
XBL 823-8620

Figure 44. The allowed configurations of n-hexane. All configurations that involve adjacent gauche rotations of opposite sign are excluded.

unknowns, as was mentioned in section 3.2.5. Now it is obvious that for a system like n-hexane, the number of unknowns (there will be 45) will vastly exceed the number of independent proton-proton couplings (there are 10 if the methyl groups are deuterated). Thus equation 124 must be simplified if we are to proceed.

One approach is to consider only the most probable configurations, that is, the all-trans and the single gauche configurations. This is a reasonable first order approximation since many of the multiple gauche configurations occur with very low probability even in isotropic systems (100). In fact, all configurations involving opposite gauche rotations on adjacent bonds (g^+g^-), are forbidden due to steric repulsion. Therefore we only consider the configurations: ttt, $g^{\pm}tt$, $ttg^{\pm}$, and $tg^{\pm}t$.

Now since the 4-methylene chain (n-hexane-1,1,1,6,6,6-d_6) is symmetrically substituted, the configurations $ttg^{\pm}$ and $g^{\pm}tt$ have identical ordering matrices and equal configurational probabilities. Thus equation 124 involves only 3 independent order matrices and we have at most 15 unknowns. This still exceeds the number of independent couplings, but the number of unknowns may still be reduced by configurational symmetry.

From figure 44b, we see that the $ttg^{\pm}$ (=$g^{\pm}tt$) configuration has no symmetry and we expect all five components of the ordering tensor to be nonzero.

Figure 44a shows the ttt configuration of n-hexane. We assign the coordinate system as follows: the z axis is parallel to the vector connecting alternate carbon nuclei, the x axis bisects the H-C-H angle, and the y axis completes a right-handed coordinate system. We see that there are four symmetry operations: E, C_2^y, σ_{xz} and i. The inversion center is located at the midpoint of the central carbon-carbon bond. We designate $P(\Omega)$ as the probability that an excursion of $\Omega = (\alpha, \beta, \gamma)$ occurs from the coordinate axes and we get

$$C_2^y \longrightarrow P(-\alpha, \pi-\beta) = P(\alpha,\beta) \tag{126a}$$

$$\sigma_{xz} \longrightarrow P(-\alpha) = P(\alpha) \tag{126b}$$

$$i \longrightarrow P(\pi+\alpha, \pi+\beta) = P(\alpha,\beta) \quad . \tag{126c}$$

Equations 126 imply that only $S_{zz}(ttt)$ and $S_{xx}(ttt) - S_{yy}(ttt)$ are nonzero.

Figure 44c shows the $tg^{\pm}t$ configuration. The z-axis is assumed to be parallel to the central carbon-carbon (C-C) bond, and the y-axis bisects the angle between the second and fourth C-C bonds. The x-axis completes a right-handed coordinate system. There are two symmetry operations, E and C_2^y and we find that

$$C_2^y \longrightarrow P(-\alpha,\pi-\beta) = P(\alpha,\beta) \tag{127}$$

which implies that only $S_{zz}(tg^{\pm}t)$, $S_{xx}(tg^{\pm}t) - S_{yy}(tg^{\pm}t)$, and $S_{xz}(tg\ t)$ are nonzero.

In summary, we have reduced the problem to 10 unknowns which involve the ordering parameters:

$$S(ttt) = S^1 \quad \Rightarrow S^1_{zz} \text{ and } S^1_{xx} - S^1_{yy} \tag{128a}$$

$$S(tg^{\pm}t) = S^2 \quad \Rightarrow S^2_{zz},\ S^2_{xx} - S^2_{yy}, \text{ and } S^2_{xz} \tag{128b}$$

$$S(g^{\pm}tt) = S(ttg\ ) \Rightarrow S^3 = S^3_{zz},\ S^3_{xx} - S^3_{yy},\ S^3_{xz},\ S^3_{xy}, \text{ and } S^3_{yz} \tag{128c}$$

and the configurational probabilities:

$$P_{ttt} = P_1 \tag{129a}$$

$$P_{tg^{\pm}t} = P_2 \tag{129b}$$

$$P_{ttg^{\pm}} = P_{g^{\pm}tt} = P_3 \tag{129c}$$

The ten unknowns of the problem can be obtained through the simulation of the 6 quantum spectrum. A set of 10 coupling constants is calculated from a set of $P_nS(n)$'s, and is used to generate a theoretical 6-quantum spectrum. If necessary, the fit may be improved by an iterative calculation in which the coupling constants are treated as parameters.

Another simplification of equation 124 may be obtained by assuming that for each configuration, molecular reorientation can be described by the single order parameter $S_{zz}(n)$. $S_{zz}(n)$ measures the tendency of the z-axis of the molecular-fixed coordinate system of the n^{th} configuration to align parallel to the z-axis of the director coordinate system. Now we can assume that $S_{zz}(n)$ is the only nonzero order parameter if the molecular z-axis is an axis of three-fold symmetry or higher. But the approximation might be made that if $S_{zz}(n)$ is much larger than the other order parameters, the products $P_n(S_{xx}(n) - S_{yy}(n)$, $P_n(S_{xz}(n)$ etc. may be neglected. Measurements of $S_{xx}(n) - S_{yy}(n)$ and $S_{xz}(n)$ for chain molecules in liquid crystalline phases have appeared in the literature (101) and indicate that $S_{xx}(n) - S_{yy}(n)$ and $S_{xz}(n)$ are better than an order of magnitude smaller than $S_{zz}(n)$. Those measurements, however, were obtained for alkyl chain protons (or deuterons) on the mesogens themselves - (PAA, pentylcyanobiphenyl)- and n-hexane cannot be expected to order in exactly the same manner as the chain moiety of a liquid crystal mesogen. In particular, we expect that the approximation is most questionable for the very nonlinear configurations such as $tg^{\pm}g$ or $g^{\pm}g^{\pm}g$ which tend to have the least anisotropic shapes. Such configurations, however, may occur with a very low probability in liquid crystalline systems, so the approximation may be useful.

We also note that the $S_{zz}(n)$'s are given to be different for each configuration. Now it is often assumed in the literature that the $S_{zz}(n)$'s for all configurations are equal. While such an assumption allows calculation of the relative configurational probabilities, it is only strictly valid for configurations related by symmetry even if the rate of internal motion is far greater than the rate of molecular reorientation (102).

In summary, the second model includes seven unknowns which are the products $P_n S_{zz}(n)$ for the configurations ttt, $ttg^{\pm}$ $(=g^{\pm}tt)$, $tg^{\pm}t$, $g^{\pm}tg^{\pm}$, $g^{\pm}tg^{\pm}$, $tg^{\pm}g^{\pm}$ $(=g^{\pm}g^{\pm}t)$, and $g^{\pm}g^{\pm}g^{\pm}$. The configurations $tg^{\pm}g^{\mp}$, $g^{\pm}g^{\mp}g^{\pm}$, and $g^{\mp}g^{\pm}g^{\pm}$ are neglected since they result in severe steric hindrances.

A third model would involve only the "linear" configurations with such configurations as $g^{\pm}g^{\pm}t$ and $g^{\pm}g^{\pm}g^{\pm}$ being neglected. Such a model would require five unknowns.

Another model which has appeared in the liquid crystal literature (47) and the lipid literature (103) includes only the all-trans configuration and "kink" configurations $(\ldots tg^{\pm}tg^{\pm}t\ldots\ldots)$ Kink configurations are expected to be abundant in long alkyl chains in ordered phases since they perturb least the linear structure of the chain. While such a model may be appropriate for systems of long chains, the model is less applicable to a 5 bond chain, where the single gauche configurations are no less "linear" than the $g^{\pm}tg^{\pm}$ configurations.

3.4 Experimental Results and Discussion

3.4.1 Chemical Synthesis of n-hexane-1,1,1,6,6,6-d_6

(i) $CD_3I + Li \xrightarrow{ET_2O} CD_3Li + LiI$

In a 200 ml, three-neck flask, equipped with a condensor, dropping funnel, and magnetic stir bar, 1.4 gm of lithium wire cut into 50 pieces were added to 30 ml of dry ether under an argon atmosphere (104). 10gm (69 nmoles) of Methyl-d_3 iodide (Aldrich Chemical, >99%, Gold Label) in 30 ml of dry ether were added dropwise to the stirred and gently-heated solution (reflux maintained) over a period of 1.5 hours. The reflux was continued only shortly after the addition. The flask was then immersed in a 40°C oil bath and most of the ether was removed by an argon stream. Then the flask was cooled with an ice bath and tetrahydrofuran (THF) was added slowly and the solution was allowed to warm to room temperature. The solution appeared homogeneous with the exception of the unreacted lithium.

(ii) $CD_3Li + CuI \xrightarrow{THF} (CD_3)_2CuLi + LiI$

The methyllithium-d_3 solution was transferred by syringe to a dropping funnel and was added dropwise to a suspension of 4.75 gm (25 mmoles) of cuprous iodide (under argon) in 50 ml of THF in a 200 ml flask (105). The temperature of the reaction mixture was maintained at slightly below 0°C.

(iii) $(CD_3)_2CuLi + Br(CH_2)_4Br \longrightarrow CD_3(CH_2)_4CO_3$

At the conclusion of the addition, 3.2 gm (1.8 ml, 15 mmole) of 1,4-dibromobutane were added dropwise, while maintaining a temperature of 0^o - 10^oC. The solution was subsequently allowed to warm to room temperature and was stirred overnight. 40 ml of decane and 5 ml of water were added and the solution was filtered. Then the solution was washed with 300 ml of a dilute solution of sodium thiosulphate, and then washed four more times with water to remove most of the THF and ether. The decane solution was dried with calcium sulphate, decanted, and distilled with a small fractionary column. The distillate was first washed with cold sulfuric acid and then water. The n-hexane-1,1,1,6,6,6,-d_6 was dried by vacuum distillation from 4Å molecular sieve. Gas chromatography (6' x 1/8" .1% SP-1000 on 80/100 mesh Carbopack C) at 90^o - 22^o indicated greater than 99% deuteration. Mass spectrometry indicated 99.2% isotopic purity. The yield was .54 gm (39%).

A high resolution nmr spectrum of n-hexane-1,1,1,6,6,6-d_6 in $CDCl_3$ (V_H = 180 Mhz, deuterium decoupling, TMS) is shown in figure 45. The single peak (4 hz full width at half maximum) downfield

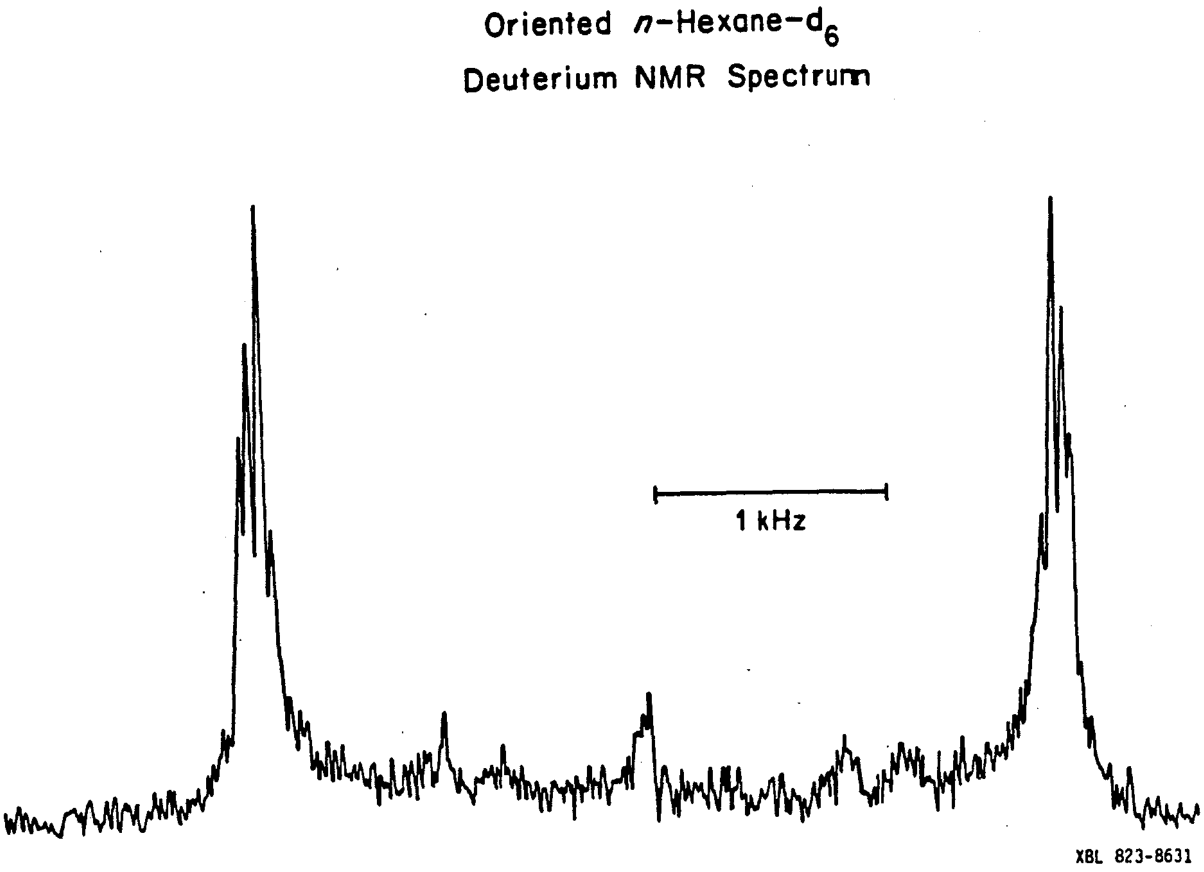

Figure 47. The proton decoupled deuterium nmr spectrum of oriented n-hexane-d_6 using a Hahn spin echo pulse sequence. The fine structure on the deuterium quadrupolar satellites is due to intramethyl dipolar couplings.

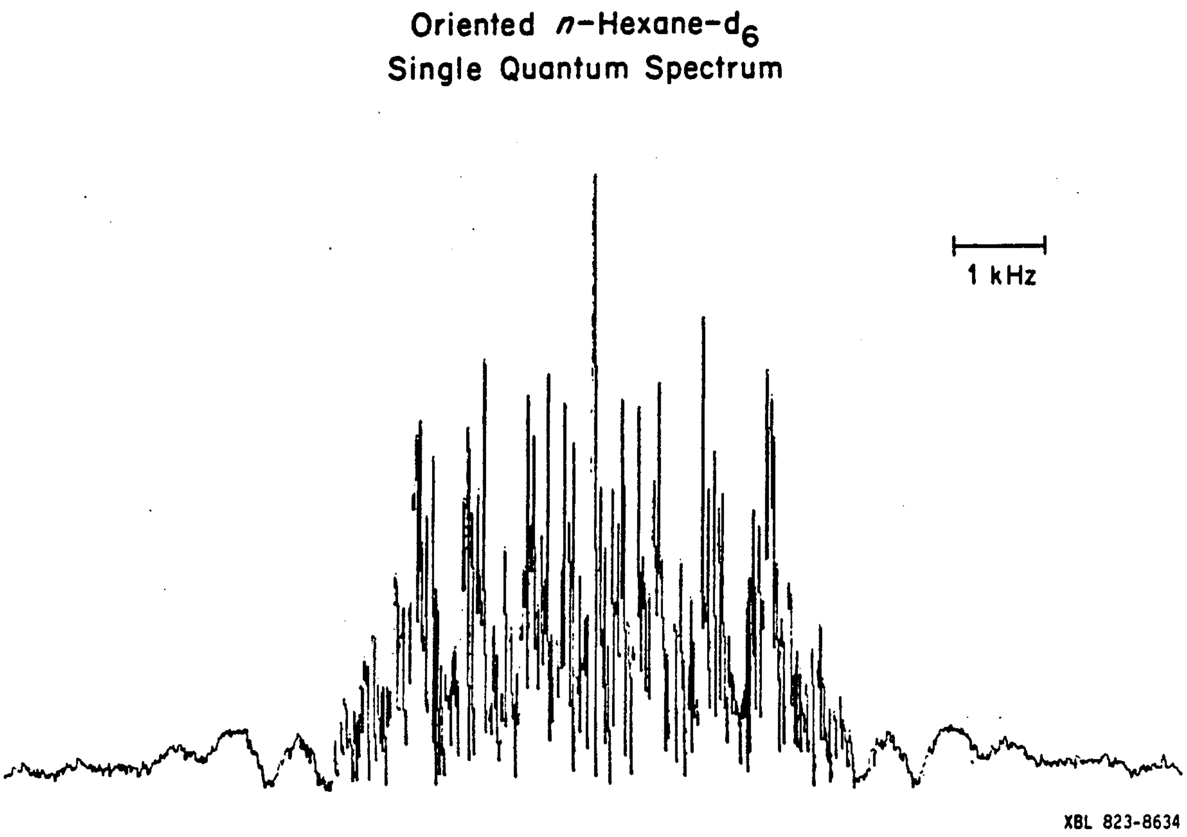

Figure 48. The proton single quantum nmr spectrum of n-hexane-d_6 obtained using a Hahn spin echo pulse sequence with deuterium decoupling.

complex spectrum (the power spectrum is shown in figure 48). Linewidths (full width at half maximum) were about 10 - 15 hz. No attempt was made to analyze the spectrum.

3.4.4 Multiple Quantum Spectra

Multiple quantum free induction decays of n-hexane-d_6 oriented in E-15320 were obtained at 33°C using the 4-pulse sequence described in section 3.2.4. TPPI was used to separate the different multiple quantum orders, with appropriate phase shifts being generated by a Daico 100D0898 digitally-controlled analog phase shifter (see section 4.7). All multiple quantum decays were obtained with deuterium decoupling during the preparation, evolution, and mixing periods.

Each multiple quantum experiment involved the accumulation of 4096 points at a timing increment of 10 μsec per point. The multiple quantum signal was observed to decay for only about one time constant, so signal truncation probably limits the resolution. Fifteen multiple quantum experiments were performed for preparation times ranging between 2 msec and 15 msec. The fifteen decays were Fourier transformed (8192 points) and the power spectra were added together, with appropriate scaling.

Figure 49 shows the 5 and 6 quantum regions and figure 50 shows the 6, 7, and 8 quantum regions. Linewidths are observed to be about 20 hz. The frequencies of the lines in the 6 and 7 quantum regions, measured relative to the center of each order, appear in table 33. As expected, the 7 quantum spectrum consists of two pairs of lines, and the central line is an artifact caused

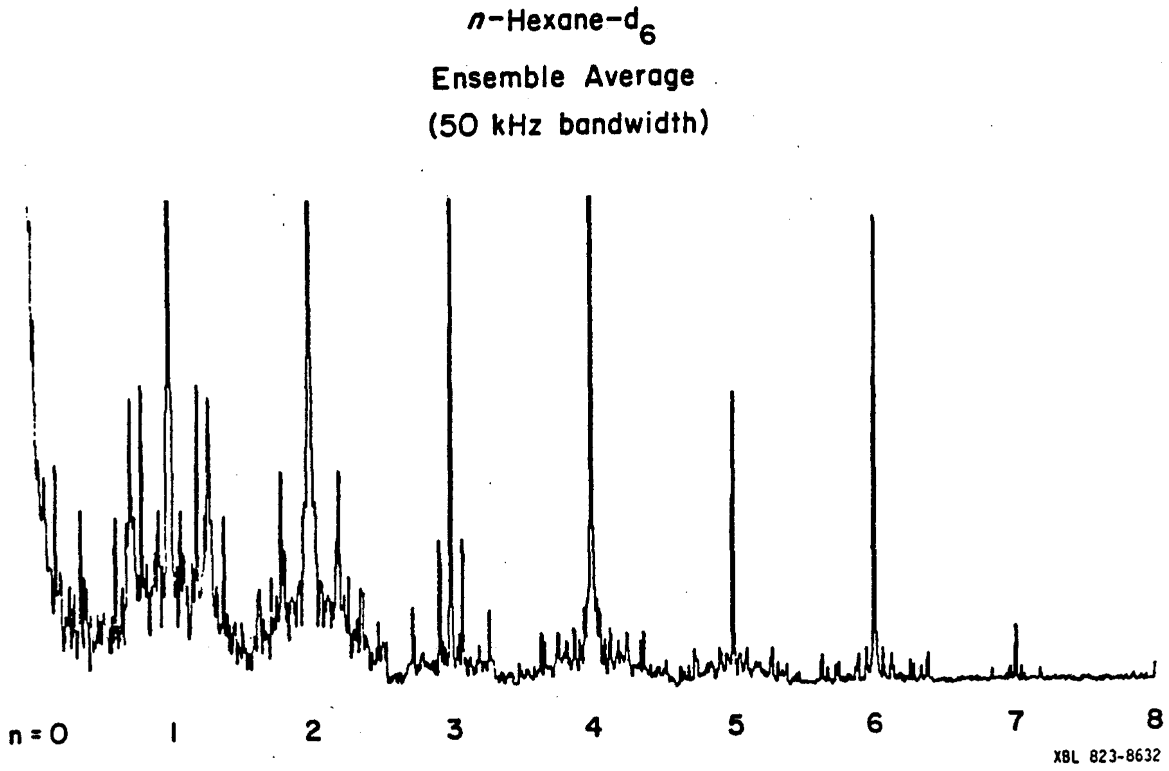

Figure 49.

(a) The multiple quantum proton nmr spectrum of oriented n-hexane-d_6 obtained using a TPPI pulse sequence with deuterium decoupling.

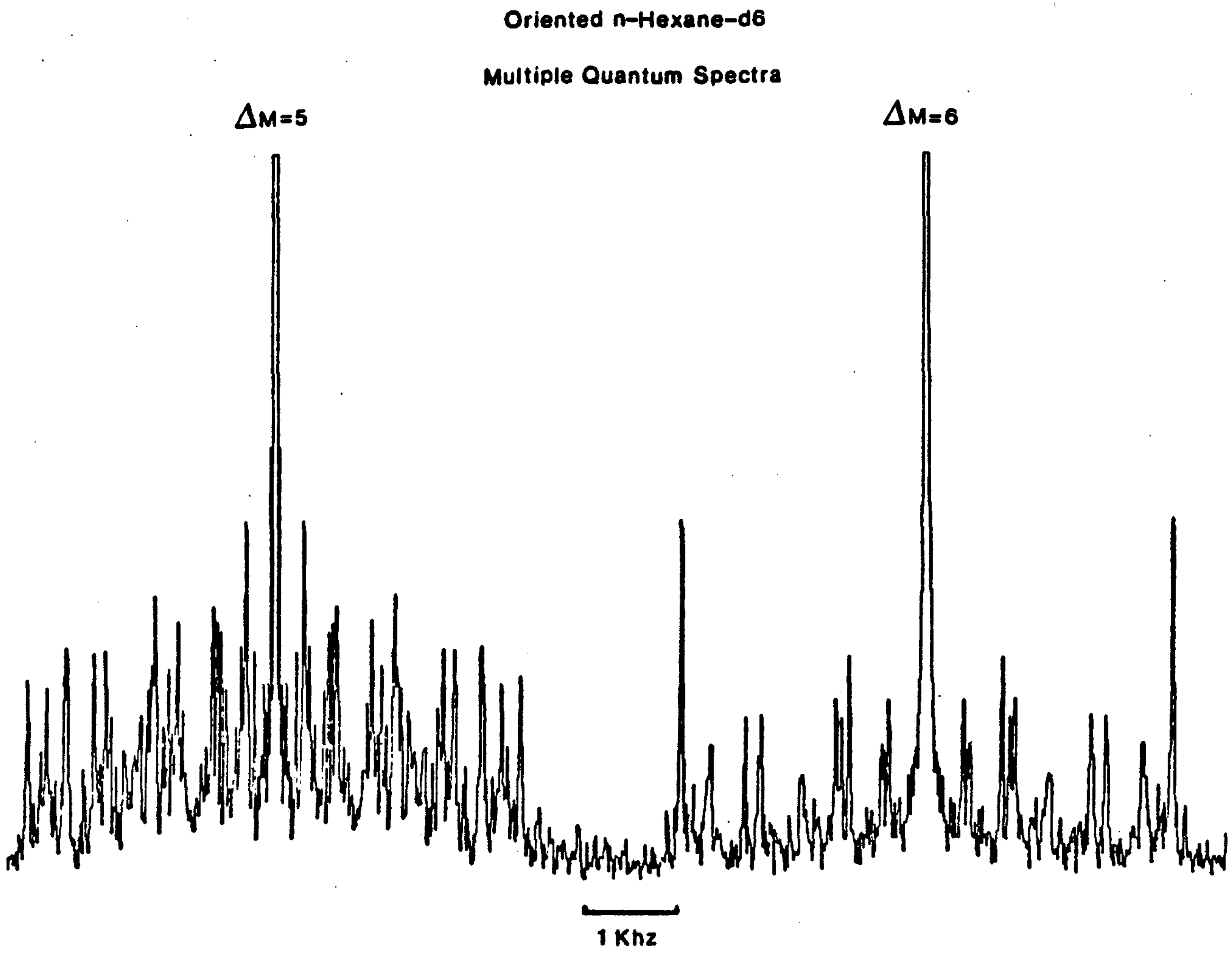

Figure 49.

(b) Expansion of the five and six quantum regions.

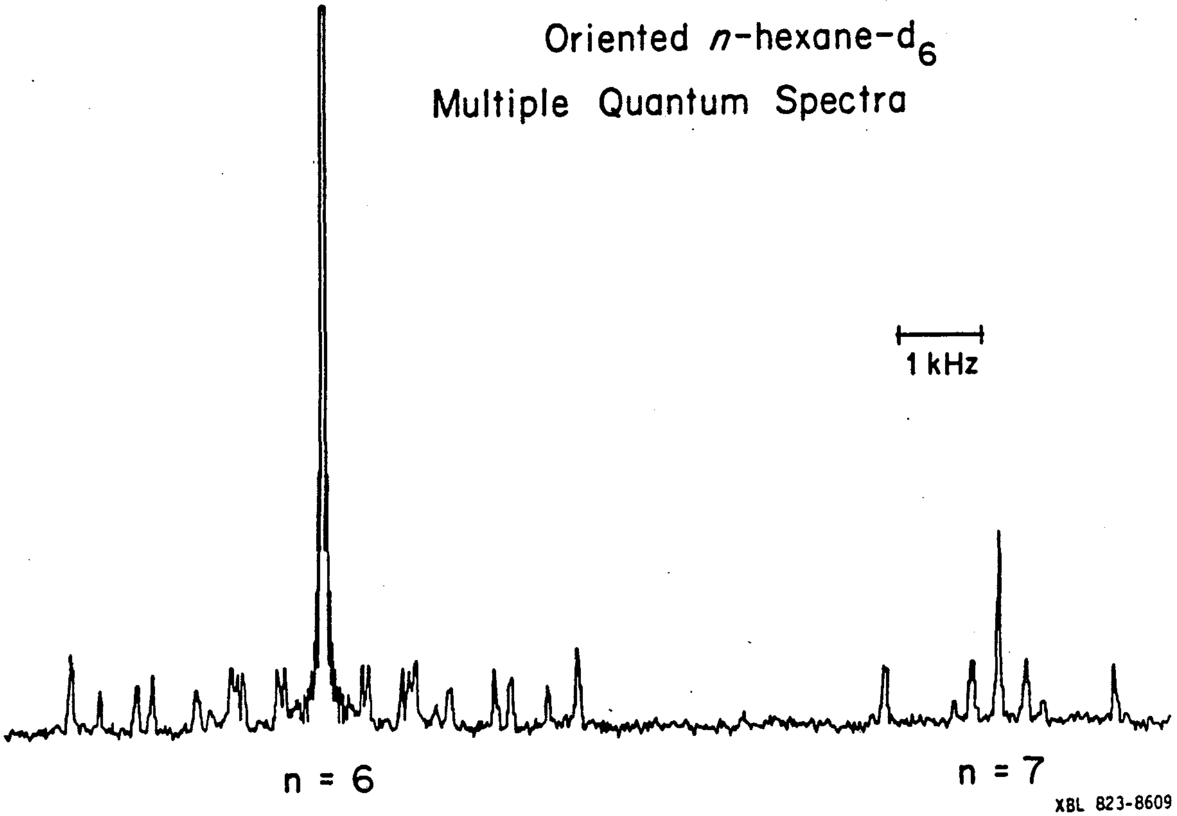

Figure 50. The six and seven quantum order of the proton multiple quantum spectrum of n-hexane-d_6.

by modulation of the pulse amplitude by the Daico phase shifter.

Table 3.3: Experimental Six and Seven Quantum Transition Frequncies*

$\Delta m = 6$	$\Delta m = 7$
±2298 hz	± 1044 hz
±2046	± 252
±1698	
±1554	
±1254	
±1146	
±1026	
± 846	
± 798	
± 714	
± 414	
± 354	

* Frequencies are measured relative to the center of the multiple quantum orders ($6\Delta\omega$ and $7\Delta\omega$).

The 6 quantum spectrum consists of 12 pairs and a central peak. Although 14 pairs of lines are expected, we will show in the next section that 2 pairs are expected to occur very close to the central lines and so are unresolved in the power spectrum.

3.4.5 Calculations and Discussion

In this section we present a preliminary analysis of the data presented in section 3.4.4. In particular we will calculate proton-proton coupling constants for n-hexane-d_6 using the expression

$$D(ij) = T_{20}^{dir}(ij) = -\frac{h\gamma^2}{4\pi^2} \sum_n (r_{ijn})^{-3} P_n S_{zz}(n)(3\cos^2\beta_n - 1) \qquad (131)$$

which is a simplification of equation 125. We will also assume that $S_{zz}(n)$ does not vary much with the configuration, so equation 131 is simplified to

$$D(ij) \sim -\frac{h\gamma^2}{4\pi^2} S_{zz} \sum_n (r_{ijn})^{-3} P_n (3\cos^2\beta_n - 1) \quad . \qquad (132)$$

Sets of average proton-proton dipole-coupling constants will be calculated for each of the motional models described in section 3.3.2. From the spectrum of isotropic n-hexane-d_6 we find that the scalar coupling between the protons of different methylene groups is negligible as is the isotropic chemical shift difference. Though the difference in anisotropic chemical shifts is also expected to be small, no data is available in the literature for n-hexane. Admitting ignorance, we will therefore neglect the anisotropic shift difference and assume that the internal Hamiltonian is

$$\mathcal{H} = \sum_{i<j} D_{ij}(3I_{zi}I_{zj} - I_i \cdot I_j) \qquad (133)$$

where D_{ij} is given by equation 132. Assuming that the internal Hamiltonian is given by equation 133, the set of D_{ij}'s calculated for each motional model will be used to calculate theoretical six and seven quantum spectra.

In order to calculate the geometric parameters $(r_{ijn})^{-3}(3\cos^2\beta_n-1)$, the coordinates of each proton nucleus were calculated for each configuration assuming that the carbon-carbon bond distance is 1.54Å, the carbon-carbon bond distance is 1.11Å, all bond angles are 109.45°, and rotational isomers are related by 120° rotations about the carbon-carbon bonds. A complete listing of the proton nuclear coordinates for all configurations not involving adjacent gauche rotations of opposite sign ($g^{\pm}g^{\mp}t$, $g^{\pm}g^{\mp}g^{\pm}$, $g^{\pm}g^{\mp}g^{\mp}$) is given in appendix 3.2.

Using the nuclear coordinates listed in appendix 3.2 the internuclear distance r_{ijn} was calculated for each nuclear pair in each configuration. Similarly the angle β_n between the internuclear vector and the molecular z axis was calculated for each nuclear pair in each configuration using the identity

$$\beta_n = \tan^{-1} \frac{(x_n{}^2 + y_n{}^2)^{1/2}}{Z_n} \tag{134}$$

Finally, the coupling constant of nuclei i and j for the n^{th} configuration was calculated by the program CPARAM using the expression

$$D_n(ij) = -\frac{hy^2}{4\pi^2}(r_{ijn})^{-3}(3\cos^2\beta_n-1) \tag{135}$$

For two protons, $-\frac{hy^2}{4\pi^2} = -240.14\ \frac{\text{khz}}{\text{Å}^3}$. A complete listing of the coupling constants (in units of kilohertz is given in appendix 3.3)

It remains to calculate a set of average coupling constants for each model using equation 132. This requires that each configurational coupling constant, given by equation 135, be weighted by an amount P_n, the configurational probability. We define the configurational probability as the statistical weight of the configurations incidence divided by the sum of the statistical weights of all feasible configurations. The statistical weight of the n^{th} configuration for an m-bond alkyl chain, assuming interdependent rotational potentials u

$$\Omega_n = \sum_{i=1}^{m-1} u_{\alpha\beta i} \tag{136}$$

where i labels the bond, $\alpha = t, g^{\pm}$, $\beta = t, g^{\pm}$ and we excluded any configuration that involves adjacent gauche rotations of opposite sign.

The term $u_{\alpha\beta i}$ is defined as

$$u_{\alpha\beta i} = \exp(-E_{\alpha\beta}/RT)_i \quad . \tag{137}$$

Thus the sum over statistical weights is the partition function

$$Z = \sum_n \Omega_n \quad , \tag{138}$$

and the configurational probability is given by

$$P_n = Z^{-1} \prod_{i=2}^{m-1} u_{\alpha\beta i} \quad . \tag{139}$$

To proceed we muct calculate sets of P_n's for each model. As a first approximation we assume a simple weighting of the configurational probability according to the number of bonds existing in gauche isomeric states, and we assume that for a given bond the probability of a trans state occurring is twice that of a gauche state. Furthermore, a probability of zero is assigned to any configuration in which adjacent bonds exist in gauche states of opposite rotation (e.g. $tg^{\pm}g^{\mp}$). Given these assumptions, configurational probabilities for each of the models discussed in section 3.3.2 were calculated and are listed in table 3.4.

Table 3.4: Calculated Configurational Probabilities for the Motional Models of n-hexane-d_6

Model	P_{ttt}	$P_{tg^{\pm}t}$	$P_{ttg^{\pm}}(=g^{\pm}tt)$	$P_{g^{\pm}tg^{\mp}}$	$P_{tg^{\pm}g^{\pm}}(=g^{\pm}g^{\pm}t)$	$P_{g^{\pm}+g^{\pm}}$	$P_{g^{\pm}g^{\pm}g^{\pm}}$
1	.25	.125	.125	0	0	0	0
2	.16	.08	.08	.04	.04	.04	.02
3	.2	.1	.1	.05	0	.05	0

We also note that the symmetry of a three bond chain requires that the following identities exist

$$D_{12} = D_{78} \tag{140a}$$

$$D_{13} = D_{24} = D_{57} = D_{68} \tag{140b}$$

$$D_{14} = D_{23} = D_{58} = D_{67} \tag{140c}$$

$$D_{15} = D_{26} = D_{37} = D_{48} \tag{140d}$$

$$D_{16} = D_{25} = D_{38} = D_{47} \tag{140e}$$

$$D_{17} = D_{28} \tag{140f}$$

$$D_{18} = D_{27} \tag{140g}$$

$$D_{34} = D_{56} \tag{140h}$$

$$D_{35} = D_{46} \tag{140i}$$

$$D_{36} = D_{45} \tag{140j}$$

and so there exist 10 independent coupling constants.

Using the probabilities given in table 3.4, the configurational coupling constants given in appendix 3.3, and the identities 140a-j, sets of average coupling constants may be calculated for each of the three models discussed in section 3.3.2 using equation 132. The results are tabulated in table 3.5. Using these average coupling constants, 6 and 7 quantum spectra were calculated using the program WIMP76, which is described in detail in reference 82. Theoretical spectra generated by WIMP76 are shown in figures 52a - e. Calculated frequencies are listed in table 3.6. Figure 52a shows the 6 and 7 quantum spectra assuming the existence only the "all trans" rotational isomer. Clearly the fit must be improved by the addition of other rotational isomers.

Figures 51b-d show theoretical 6 and 7 quantum spectra for the cases in which additional rotational isomers are included. Figure 51b shows the case of inclusion of the "single gauche" isomers, g±tt(=ttg±) and tg±t. Figure 51c shows the case in which all feasible configurations are included and figure 51d shows the case in which only the "linear" configurations are included. In the latter case such configurations as g±g±t and g±g±g± have been omitted. It is clear that figure 51d shows the closest correspondence to the experimental data.

The question remains, can the fit to experimental data be improved for any of the three models by an adjustment of the quantities $S_{zz}P_n$? One way to do this is to adjust the average coupling constants $D_{(ij)}$ iteratively using a "least squares" algorithn with the object of minimizing the difference between the theoretical and experimental line positions ( ). An improved set of D_{ij}'s could then be obtained and refined values of $S_{zz}(n)P_n$

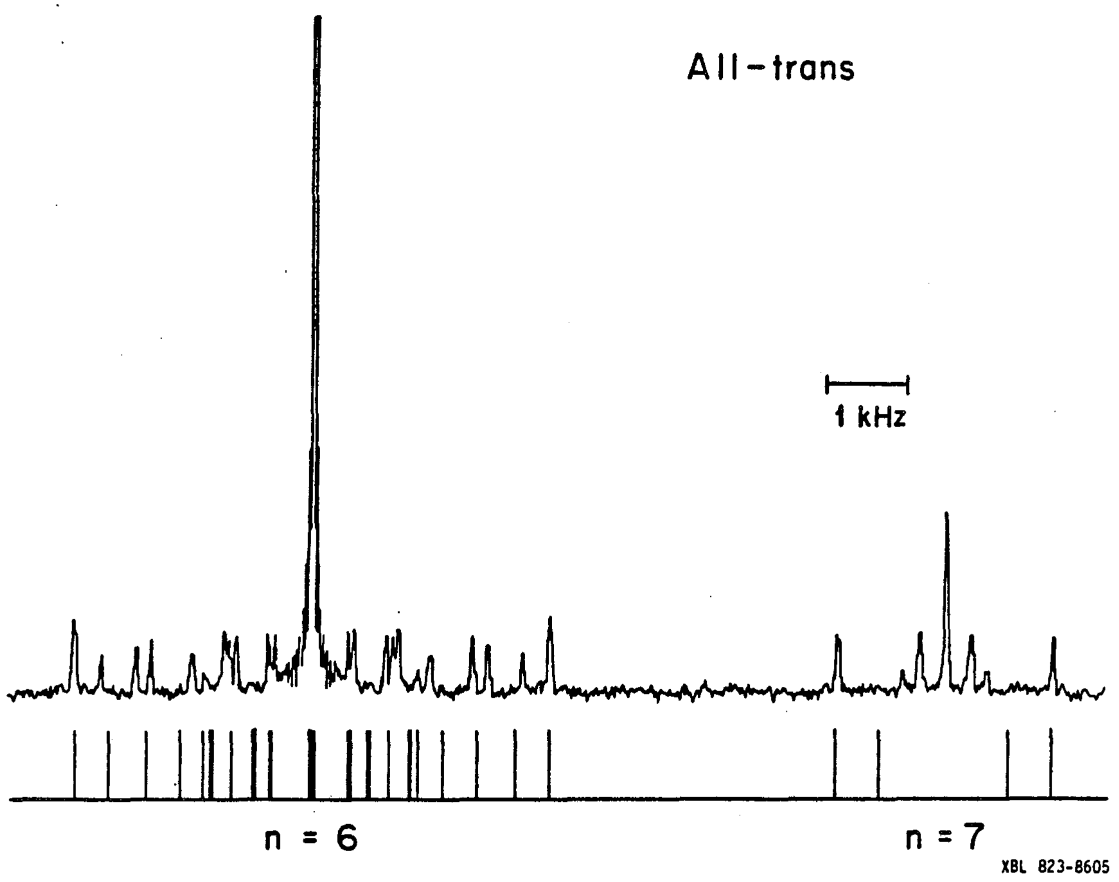

Figure 51. Spectral simulations of the six and seven quantum orders of n-hexane-d_6. It is assumed that P (trans)/P (gauche) = 2.

(a) All trans (ttt) only.

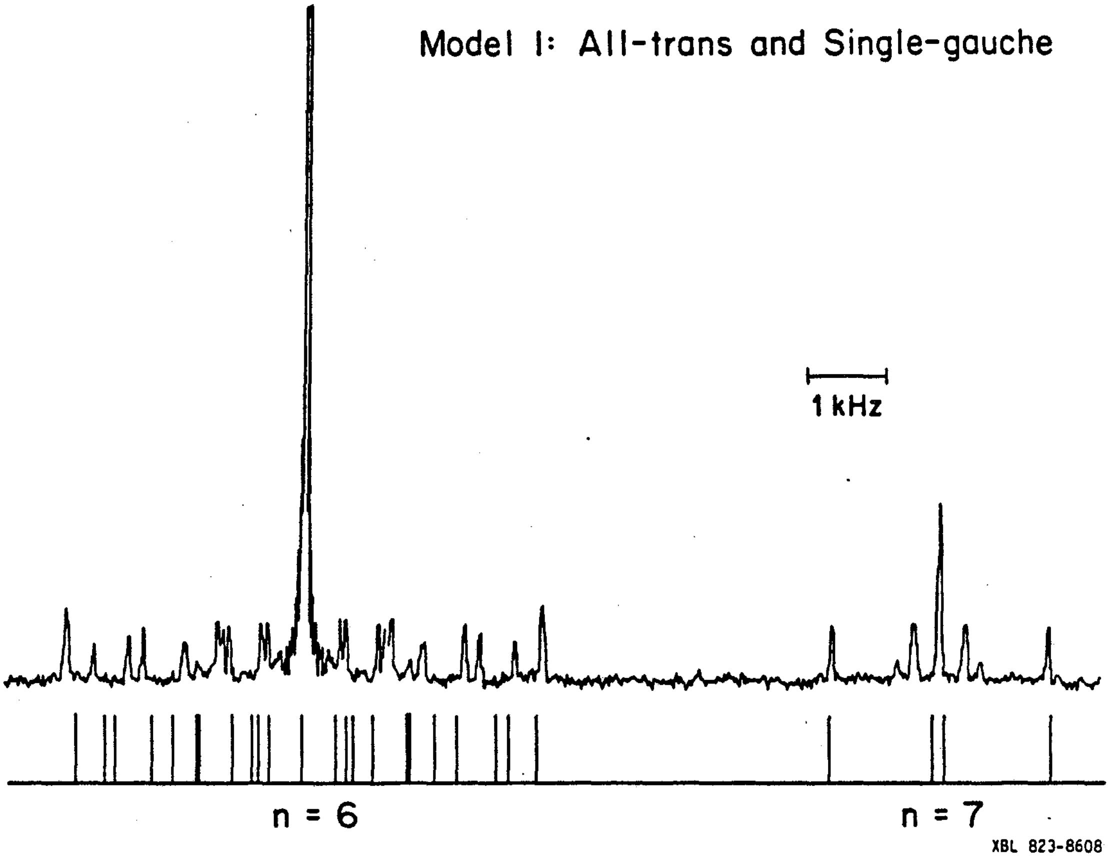

Figure 51.

(b) All trans (ttt) and single gauche ($g^{\pm}tt$ and $tg^{\pm}t$) only.

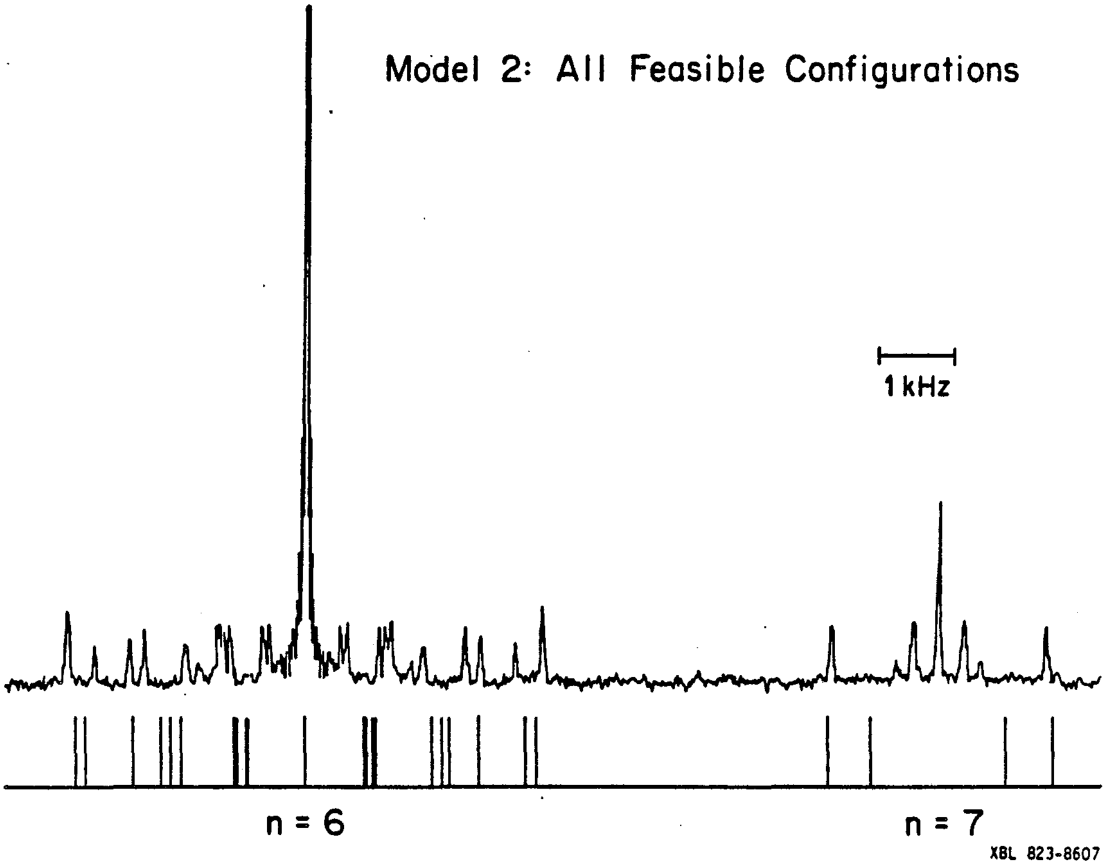

Figure 51.

(c) ttt, $g^{\pm}tt$, $tg^{\pm}t$, $g^{\pm}tg^{\mp}$, $g^{\pm}tg^{\pm}$, $g^{\pm}g^{\pm}t$, $g^{\pm}g^{\pm}g^{\pm}$.

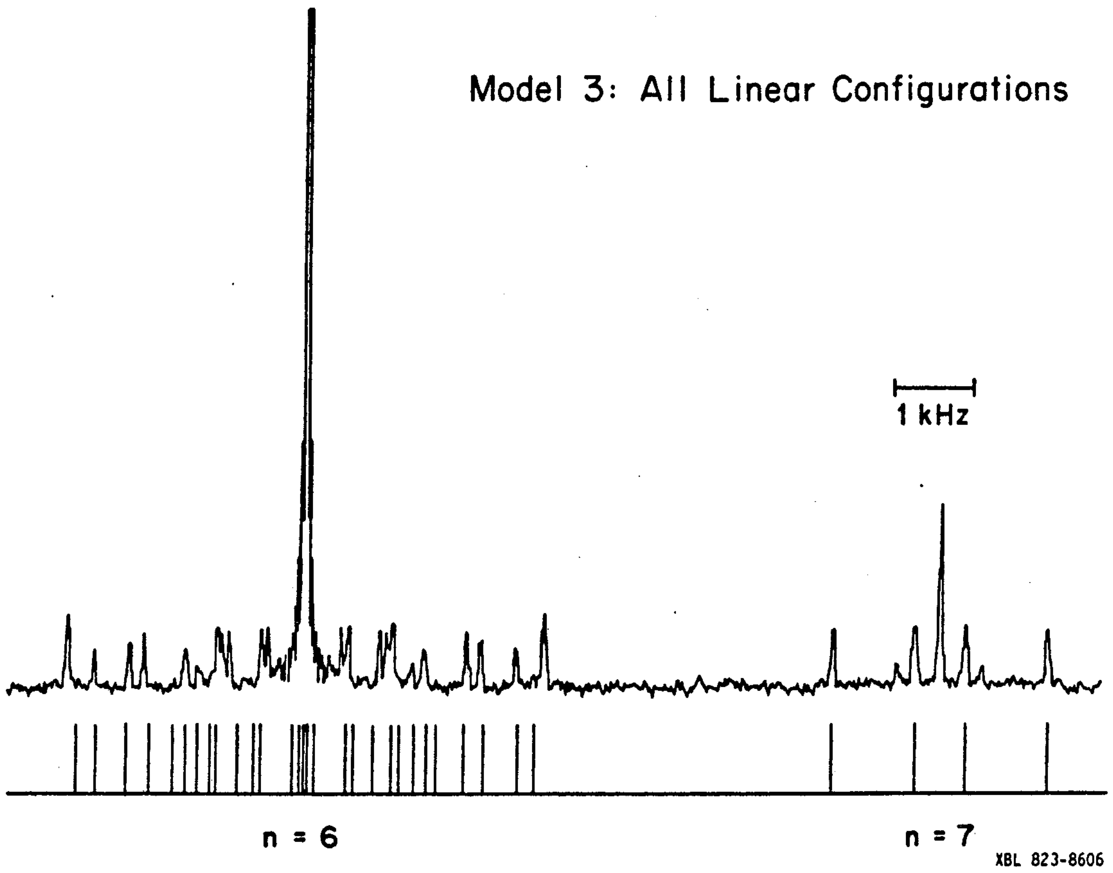

Figure 51.

(d) ttt, $g^{\pm}tt$, $tg^{\pm}t$, $g^{\pm}tg^{\mp}$, $g^{\pm}tg^{\pm}$.

Table 3.5: Calculated Averaged Dipolar Coupling Constants for the Motional Models of n-hexane-d_6*

$D_{(ij)}$	Model 1	Model 2	Model 3
12	1642.20	847.10	1434.47
13	113.77	37.20	4.43
14	69.81	40.30	-23.20
15	-1018.56	-764.90	-915.11
16	561.49	-621.60	-639.74
17	-301.54	-363.70	-420.00
18	-160.26	-384.00	-152.75
23	69.81	40.30	-23.20
24	113.77	37/20	4.43
25	-561.49	-621.60	-639.74
26	-1018.56	-764.90	-915.11
27	-160.26	-384.00	-152.75
28	-301.54	-363.70	-420.00
34	2080.48	2252.00	2161.37
35	67.70	5.60	89.97
36	14.75	-30.60	29.79
37	-1018.56	-764.90	-915.11
38	-561.49	-621.60	-639.74
45	14.75	-30.60	29.79
46	67.70	5.60	89.97
47	-561.49	-621.60	-639.74
48	-1018.56	-764.90	-915.11
56	2080.48	2252.00	2161.37
57	113.77	37.20	4.43
58	69.81	40.30	-23.20
67	69.81	40.30	-23.20
68	113.77	37.20	4.43
78	1642.20	847.10	1434.47

---

* In units of hertz.

Table 3.6: Calculated Six and Seven Quantum Transition Frequencies of the Motional Models of n-hexane-d_6*

$\Delta m = 6$

Model 1	Model 2	Model 3
±2257	±2223	±2219
±2006	±2136	±2050
±1922	±1724	±1770
±1369	±1435	±1504
±1253	±1435	±1323
±1015	±1378	±1178
±997	±1268	±1051
±655	±720	±958
±477	±712	±881
±417	±609	±622
±314	±589	±471
±257	±227	±414
±137	±191	±218
-	-	55

$\Delta m = 7$

±1063	±1080	±1053
±40	±644	±270

---

* In units of hertz, measured from the center of the multiple quantum order.

could be calculated by the solution of a set of simultaneous equations of the form of equation 130.

Iterative improvements of the spectral simulations shown in figures 51b-d were attempted using the program MQITER. MQITER has been thoroughly described in reference 88 so we only comment that the parameters used were the 10 independent coupling constants and these parameters were adjusted via a least squares algorithm to minimize the differences between the experimental and calculated six and seven quantum transition frequencies. Twenty-six five quantum transitions were also included in the calculation. Of the three models considered in this study only the model involving "linear" configurations (figure 51d) converged after a small improvement in rms error (48 to 45 hz). The other models (figures b and c) diverged after a single iteration. However, the rms improvement in the third model was mainly in the five quantum spectrum, while the "refined" fit is actually poorer in the six and seven quantum spectra (see table 3.7). This clearly indicates that the iteration is converging to a local minimum, a situation that often occurs in least-squares algorithms (104).

WIMP76 also generates transitions intensities for individual preparation times and for "ultimate" ensemble averages. The spectrum resulting from the coaddition of several multiple quantum power spectra (corresponding to different preparation times) is called an ensemble average. If a very large number of power spectra are added, convergence to an ultimate ensemble average is expected (82). Figure 52 compares the experimental ensemble average of the six and

Table 3.7: Calculated Six and Seven Quantum Transition Frequencies for Model 3: MQITER*

m = 6

±2213

±2075

±1819

±1511

±1335

±1180

±1061

±981

±873

±590

±487

±434

±94

±59

m = 7

±1084

±250

---

* in units of hertz

seven quantum spectra with the calculated ultimate ensemble average. There is no agreement, indicating that the experimental average has not converged to the "ultimate value".

3.4.6 Conclusions

In this chapter multiple quantum nmr spectroscopy has been applied to the study of the configurational statistics of an alkyl chain molecule, n-hexane-d_6, dissolved in a nematic liquid crystal. Specifically, high resolution multiple quantum spectra have been obtained by using a 180° pulse in the middle of the evolution time (t_1) to refocus magnetic field inhomogeneity together with TPPI to separate the various multiple quantum orders. Theoretical six and seven quantum spectra have been calculated assuming various configurational populations and assuming a rotational isomeric model of chain motion. It has been found that the closest agreement with experiment results assuming the following probabilities

$$P_{ttt} = .2$$

$$P_{ttg^\pm} = P_{g^\pm tt} = P_{tg^\pm t} = .1$$

$$P_{g^\pm tg^\mp} = P_{g^\pm tg^\pm} = .05$$

$$P_{g^\pm g^\pm t} = P_{tg^\pm g^\pm} = P_{g^\pm g^\pm g^\pm} = 0$$

A refinement of the above probabilities was attempted using the dipolar couplings as parameters and iterating on several five quantum lines and all the six and seven quantum lines. The result

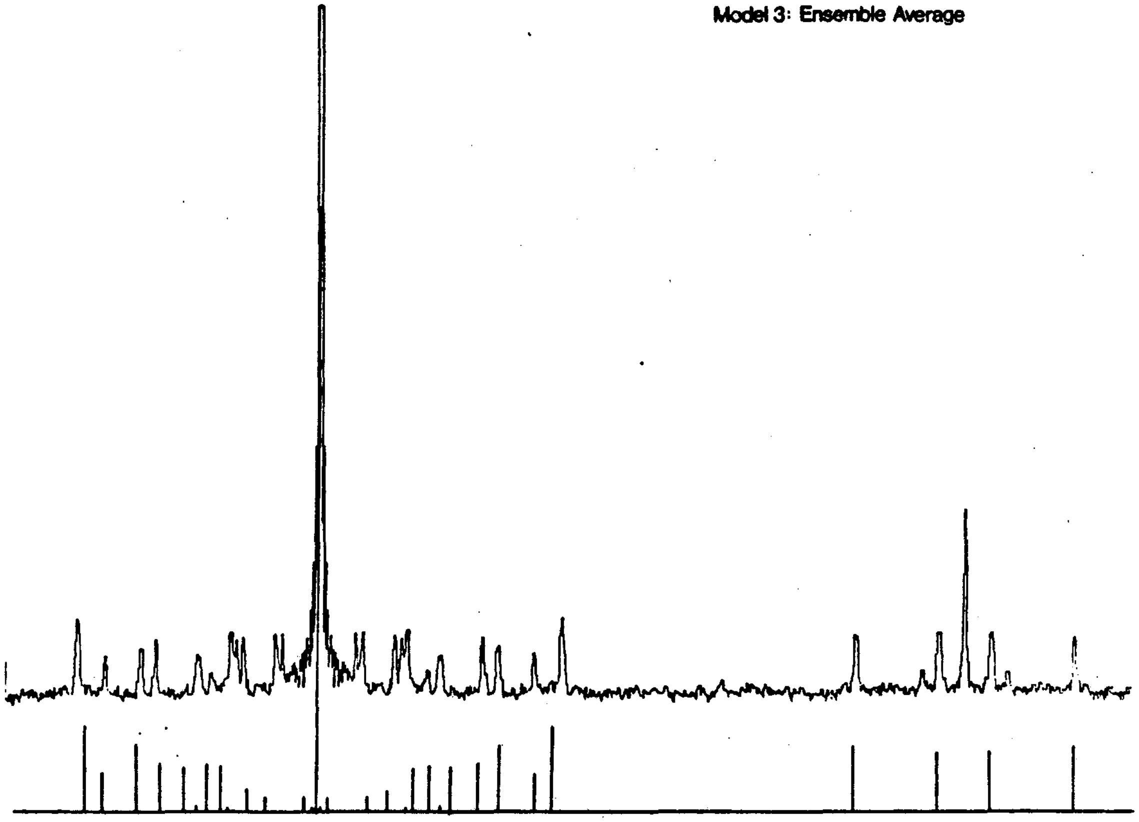

Figure 52. Comparison of the experimental six and seven quantum spectra with the "ultimate ensemble average" generated by WIMP76.

was that the five quantum fit improved slightly at the expense of the six and seven quantum fits. Therefore the calculation seem to have converged to a nonglobal minimum.

Appendix 3.1: Matrix Form for $\exp(-i\mathcal{H}^D_{yy}\tau)$

We define $\mathcal{H}^D_{yy}$ as

$$\mathcal{H}^D_{yy} = e^{-i\frac{\pi}{2}I_x}\ \mathcal{H}^D_{zz}\ e^{i\frac{\pi}{2}I_x}$$

$$= {}^{d}/4(3I_y{}^2 - I^2)$$

$$= \frac{3d}{8}\begin{bmatrix} 1 & 0 & -\sqrt{3} & 0 \\ 0 & 1 & 0 & -\sqrt{3} \\ -\sqrt{3} & 0 & 1 & 0 \\ 0 & -\sqrt{3} & 0 & -1 \end{bmatrix} = \frac{3d}{8} M \qquad (1)$$

Now expand $\exp(-i\mathcal{H}^D_{yy}\tau)$ in a Taylor series

$$\exp(-i\mathcal{H}^D_{yy}\tau) = 1 - i\mathcal{H}^D_{yy}\tau - \frac{(\mathcal{H}^D_{yy}\tau)^2}{2!} + \frac{i(\mathcal{H}^D_{yy}\tau)^3}{3!} + \ldots.. \qquad (2)$$

and use the identities

$$(\mathcal{H}^D_{yy})^{2k} = ({}^{3d}/4)^{2k}\ \underset{\sim}{1} = (d')^{2k} \qquad (3a)$$

$$(\mathcal{H}^D_{yy})^{2k+1} = {}^{1}/2({}^{3d}/4)^{2k+1}\ M = \frac{(d')^{2k+1}}{2}\ M \qquad (3b)$$

to obtain the final result

$$\exp(-i\mathcal{H}^D_{yy}\tau) = \sum_{k=0}^{\alpha} (-)^k \frac{(d'\tau)^{2k}}{(2k)!} - {}^{i}/2\ M \sum_{k=0}^{\alpha} (-)^k \frac{(d'\ )^{2k+1}}{(2k+1)!}$$

$$= \cos(d'\tau) - {}^{i}/2\ M \sin(d'\tau) \qquad (4)$$

Appendix 3.2: Nuclear Coordinates for the Methylene Protons of n-hexane

In this appendix, the nuclear coordinates of the methylene protons for all allowed configurations of n-hexane. If the molecular coordinate system used does not coincide with the all trans coordinate system (figure 42), the Cartesian rotation matrix $\mathcal{R}(\alpha, \beta, \gamma)$ relating the two coordinate systems will be specified. $\mathcal{R}(\alpha, \beta, \gamma)$ is defined as:

$$\mathcal{R}(\alpha,\beta,\gamma) = \begin{bmatrix} \cos\alpha\cos\beta\cos\gamma-\sin\alpha\sin\gamma & \sin\alpha\cos\beta\cos\gamma+\cos\alpha\sin\gamma & -\sin\beta\cos\gamma \\ -\cos\alpha\cos\beta\sin\gamma-\sin\alpha\cos\gamma & -\sin\alpha\cos\beta\sin\gamma+\cos\alpha\cos\gamma & \sin\beta\sin\gamma \\ \cos\alpha\sin\beta & \sin\alpha\sin\beta & \cos\beta \end{bmatrix} \tag{1}$$

In the tabulation that follows, P_i referes to the point coordinates of nuclei i. $P_i = (x_i, y_i, z_i)$. Coordinates are in units of Angstroms.

a. All trans

P_1	(-1.09, .91, -1.89)	P_5	(-1.09, .91, .63)
P_2	(-1.09, -.91, -1.89)	P_6	(-1.09, -.91, .63)
P_3	(1.09, .91, -.63)	P_7	(1.09, .91, 1.89)
P_4	(1.09, -.91, -.63)	P_8	(1.09, -.91, 1.89)

b. single gauche

ttg^-

P_1	(-1.09, .91, -1.89)	P_5	(-1.09, .91, .63)
P_2	(-1.09, -.91, -1.89)	P_6	(-1.09, -.91, .63)
P_3	(1.09, .91, -.63)	P_7	(1.09, -.91, 1.89)
P_4	(1.09, -.91, -.63)	P_8	(-.198, 0, 2.80)

ttg^+

P_1	(-1.09, .91, -1.89)	P_5	(-1.09, .91, .63)
P_2	(-1.09, -.91, -1.89)	P_6	(-1.09, -.91, .63)
P_3	(1.09, .91, -.63)	P_7	(1.09, -.91, 1.89)
P_4	(1.09, -.91, -.63)	P_8	(-.198, 0, 2.80)

g^+tt

P_1	(-1.09, -.91, -1.89)	P_5	(-1.09, .91, .63)
P_2	(.198, 0, -2.8)	P_6	(-1.09, -.91, .63)
P_3	(1.09, .91, -.63)	P_7	(1.09, .91, 1.89)
P_4	(1.09, -.91, -.63)	P_8	(1.09, -.91, 1.89)

g^-tt

P_1	(.198, 0, -2.8)	P_5	(-1.09, .91, .63)
P_2	(-1.09, .91, -1.89)	P_6	(-1.09, -.91, .63)
P_3	(1.09, .91, -.63)	P_7	(1.09, .91, 1.89)
P_4	(1.09, -.91, -.63)	P_8	(1.09, .91, 1.89)

$tg^{+}t$

The molecular coordinate system of this configuration is related to that of ttt by the Euler angles Ω = (180, 35.25, 60)

$$\underset{\sim}{R}\,(180,35.25,60) = \begin{bmatrix} -.409 & -.866 & -.289 \\ .707 & -.500 & .500 \\ -.577 & 0 & .817 \end{bmatrix}$$

P_1	(.204, -2.17, -.915)	P_5	(1.05, 0, 1.14)
P_2	(1.78, -1.26, -.915)	P_6	(-.524, .91, 1.14)
P_3	(-1.05, 0, -1.14)	P_7	(-.204, -2.17, .915)
P_4	(524, .91, -1.14)	P_8	(-1.78, -1.26, .915)

$tg^{-}t$

The molecular coordinate system is related to that of ttt by the transformation:

$$\underset{\sim}{R} = \begin{bmatrix} .409 & -.866 & .289 \\ .707 & .5 & .5 \\ -.577 & 0 & .817 \end{bmatrix}$$

c. Double Gauche

$g^{-}tg^{+}$

P_1	(.198, 0, -2.80)	P_5	(-1.09, .91, .63)
P_2	(-1.09, .91, -1.89)	P_6	(-1.09, -.91, .63)
P_3	(1.09, .91, -.63)	P_7	(1.09, -.91, 1.89)
P_4	(1.09, -.91, -.63)	P_8	(-.198, 0, 2.80)

tg^+g^+

P_1	(-1.09, .91, -1.89)	P_5	(.2, 0, 1.54)
P_2	(-1.09, -.91, -1.89)	P_6	(-1.09, .91, .63)
P_3	(1.09, .91, -.63)	P_7	(-1.98, -1.26, -.28)
P_4	(1.09, -.91, -.63)	P_8	(-1.98, -1.26, 1.54)

tg^-g^-

P_1	(-1.09, .91, -1.89)	P_5	(-1.09, -.91, .63)
P_2	(-1.09, -.91, -1.89)	P_6	(.2, 0, 1.54)
P_3	(1.09, .91, -.63)	P_7	(-1.98, 1.26, 1.54)
P_4	(1.09, -.91, -.63)	P_8	(-1.98, 1.26, -.28)

g^+tg^-

P_1	(-1.09, -.91, -1.89)	P_5	(-1.09, .91, .63)
P_2	(.198, 0, -2.80)	P_6	(-1.09, -.91, .63)
P_3	(1.09, .91, -.63)	P_7	(-.198, 0, 2.80)
P_4	(1.09, -.91, -.63)	P_8	(1.09, .91, 1.89)

g^-tg^-

P_1	(-1.09, -.91, -1.09)	P_5	(-1.09, .91, .63)
P_2	(.198, 0, -2.8)	P_6	(-1.09, -.91, .63)
P_3	(1.09, .91, -.63)	P_7	(1.09, -.91, 1.89)
P_4	(1.09, -.91, -.63)	P_8	(-.198, 0, 2.80)

g tg

P_1	(.198, 0, -2.8)	P_5	(-1.09, .91, .63)
P_2	(-1.09, .91, -1.89)	P_6	(-1.09, -.91, .63)
P_3	(1.09, .91, -.63)	P_7	(-.198, 0, 2.8)
P_4	(1.09, -.91, -.63)	P_8	(1.09, .91, 1.89)

g^+g^+t

P_1	(1.98, 1.26, -1.54)	P_5	(-1.09, .91, .63)
P_2	(1.98, 1.26, .28)	P_6	(-1.09, -.91, .63)
P_3	(1.09, -.91, -.63)	P_7	(1.09, .91, 1.89)
P_4	(-.2, 0, -1.54)	P_8	(1.09, -.91, 1.89)

g^-g^-t

P_1	(1.98, -1.26, .28)	P_5	(-1.09, .91, .63)
P_2	(1.98, -1.26, -1.54)	P_6	(-1.09, -.91, .63)
P_3	(-.2, 0, -1.54)	P_7	(1.09, .91, 1.89)
P_4	(1.09, .91, -.63)	P_8	(1.09, -.91, 1.89)

d. Triple Gauche

$g^+g^+g^+$

THe molecular coordinate system of the $g^+g^+g^+$ configuration is related to the ttt coordinate system by the Euler angles $\Omega = (-60, 90, 0)$.

$$R(-60,90,0) = \begin{bmatrix} 0 & 0 & -1 \\ .866 & .5 & 0 \\ .5 & -.866 & 0 \end{bmatrix}$$

P_1	(1.89, -1.40, .243)	P_5	(-1.54, .173, .1)
P_2	(2.80, .171, .099)	P_6	(-.63, -.489, -1.33)
P_3	(.63, 1.40, -2.43)	P_7	(.28, -2.34, .1)
P_4	(.63, .489, 1.33)	P_8	(1.54, -2.34, .1)

$g^{-}g^{-}g^{-}$

The molecular coordinate system of the $g^{+}g^{+}g^{+}$ configuration is related to the ttt coordinate system by the Euler angles Ω = (60, 90, 180).

$$R\,(60,90,180) = \begin{bmatrix} 0 & 0 & -1 \\ .866 & -.5 & 0 \\ .5 & .866 & 0 \end{bmatrix}$$

P_1	(2.80, .171, .099)	P_5	(-.63, -.489, -1.33)
P_2	(1.89, -1.40, .243)	P_6	(-1.54, .173, .1)
P_3	(.63, .489, 1.33)	P_7	(-1.54, -2.34, .1)
P_4	(.63, 1.40, -.243)	P_8	(.28, -2.34, .1)

Appendix 3.3: Dipolar Couplings for n-hexane-d_6

In this appendix is tabulated the dipolar couplings between the methylene protons for all allowed configurations of n-hexane. Dipolar couplings were calculated using the equation

$$D_{(ij)} = -\frac{h\gamma^2}{4\pi^2}(r_{ijn})^{-3}(3\cos^2\beta_n - 1) \qquad (1)$$

where r_{ijn} is the distance between i and j in the nth configuration, and β_n is the angle between the z axis of the principal axis system and the z axis of the molecular axis system in the nth configuration. The internuclear distance r_{ijn} and β_n were calculated from the coordinates given in appendix 3.2. All couplings are in units of kilohertz. The symbol "ij)" before each coupling signifies the nuclei involved, numbered according to the convention given in figure 42.

a. All trans

12)	19.9169
13)	1.8711
14)	2.0282
15)	-15.0059
16)	-3.8839
17)	-1.8082
18)	-1.0425
23)	2.0282
24)	1.8711
25)	-3.9939
26)	-15.0059
27)	-1.0425
28)	-1.8082
34)	19.9169
35)	1.8711
36)	2.0282
37)	-15.0059
38)	-3.8839
45)	2.0282
46)	1.8711
47)	-3.8839
48)	-15.0059
56)	19.9169
57)	1.8711
58)	2.0282
67)	2.0282
68)	1.8711
78)	19.9169

b. Single Gauche

ttg^-

12) 19.9169
13) 1.8711
14) 2.0282
15) -5.0059
16) -3.8839
17) -1.8762
18) -1.8082

23) 2.0282
24) 1.8711
25) -3.8839
26)-15.0059
27) -1.8762
28) -1.0425

34) 19.9169
35) 1.8711
36) 2.0282
37) -3.2950
38)-15.0059

45) 2.0282
46) 1.8711
47) -3/2950
48) -3.8839
56) 19.9169
57) -9.2732
58) 1.8711

67) -9.2732
68) 2.0282
78) 4.9854

ttg^+

12) 19.9169
13) 1.8711
14) 2.0282
15)-15.0059
16) -3.8839
17) -1.0425
18) -1.8702

23) 2.0282
24) 1.8711
25) -9.8839
26)-15.0059
27) -1.8082
28) -1.8762

34) 19.9169
35) 1.8711
36) 2.0282
37) -3.8839
38) -3.2950

45) 2.0282
46) 1.8711
47)-15.0059
48) -3.2950
56) 19.9169
57) 2.0282
58) -9.2732

67) 1.8711
68) -9.2732
78) 4.9854

g^+tt

12) 4.9854
13) 2.0282
14) 1.8711
15) -3.8839
16)-15.0059
17) -1.0425
18) -1.8082

23) -9.2732
24) -9.2732
25) -3.2950
26) -3.2950
27) -1.8762
28) -1.8762

34) 19.9169
35) 1.8711
36) 2.0282
37)-15.0059
38) -3.8839

45) 2.0282
46) 1.8711
47) -3.8839
48)-15.0059
56) 19.9169
57) 1.8711
58) 2.0282

67) 2.0282
68) 1.8711
69) 19.9169

gtt

12)	4.9854	23)	1.8711	34)	19.9169	45)	2.0282	67)	2.2082
13)	-9.2732	24)	2.0282	35)	1.8711	46)	1.8711	68)	1.8711
14)	-9.2732	25)	-15.0059	36)	2.0282	47)	-3.8839	78)	19.9169
15)	-3.2950	26)	-3.8839	37)	-15.0059	48)	-15.0059		
16)	-3.2950	27)	-1.8082	38)	-3.8839	56)	19.9169		
17)	-1.8762	28)	-1.0425			57)	1.8711		
18)	-1.8762					58)	2.0282		

$tg^{+}t$

12)	19.9215	23)	3.9441	34)	19.9785	45)	-11.1853	67)	3.9488
13)	7.3549	24)	7.3463	35)	-2.5119	46)	-11.2218	68)	7.3463
14)	3.9488	25)	-7.4939	36)	-11.1853	47)	.2464	78)	19.9215
15)	-1.2549	26)	.2465	37)	-1.2549	48)	.2465		
16)	.2464	27)	-1.2382	38)	-7.4939	56)	19.9785		
17)	-33.8463	28)	.6982			57)	7.3549		
18)	-1.2382					58)	3.9441		

$tg^{-}t$

12)	19.9215	23)	3.9488	34)	19.9785	45)	-11.1853	67)	3.9441
13)	7.3463	24)	7.3549	35)	-11.2218	46)	-2.5119	68)	7.3549
14)	3.9441	25)	.2464	36)	-11.1853	47)	-7.4939	75)	19.9215
15)	.2465	26)	-1.2549	37)	.2465	48)	-1.2549		
16)	-7.4939	27)	-1.2382	38)	.2464	56)	19.9785		
17)	.6982	28)	-33.8463			57)	7.3463		
18)	-1.2382					58)	3.9488		

c. Double Gauche

g^+tg^+

12)	4.9854	23)	-9.2732	34)	19.9169	45)	2.0282	67)	1.8711
13)	2.0282	24)	-9.2732	35)	1.8711	46)	1.8711	68)	-9.2732
14)	1.8711	25)	-3.2950	36)	2.0282	47)	-15.0059	78)	4.9854
15)	-3.8839	26)	-3.2950	37)	-3.8839	48)	-3.2950		
16)	-15.0059	27)	-1.8702	38)	-3.2950	56)	19.9169		
17)	-1.8082	28)	-1.3471			57)	2.0282		
18)	-1.8762					58)	-9.2732		

g^-tg^-

12)	4.9854	23)	1.8711	34)	19.9169	45)	2.0282	67)	-9.2732
13)	-9.2732	24)	2.0282	35)	1.8711	46)	1.8711	68)	2.0282
14)	-9.2732	25)	-15.0059	36)	2.0282	47)	-3.2950	78)	4.9854
15)	-3.2950	26)	-3.8839	37)	-3.2950	48)	-3.8839		
16)	-3.2950	27)	-1.8762	38)	-15.0059	56)	19.9169		
17)	-1.3471	28)	-1.8082			57)	-9.2732		
18)	-1.8762					58)	1.8711		

g^-tg^+

12)	4.9854	23)	1.8711	34)	19.9169	45)	2.0282	67)	1.8711
13)	-9.2732	24)	2.0282	35)	1.8711	46)	1.8711	68)	-9.2732
14)	-9.2732	25)	-15.0059	36)	2.0282	47)	-15.0059	78)	4.9854
15)	-3.2950	26)	-3.8839	37)	-3.8839	48)	-3.2950		
16)	-3.2950	27)	-1.0425	38)	-3.2950	56)	19.9169		
17)	-1.8962	28)	-1.8762			57)	2.0282		
18)	-1.3471					58)	-9.2732		

g^+tg^-

12) 4.9854
13) 2.0282
14) 1.8711
15) -3.8839
16)-15.0059
17) -1.8762
18) -1.0425
23) -9.2732
24) -9.2732
25) -3.2950
26) -3.2950
27) -1.3471
28) -1.8762
34) 19.9169
35) 1.8711
36) 2.0282
37) -3.2950
38) -15.0059
45) 2.0282
46) 1.8711
47) -3.2950
48) -3.8839
56) 19.9169
57) -9.2732
58) 1.8711
67) -9.2732
68) 2.0282
78) 21.9854

tg^+g^+

12) 19.9169
13) 1.8711
14) 2.0282
15) -3.2912
16)-15.0059
17) .2041
18) -1.7475
23) 2.0282
24) 1.8711
25) -3.2912
26) -3.8839
27) -22.2626
28) -4.7433
34) 19.9169
35) -9.2905
36) 1.8711
37) 2.1731
38) .3674
45) -9.2905
46) 2.0282
47) 3.8413
48) .0203
56) 4.9969
57) -.1181
58) 7.5214
67) 4.5809
68) 4.509
78) -39.8337

tg^-g^-

12) 19.9169
13) 1.8711
14) 2.0282
15) -3.8839
16) -3.2912
17) -4.7430
18)-22.2626
23) 2.0282
24) 1.8711
25) -15.0059
26) -3.2912
27) -1.7475
28) .2401
34) 19.9169
35) 2.0282
36) -9.2905
37) .0203
38) 3.8413
45) 1.8711
46) -9.2905
47) .3674
48) 2.1731
56) 4.9869
57) 4.5809
58) 4.5809
67) 7.5214
68) -1.1181
78) -39.8337

$g^{+}g^{+}t$

12)	-39.8337	23)	4.5809	34)	4.9969	45)	-9.2905	67)	2.0282
13)	4.5809	24)	-.1181	35)	2.0282	46)	-9.2905	68)	1.8711
14)	7.5214	25)	3.8413	36)	1.8711	47)	-3.2912	78)	19.9169
15)	.0208	26)	2.1731	37)	-3.8839	48)	-3.2912		
16)	.3674	27)	-22.2626	38)	-15.0059	56)	19.9169		
17)	-4.7433	28)	.2041			57)	1.8711		
18)	-1.7475					58)	2.0282		

$g^{-}g^{-}t$

12)	-39.8337	23)	7.5214	34)	4.9969	45)	1.8711	67)	2.0282
13)	-.1181	24)	4.5804	35)	-9.2905	46)	2.0282	68)	1.8711
14)	4.5809	25)	.3674	36)	-9.2905	47)	-15.0059	78)	19.9169
15)	2.1731	26)	.0203	37)	-3.2912	48)	-3.8839		
16)	3.8413	27)	-1.7475	38)	-3.2912	56)	19.9169		
17)	.2041	28)	-4.7433			57)	1.8711		
18)	-22.2626					58)	2.0282		

d. Triple Gauche

$\underline{g^+ g^+ g^+}$

12)	19.5037	23)	7.1111	35)	7.1155	48)	1.5239
13)	3.7037	24)	2.1231	36)	3.3165	56)	-16.9917
14)	3.3165	25)	1.4688	37)	2.1818	57)	4.0194
15)	2.2202	26)	1.2730	38)	1.4437	58)	7.5658
16)	.9252	27)	2.6669	45)	2.1306	67)	.1983
17)	18.0452	28)	.9525	46)	-4.8558	68)	.1983
18)	2.6498	34)	-24.9182	47)	2.1230	78)	19.9169

$\underline{g^- g^- g^-}$

12)	19.5037	23)	3.3165	35)	-4.8558	48)	2.1818
13)	2.1231	24)	3.7037	36)	2.1306	56)	-16.9917
14)	7.1111	25)	.9252	37)	1.5239	57)	.1983
15)	1.2730	26)	2.2202	38)	2.1230	58)	.1983
16)	1.4688	27)	2.6498	45)	3.3165	67)	7.5658
17)	.9525	28)	18.0452	46)	7.1155	68)	4.0194
18)	2.6669	34)	-24.9182	47)	1.4437	78)	19.9169

Appendix 3.4: Program CPARAM

Chapter 4: A HIGH FIELD NMR SPECTROMETER

4.1 Introduction

The nmr spectrometer that will be described in this chapter is the fourth spectrometer to be built in the laboratory of A. Pines. It has therefore been designated "delta".

This chapter is divided into nine sections and one appendix. Sections two through five document the analog electronics of the delta. In section 2 is described the manner in which low power r.f. pulses are generated at the various nuclear resonance frequencies. In section 3 are described the high power r.f. amplifiers which are used to produce r.f. pulses at power levels in excess of 300 watts at the proton Larmor frequency and 2 kilowatts at the deuterium Larmor frequency. Finally the broadband r.f. receiver is described in section 4, and the phase sensitive detector is described in section 5.

Sections 6, 7 and 8 document what may be called the digital electronics of the delta. Section 6 covers the acquisition system. Section 7 deals with the phase-shifter controller and in section 8 the pulse programmer is described.

Section 9 describes the general features of a program that is used by a Z-80 microprocessor to drive the pulse programmer. The program is especially suited for executing multiple quantum pulse sequences and other types of two dimensional experiments. The source version of the program is listed in the appendix to this chapter.

Before proceeding, brief mention should be made of the superconducting magnet. The magnet consists of a main solenoid of niobium-titanium alloy (Bruker BZH-01840070) housed in an Oxford dewar system. Three superconducting x, y, and z shim coils are also present. The persistent current of the main superconducting solenoid is about 34 amps corresponding to a field of approximately 84 kiloGauss at the shim center. The proton Larmor frequency is 360 Mhz and the deuterium Larmor frequency is 55 Mhz.

The superconducting solenoid is contained within a liquid helium dewar which has a capacity of about 25 liters. The helium dewar is in turn surrounded by a radiation shield and a liquid nitrogen dewar, which has a capacity of about 30 liters. The liquid nitrogen dewar requires refilling about once every four to five days and the liquid helium dewar requires refilling about once every 60 days.

4.2 Frequency and Phase Generation

In this section we describe the manner in which the various nuclear magnetic resonance frequencies are generated. As we found in chapters two and three, time domain nmr experiments often require that pulses within a sequence be phase shifted relative to one another. Therefore, the nmr spectrometer must be capable of producing pulses at the same nuclear frequency but with varying phases. In this section we also describe the manner in which phase shifts are generated.

Since the phase shift of an r.f. wave in a coaxial transmission cable is proportional to its frequency, phase generation networks rarely operate at high frequencies. Therefore, in most nmr spectrometers, phase generation is usually done at some low intermediate frequency (IF) and the nmr frequency is generated by mixing the phase-shifted IF with a second frequency, called the local oscillator (LO) frequency. In the delta spectrometer, the IF is 30 Mhz. Accordingly the proton LO is about 390 Mhz and the deuterium LO is about 85 Mhz.

The delta spectrometer is capable of producing pulsed irradiations at two different r.f. frequencies simultaneously. This is a requirement for any double resonance experiment. The frequency and phase generation networks are therefore dual channel. One channel is designed to produce pulsed irradiations at the proton resonance frequency (∿360 Mhz), while the second channel can easily be adapted to produce irradiations at virtually any frequency up to 350 Mhz. Since the second channel is often operated at the deuterium frequency (∿55 Mhz) we will describe it in that configuration. A schematic of the frequency generation network is shown in figure 53. The quadrature phase generation network is shown in figure 55.

4.2.1 LO Generation (figure 53)

The proton LO frequency of 390 Mhz is generated as follows. A signal at 130 Mhz at a level of .5 Vpp (volts peak-to-peak) is produced by a PTS-160 frequency synthesizer (.1 hz resolution) equipped with an internal reference crystal. The third harmonic is generated by a step diode (HP 5082-0112, see figure 54). The fundamental and higher frequency responses are removed by an LC circuit tuned to 390 Mc (figure 55). The 390 Mhz LO signal is then amplified

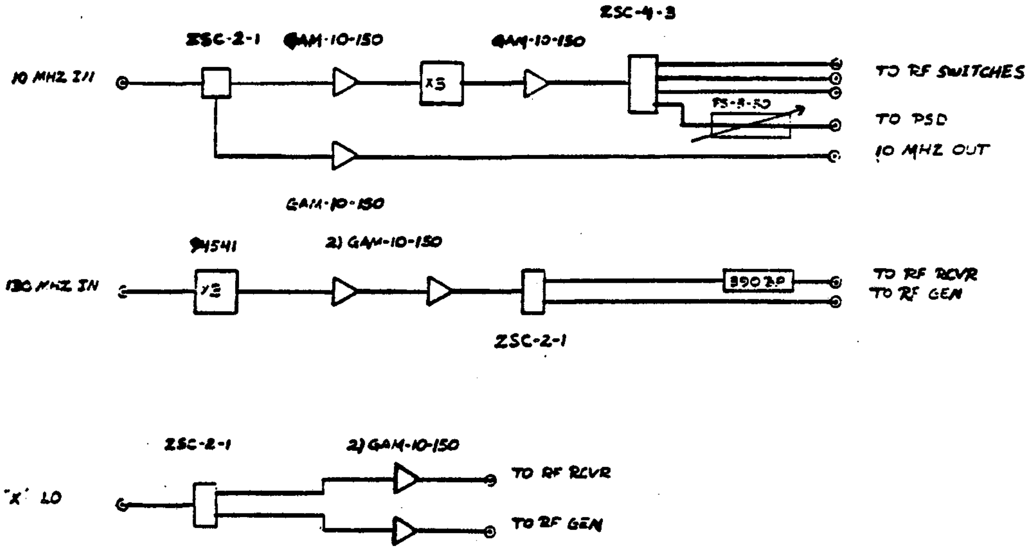
ZSC-4-3
ZSC-2-1
GAM-10-150
GAM-10-150
10 MHZ IN
X5
TO RF SWITCHES
PS-3-50
TO PSD
10 MHZ OUT
GAM-10-150
94541
2) GAM-10-150
130 MHZ IN
X2
390 BP
TO RF RCVR
TO RF GEN
ZSC-2-1
ZSC-2-1
2) GAM-10-150
"X" LO
TO RF RCVR
TO RF GEN

Figure 53. Delta Spectrometer: Frequency Multiplier.

to about 2.0 Vpp by two Merrimac GAM-10-150 10 dB amplifiers, and split by a Minicircuits ZSG-2-1 hybrid power divider (the two outputs are in phase). After passing through a Texscan 390 Mhz bandpass filter (20 Mhz pass band) one output channel goes to the r.f. receiver (see section 4.4) if the observed nucleus is proton and the other channel goes to the r.f. generation (section 4.2.4). Each output should be approximately 1.2 Vpp.

The deuterium LO frequency of 85 Mhz is produced by a second PTS-160 frequency synthesizer. This second synthesizer (.1 hz resolution) has no internal frequency reference and so must be "locked" to the first PTS-160. The 85 Mhz signal, at a level of .5-.6 Vpp, is split by a Minicircuits ZSC-2-1 hybrid power divider. Each output channel is amplified by a Merrimac GAM-10-150 to a level of approximately 1.2 Vpp, and one channel goes to the r.f. generation (section 4.2.4) while the other channel goes to the r.f. detector if the observed nucleus is deuterium. If the observed nucleus is not deuterium, the output is terminated.

The PTS-160 is capable of producing frequencies of up to 160 Mhz, and so any LO frequency not exceeding 160 Mhz may be synthesized directly. If a nuclear frequency exceeds 190 Mhz, the appropriate LO frequency may be obtained by using an r.f. frequency doubler.

4.2.2 IF Generation (figure 53)

As mentioned above, the intermediate frequency (IF) used in the delta spectrometer is 30 Mhz. A reference frequency of 10 Mhz at a level of about 1 Vpp is available at the rear of the proton PTS-160. The 10 Mhz reference is only available if the synthesizer has an

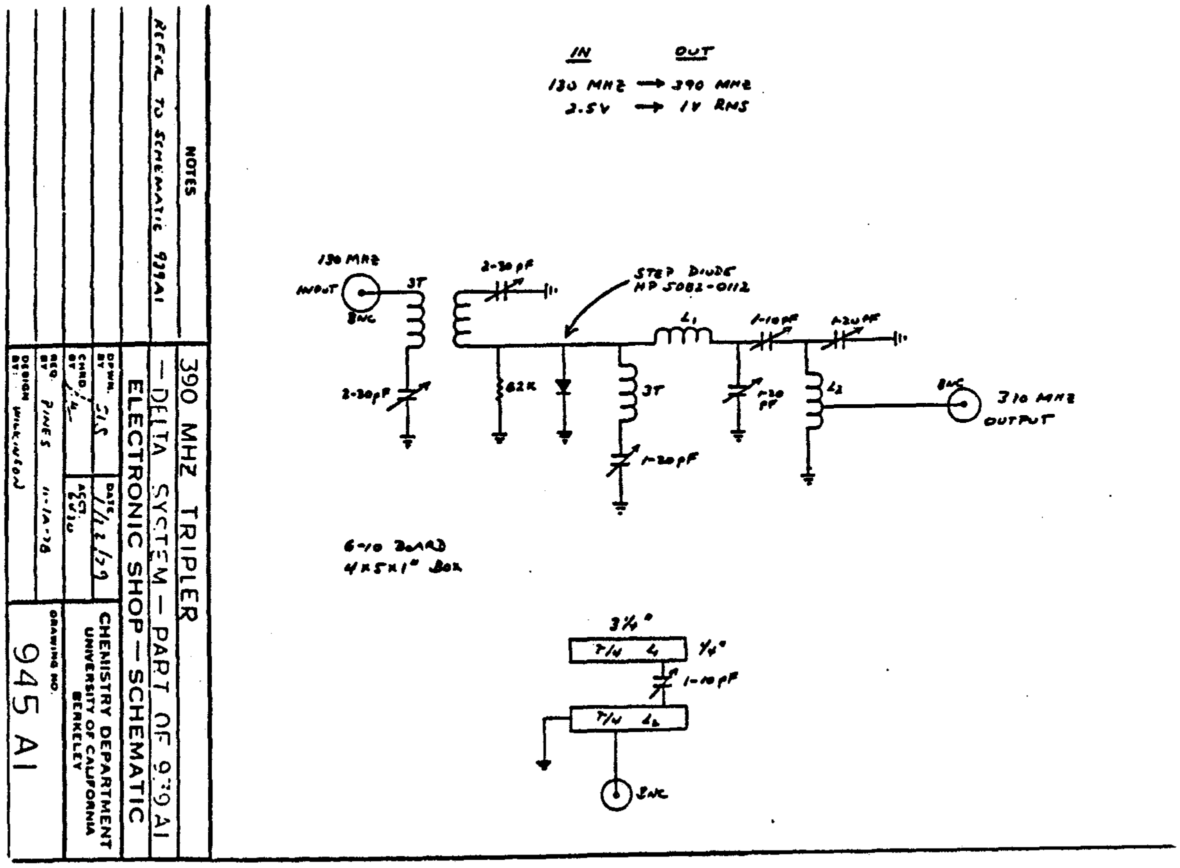
IN
OUT
130 MHZ → 390 MHZ
2.5V → 1V RMS
130 MHZ
INPUT
BNC
3T
2-30pF
2-30pF
STEP DIODE
HP 5082-0112
L1
1-10pF
2-20pF
62K
3T
1-20pF
1-20 PF
L2
BNC
390 MHZ
OUTPUT
6-10 BOARD
4x5x1" BOX
3¼"
T/4 L1
¼"
1-10pF
T/4 L2
BNC
NOTES
REFER TO SCHEMATIC 939A1
390 MHZ TRIPLER
— DELTA SYSTEM — PART OF 939 A1
ELECTRONIC SHOP — SCHEMATIC
DRWN. BY SJS
DATE 1/12/79
CHKD. BY
ACCT. 2410
REQ. BY PINES 11-12-78
DESIGN BY: WILKINSON
CHEMISTRY DEPARTMENT
UNIVERSITY OF CALIFORNIA
BERKELEY
DRAWING NO.
945 A1

Figure 54. Delta Spectrometer: 390 Mhz Tripler.

internal reference or if it is locked to an external reference. The 10 Mhz reference is split by a Minicircuits ZSC-2-1 hybrid power divider (figure 54) and each output is amplified to approximately 2 Vpp by a Merrimac GAM-10-150. One output is again split by a hybrid power divider, and the two outputs are used to lock the second PTS-160 and to provide a reference frequency for the pulse programmer (see section 4.8). The other 10 Mhz channel, at a level of about 2 Vpp, is connected to crossed diodes (1N914) to ground. The 10 Mhz fundamental and the higher harmonics are separated from the third harmonic by a homebuilt 30 Mhz bandpass filter. The 30 Mhz IF is amplified to about 1.5 Vpp by a Merrimac GAM-10-150 and split by a Minicircuits ZSG-4-3 4-way hybrid power divider. Three of the outputs, each at about .5-.6 Vpp are connected to the quadrature phase generation network (see section 4.2.3) and the fourth output is passed through a Merrimac PS-3-30 continuously variable phase adjuster, which can produce phase delays of up to 180°. The output of the PS-3-30 is connected to the phase sensitive detector (section 4.5).

4.2.3 Quadrature Phase Generation (figure 55)

A basic feature of any nmr spectrometer is the ability to produce pulsed irradiations with different phases, and a common requirement is that the phases be in quadrature. The delta spectrometer has quadrature phase generation networks in both r.f. channels. In addition there is an auxiliary IF channel which may be set to a different amplitude relative to either of the quadrature networks. This is a useful feature if one wishes to do double quantum experiments. The auxiliary IF channels may also be used as the reference phase

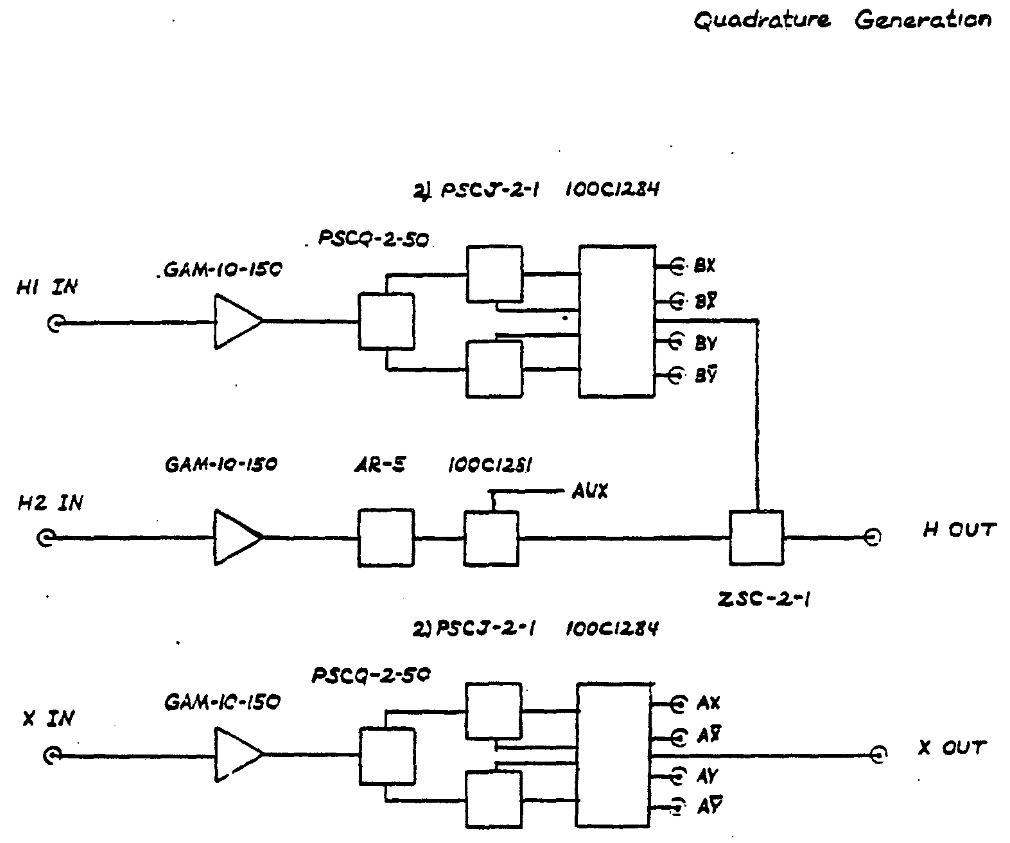
Quadrature Generation
2) PSCJ-2-1 100C1284
PSCQ-2-50
GAM-10-150
H1 IN
BX
BX̄
BY
BȲ
GAM-10-150
AR-5
100C1251
AUX
H2 IN
H OUT
ZSC-2-1
2) PSCJ-2-1 100C1284
PSCQ-2-50
GAM-10-150
X IN
AX
AX̄
AY
AȲ
X OUT

Figure 55. Delta Spectrometer: Quadrature Generation.

channel in TPPI experiments if the output of the proton quadrature network is connected to the digitally-controlled analog phase shifter described in section 4.7.3.

The quadrature generation networks of the proton and deuterium channels are identical since the IF's are both 30 Mhz. The 30 Mhz signal (.5-.6 Vpp) from the IF generation is amplified to about 1.4 Vpp by a GAM-10-150 (figure 56), and enters the quadrature generation network which is composed of a set of three 2-way hybrid power dividers mounted on a PC board. The first divider is a Minicircuits PSCQ-2-50 whose outputs are about 90° out of phase (x and y). The x and y signals are each divided by a Minicircuits PSCJ-2-1, whose outputs are 180° out of phase. Thus 4 phases in quadrature (x, y, -x, and -y) are produced. The phases may be fine-adjusted by varying lengths of coaxial cable between the outputs of the quadrature network and the inputs of the r.f. switch.

The four quadrature phase channels are connected to the inputs of a DAICO 100C1284 single-pole-four throw (SP4T) balanced diode switch. Each switch is digitally controlled (1 = closed, ϕ = open) and completely TTL-compatible. An open switch attenuates the input by better than 60dB at 30 Mhz and the switching time, defined as the time from 0 to one half the envelop maximum is about 100 nsec. The diodes in the switches produce antisymmetric transients whose intensities are a function of the d.c. power level (B^{+}). These transients are at low frequencies (<2 Mhz) and may be removed by bandpass filtering.

The amplitude of the auxillary IF channel (figure 55) is adjusted

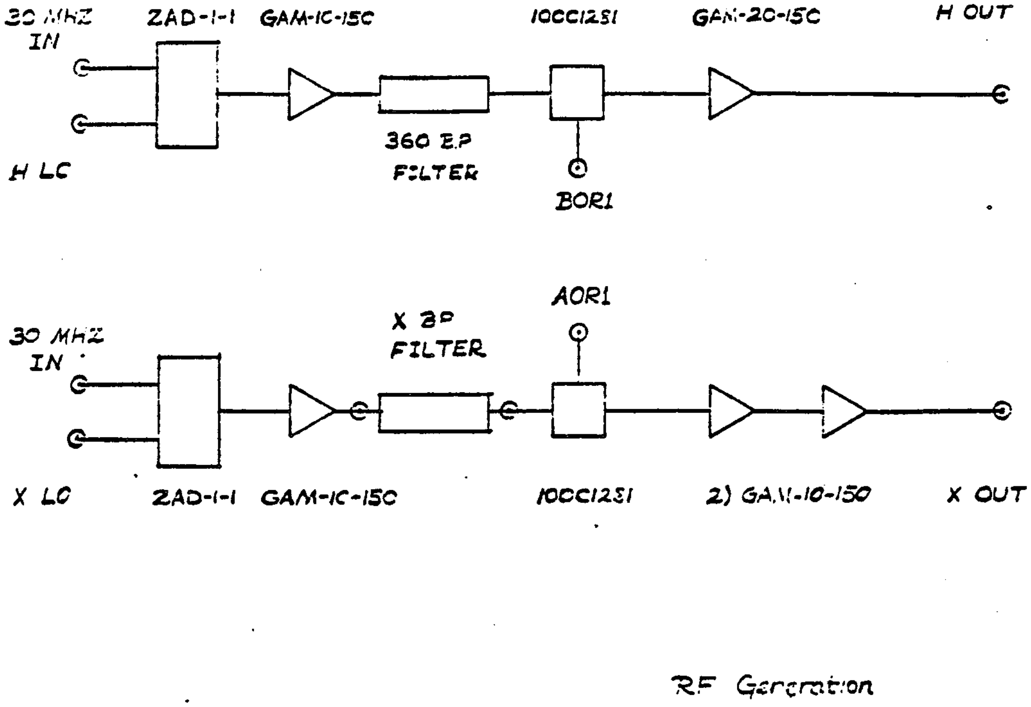
30 MHZ IN
H LO
ZAD-1-1
GAM-10-15C
360 BP FILTER
10CC1251
BOR1
GAM-20-15C
H OUT
30 MHZ IN
X LO
ZAD-1-1
GAM-10-150
X BP FILTER
AOR1
10CC1251
2) GAM-10-150
X OUT
RF Generation

Figure 56. Delta Spectrometer: Radio Frequency Generation.

by a Merrimac AR-5 continuously variable, mechanically-controlled attenuator. Maximum attenuation is -20dB (1/10 in voltage). R.F. switching is performed by a Daico 100C1281 single-pole-single-throw (SPST) balanced diode switch.

If the auxillary channel is to be used as a proton IF channel, the outputs of the Daico 100C1281 and the proton Daico 100C1284 should be combined using a ZSC-2-1. The output of the ZSC-2-1 is passed through a 30 Mhz bandpass filter (3 Mhz pass band) in order to remove the switching transients. The output level of the filter should be about .2 Vpp.

4.2.4 R.F. Generation (figure 56)

It remains to combine the pulsed IF signal at 30 Mhz with the LO frequency to produce the nuclear resonance frequency. This is done in the r.f. generation section. The r.f. generation schemes are identical for proton and deuterium, so we will only discuss the proton frequency generation.

The pulsed IF signal at a level of about .2 Vpp is mixed with the continuous proton LO signal which is at a level of about 1.2 Vpp. The mixer is a Minicircuits ZAD-1-1 standard level double balanced mixer. Care should be taken to maintain the relative levels of the LO and the IF signals at the mixer inputs since they have been adjusted to minimize spurious responses (106). The output of the mixer should be predominantly two sidebands at 360 Mhz and 420 Mhz. If the mixer has been properly balanced each sideband should not be much less than .1 Vpp. After amplification by a GAM-10-150 the

420 Mhz sideband is removed by filtering (Texscan 360 Mhz bandpass). The 360 Mhz signal is then gated by a second Daico 100C1281 SPST r.f. switch, amplified by a Merrimac GAM-20-150 (gain - 20 dB), and filtered again to remove the switching transients. The signal at the output of the second 360 Mhz filter should be about 3 Vpp.

4.3 R.F. Power Amplifiers

4.3.1 360 Mhz Power Amplifiers

The low power proton pulse (∿20 mw at 360 Mhz) is amplified in two stages. The first stage is a 30 watt solid state power amplifier with a 50 Mhz bandwidth (350-400 Mhz). The second stage is a high power solid state amplifier capable of generating a pulsed output of 350 watts at 360 Mhz. The amplifier is based on three MRF-327's in a parallel configuration (see figure 58) in which the collectors are coupled together by $^{\lambda}/4$ lines. To initialize operation after powering up, a momentary switch is engaged that closes a relay which applies power to the collectors of the three MRF-327's. If any one of the MRF-327's should short out, causing the collector voltage to drop, the output of the 7410 (three way NANDgate) will go high, opening the relay and shutting down the amplifier. The $^{\lambda}/4$ lines which couple the collectors together prevent damage to the other two MRF-327's if one MRF-327 should short out.

While the amplifier should operate into a 50 ohm load, it is capable of withstanding extreme "mismatches" and will not be damaged even if it is disconnected from the load while pulsing (the practice is not recommended, though).

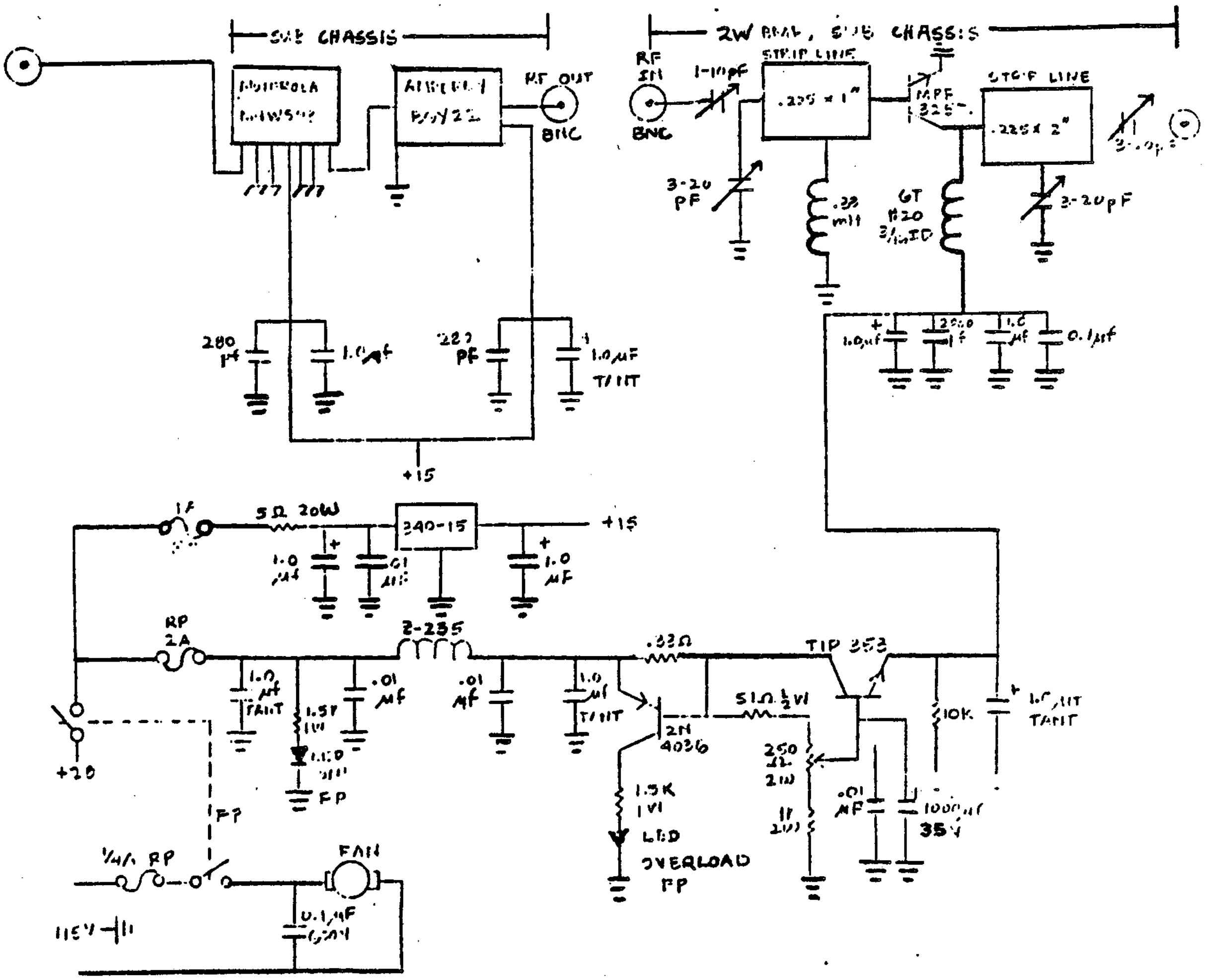
SUB CHASSIS
MOTOROLA
MHW592
ANZAC
RF OUT
BNC
280 pf
1.0 μf
220 PF
1.0 μF TANT
+15
2W AMP, SUB CHASSIS
RF IN
BNC
1-10 pF
STRIP LINE
.225 × 1"
MPF
STRIP LINE
.225 × 2"
3-20 PF
.33 mH
GT
#20
3/16 ID
3-20 pF
1.0 μf
0.1 μf
1.0 μF
1 F
5 Ω 20W
340-15
+15
1.0 μF
.01 μF
1.0 μF
RP
2A
Z-235
.33 Ω
TIP
1.0 μf TANT
1.5K 1W
LED
FP
.01 μF
.01 μF
1.0 μf TANT
2N 4036
51 Ω ½W
250 Ω 2W
10K
1.0 μF TANT
1.5K 1W
LED
OVERLOAD
FP
.01 μF
1000 μF
35V
+20
FP
¼A RP
FAN
0.1 μF
115V

Figure 57. Delta Spectrometer: 360 Mhz Driver.

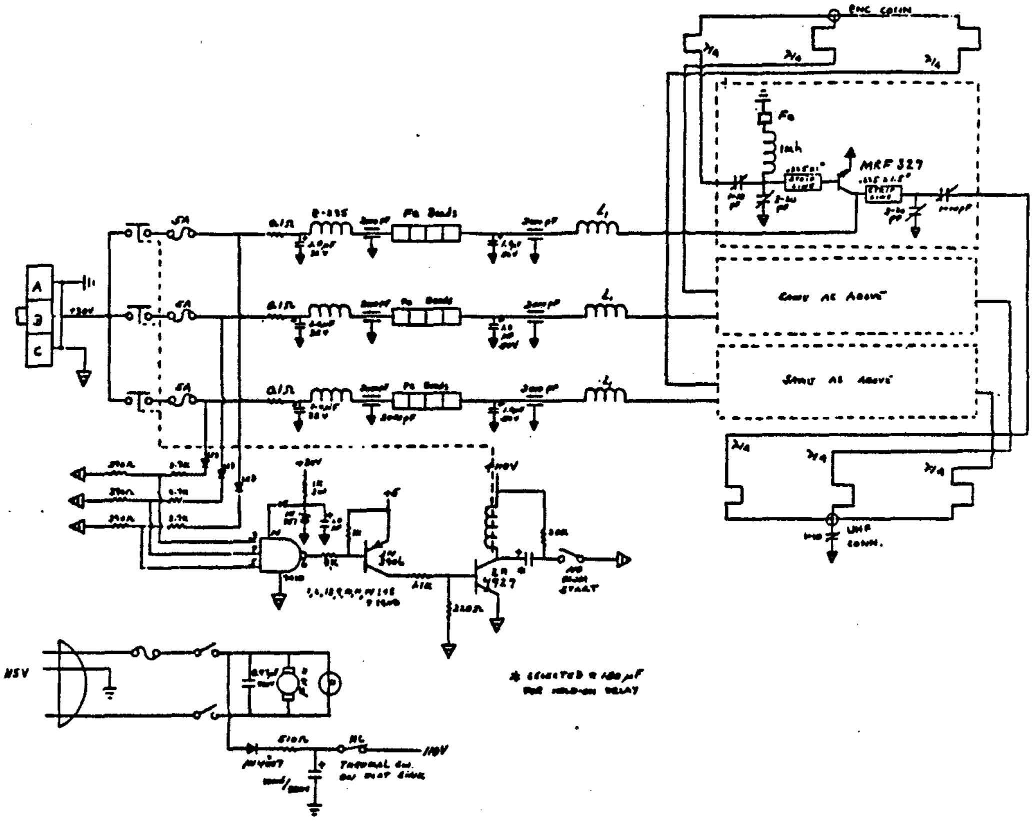
BNC CONN
λ/4
λ/4
λ/4
Fe
1mh
MRF 327
5A
5A
5A
0.1Ω
0.1Ω
0.1Ω
Fe Beads
Fe Beads
Fe Beads
L1
L1
L1
SAME AS ABOVE
SAME AS ABOVE
A
B
C
λ/4
λ/4
λ/4
UHF CONN.
115V
110V
* SELECTED ≈ 100 μF FOR HOLD-ON DELAY

Figure 58. Delta Spectrometer: 360 Mhz Transmitter.

4.3.2 Other High Power Amplifiers

The deueterium channel uses an AR-200L high power, broadband r.f. transmitter. The AR200-L is capable of delivering 500 watts into a 50 ohm load in pulsed mode for frequencies up to 200 Mhz. The input voltage to the AR-200L should not exceed 3 Vpp. If higher power is desired the AR-200L may be used to drive a Drake L-7 amplifier which has been altered to operate between 45 and 55 Mhz. Given an input of about 200 watts, the Drake L-7 will deliver 2000 watts into a 50 ohm load in pulsed mode.

4.4 R.F. Receiver (figure 59)

In chapter 1 it was pointed out that the linear absorption spectrum is obtained by Fourier transforming the nuclear free induction decay. However, the FID corresponds to a signal in a frame which rotates around the laboratory z-axis (specified by the magnetic field direction) at the Larmor frequency or within a few 1000 hertz of the Larmor if the r.f. field is off resonance. Electronically this means that the Larmor frequency is a carrier which is removed in the r.f. receiver, and the resultant audio frequency signal corresponds to the rotating frame FID. The nmr carrier is of the superheterodyning type since it removes the carrier in two stages, and is in most respects similar to a conventional radio receiver.

4.4.1 Preamplifier

The first stage of the r.f. receiver is the preamplifier. Since the FID at the input is at very low power levels (less than -80 dB), the thermal noise introduced by the preamplifier must be minimal.

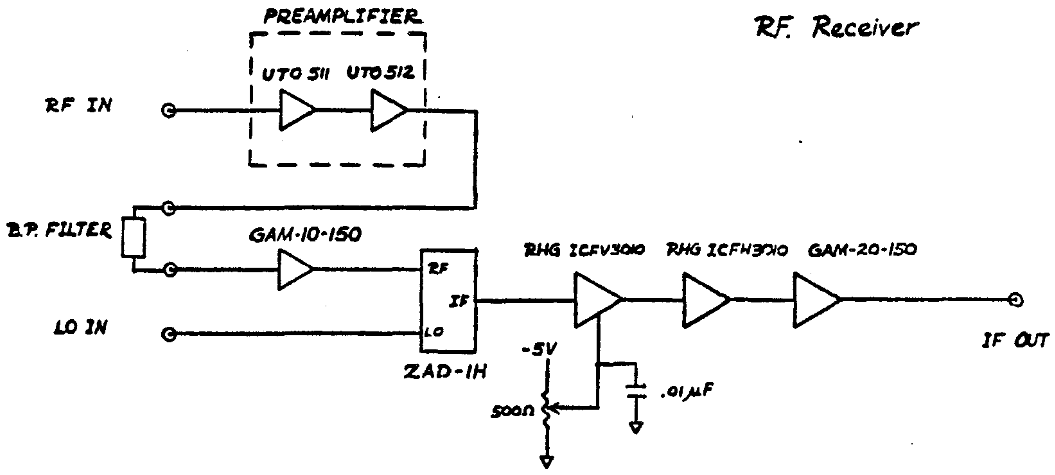
PREAMPLIFIER
RF. Receiver
UTO 511
UTO 512
RF IN
B.P. FILTER
GAM-10-150
RHG ICFV3010
RHG ICFH3010
GAM-20-150
RF
IF
LO
LO IN
ZAD-1H
-5V
500Ω
.01μF
IF OUT

Figure 59. Delta Spectrometer: Radio Frequency Receiver.

The delta spectrometer utilizes a two stage preamplifier. The first stage is an Avantek UTO 511 with a gain of 15 dB and has sufficient bandwidth to cover all frequencies of interest (-- 400 Mhz). The noise figure is 2.5 dB. The second stage is an Avantek UTO 512 with 20 dB of gain and a noise figure of about 4 dB. The preamplifier can recover from saturation in about 15 μsec.

After the preamplifier the signal is filtered. The filter should have a center frequency at the nuclear resonance frequency (proton = 360 Mhz, deuterium = 55 Mhz etc.) and as low an insertion loss as possible (<3 dB). On the delta, the receiver filters are attached externally to the receiver chassis to enable easy conversion between nuclear frequencies. After filtering the signal is again amplified by a Merrimac GAM-10-150.

The first heterodyning consists of taking the difference frequency between the Larmor frequency and the local oscillator (see section 4.2.1). This is accomplished by mixing the local oscillator with the nuclear FID using a Minicircuits ZAD-1-H high level double-balanced mixer. High level mixers should always be used in nmr receivers to avoid large conversion loss changes due to input signal level fluctuations. The output of the ZAD-1-H consists of two side bands corresponding to the sum and difference frequencies. In the case of protons the Larmor frequency is 360 Mhz and the LO is 390 Mhz, so the sidebands are at 30 Mhz and 750 Mhz.

A $.6 \times 10^{-4}$ Vpp signal at 360 Mhz at the input of the preamplifier should result in a signal level of $.8 \times 10^{-2}$ Vpp for the 30 Mhz sideband at the output of the ZAD-1-H.

4.4.2 IF Amplifiers

The IF amplifiers serve to increase the power level of the 30 Mhz sideband. The upper sideband is suppressed since several of the IF amplifiers are tuned.

There are three IF amplifiers (see figure 59). The first amplifier is an RHG ICFV 3010 which is tuned to 30 Mhz with a bandwidth of 5 Mhz. The gain of the amplifier is 25 dB which is variable over a range of 20 dB. The gain is voltage-controlled and is adjusted by a front panel potentiometer.

The second amplifier is an RHG ICFN 3010 with a fixed gain of 25 dB. This amplifier is also tuned to 30 Mhz and has a 5 Mhz bandwidth. For an input level of $.8 \times 10^{-2}$ Vpp to the ICFV 3010, the output of the ICFN 3010 should be about 2.5 Vpp with the ICFV 3010 at full gain.

The third amplifier is a Merrimac GAM-20-150 which has 20 dB of gain.

4.5 Phase Sensitive Detector (figure 60)

4.5.1 Dual Channel Detector

The phase sensitive detector operates as follows. The IF signal from the receiver is split by a Merrimac PD 2-50 hybrid power divider. Similarly, the IF reference signal from the frequency generation (see section 4.2.2) system is split by a Minicircuits QH-2-30 hybrid power divider, the outputs of which are 90° out of phase. The second heterodyning is now accomplished by mixing the IF signals using two Minicircuits ZAD-I-H high level double-balanced

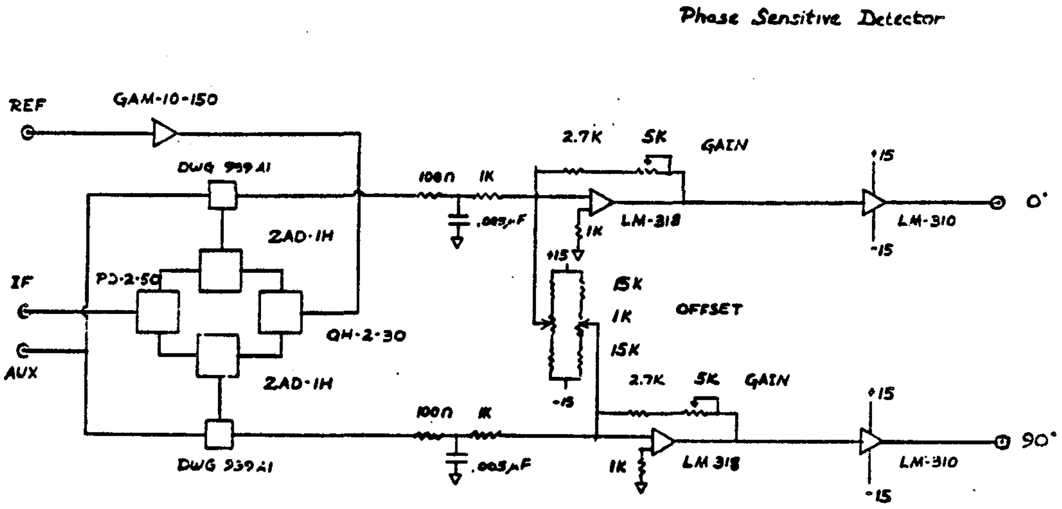
Phase Sensitive Detector
REF
GAM-10-150
DWG 939A1
ZAD-1H
IF
PD-2-50
AUX
QH-2-30
ZAD-1H
DWG 939A1
100Ω
1K
.005μF
2.7K
5K
GAIN
LM-318
1K
+15
15K
1K
15K
OFFSET
-15
+15
LM-310
-15
0°
2.7K
5K
GAIN
100Ω
1K
.005μF
1K
LM 318
+15
LM-310
-15
90°

Figure 60. Delta Spectrometer: Phase Sensitive Detector.

mixers. The outputs of the mixers are given by the equations

$$S_{x'} = (A\cos(\omega_{IF}+\mathcal{H})t)\ (B\cos(\omega_{IF}t+\psi))$$

$$= \frac{AB}{2}\ (\cos((2\omega_{IF}+\mathcal{H})t+\psi) + \cos(\mathcal{H}_t+\psi) \qquad (1)$$

$$S_{y'} = (A\cos(\omega_{IF}+\mathcal{H})t)\ (B\sin(\omega_{IF}t+\psi)$$

$$= \frac{AB}{2}\ (\sin((2\omega_{IF}+\mathcal{H})t+\psi) + \sin(\mathcal{H}_t+\psi) \qquad (2)$$

The phase term ψ may be varied by changing the phase of the reference IF which is done in the IF generation (see section 4.2.2)

4.5.2 Audio gain and D.C. level adjust

The outputs of the phase sensitive detector are gated by analog r.f. switches (figure 61) which are controlled by the pulse programmer. The switches are closed only during detection and are otherwise open in order to prevent ringing of the audio filters by pulse leak-through. Open switches attenuate input by -63 dB.

After the "blanking" switches is the first audio gain stage. This consists of an LM-318 operational amplifier with a potentiometer in the feedback loop adjusted to provide a gain of 14 dB. After the LM-318 is an LM-310 voltage follower.

The d.c. voltage level in each channel is adjusted by two front panel potentiometers which change the d.c. levels at the summing points of the LM-318's. The d.c. levels may be swept about ±.5 at the output of the LM-310.

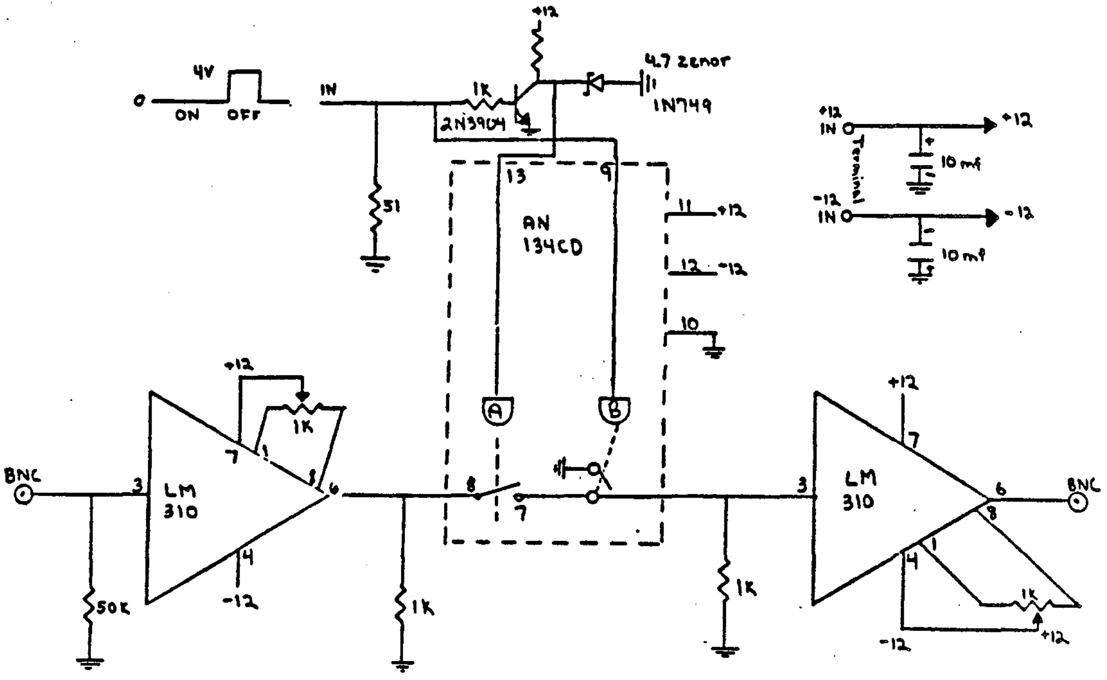
+12
4.7 zenor
1N749
4V
0
ON
OFF
IN
1K
2N3904
51
13
9
AN
134CD
11 +12
12 -12
10
+12
IN
Terminal
+
10 mf
-12
IN
-
10 mf
+12
-12
+12
1K
BNC
3
LM
310
7
1
8
6
4
-12
50K
1K
A
B
8
7
+12
7
3
LM
310
6
BNC
8
1
4
1K
1K
-12
+12

IN	A	B
0	ON	OFF
1	OFF	ON

4 × 2¼ × 1⅝ Box

63 DB ISOLATION

Ref. drawing 662A2

Figure 61. Delta Spectrometer: Analog Blanking Switch.

4.5.3 Audio Filters

The audio filters are Rockland 452 dual channel Butterworth filters. The filter mode is low pass and the unit has 20 dB of gain.

4.6 Data Acquisition (figure 62)

The purpose of the data acquisition system is to accurately digitize the analog signals at the output of the audio filters. When digitized data is available in the memory of the data acquisition system, an "interrupt" is generated which signals the Nova 820 computer that data is available at the data channel inputs. The Nova 820 will then initialize the data channel transfer.

4.6.1 Sample-and-Hold Amplifier

In order for the analog-to-digital converters (ADC) to accurately convert analog signals to sequences of binary words, the voltages at the inputs of the ADC's must be very stable for the duration of the conversion. This is accomplished by the sample-and-hold amplifiers. After the audio filters each analog data channel goes to a Datel SHM-2 sample-and-hold amplifier. The SHM-2 is composed of an operational amplifier with a 200 pf capacitor to ground at the input. The input is gated by an electronic switch. When the central voltage to the switch driver is logically low, the switch closes and capacitor is charged to its peak value. When the control voltage to the switch driver is logically high the switch opens and the input voltage is "held". The mode control is TTL compatible. The inputs to SHM-2's should not exceed ±10 volts.

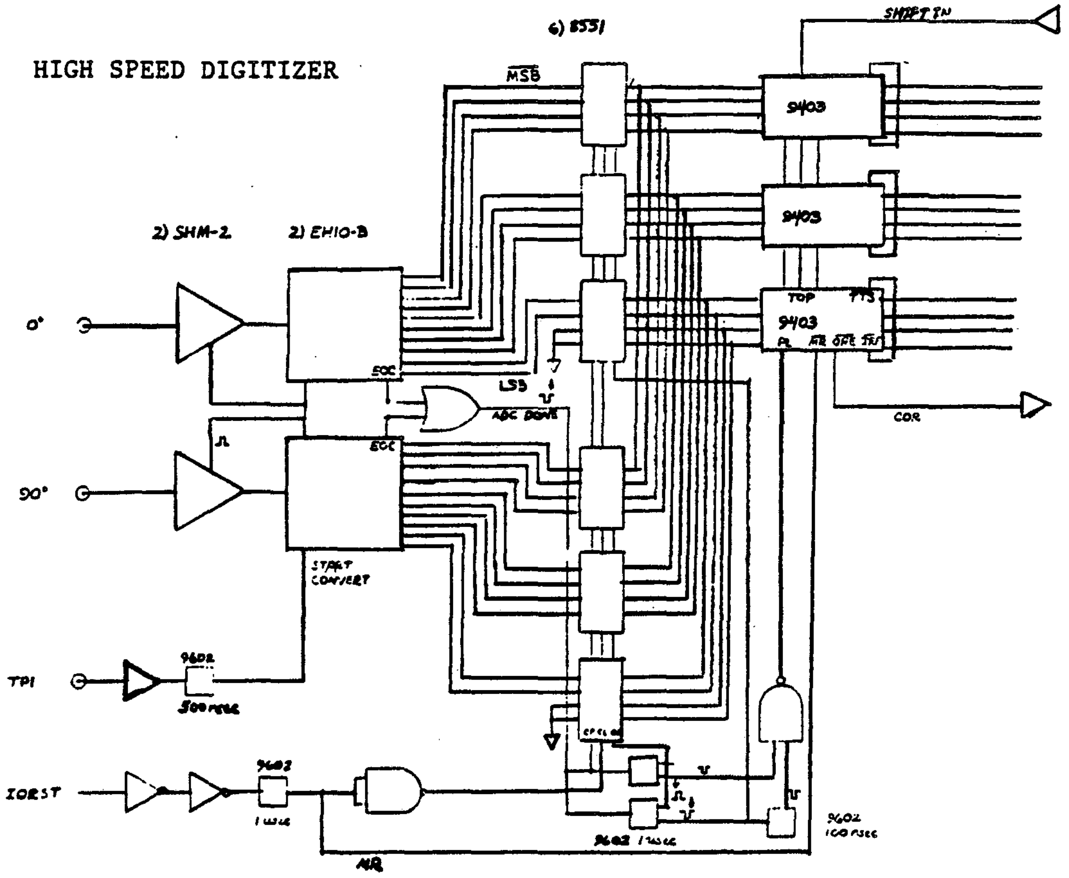
HIGH SPEED DIGITIZER
6) 8551
SHIFT IN
MSB
9403
9403
TOP
9403
PL
MR
OE
COR
2) SHM-2
2) EH10-B
0°
EOC
LSB
ADC DONE
EOC
90°
START CONVERT
TPI
9602
500 nsec
IORST
9602
1 μsec
9602 1 μsec
9602 100 nsec
MR

Figure 62. High Speed Digitizer.

4.6.2 Analog-to-Digital Converters

The voltages at the outputs of the sample-and-hold amplifiers are converted to 10 bit digital words by the analog-to-digital converters (what else?). ADC's operate in the following manner. The capacitor that was charged by the sampled voltage pulse, is discharged by a constant current. The end of the discharge is detected by a voltage comparator in the ADC, and the discharge time is measured by a counter and a clock oscillator. The delta acquisition system utilizes 2 Datel ADC-EH10B analog-to-digital converters. Initially, the end-of-conversion flag (EOC) is low on each ADC, causing the SHM-2's to go into "sample" mode. When the ADC's receive a start-convert pulse, which is provided by the pulse programmer, the EOC flags go high causing the SHM-2's to go into "hold" mode (see figure 62). At the end of the conversion, which requires 2 μsec, the EOC flags go low causing the SHM-2's to return to sample mode. The 10 bit outputs of the ADC's are valid as soon as the EOC status goes low,

The ADC's are operated in bipolar mode, meaning that they will accept analog voltages within the range ±5 V. The start convert flag is TTL compatible.

4.6.3 Fifo Buffer Memory and Data Channel Interface

At the end of a conversion, two 10 bit words are available, one at the output of each ADC. The problem is how to get both words which are in parallel at the ADC output, arranged in serial for the data channel transfer into the Nova 820 memory. This is accomplished in the following way (see figure 62). The EOC status flags are connected to the inputs of a 7402 NOR gate. When the EOC's go high, the output of the 7402 goes low. The rising edge of the 7402 output pulse clocks a set of three 8551 tri-state latches which latch one of the 10 bit words. The outputs of the latches are connected to the input registers of three 9403 (4 x 16 bit) first-in-first-out (FIFO) memories. The rising edge of the same pulse performs two other functions. Firstly, it triggers a 100 nsec 9602 monostable which, after propagating down a NAND date delay, triggers the parallel load (PL) function of the three parallel 9403's, causing the latched data word to be transferred to the memory stacks. Secondly, another 100 nsec monostable is triggered. The rising edge of the positive (Q) output triggers the high impedance state in the first set of 8551's and the rising edge of the negative ($\bar{Q}$) output, occurring 100 nsec later, triggers a second set of parallel 8551's which latch the second 10 bit word. The rising edge of the same $\bar{Q}$ output triggers yet another 100 nsec 9602 monostable which in turn triggers the PL function of the 9403 FIFO memories, causing the second 10 bit data word to be transferred to the memory stacks. It should be mentioned that the 10 bits corresponding to the output of the ADC, are arranged as the 10 most significant bits of a 12 bit word. The least significant two bits are grounded at the 8551 inputs.

What has been accomplished is that the two 10 bit data words appearing in parallel at the outputs of the ADC's have been transferred serially to the stack of a memory buffer composed of three parallel 9403 FIFO's. The first word to enter the FIFO stack is immediately transferred to the output register of the FIFO, which causes the output register empty (ORE) status flag to go high. A high condition at the ORE status ports of the 9403 memory buffer causes a data channel enable request (RQENB) to occur on the Nova 820 data acquisition interface. For details on the data channel timing logic, the reader is referred to the Data General Corporation documentation (107). We will only briefly outline the interaction between the interface and the buffer memory.

The advantage of a data channel transfer over a program transfer is that the former transfer is only initiated by the CPU. When the Nova 820 is ready to accept data through the data channel, the "busy-done" flag on the interface is initialized to busy. In addition, two sets of 74177 synchronous counters are loaded with the number of words to be transferred and the initial memory address. The interface then generates a "shift-out" pulse which causes the data on the output registers of the buffer memory to be latched into the input data register on the interface. The pulse also transfers the next word from the buffer memory stack into the output registers and updates the memory address and the word count. The interface will continue to furnish "shift out" pulses until the word count reaches zero, at which time the "busy-done" flag will be reset to "done" and the transfer is concluded. All of this occurs without the necessity of a program-controlled transfer through the accumulator, a process that would take much longer. The data acquisition system can digitize accurately in dual channel mode at a maximum rate of 333 kHz.

4.7 A Digitally Controlled Analog Phase Shifter

In chapter 3 we found that multiple quantum pulse sequences often require phase shifts of other than 90°, 180° or 270°, and so some other method than the quadrature phase generation network described in section 4.2.3 is required. Digitally controlled narrow band analog phase shifters capable of generating phase shifts in units of $^{2\pi}/256$ are commercially available. One example is the Daico 100D0898 which produces a phase shift between the input and output ports specified by an eight bit control word, at rates of up to 500 khz. The delta spectrometer may be arranged for a TPPI experiment by placing the phase shifter between one of the outputs of the IF generation (section 4.2.2) and an input to one of the quadrature phase generation networks (section 4.2.3). The auxiliary phase IF channel may be used as the fixed phase channel.

Figure 63 shows a digital circuit designed to deliver a sequence of control words to the phase shifter. By changing the select bits on the 74153 multiplexers (A4, A5) a phase shift is specified by a control word from a front panel toggle wheel switch or from the outputs of two 7483 binary adders (A2 and A3). The 7483 sum together control words from two independent circuits.

TPPI requires a simple incrementation of the phase and so a "wrap-around" adding circuit suffices. A unit phase increment is set from a front panel toggle wheel switch. The unit phase increment is added to the previous sum by two 7483's (C4 and C5). The 74175 latches (B5, B6, C2 and C3) are clocked by pulsing the "INC" line, and are cleared by pulsing the "RESET" line. Both the INC and

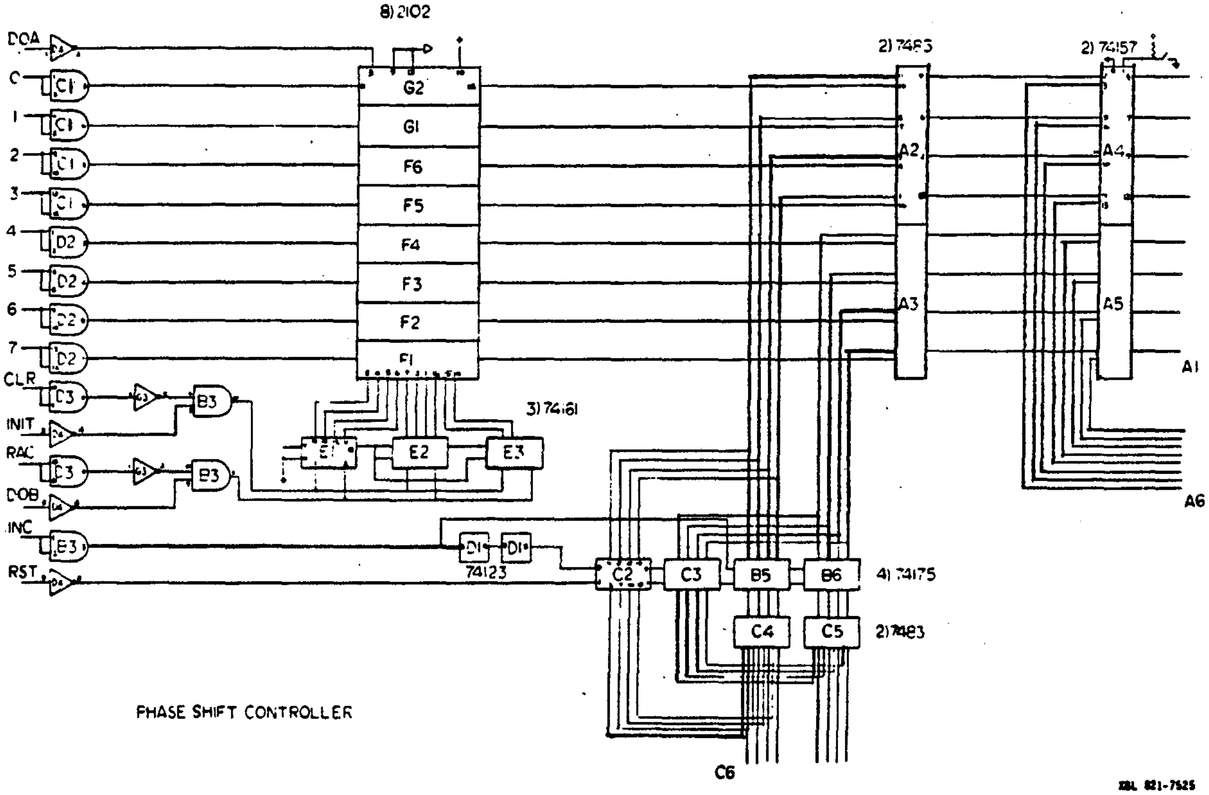
8) 2102
DOA
C
1
2
3
4
5
6
7
CLR
INIT
RAC
DOB
INC
RST
C1
D2
C3
B3
G2
G1
F6
F5
F4
F3
F2
F1
3) 74161
E1
E2
E3
D1
74123
C2
C3
B5
B6
4) 74175
C4
C5
2) 7483
C6
2) 7483
A2
A3
2) 74157
A4
A5
A1
A6
PHASE SHIFT CONTROLLER
XBL 821-7525

Figure 63. Delta Spectrometer: Digitally Controlled R.F. Phase Shifter.

RESET lines are under pulse programmer control.

More intricate sequences of control words may be obtained from the random access memory (RAM). Up to 1024 control words may be loaded into 8 parallel 2102-1 x 1024 bit RAM memories (F1-G2). The memory address is specified by the 3 74161 asynchronous counters (E1-E3) which may be updated by pulsing either the DOB line or the RAC line. The RAC line is under pulse programmer control, and the DOB line is under minicomputer control. The counters may be initialized either by pulsing the CLR line which is under minicomputer control, or the INIT line which is under pulse programmer control. The operation of the RAM memory is as follows. An eight bit control word is specified by the outputs of the eight line receivers (C1-D2) is loaded into the RAM memory by pulsing DOA. By pulsing DOB the RAM address counter (RAC) is advanced and the process is repeated. Since the RAM memory is write-enabled whenever $\overline{\text{DOA}}$ is high, the memory may be output simply by pusling RAC. The memory address counter may be reset by pulsing INIT.

By using the RAM memory in combination with the "wrap-around" adder, all of the complex phase shifts required by multiple quantum selective excitation pulse sequences may be performed.

4.8 Pulse Programmer

4.8.1 Introductory Remarks

The pulse programmer is the device that produces the complicated sequences of logic pulses that operate the various r.f. switches in the spectrometer and trigger the data acquisition system. It is eventually the pulse programmer that defines the complexity of the experiments that may be attempted on a spectrometer, and therefore it is desirable that it be as versatile as possible.

The design of the pulse programmer to be described is due to Dr. David Ruben, and the basic idea is as follows. The heart of the programmer is a Zilog Z-80 microprocessor. The microprocessor receives a series of commands that describe in terms of some type of programmed code, a pulse sequence. This sequence of commands will be called the pulse program. Now the microprocessor stores the pulse program in its memory, determines the structure of the pulse sequence by decoding the program, and outputs the appropriate pattern of logic pulses to its bus. The idea is very simple in principle but the difficulty is that the microprocessor cannot possibly output logic pulses at the rates required in nmr experiments. In fact, execution times for even the simplest instructions, for example a transfer between the primary accumulator and one of the secondary accumulators, may require 10 clock cycles, so it is clear that the microprocessor cannot directly control the spectrometer.

A solution to the problem is to interface the Z-80 to a buffer memory. The Z-80 will load the memory with a set of control words that specify which r.f. switches will be opened and for how long, and the memory contents will then be output to appropriate TTL control logic. For example, that part of the control word that specifies the r.f. switch to be opened (we will call it the gate word) will be latched, and the part of the control word that specifies the length of time that the switch will remain opened (we will call it the timing word) will be loaded into a set of synchronous counters. The counters are, in turn, clocked by a crystal oscillator, and when the count is concluded, the next control word is output from the memory buffer.

We see that now the microprocessor need only output control words at a rate fast enough to keep the buffer memory from "emptying". The question remains, can the memory buffer perform writes rapidly enough? The answer is that static RAM memory can perform writes at rates sufficient for nmr applications.

4.8.2 General Structure

We will now describe in a general way, the structure of the pulse programmer. The pulse programmer is divided into two sections. The first section consists of the Z-80 CPU board,the IO (input-output) controller board, and a 16K RAM memory board. It is not our intention to describe the architecture of the CPU, but we will mention some of its salient features so that its interaction with the buffer memory can be easily understood. The reader is referred to volume 2 of the 3 volume series by Osborne and Associates for details on the Z-80 archtitecture (108).

The heart of the CPU board is the Z-80 microprocessor. The Z-80 is an enhancement of the Intel 8080. It is a "single chip" 40 pin microprocessor, which utilizes a single system clock signal and requires only a single power supply of ±5 V. The data word length is eight bits and there are 16 memory address bits. The CPU also contains a 2702 (8 x 1024) EPROM which is used to store the operating system "HDT", and IK (8 x 1024) of static RAM memory. An additional 16K of static RAM memory is located on a separate board which consists of a matrix of 32 2114L's.

The CPU, IO controller, and 16K RAM memory are designed to utilize the Chem μ80 bus which is standard in the U.C. Berkeley Department of Chemistry. The bus signals of interest to us are:

a) DB0 - DB7: these 8 bits compose the basic data word.

b) A0 - A15: these bits specify the memory location or IO device with which the CPU will interact.

c) $\overline{\mathrm{WRITE}}$: when the CPU executes a write-to-memory, this bus line will be pulled low and the memory address will be specified by A0 - A15. The data word stored at the specified memory address will appear on the bus lines D0 - DB7.

d) $\overline{\mathrm{IN}}$: when the CPU executes a read from an IO port, this bus line goes low. The IO port number appears on A0 - A15 and the input from the port will appear on DB0 - DB7.

e) $\overline{\mathrm{RESET}}$: when this line is pulled low, the Z-80 program pointer will be relocated to the first page (1 page = 256 words) of memory.

The second section of the pulse programmer consists of the buffer memory and the TTL control logic which the Z-80 uses to control the r.f. switches and the data acquisition system. A control word is composed of a 16 bit gate word and a 16 bit time word. Therefore, in order for the Z-80 to output a single control word, four writes to memory must be executed. The pulse programmer buffer memory is composed of two parts, a FIFO memory and a RAM memory. The FIFO memory consists of 8 parallel 9403's, which can hold up to 16 control words, and the RAM memory consists of 8 parallel 2101-1's which can hold up to 256 control words.

The 9403 FIFO memory can be clocked out at a maximum rate of 12 Mhz, which is certainly fast enough for nmr applications. The FIFO memory can be used to output any pulse sequence that does not require long (>16) trains of short pulse (<200 usec) separated by short delays (<200 usec). This limitation is due to the fact that the microprocessor cannot load the FIFO any faster than once every 200 usec, and so if more than 16 pulses and delays of durations less than 200 usec are required, the FIFO will be unloaded faster than the Z-80 can load it, and timing errors will result.

The 2101 RAM memory is normally used to output trains of short pulses and delays. The Z-80 simply preloads the RAM with the appropriate control words, and the RAM memory contents is output by an address counter during the experiment. The 2101 memory can perform writes at a maximum rate of 2 Mhz.

4.8.3 Pulse Programmer Operation: Buffer Memory Input

Before the Z-80 can execute a write to the FIFO memory the input registers of the 8 parallel fifos must be clear. Therefore, before attempting a data transfer to the FIFO, the Z-80 examines the status of the input register ports ($\overline{\text{IRF}}$) (see figure 64). The $\overline{\text{IRF}}$ ports of four of the 8 9403's are AND'ed together and input to an

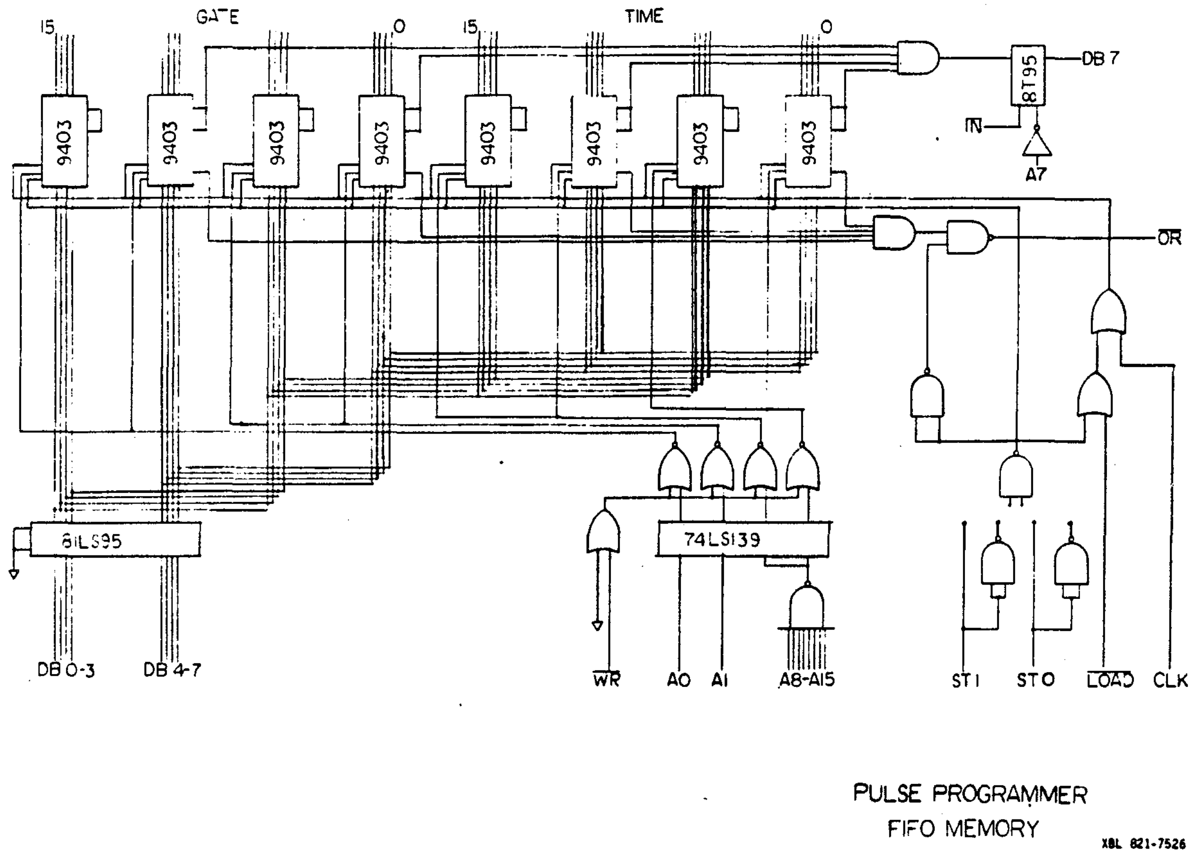
15
GATE
0
15
TIME
0
9403
9403
9403
9403
9403
9403
9403
9403
8T95
DB 7
IN
A7
OR
81LS95
74LS139
DB 0-3
DB 4-7
WR
A0
A1
A8-A15
ST1
ST0
LOAD
CLK
PULSE PROGRAMMER
FIFO MEMORY
XBL 821-7526

Figure 64. Pulse Programmer: Fifo Memory.

8T95 Tristate buffer. When the Z-80 wishes to check the $\overline{\text{IRF}}$ status ports, the $\overline{\text{IN}}$ bus line is pulled low and the A7 address line goes high, causing the 8T95 to switch out of its high impedence state. As a result the $\overline{\text{IRF}}$ status is transferred to DB7. If the input registers are empty, $\overline{\text{IRF}}$ is high, causing DB7 to go high, and the Z-80 will then proceed with a transfer. If DB7 is low, indicating that the input registers are full, the Z-80 will not proceed with the transfer but will continue to examine the $\overline{\text{IRF}}$ status until the input registers are cleared.

In order to transfer a single 32 bit control word, the Z-80 must execute a write to each of the 4 FIFO pairs. The beginning memory address of the FIFO memory in hexidecimal is FF80. The eight most significant bits are decoded. The two least significant address bits A0 and A1 specify which FIFO pair will receive input. Therefore, when the Z-80 executes a write to the FIFO, the $\overline{\text{WRITE}}$ bus line goes low and bits A5 through A15 go high causing the output of a 7430 to go low which enables a 74139 binary decoder. The 74139 inputs are the FIFO pair code specified by A0 and A1. The decoder output, NOR'ed with WRITE, causes the parallel load port (PL) on the appropriate FIFO pair to go high, which loads the 8 bit word specified by DB0-DB7 into the input register, causing $\overline{\text{IRF}}$ to go low. Since $\overline{\text{IRF}}$ is connected to the stack transfer control ($\overline{\text{TTS}}$), as soon as data appears in the input register, it is transferred to the stack. If the stack is not occupied, the data will appear at the output register, causing the output register-status port ($\overline{\text{ORE}}$) to go high.

Data transfer to the RAM memory is done in a similar manner (see figure 65). The beginning address of the RAM memory is F000.

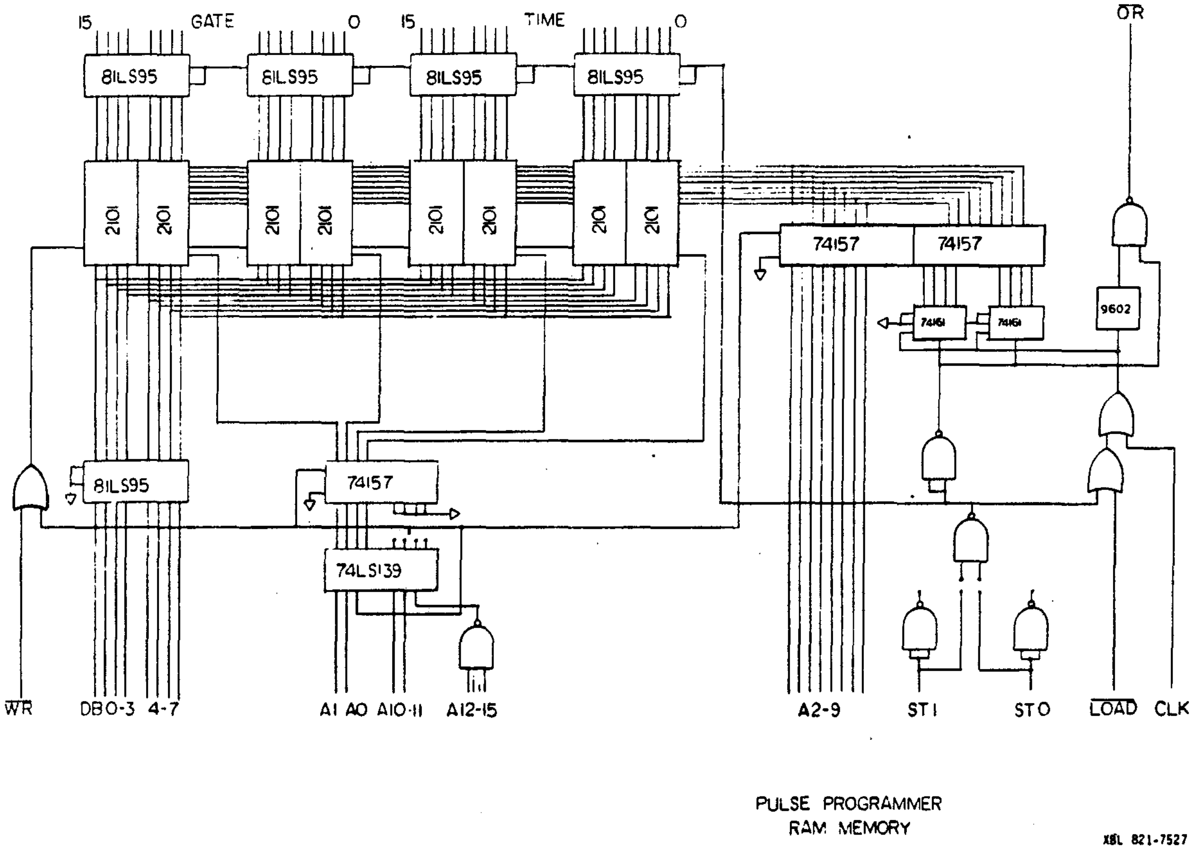
15
GATE
0
15
TIME
0
OR
81LS95
81LS95
81LS95
81LS95
2101
2101
2101
2101
2101
2101
2101
2101
74157
74157
74161
74161
9602
81LS95
74157
74LS139
WR
DBO-3
4-7
A1
A0
A10-11
A12-15
A2-9
ST1
STO
LOAD
CLK
PULSE PROGRAMMER
RAM MEMORY
XBL 821-7527

Figure 65. Pulse Programmer: Ram Memory.

Memory address bits A0 and A1 specify which RAM pair will receive data and address bits A2 to A9 specify the memory location. When the CPU executes a write to the RAM memory the $\overline{\text{WRITE}}$ line goes low causing the write enable ($\overline{\text{WE}}$) lines to go low on all the RAM's. But data transfer will only occur to that RAM pair whose chip enable ($\overline{\text{CE1}}$) lines are pulled low as a result of the decoding of A0 and A1. When the RAM memory is not being addressed by the Z-80, $\overline{\text{WE}}$ is high and all $\overline{\text{CE1}}$ lines are low, which causes all RAM's to be output enabled.

4.8.4 Pulse Programmer Operation: Buffer Memory Output

We will now discuss the manner in which the buffer memory outputs control words. It has already been mentioned that the control word is 32 bits in length, consisting of a 16 bit gate word and a 16 bit time word. The 2 most significant bits of the time word are used to enable the *next* memory device to be the output source. The 2 bit code "source" code is:

00 = FIFO
01 = RAM 1
02 = RAM 2
03 = RAM 3

Initially, the FIFO is enabled.

Suppose the Z-80 writes a 32 bit control word to the FIFO memory (see figure 64). If the stack is empty the data "fall through" to the output register, causing the output register status port ($\overline{\text{ORE}}$) to go high, which in turn causes the $\overline{\text{OR}}$ (output register) line to go

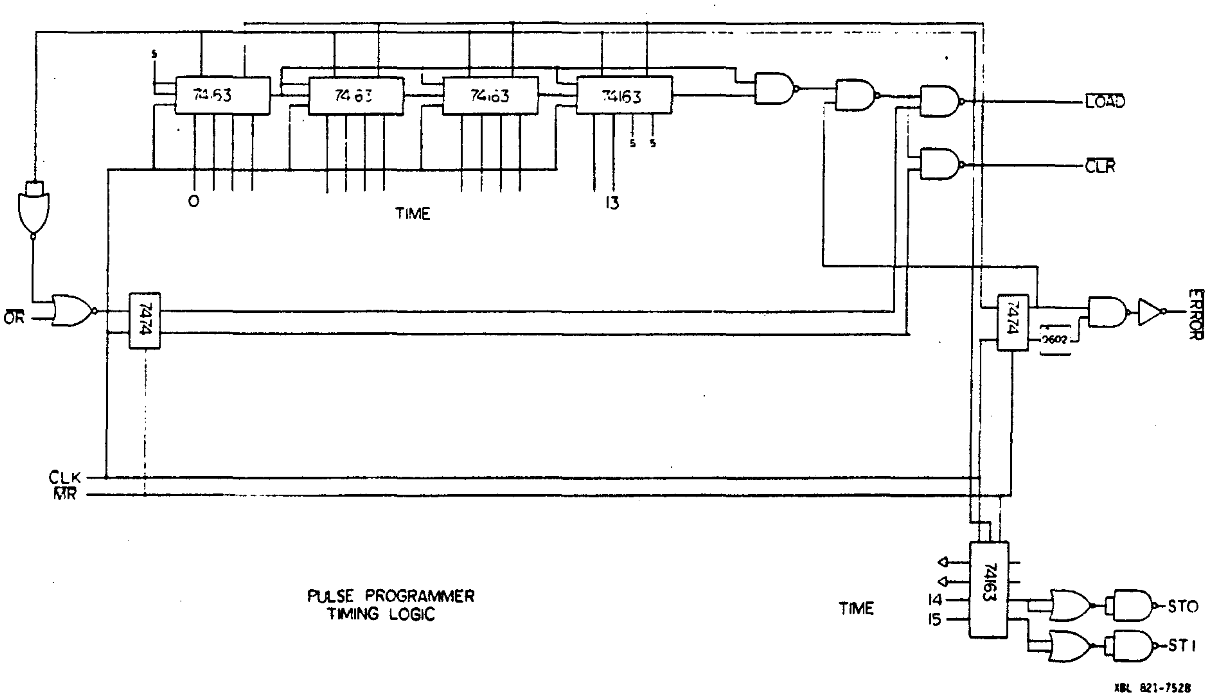
74163
74163
74163
74163
0
TIME
13
5
5
5
LOAD
CLR
OR
7474
7474
9602
ERROR
CLK
MR
PULSE PROGRAMMER
TIMING LOGIC
TIME
14
15
74163
ST0
ST1
XBL 821-7528

Figure 66. Pulse Programmer: Timing Logic.

low. This signals the timing logic (see figure 66) that data is available in the buffer memory output register and the timing logic responds by pulling the $\overline{\text{LOAD}}$ line low for one clock cycle (100 nsec), which causes the gate control word to be transferred to the outputs of a set of latches (see figure 67), the timing word (14 bits) to be loaded into a set of synchronous binary counters, and the 2 bit source code to be latched. The timing word is the two's complement of the length of the logic pulse, and since the pulse programmer uses a 10 Mhz clock, the maximum pulse length per control word is 1638.3 μsec.

When the count has been concluded the timers generate a "carry out" pulse which again causes the $\overline{\text{LOAD}}$ line to go low for one clock cycle. If the FIFO is enabled by a source code of 0, the "transfer out parallel" line (TOP) will be pulled low causing the next control word in the stack to be transferred to the output register and the process repeats itself. If the RAM is enabled by a source code of 1, 2, or 3, the $\overline{\text{LOAD}}$ pulse will cause the control word on the outputs of the RAM to be processed and the RAM address counter will be advanced. In addition a monostable will be triggered that causes the $\overline{\text{OR}}$ line to go high for 500 nsec.

An error condition, indicated by the front panel "ERROR" diode, occurs if the $\overline{\text{LOAD}}$ line goes low while the $\overline{\text{OR}}$ line is high. This will occur if an attempt is made to obtain a control word from the FIFO when the output register is empty of if an attempt is made to clock out the RAM at a rate in excess of 2 Mhz. An error condition results in the clearing of the gate word latches.

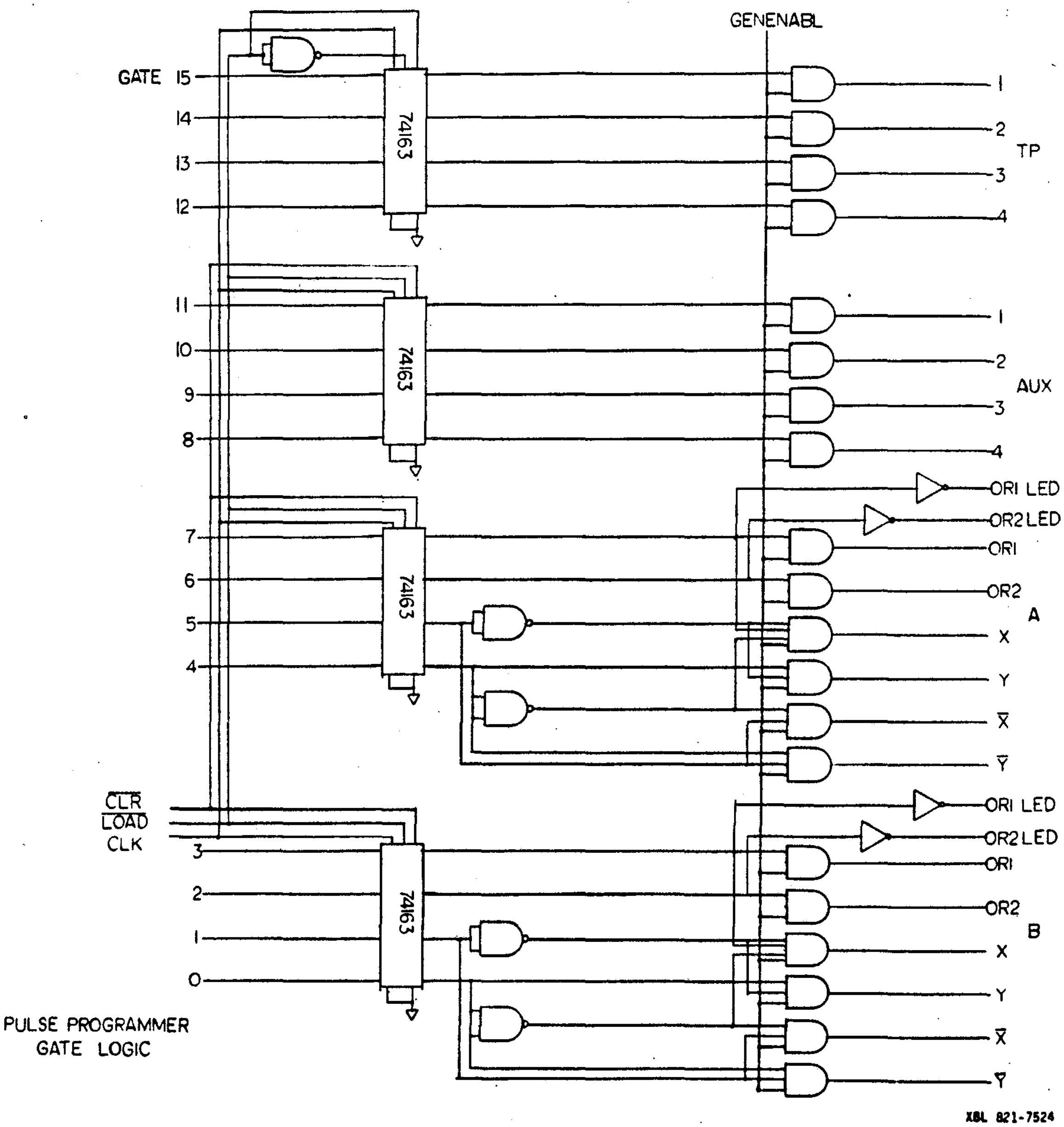
GENENABL
GATE 15
14
13
12
11
10
9
8
7
6
5
4
3
2
1
0
74163
74163
74163
74163
CLR
LOAD
CLK
1
2
3
4
TP
1
2
3
4
AUX
ORI LED
OR2 LED
ORI
OR2
A
X
Y
X̄
Ȳ
ORI LED
OR2 LED
ORI
OR2
B
X
Y
X̄
Ȳ
PULSE PROGRAMMER
GATE LOGIC
XBL 821-7524

Figure 67. Pulse Programmer: Gating Logic.

4.8.5 Front Panel Controls

In this section, we describe the front panel controls of the pulse programmer:

Reset: When this button is pushed, the program memory pointer of the Z-80 is initialized to the first memory page causing program execution to halt. The output ports of the pulse programmer are disabled (see figure 67). In addition, the master reset (MR) port on the 9403's goes low, initializing all FIFO memory functions, the source word latch is cleared, and the gate word latches are cleared as are the counters.

Enable/
Disable: When the disable button is pushed, the output ports are disabled but pulse program execution is not interrupted. The disable button may be used as a "panic button" if, for instance, a programming error causes an output port to "hang" in a high state. The output ports are reopened by pushing the enable button.

Start/
Stop: These buttons are not active on the Delta pulse programmer. They are intended to be used to interrupt pulse program execution without executing a reset.

4.9 Pulse Programmer: Software

4.9.1 General Program Structure

We will now discuss the general structure of the program that is used to operate the pulse programmer.

The program may be imagined as consisting of two principal sections. The first section includes those subroutines that allow the operator to input and edit pulse programs, input pulse program parameters such gate codes and delay times, and execute pulse programs. The commands that the operator used to accomplish such tasks are called console commands. When the operator wishes to execute a task, he/she enters the appropriate command on the console, and a subroutine called the command processor obtains the command string, interprets the string, and transfers control to the appropriate subroutine which then executes the task. When the task execution is completed, program control is returned to the command processor subroutine.

The second section is composed of those subroutines that drive the pulse programmer. Pulse sequences to be output to the spectrometer r.f. switches and data acquisition system are specified by entering pulse programs into the memory of the microprocessor. Pulse programs are composed of sequences of commands and parameters that specify such tasks as outputting control words to the pulse program buffer memories (FIFO memory or RAM memory), executing software loops, and setting or changing pulse program parameters such as delay times and pulse lengths.

Before describing each section of the program, some general features of the program should be mentioned.

The source version of the program, listed in appendix 1, is stored in the five RDOS files called UPCODE1.SR, UPCODE2.SR etc. The source files are backed up on floppy disk. In order to obtain an executable version of the program, the five source files are appended together into a single file that must be called PROG.SR. This source file is assembled by the program UPASM which resides in the directory UP on the removable disks of the Nova 2 and both Nova 820's. UPASM also exists on floppy disk and may be executed on the MP-200. A typical assembly requires about 20 minutes. Two files are output by UPASM. PROG.LS is a memory map of the program and PROG.AB is the executable binary version.

The program is loaded into the Z-80 memory by the program UPLOAD which also resides in the directory UP. But before UPLOAD can be executed, two things must be done. First, the binary version PROG.AB must be reorganized into a format that can be stored in the Z-80 memory. This is accomplished by executing the program ABIM which resides in UP. The output file is PROG.IM. Second PROG.IM must be renamed UP.IM, which is the file whose contents UPLOAD sends to the Z-80 memory.

The entry point of the program is on page $16_{10}(10_{16})$ of the Z-80 memory. In order to execute the program, input 10.G to the console. The entire program occupies about 5.5 K of memory. The first 16 pages (10_{16} to 20_{16}) are the system routines. The next page is the register page which is used to store the various pulse program parameters. Since gate words and time words are 16 bits (= 2 bytes = 1 word) long, the page is divided into 128 evenlynumbered registers. A valid register name is any even hexidecimal number and including 00 and FE. Following the register page is the line table page. The line table indicates which line numbers are in use by storing a FF at any unused number. Following the line table page are four pages that are used to store the pulse program.

4.9.2 Console Commands

"10.G" causes execution of the program. The program first initializes various system buffers and outputs a starting message:

```
UPCODE VERSION X.Y.
```

X is the version number and is characterized by the command set. Y is the number of pulse programline permitted. Currently X = 3 and T = 255.

Program control is then dispatched to the command processor subroutine (CMDPRS) which outputs a symbol CMD> to the terminal. The appearance of CMD> means that CMDPRS is waiting for a command line to be input. The command line format is:

```
COM   OP1   OP2
```

where COM is the command and OP1 and OP2 are operands used in executing the command task.

Once the command line has been received, CMDPRS calls the subroutine SCOM which searches the command text table for a match with COM. If no match is found an error message is output by SCOM and control is returned to CMDPRS. If a match is found control is dispatched to the appropriate "handler" subroutine by a jump table.

Version 3 has eight console commands:

1) CL

This command clears the pulse program by setting all line number flags to FF.

2) EC VAL

If VAL is zero, the echo flag (ECHO) is cleared which blocks echoing of input. If the echo is off, all command lines must begin with control-B and must be terminated by control-E. The echo should always be turned off if the program is to interact with SPEC. If VAL is nonzero, the echo flag is set to 1 and input is echoed.

3) VA REG

REG is a valid register name. This command is used to obtain the contents of the register specified by REG. Three numbers are output. The first number is the contents of the register in hexadecimal. The second number is the positive decimal version and the third number is the negative decimal version. The number may be interpreted as a positive or negative decimal number depending upon its application. If the contents of the register is to be used as a timing word, then the negative decimal version is of interest. If the contents of the register is to be used as a program counter, the positive decimal version is of interest.

4) LO REG VAL

Execution of LO causes a register, designated by REG, to be set to the value specified by VAL. VAL must be a hexinumber. For example

```
LO E0 F0F0
```

causes the register E0 to be set to the value $F0F0_{16}$.

5) DF REG VAL

Execution of DF causes a register, designated by REG, to be set to a value specified by VAL. VAL must be a positive or negative decimal number. REG must be a valid register name in hexidecimal. For example

```
DF E0 100
```

causes E0 to be set to $100_{10} = 64_{16}$.

6) LI LNI LN2

Execution of LI causes the current pulse program to be listed. The first line to be listed is specified LN1. The last line to be listed is LN2. LN1 and LN2 must be valid hexidecimal line numbers. For example:

```
L1 00 10
```

cause all program lines between and including 00 and 10_{16} to be listed.

7) ED

Execution of ED causes entry into the pulse program editor indicated by the appearance of ED> on the terminal screen. ED> indicates that the editor is waiting for input. Pulse program command lines have the format

```
LN COM OP1 OP2
```

where LN is a valid line number, COM is a pulse program command (see section 4.9.3), and OP1 and OP2 are operands used by the command subroutine. A valid line number is any hexidecimal number between 00 and FE.

When a command line is input, the editor checks to see if the line number is valid. If the line number is valid the editor checks to see if the line number is not in use. If it is not in use, it sets the flag to LN.

Next the editor calls SCOM which searches the pulse program text table for a match with COM. If no match is found an error message is output and control is returned to the editor. If a match is found the command number, specified by the command's position in the text table, is stored in the public pulse program. The operand numbers OP1 and OP2 are also stored in the pulse program area.

A pulse program line may be removed by typing LN↓. For example

```
10↓
```

will cause the line 10 to be deleted.

The editor may be exited by typing Q↓.

8) GO LN

GO initiates pulse program execution at the line number specified by LN. If LN is unused an error will be returned. GO calls the subroutine PP which examines the line table for line numbers in use. When a line number is encountered that is in use, PP obtains the command number and the operands OP1 and OP2 from the pulse program area and dispatches control to the appropriate subroutine with a jump table. When the command has been executed, control is returned to PP. PP will continue to search the line table until line FF is encountered, indicating the end of the table, or a halt command is encountered in the pulse program. In either case control is returned to the command processor.

4.9.3 Pulse Program Commands

Version 3 has 22 pulse program commands. What follows is a description of each command.

1) CO REG1 REG2

This instruction causes the contents of register 1 (C(REG1) to be compared to the contents of register 2 (C(REG2). The comparison code COMP is set as follows:

(i) If C(REG1).EQ.C(REG2), COMP = 01
(ii) If C(REG1).LT.C(REG2), COMP = 02
(iii) If C(REG1).GT.C(REG2), COMP = 04

2) BR LN CODE

This instruction causes a branch to be performed to the line number specified by LN if (CODE.AND.COMP).NE.0. Suppose the contents of REG1 and REG2 were compared and COMP was set accordingly. Then the branch condition code may be defined as follows:

CODE = 0, a branch to LN never occurs

CODE = 1, a branch to LN occurs if C(REG1).EG.C(REG2)

CODE = 2, a branch to LN occurs if C(REG1).LT.C(REG2)

CODE = 3, a branch to LN occurs if C(REG1).LE.C(REG2)

CODE = 4, a branch to LN occurs if C(REG1).GT.C(REG2)

CODE = 5, a branch to LN occurs if C(REG1).GE.C(REG2)

CODE = 6, a branch to LN occurs if C(REG1).NE.C(REG2)

CODE = 7, a branch always occurs to LN

3) DE REG1 REG2

The contents of register 1 is decremented by the contents of register 2. The result is left in register 1.

4) HA

When the subroutine PP encounters this command, pulse program execution ceases and program control is returned to the command processor. A HA command must be used to separate the portion of the pulse program that loads the FIFO memory. from the portion of the pulse program that loads the RAM memory.

5) HN REG1

This instruction causes a delay in units of .1 nsec to be output to the FIFO memory.

C(REG1) is the length of the delay in units of .1 nsec and may not exceed 16383. C(REG2) is the gate word (see section 4.9.4).

6) IN REG1 REG2

This instruction causes the contents of register 1 to be incremented by the contents of register 2. The result is left in register 1.

7) 01(02,03) REG1 REG2

This instruction causes a delay to be output to the RAM 1 (2,3) memory. Currently, only RAM 1 exists in the pulse programmer. C(REG1) is the two's complement of the delay in units of .1 usec. C(REG2) is the gate word.

8) OD REG1 REG2

This instruction causes a delay to be output to the FIFO memory. The length of the delay is defined by C(FE)*C(REG1). C(REG1) is the unit time delay in units of .1 usec. C(REG1) may not exceed 8192_{10}.C(FE) is a multiplier. For example, if C(REG1) = 5000_{10} and C(FE) = 10_{10}, a delay of 5msec is output to the FIFO.

If a single OD command occurs within a pulse program, C(REG1) may be any time less than 819.2 usec. If, however, two OD commands occur within a pulse program C(REG1) should not be less than about 150 usec, otherwise timing errors may occur.

C(REG2) is the gate word.

9) OF REG1 REG2

This instruction causes a delay to be output to the FIFO. C(REG1) is the two's complement of the delay in units of .1 usec C(REG2) is the gate word.

10) PA NIS

This instruction causes the "next instruction source" code SOURCE to be set to NIS. The two most significant bits of all timing words output to the pulse program memory following execution of a PA command are defined by SOURCE. The source code is

00 = FIFO   02 = RAM 2

01 = RAM 1   03 = RAM 3

11) R1 (R2,R3)

This instruction causes initialization of the RAM 1 (R2,R3) address counter to $F000_{10}$ ($F400_{16}$, $F800_{16}$).

12) RE

This instruction only works on a pulse programmer with a functioning start/stop button. When this command is encountered, program execution ceases and control is despatched to the command processor if the stop button has been pushed. Control will remain with the command processor until the start button is pushed, and the program execution will continue at the line following the RE command.

13) SB REG1 REG2

When an SB command is encountered, C(REG1) is decremented by one and the result is left in REG1. If the result is nonzero, a program branch occurs to the line number specified by C(REG2).

14) SC REG1 REG2

This instruction causes a delay to be output to the FIFO in units of seconds. C(REG1) is the delay in units of seconds and may not exceed 255_{10}. C(REG2) is the gate word.

15) MS REG1 REG2

This instruction causes a delay to be output to the FIFO in units of milliseconds. C(REG1) is the delay in units of milliseconds. C(REG2) is the gate word.

16) US REG1 REG2

This instruction causes a delay to be output to the FIFO in units of microseconds. C(REG1) is the delay in units of usec and may not exceed 8192. C(REG2) is the gate word.

17) SE REG1 REG2

When this instruction is encountered, the contents of register 1 is set to the contents of register 2.

18) TI REG1 REG2

This instruction causes a train of delays to be output to RAM 1. C(REG1) is the number of delays in the train and may not exceed 255_{10}. C(REG2) is the gate word. The two's complement of the delay in units of .1 usec must be stored in register D2.

4.9.4 Construction of Gate Words

From figure 67 it may be seen that there are twenty output ports available at the rear panel of the pulse programmer. Control of the voltage level at each port is effected by delivering an appropriate 16 bit hexidecimal-coded gate word to the buffer memory.

The four bits composing the most significant nibble control the "triggering pulse" ports. A high bit within the most significant nibble will cause one of the trigger ports to go high for one clock cycle (100 nsec). TP1 corresponds to the most significant bit (2^3), TP2 to the next lower bit (2^2) and so on. If one wished to open TP1 and TP4 simultaneously, the value of the nibble would be 9.

The next nibble controls the auxiliary ports. A high bit within this nibble will cause the voltage at the appropriate port to go high for a time specified by the time word. If one wishes to open auxiliary port 2 (AUX 2) and AUX3, the value of the nibble word would be 6.

The next nibble controls the A gates which in turn control the r.f. switches of the deuterium channel of the spectrometer. The quadrature phase channels are controlled by the decoding of the two least significant bits of the nibble by a 74LS139. The code is

AX = 00 A-X = 10

AY = 01 A-Y = 11

The two most significant bits correspond to the AOR2 and AOR2 gates. The complements of the OR bits are logically NOR'ed with the complements of the A bits so to open one of the A gates, one of the OR gates must be opened. To cause the A-X gate to open the valves of the nibble would be A.

The next nibble controls the states of the B gates which in turn control the r.f. switches of the proton channel. Control of the B gates is identical to control of the A gates. Thus to open the BY gate the value of the nibble is 9.

A gate word is constructed by a concantenation of the four nibbles. Therefore to open the gates TP1, TP2, AUX2, AUX3, A-X, and BY the gate word is C6A9.

Appendix 4.1 : Source Listing of Microprocessor Code

```
        ORG     1000
FIRST   EQU     .
/
/MAIN
/
/ENTRY POINT FOR UP OPERATING SYSTEM
/
MAIN    CALL    INIT            /INITIALIZE SYSTEM PARAMETERS
        CALL    CRLF            /OUTPUT CR AND LF
        CALL    SMSG            /OUTPUT START MESSAGE
        JMP     CMDPRS          /GET COMMAND
/
/INIT
/INITIALIZES SYSTEM PARAMETERS
INIT
        XRA     A               /ZERO A
        STA     RCYCLE          /INIT RECYCLE STATUS TO OFF
        STA     SOURCE          /INIT INSTRUCTION FIELD TO FIFO
        STA     COMP            /INIT COMP TO NEVER
        STA     OCHAR           /INIT OUTPUT CHARACTER INDEX
        STA     ICHAR           /INIT INPUT CHARACTER INDEX
        MVI     A,01            /GET ONE INTO A
        STA     ECHO            /TURN ON ECHO
        MVI     L,00            /GET 0 INTO L
        MVI     H,SRAM1         /SRAM1 INTO H,L
        SHLD    RAC1            /INIT RAC1
        MVI     H,SRAM2         /SRAM2 INTO H,L
        SHLD    RAC2            /INIT RAC2
        MVI     H.SRAM3         /SRAM3 INTO H,L
        SHLD    RAC3            /INIT RAC3
        RET                     /RETURN
/
/SMSG
/ROUTINE TO OUTPUT START MESSAGE
SMSG    LXI     H,1$            /POINT TO START MESSAGE
        CALL    PSTR            /GET STRING INTO OUTPUT BUFFER
        CALL    PLINE           /OUTPUT MESSAGE
        RET                     /RETURN
/MSG
1$      TXT     /UPCODE VERSION 3.255/
        DB      0
/
/PSTR
/
/ROUTINE TO GET CHAR STRING INTO OUTPUT BUFFER
/H.L CONTAINS POINTER TO STRING. STRING TERMINATED BY NULL BYTE
/ALL REGISTERS EXCEPT A PRESERVED
/
PSTR    PUSH    H               /SAVE H,L
1$      MOV     A.M             /GET NEXT CHAR
        ORA     A               /CHECK FOR NULL BYTE
        JZ      2$              /YES. DONE.
        CALL    PCHAR           /OUTPUT CHAR
        INX     H               /UPDATE STRING POINTER
        JMP     1$              /BACK FOR MORE
2$      POP     H               /GET H.L AGAIN
        RET                     /RETURN
/
```

```
/PCHAR
/
/ROUTINE TO PUT NEXT CHAR INTO OUTPUT BUFFER
/BUFFER IS NOBUF BYTES IN SIZE
/ALL REGISTERS PRESERVED
/
PCHAR   PUSH    B               /SAVE B.C
        PUSH    D               /SAVE D,E
        PUSH    H               /SAVE H,L
        MOV     B.A             /SAVE CHAR
        MVI     E.NOBUF         /GET BUFFER SIZE
        LDA     OCHAR           /GET CHAR INDEX
        CMP     E               /CHECK FOR .LT. MAX
        JNC     1$              /NO. DONE.
        MOV     L.A             /MOVE CHAR INDEX INTO H,L
        MVI     H,00
        INR     A               /UPDATE CHAR INDEX
        STA     OCHAR           /SAVE CHAR INDEX
        LXI     D.OBUF          /POINT TO OUTPUT BUFFER
        DAD     D               /POINT TO NEXT CHAR
        MOV     M.B             /SAVE NEXT CHAR
1$      MOV     A.B             /GET CHAR AGAIN
        POP     H               /GET H,L AGAIN
        POP     D               /GET D.E AGAIN
        POP     B               /GET B.C AGAIN
        RET                     /RETURN
/
/PLINE
/
/ROUTINE TO OUTPUT LINE WITH CR
/LENGTH OF LINE IS OCHAR
/ALL REGISTERS EXCEPT A RESTORED
/
PLINE   CALL    PLINE1          /OUTPUT LINE
        CALL    CRLF            /OUTPUT CR AND LF
        RET                     /RETURN
/
/PLINE1
/ROUTINE TO OUTPUT LINE
/LENGTH OF LINE IS OCHAR CHARACTERS
PLINE1  PUSH    B               /SAVE B.C
        PUSH    H               /SAVE H,L
        MVI     A.02            /GET CNTRL-B
        CALL    OUTPUT          /OUTPUT CNTRL-B
        LDA     OCHAR           /GET LINE LENGTH
        ORA     A               /CHECK FOR ZERO
        JZ      2$              /YES
        MOV     B.A             /INIT LOOP COUNTER
        LXI     H.OBUF          /POINT TO OUTPUT BUFFER
1$      MOV     A.M             /GET NEXT CHAR
        CALL    OUTPUT          /OUTPUT NEXT CHAR
        INX     H               /UPDATE CHAR BUFFER
        DCR     B               /UPDATE LOOP COUNTER
        JNZ     1$              /BACK FOR MORE
2$      MVI     A.05            /GET CNTRL-E
        CALL    OUTPUT          /OUTPUT CNTRL-E
        XRA     A               /ZERO A
        STA     OCHAR           /INIT LINE LENGTH
        POP     H               /GET H,L AGAIN
        POP     B               /GET B,C AGAIN
        RET                     /RETURN
/
/OUTPUT
/BASIC CONSOLE OUTPUT ROUTINE
OUTPUT  STA     CHAR            /SAVE CHARACTER
1$      IN      TTS             /GET RMTTO
        ANI     RMTTO           /CHECK FOR COMPLETION
        JZ      1$              /NO
        LDA     CHAR            /GET CHARACTER AGAIN
        OUT     TTO             /OUTPUT CHAR
        RET                     /RETURN
/
/CRLF
/OUTPUT CR,LF TO CONSOLE
/
CRLF
        MVI     A,0D            /GET CR
        CALL    OUTPUT          /OUTPUT CR
        MVI     A,0A            /GET LF
        CALL    OUTPUT          /OUTPUT LF
        RET                     /RETURN
/
/CMDPRS
/COMMAND PROCESSOR
/
CMDPRS
/GET COMMAND
1$      CALL    DSPTCH          /DISPATCH CONTROL
        CPI     0FF             /CHECK FOR DISPATCH TO PP
        JZ      PP              /DISPATCH CONTROL TO PP
        CALL    PRMPT           /OUTPUT CNTRL-F
        LDA     ECHO            /CHECK ECHO STATUS
        ANA     A               /CHECK FOR ECHO OFF
        JZ      2$              /ECHO OFF. SKIP CMDPRS PROMPT.
        LXI     H,3$            /POINT TO PROMPT
        CALL    PSTR            /OUTPUT STRING
        CALL    PLINE1          /OUTPUT CMDPRS PROMPT
2$      CALL    GLINE           /GET INPUT
        CALL    GCHAR           /GET FIRST CHAR
        ANA     A               /CHECK FOR NULL
        JZ      1$              /TRY AGAIN
        LXI     D.TOPSO         /GET START OF OPCODE STRING TABLE
        LXI     H.IBUF          /POINT TO INPUT BUFFER
        CALL    SCOM            /SEARCH FOR MATCH
        CPI     0FF             /CHECK FOR ERROR
        JZ      1$              /YES. TRY AGAIN
        JMP     TJMPO           /CALL HANDLER
/MSG
3$      TXT     /CMD> /
        DB      0
/
/SCOM
/ROUTINE TO SEARCH OPCODE TABLE FOR MATCH WITH STRING
/H.L CONTAINS POSITION POINTER
/D.E CONTAINS TABLE POINTER. NULL TERMINATES TABLE
/INDEX OF MATCH RETURNED IN A. -1 RETURNED IF NO MATCH
SCOM    PUSH    B               /SAVE B,C
        PUSH    D               /SAVE D,E
        PUSH    H               /SAVE H,L
        MVI     C.00            /INIT TABLE INDEX
```

```
1$      PUSH    H               /SAVE STRING POINTER
        MVI     B,02            /SAVE LOOP CONTER
2$      LDAX    D               /GET NEXT CHAR OF ENTRY
        CMP     M               /COMPARE WITH NEXT CHAR OF STRING
        JNZ     3$              /NOT EQUAL
        INX     D               /UPDATE TABLE POINTER
        INX     H               /UPDATE STRING POINTER
        DCR     B               /UPDATE LOOP COUNTER
        JNZ     2$              /TRY AGAIN
        POP     H               /GET STRING POINTER
        MOV     A,C             /GET TABLE INDEX
        JMP     4$              /DONE
3$      INX     D               /UPDATE TABLE POINTER
        DCR     B               /UPDATE LOOP COUNTER
        JNZ     3$              /BACK FOR MORE
        INR     C               /UPDATE TABLE INDEX
        POP     H               /GET STRING POINTER AGAIN
        LDAX    D               /GET FIRST CHAR
        ORA     A               /CHECK FOR ZERO
        JNZ     1$              /NO. TRY FOR MATCH AGAIN
        LXI     H,5$            /POINT TO MSG
        CALL    PSTR            /GET STRING
        CALL    PLINE           /OUTPUT MESSAGE
        MVI     A,0FF           /SIGNAL ERROR
4$      POP     H               /GET H,L
        POP     D               /GET D,E
        POP     B               /GET B,C
        RET                     /RETURN
/MSG
5$      TXT     /(SCOM   ) INVALID COMMAND/
        DB      0
/
/PRMPT
/OUTPUTS PROMPT TO CONSOLE
/
PRMPT
1$      IN      1               /CHECK FOR RMTTO
        ANI     01              /WAIT FOR COMPLETION
        JZ      1$              /NO
        MVI     A,06            /YES. GET CNTRL-F
        OUT     TTO             /OUTPUT CNTRL-F
        RET                     /RETURN
/
/GLINE
/
/INPUTS LINE. MAX LENGTH OF LINE IS NIBUF BYTES
/ALL REGISTERS EXCEPT A PRESERVED
GLINE   PUSH    B               /SAVE B,C
        PUSH    H               /SAVE H,L
1$      LDA     ECHO            /GET ECHO STATUS
        ANA     A               /CHECK ECHO STATUS
        JNZ     3$              /ECHO ON
2$      CALL    INPUT           /GET INPUT
        CPI     02              /CHECK FOR CNTRL-B
        JNZ     2$              /NO, TRY AGAIN
3$      LXI     H,IBUF          /POINT TO INPUT BUFFER
        MVI     B,00            /INIT INPUT LINE LENGTH
4$      CALL    INPUT           /GET INPUT
        CPI     0A              /CHECK FOR LF
        JNZ     5$              /NO
        LDA     ECHO            /GET ECHO STATUS AGAIN
        ANA     A               /CHECK ECHO STATUS AGAIN
        JNZ     10$             /ECHO ON. DONE
        JZ      4$              /TRY AGAIN
5$      CPI     7F              /CHECK FOR RUBOUT
        JNZ     6$              /NO
        CALL    BS              /OUTPUT BS
        JMP     4$              /TRY AGAIN
6$      CPI     05              /CHECK FOR CNTRL-E
        JNZ     7$              /NO
        LDA     ECHO            /GET ECHO STATUS AGAIN
        ANA     A               /CHECK ECHO STATUS AGAIN
        JZ      10$             /ECHO OFF. DONE.
        JMP     4$              /ECHO ON. DISREGARD.
7$      MOV     M.A             /SAVE CHAR
        INX     H               /UPDATE BUF POINTER
        INR     B               /UPDATE LINE LENGTH
        MOV     A.B             /MOVE TO A
        CPI     NIBUF           /CHECK FOR .LT. MAX
        JC      4$              /BACK FOR MORE
8$      CALL    INPUT           /GET NEXT CHAR
        CPI     7F              /CHECK FOR RUBOUT
        JZ      1$              /TRY AGAIN
        CPI     05              /CHECK FOR CNTRL-E
        JNZ     9$              /NO
        LDA     ECHO            /GEET ECHO STATUS AGAIN
        ANA     A               /CHECK ECHO STATUS
        JZ      10$             /ECHO OFF. DONE.
        JMP     8$              /ECHO ON. DISREGARD.
9$      CPI     0A              /CHECK FOR LF
        JNZ     8$              /TRY AGAIN
        LDA     ECHO            /GET ECHO STATUS
        ANA     A               /CHECK ECHO STATUS
        JZ      8$              /ECHO OFF. TRY AGAIN.
10$     MOV     A.B             /GET LINE LENGTH
        INR     A               /UPDATE LINE LENGTH
        STA     NICHAR          /SAVE LINE LENGTH
        XRA     A               /CLEAR A
        MOV     M.A             /NULL LAST BYTE
        STA     ICHAR           /INIT CHAR INDEX
        POP     H               /GET H.L AGAIN
        POP     B               /GET B,C AGAIN
        RET                     /RETURN
/
/BS
/ROUTINE TO OUTPUT BACK SPACE
BS      MOV     A.B             /GET LINE LENGTH INTO A
        ANA     A               /CHECK FOR ZERO
        JZ      1$              /EXIT
        MVI     A,08            /GET BS CHARACTER
        CALL    OUTPUT          /OUTPUT CHAR
        MVI     A,20            /GET SP CHAR
        CALL    OUTPUT          /OUTPUT SPACE
        MVI     A,08            /GET BS CHAR
        CALL    OUTPUT          /OUTPUT BACK SPACE
        DCX     H               /UPDATE POINTER
        DCR     B               /UPDATE LINE LENGTH
1$      RET                     /RETURN
/
/INPUT
```

```
/BASIC CONSOLE INPUT ROUTINE
INPUT   LDA     ECHO            /GET ECHO FLAG
        ANA     A               /CHECK FOR ECHO
        JNZ     2$              /ECHO CHAR
1$      IN      TTS             /GET INPUT STATUS
        ANI     RMTTI           /CHECK FOR INPUT READY STATUS
        JZ      1$              /NO. TRY AGAIN
        IN      TTI             /GET INPUT
        ANI     7F              /MASK TO 7 BITS
        JMP     4$              /DONE. EXIT
2$      IN      TTS             /GET INPUT
        ANI     RMTTI           /CHECK FOR READY STATUS
        JZ      2$              /NO. TRY AGAIN
        IN      TTI             /GET INPUT
        ANI     7F              /MASK TO 7 BITS
        CPI     7F              /CHECK FOR RUBOUT
        JZ      4$              /EXIT
        CPI     0D              /CHECK FOR CR
        JNZ     3$              /NO
        CALL    CRLF            /OUTPUT CRLF
        JMP     4$              /EXIT
3$      CALL    OUTPUT          /ECHO CHAR
4$      RET                     /RETURN
/
/GCHAR
/ROUTINE TO GET NEXT CHAR FROM INPUT BUFFER
/BUFFER IS NICHAR BYTES IN LENGTH
/ALL REGISTERS EXCEPT A PRESERVED
GCHAR   PUSH    D               /SAVE D,E
        PUSH    H               /SAVE H,L
        LDA     NICHAR          /GET NUMBER OF CHAR IN INPUT BUFFER
        MOV     E.A             /SAVE IN E
        LDA     ICHAR           /CHECK CHAR INDEX
        CMP     E               /CHECK FOR .LT. MAX
        JC      1$              /YES
        XRA     A               /CLEAR A
        JMP     2$              /DONE
1$      MOV     L.A             /MOVE CHAR INDEX TO A
        MVI     H,00            /
        INR     A               /UPDATE CHAR INDEX
        STA     ICHAR           /SAVE CHAR INDEX
        LXI     D.IBUF          /POINT TO INPUT BUFFER
        DAD     D               /POINT TO NEXT CHAR
        MOV     A.M             /GET NEXT CHAR
        POP     H               /GET H.L AGAIN
        POP     D               /GET D,E AGAIN
2$      RET                     /RETURN
/
/HSW
/ROUTINE TO CONVERT HEX STRING TO 16 BIT WORD
/RESULT STORED IN B,C
/ERROR CODE RETURNED IN A
HSW     PUSH    D               /SAVE D,E
        PUSH    H               /SAVE H,L
/INIT
        XRA     A               /CLEAR A
        MOV     E,A             /E WILL HOLD LS NIBBLE
        MOV     D,E             /
        MOV     C.D             /
        MOV     B.C             /B WILL HOLD MS NIBBLE
```

```
/GET NEXT CHAR
1$        CALL      GCHAR                 /GET CHAR
          CPI       ' '                   /CHECK FOR SP
          JZ        4$                    /YES. DONE
          ORA       A                     /CHECK FOR NULL
          JZ        4$                    /YES. DONE
/CONVERT
          CPI       '0'                   /CHECK FOR .GE. '0'
          JC        5$                    /NO. ERROR
          CPI       '9'+1                 /CHECK FOR .LE. '9'
          JNC       2$                    /NO
          SUI       '0'                   /CONVERT TO NIBBLE
          JMP       3$                    /
2$        CPI       'A'                   /CHECK FOR .GE. 'A'
          JC        5$                    /NO. ERROR
          CPI       'F'+1                 /CHECK FOR .LE. 'F'
          JNC       5$                    /NO. ERROR
          SUI       'A'                   /CONVERT TO NIBBLE
          ADI       0A                    /ADD 10
/SAVE NIBBLE
3$        MOV       B.C                   /SHIFT
          MOV       C.D                   /
          MOV       D.E                   /
          MOV       E.A                   /SAVE LS NIBBLE
          JMP       1$                    /BACK FOR MORE
/ASSEMBLE WORD
4$        MOV       A.B                   /GET MORE SIGNIFICANT NIBBLE
          RLC                             /SHIFT
          RLC
          RLC
          RLC
          ORA       C                     /ADD LSB
          MOV       B.A                   /SAVE HIGH ORDER RESULT
          MOV       A.D                   /GET MORE SIGNIFICANT NIBBLE
          RLC
          RLC
          RLC
          RLC
          ORA       E                     /ADD LESS SIGNIFICANT NIBBLE
          MOV       C,A                   /SAVE LOW ORDER RESULT
/NO ERROR
          XRA       A                     /SIGNAL NO ERROR
          JMP       6$                    /DONE
/ERROR
5$        LXI       H,7$                  /POINT TO MESSAGE
          CALL      PSTR                  /OUTPUT STRING
          CALL      PLINE                 /OUTPUT ERROR
          MVI       A.OFF                 /SET A TO ERROR
/RETURN
6$        POP       H                     /GET H,L RESULT
          POP       D                     /GET D,E RESULT
          RET                             /RETURN
/MSG
7$        TXT       /(HSW    ) ILLEGAL CHAR/
          DB        0
/
          ORG       1400
/
/ED
/ROUTINE TO EDIT PULSE PROGRAM
```

```
/
ED
1$      CALL    PRMPT           /OUTPUT CNTRL-F
        LDA     ECHO            /GET ECHO STATUS
        ANA     A               /CHECK FOR ECHO OFF
        JZ      2$              /ECHO OFF. SKIP EDITOR PROMPT
        LXI     H.10$           /POINT TO EDITOR PROMPT
        CALL    PSTR            /OUTPUT STRING
        CALL    PLINE1          /OUTPUT LINE
2$      CALL    GLINE           /GET NEXT LINE
        CALL    GCHAR           /GET FIRST CHARACTER
        CPI     51              /CHECK FOR Q CHAR (QUITE)
        JZ      9$              /YES. EXIT EDITOR
        ANA     A               /CHECK FOR NULL CHAR
        JZ      1$              /TRY AGAIN
        XRA     A               /CLEAR A
        STA     ICHAR           /INIT CHAR POINTER
        CALL    HSW             /CONVERT LINE NUMBER
        CPI     0FF             /CHECK FOR ERROR
        JZ      1$              /TRY AGAIN
        MOV     A,B             /GET B INTO A
        ORA     A               /CHECK FOR OVERFLOW
        JZ      3$              /CONTINUE
        LXI     H.11$           /POINT TO ERROR MSG
        JMP     8$              /OUTPUT ERROR
3$      MOV     A.C             /GET LINE NUMBER INTO A
        STA     LN              /STORE AT LN
        MVI     A,02            /GET 02 INTO A
        STA     ICHAR           /SAVE AT ICHAR
        CALL    GCHAR           /GET NEXT CHARACTER
        CPI     ' '             /CHECK FOR SPACE
        JZ      5$              /YES. CONTINUE.
        ANA     A               /CHECK FOR NULL
        JZ      4$              /YES. DELETE LINE
        LXI     H.12$           /POINT TO ERROR MSG
        JMP     8$              /OUTPUT ERROR
4$      CALL    IDEL            /DELETE LINE
        JMP     1$              /BACK FOR MORE
5$      LXI     D.TOPS11        /GET START OF OPCODE STRING TABLE
        LXI     H.IBUF          /POINT TO  INPUT BUFFER
        INX     H               /POINT TO OPCODE STRING
        INX     H
        INX     H
        CALL    SCOM            /SEARCH FOR MATCH
        CPI     0FF             /CHECK FOR ERROR
        JZ      1$              /TRY AGAIN
        STA     OPCODE          /SAVE AT OPCODE
        MVI     A,05            /GET 05 INTO A
        STA     ICHAR           /SAVE AT ICHAR
        CALL    GCHAR           /GET NEXT CHARACTER
        CPI     ' '             /CHECK FOR SPACE
        JZ      6$              /CONTINUE
        LXI     H.12$           /POINT TO ERROR MSG
        JMP     8$              /OUTPUT ERROR
6$      CALL    OPEVAL          /EVALUATE FIRST OPERAND
        CPI     0FF             /CHECK FOR ERROR
        JZ      1$              /TRY AGAIN
        MOV     A.C             /GET OPERAND
        STA     OP1             /SAVE AT OP1
        MVI     A.08            /GET 08 INTO A
        STA     ICHAR           /SAVE AT ICHAR
        CALL    GCHAR           /GET NEXT CHARACTER
        CPI     ' '             /CHECK FOR SPACE
        JZ      7$              /CONTINUE
        LXI     H,12$           /POINT TO ERROR MSG
        JMP     8$              /OUTPUT ERROR
7$      CALL    OPEVAL          /EVALUATE SECOND OPERAND
        CPI     0FF             /CHECK FOR ERROR
        JZ      1$              /TRY AGAIN
        MOV     A,C             /GET SECOND OPERAND
        STA     OP2             /SAVE AT OP2
        CALL    IADD            /ADD INSTRUCTION TO PP AREA
        JMP     1$              /BACK FOR MORE
8$      CALL    PSTR            /OUTPUT STRING
        CALL    PLINE           /OUTPUT LINE
        JMP     1$              /TRY AGAIN
9$      JMP     CMDPRS          /EXIT EDITOR
/MSG
10$     TXT     /ED> /
        DB      0
11$     TXT     /(ED     ) INVALID LINE NUMBER/
        DB      0
12$     TXT     /(ED     ) INPUT FORMAT ERROR/
        DB      0
/WDS
/ROUTINE TO CONVERT WORD TO DECIMAL STRING
/ALL REGISTERS EXCEPT A PRESERVED
WDS     PUSH    B               /SAVE B,C
        PUSH    D               /SAVE D,E
        PUSH    H               /SAVE H.L
        LXI     H,2710          /GET 10000 INTO H,L
        MVI     D,04            /INIT PLACE COUNTER
/MAIN LOOP
1$      MVI     E,00            /INIT LOOP COUNTER
2$      MOV     A,C             /GET LS BYTE INTO A
        SUB     L               /SUBTRACT LS BYTE
        MOV     C,A             /GET RESULT INTO C
        MOV     A,B             /GET MS BYTE INTO A
        SBB     H               /SUBTRACT MS BYTE
        MOV     B,A             /GET RESULT INTO B
        JC      3$              /RESULT .LT. 0
        INR     E               /UPDATE LOOP COUNTER
        JMP     2$              /BACK FOR MORE
3$      DCR     D               /UPDATE PLACE COUNTER
        MOV     A,E             /GET LOOP COUNTER INTO A
        ADI     30              /CONVERT TO CHAR
        CALL    PCHAR           /OUTPUT CHAR
/RESTORE B,C TO LAST RESULT
        MOV     A,C             /GET LS BYTE INTO A
        ADD     L               /ADD LS BYTE
        MOV     C,A             /GET RESULT INTO C
        MOV     A,B             /GET MS BYTE INTO A
        ADC     H               /ADD MS BYTE
        MOV     B,A             /GET RESULT INTO B
/DETERMINE CURRENT DECIMAL PLACE
        MOV     A,D             /GET PLACE COUNTER INTO A
        CPI     03              /CHECK FOR 1000 PLACE
        JNZ     4$              /TRY AGAIN
        LXI     H,03E8          /GET 1000 INTO H,L
        JMP     1$              /BACK FOR MORE
```

```
4$      CPI     02                      /CHECK FOR 100 PLACE
        JNZ     5$                      /TRY AGAIN
        LXI     H,0064                  /GET 100 INTO H,L
        JMP     1$                      /TRY AGAIN
5$      CPI     01                      /CHECK FOR 10 PLACE
        JNZ     6$                      /TRY AGAIN
        LXI     H,000A                  /GET 10 INTO H,L
        JMP     1$                      /BACK FOR MORE
6$      MOV     A,C                     /GET NUMBER INTO A
        ADI     30                      /CONVERT TO CHAR
        CALL    PCHAR                   /OUTPUT CHAR
        POP     H                       /GET H,L AGAIN
        POP     D                       /GET D,E AGAIN
        POP     B                       /GET B,C AGAIN
        RET                             /RETURN
/
/DF REG VAL
/ROUTINE TO LOAD A REGISTER WITH A VALUE
/REG IS THE NAME OF THE REGISTER
/VAL IS THE VALUE TO BE LOADED (DECIMAL)
/
DF      MVI     A,02                    /GET 02 INTO A
        STA     ICHAR                   /INIT CHAR INDEX
        CALL    GCHAR                   /GET CHAR
        CPI     ' '                     /CHECK FOR SP
        JZ      1$                      /YES
        LXI     H,9$                    /POINT TO MSG
        JMP     7$                      /OUTPUT ERROR AND EXIT
1$      CALL    HSW                     /EVALUATE REG OPERAND
        CPI     OFF                     /CHECK FOR ERROR
        JZ      8$                      /ERROR. EXIT
        MOV     A,B                     /CHECK FOR OVERFLOW
        ORA     B
        JZ      2$                      /NO OVERFLOW
        LXI     H,10$                   /POINT TO MSG
        JMP     7$                      /OUTPUT ERROR AND EXIT
2$      MOV     A,C                     /GET LOW ORDER OPERAND INTO A
        RAR                             /CHECK FOR VALID REGISTER
        JNC     3$                      /YES
        LXI     H,10$                   /POINT TO MSG
        JMP     7$                      /OUTPUT ERROR AND EXIT
3$      LXI     H,REGS                  /GET START OF REG AREA INTO H,L
        DAD     B                       /POINT TO REG
        MVI     A,05                    /GET 5 INTO A
        STA     ICHAR                   /INIT CHAR INDEX
        CALL    GCHAR                   /GET CHAR
        CPI     ' '                     /CHECK FOR SP
        JZ      4$                      /YES
        LXI     H,9$                    /POINT TO MSG
        JMP     7$                      /OUTPUT ERROR AND EXIT
4$      MVI     A,06                    /GET 6 INTO A
        STA     ICHAR                   /INIT CHAR INDEX
        CALL    GCHAR                   /GET CHAR
        CPI     2D                      /CHECK FOR '-'
        MVI     A,OFF                   /INIT TO NEGATIVE
        STA     SIGN                    /SAVE SIGN FLAG
        MVI     A,07                    /GET 7 INTO A
        STA     ICHAR                   /INIT CHAR INDEX
        JZ      5$                      /NEGATIVE
        MVI     A,00
        STA     SIGN            /SAVE SIGN FLAG
        MVI     A,06            /GET 6 INTO A
        STA     ICHAR           /INIT CHAR INDEX
5$      CALL    DSW             /EVALUATE
        CPI     OFF             /CHECK FOR ERROR
        JZ      8$              /EXIT
        LDA     SIGN            /GET SIGN FLAG
        ANA     A               /CHECK FOR POSITIVE
        JZ      6$              /POSITIVE
        CALL    TCOMP           /NEGATIVE
6$      MOV     M.C             /LOAD LOW ORDER REGISTER
        INX     H               /UPDATE POINTER
        MOV     M.B             /LOAD HIGH ORDER REGISTER
        JMP     8$              /EXIT
7$      CALL    PSTR            /OUTPUT STRING
        CALL    PLINE           /OUTPUT LINE
8$      JMP     CMDPRS          /EXIT TO CMDPRS
/MSG
9$      TXT     /(DF    ) INPUT FORMAT ERROR/
        DB      0
10$     TXT     /(DF    ) INVALID REGISTER/
        DB      0
/
/DSW
/ROUTINE TO CONVERT DECIMAL STRING TO 16 BIT WORD
/RESULT RETURNED IN B,C
/ERROR RETURNED IN A
DSW     PUSH    H               /SAVE H.L
/INIT
        XRA     A               /CLEAR A
        MOV     C.A             /INIT B,C
        MOV     B.C
/GET NEXT CHAR
1$      CALL    GCHAR           /GET CHAR
        ORA     A               /CHECK FOR NULL BYTE
        JZ      2$              /YES. DONE.
        CPI     ' '             /CHECK FOR SP
        JZ      2$              /YES. DONE.
        CPI     '0'             /CHECK FOR .GE. '0'
        JC      3$              /NO. ERROR.
        CPI     '9'+1           /CHECK FOR .LE. '9'
        JNC     3$              /NO, ERROR.
        SUI     '0'             /CONVERT TO NIBBLE
        CALL    MPY10           /MPY CURRENT RESULT BY 10
        ADD     C               /ADD LS BYTE
        MOV     C,A             /GET RESULT INTO C
        MVI     A,00            /CLEAR A
        ADC     B               /ADD MS BYTE
        MOV     B.A             /GET RESULT INTO B
        JMP     1$              /BACK FOR MORE
2$      JMP     4$              /DONE
3$      LXI     H,5$            /POINT TO MSG
        CALL    PSTR            /OUTPUT STRING
        CALL    PLINE           /OUTPUT LINE
        MVI     A,OFF           /GET ERROR FLAG
4$      POP     H               /GET H.L BACK
        RET                     /RETURN
/MSG
5$      TXT     /(DSW   ) ILLEGAL CHAR/
        DB      0
```

```
/
/CL
/ROUTINE TO CLEAR PULSE PROGRAM AREA
CL      MVI     B,0FF           /INIT LOOP COUNTER
        MVI     A,0FF           /GET EMPTY FLAG
        LXI     H,TLINE         /POINT TO BEGINNING OF LINE TABLE
1$      MOV     M,A             /CLEAR LOCATION
        INX     H               /UPDATE TABLE POINTER
        DCR     B               /UPDATE LOOP COUNTER
        JNZ     1$              /BACK FOR MORE
        MOV     M,A             /CLEAR LAST LOCATION
        STA     PGMST           /SIGNAL EMPTY PROGRAM AREA
        JMP     CMDPRS          /RETURN
/
/IDEL
/ROUTINE TO DELETE INSTRUCTION FROM PULSE PROGRAM
/INSTRUCTION LINE NUMBER IS IN LN.
/
IDEL    PUSH    B               /SAVE B,C
        PUSH    D               /SAVE D,E
        PUSH    H               /SAVE H,L
        LDA     LN              /GET LINE NUMBER INTO A
        MOV     L,A             /GET LINE NUMBER INTO H,L
        MVI     H,00
        LXI     D,TLINE         /GET START OF LINE TABLE
        DAD     D               /POINT TO LINE NUMBER
        MVI     A,0FF           /GET EMPTY FLAG
        MOV     M,A             /SIGNAL EMPTY
        POP     H               /GET H,L AGAIN
        POP     D               /GET D,E AGAIN
        POP     B               /GET B,C AGAIN
        RET                     /RETURN
/IADD
/ROUTINE TO ADD INSTRUCTION TO PULSE PROGRAM
/
IADD    PUSH    B               /SAVE B,C
        PUSH    D               /SAVE D,E
        PUSH    H               /SAVE H,L
        XRA     A               /CLEAR A
        STA     PGMST           /SIGNAL PROGRAM AREA NOT EMPTY
        LDA     LN              /GET LINE NUMBER
        MOV     L,A             /SAVE IN H,L
        MVI     H,00
        LXI     D,TLINE         /GET START OF LINE TABLE
        DAD     D               /POINT TO LINE NUMBER
        MOV     M,A             /SET INSTR INDEX
        CALL    INSERT          /INSERT NEW INSTRUCTION
        POP     H               /GET H,L AGAIN
        POP     D               /GET D,E AGAIN
        POP     B               /GET B,C AGAIN
        RET                     /RETURN
/
/
/
/INSERT
/ROUTINE TO INSERT INSTRUCTION INTO PULSE PROGRAM
/INSTRUCTION LINE IS IN LN
/
INSERT  PUSH    D               /SAVE D,E
        PUSH    H               /SAVE H,L
```

```
         LDA      LN                   /GET LINE NUMBER OF INSTR
         MOV      L,A                  /SAVE IN H,L
         MVI      H,00
         LXI      D,TLINE              /GET START OF LINE TABLE
         DAD      D                    /POINT TO INDEX
         MOV      L,M                  /GET INDEX
         MVI      H,00
         DAD      H                    /MPY BY 4  TO GIVE OFFSET
         DAD      H
         LXI      D,PGM                /GET START OF PROGRAM AREA
         DAD      D                    /POINT TO INSTRUCTION
         LDA      OPCODE               /GET OPCODE
         MOV      M,A                  /SAVE IN INST
         INX      H                    /UPDATE INSTR POINTER
         MVI      M,00                 /INSERT NULL BYTE
         LDA      OP1                  /GET FIRST OPERAND
         INX      H                    /UPDATE INSTR POINTER
         MOV      M,A                  /SAVE IN INST
         INX      H                    /UPDATE INSTRUCTION POINTER
         LDA      OP2                  /GET SECOND OPERAND
         MOV      M,A                  /SAVE IN INST
         POP      H                    /GET H,L AGAIN
         POP      D                    /GET D,E AGAIN
         RET                           /RETURN
/
/OPEVAL
/SUBROUTINE TO EVALUATE OPERAND
/
OPEVAL   CALL     HSW                  /EVALUATE OPERAND
         CPI      OFF                  /CHECK FOR ERROR
         JZ       3$                   /EXIT
         LDA      OPCODE               /GET OPERATION CODE
         ANA      A                    /CHECK FOR BRANCH OPCODE
         JZ       3$                   /EXIT
         CPI      OC                   /CHECK FOR PA OPCODE
         JZ       3$                   /EXIT
         MOV      A,B                  /GET HIGH ORDER REGISTER
         ORA      A                    /CHECK FOR OVERFLOW
         JNZ      2$                   /ERROR
1$       MOV      A,C                  /GET LOW ORDER REGISTER
         RAR                           /CHECK FOR VALID REGISTER
         JC       2$                   /INVALID REGISTER
         XRA      A                    /CLEAR A
         JMP      3$                   /EXIT
2$       LXI      H,4$                 /POINT TO ERROR MSG
         CALL     PSTR                 /OUTPUT STRING
         CALL     PLINE                /OUTPUT LINE
         MVI      A,OFF                /GET ERROR FLAG INTO A
3$       RET                           /RETURN
/MSG
4$       TXT      /(OPEVAL) INVALID REGISTER/
         DB       0
/
/EC FLAG
/ROUTINE TO TURN ECHO ON AND OFF
/IF FLAG IS NONZERO, ECHO IS TURNED ON
/IF FLAG IS ZERO, ECHO IS TURNED OFF
/
EC       MVI      A,02                 /GET TWO INTO A
         STA      ICHAR                /INIT CHARACTER INDEX
```

```
        CALL    GCHAR           /GET NEXT CHARACTER
        CPI     ' '             /CHECK FOR SPACE
        JZ      1$              /CONTINUE
        ANA     A               /CHECK FOR NULL
        JNZ     4$              /OUTPUT ERROR MSG
        XRA     A               /CLEAR A
        STA     ECHO            /SET ECHO TO OFF
        JMP     5$              /RETURN
1$      CALL    HSW             /EVALUATE FLAG
        CPI     OFF             /CHECK FOR ERROR
        JZ      5$              /EXIT
        MOV     A,B             /GET HIGH ORDER FLAG
        ORA     A               /CHECK FOR ZERO
        JZ      2$              /CONTINUE
        MVI     A,01            /GET ONE INTO A
        STA     ECHO            /SET ECHO TO ON
        JMP     5$              /EXIT
2$      MOV     A,C             /GET LOW ORDER FLAG
        ORA     A               /CHECK FOR ZERO
        JZ      3$              /ZERO
        MVI     A,01            /GET ONE INTO A
        STA     ECHO            /SET ECHO TO ON
        JMP     5$              /EXIT
3$      XRA     A               /CLEAR A
        STA     ECHO            /SET ECHO TO OFF
        JMP     5$              /EXIT
4$      LXI     H,6$            /POINT TO ERROR MSG
        CALL    PSTR            /OUTPUT STRING
        CALL    PLINE           /OUTPUT LINE
5$      JMP     CMDPRS          /RETURN
/MSG
6$      TXT     /(EC     ) INPUT FORMAT ERROR/
        DB      0
/
/DSPTCH
/SUBROUTINE TO COMPARE RECYCLE STATUS AND
/PP START STATUS. CONTROL IS DISPATCHED AS
/FOLLOWS:
/IF PPSST=0, CONTROL IS SENT TO CMDPRS
/IF PPSST=1 AND RECYCLE=1, CONTROL IS SENT TO PP
/IF PPSST=1 AND RECYCLE=0, CONTROL IS SENT TO CMDPRS
/
DSPTCH  IN      PPS             /CHECK START STATUS
        ANI     SMPP            /CHECK FOR START CONDITION
        JZ      3$              /PP STOPPED. EXIT TO CMDPRS
1$      LDA     RCYCLE          /GET RECYCLE STATUS
        ANA     A               /CHECK FOR NO RECYCLE
        JZ      3$              /NOT RECYCLING. EXIT TO CMDPRS
2$      XRA     A               /CLEAR A
        STA     RCYCLE          /TURN OFF RECYCLE
        MVI     A,OFF           /SIGNAL TO PP
3$      RET                     /RETURN
/
/RE
/CHECKS PP START STATUS
/IF PPSST=1, CONTROL DISPATCHED TO PP
/IF PPSST=0, CONTROL DISPATCHED TO CMDPRS
/
RE      IN      PPS             /GET START STATUS
        ANI     SMPP            /CHECK FOR START
        JNZ     PP              /DISPATCH TO PP
        MVI     A.01            /GET ONE INTO A
        STA     RCYCLE          /TURN ON RECYCLE
        JMP     CMDPRS          /DISPATCH TO CMDPRS
/
/LI LN1 LN2
/ROUTINE TO LIST SECTION OF PULSE PROGRAM
/LN1 IS LOWER LINE NUMBER
/LN2 IS UPPER LINE NUMBER
/
LI      MVI     A,02            /GET TWO INTO A
        STA     ICHAR           /INIT CHAR INDEX
        CALL    GCHAR           /GET CHARACTER
        CPI     ' '             /CHECK FOR ERROR
        JZ      1$              /YES
        LXI     H,9$            /POINT TO MSG
        CALL    PSTR            /OUTPUT STRING
        CALL    PLINE           /OUTPUT LINE
        JMP     8$              /EXIT
1$      CALL    HSW             /EVALUATE FIRST OPERAND
        CPI     OFF             /CHECK FOR ERROR
        JZ      8$              /EXIT
        MOV     E.C             /SAVE FIRST OPERAND IN D,E
        MOV     D,B
        MVI     A,05            /GET 5 INTO A
        STA     ICHAR           /SAVE AT ICHAR
        CALL    GCHAR           /GET NEXT CHAR
        CPI     ' '             /CHECK FOR SP
        JNZ     LI+5            /YES
        CALL    HSW             /EVALUATE SECOND OPERAND
        CPI     OFF             /CHECK FOR ERROR
        JZ      8$              /YES. EXIT
        MOV     A,C             /SWAP OPERANDS
        MOV     C,E
        MOV     E.A
        MOV     A,B             /GET HIGH ORDER OPERAND
        ORA     A               /CHECK FOR OVERFLOW
        JNZ     2$              /ERROR
        MOV     A,D             /GET HIGH ORDER OPERAND
        ORA     A               /CHECK FOR OVERFLOW
        JZ      3$              /NO
2$      LXI     H,10$           /POINT TO MSG
        CALL    PSTR            /OUTPUT STRING
        CALL    PLINE           /OUTPUT LINE
        JMP     8$              /ERROR EXIT
3$      MOV     A,C             /GET FIRST OPERAND
        CMP     E               /CHECK FOR .LE. SECOND OPERAND
        JC      4$              /YES
        JZ      4$              /YES
        LXI     H.11$           /POINT TO MSG
        CALL    PSTR            /OUTPUT STRING
        CALL    PLINE           /OUTPUT LINE
        JMP     8$              /ERROR EXIT
4$      LXI     H,TLINE         /GET START OF LINE TABLE
        DAD     B               /POINT TO FIRST INSTR INDEX
5$      MOV     A.M             /GET NEXT INDEX
        CPI     OFF             /CHECK FOR EMPTY
        JZ      7$              /YES
        PUSH    B               /SAVE LOWER LIMIT
        PUSH    D               /SAVE UPPER LIMIT
```

```
          PUSH    H                   /SAVE LINE TABLE POINTER
          MOV     L,A                 /MOVE INSTR INDEX TO H,L
          MVI     H,00
          DAD     H                   /MPY BY 4 TO GIVE OFFSET
          DAD     H
          LXI     D,PGM               /GET BEGINNING OF PROGRAM AREA
          DAD     D                   /POINT TO INSTRUCTION
          CALL    BHS                 /CONVERT LINE NUMBER AND OUTPUT
          MVI     A,' '               /GET SPACE CHARACTER
          CALL    PCHAR               /OUTPUT
          MOV     A,M                 /GET OPCODE INDEX
          PUSH    H                   /SAVE INSTR POINTER
          MOV     L,A                 /MOVE OPCODE INDEX TO H,L
          MVI     H,00
          DAD     H                   /MPY BY 2 TO GIVE OFFSET
          LXI     D,TOPS11            /GET START OF OPPCODE STRING TABLE
          DAD     D                   /POINT TO OPCODE STRING
          MVI     B,02                /INIT LOOP COUNTER
6$        MOV     A,M                 /GET NEXT CHAR OF OPCODE STRING
          CALL    PCHAR               /OUTPUT STRING
          INX     H                   /UPDATE OPCODE STRING POINTER
          DCR     B                   /UPDATE LOOP COUNTER
          JNZ     6$                  /BACK FOR MORE
          MVI     A,' '               /GET SPACE CHAR
          CALL    PCHAR               /OUTPUT SPACE
          POP     H                   /GET INSTR POINTER BACK
          INX     H                   /UPDATE INSTR POINTER
          INX     H                   /SKIP NULL BYTE
          MOV     A,M                 /GET OP1
          MOV     C,A                 /MOVE OP1 TO B,C
          MVI     B,00
          CALL    BHS                 /CONVERT OP1 AND OUTPUT
          MVI     A,' '               /GET SPACE CHAR
          CALL    PCHAR               /OUTPUT SPACE
          INX     H                   /UPDATE INSTR POINTER
          MOV     A,M                 /GET OP2
          MOV     C,A                 /MOVE OP2 TO B,C
          MVI     B,00
          CALL    BHS                 /CONVERT OP2 AND  OUTPUT
          CALL    PLINE               /OUTPUT LINE
          POP     H                   /GET H,L AGAIN
          POP     D                   /GET D,E AGAIN
          POP     B                   /GET B,C AGAIN
7$        INX     H                   /UPDATE TABLE POINTER
          INR     C                   /UPDATE LOWER LIMIT
          JZ      8$                  /END OF TABLE. DONE
          MOV     A,C                 /GET LOWER LIMIT
          CMP     E                   /CHECK FOR .LE. UPPER LIMIT
          JC      5$                  /YES, BACK FOR MORE
          JZ      5$                  /YES. BACK FOR MORE
8$        JMP     CMDPRS              /RETURN  TO COMMAND PROCESSOR
/MSG
9$        TXT     /(LI   ). INPUT FORMAT ERROR/
          DB      0
10$       TXT     /(LI   ) INVALID LINE NUMBER/
          DB      0
11$       TXT     /(LI   ) LOW LIMIT .GT. HIGH LIMIT/
          DB      0
/
/BHS
```

```
/CONVERTS BYTE TO HEX STRING AND OUTPUTS
/C CONTAINS BYTE
/ALL REGISTERS EXCEPT A PRESERVED
BHS     MOV     A,C             /GET BYTE
        ANI     0F0             /MASK HIGH ORDER NIBBLE
        RRC                     /POSITION NIBBLE TO LS BITS
        RRC
        RRC
        RRC
        CPI     0A              /CHECK FOR .GE. 10
        JNC     1$              /YES
        ADI     '0'             /CONVERT
        JMP     2$              /
1$      SUI     0A              /SUBTRACT 10
        ADI     'A'             /CONVERT NIBBLE TO CHAR
2$      CALL    PCHAR           /OUTPUT CHAR
        MOV     A,C             /GET BYTE AGAIN
        ANI     0F              /MASK LOWER ORDER BIT
        CPI     0A              /CHECK FOR .GE. 10
        JNC     3$              /YES
        ADI     '0'             /CONVERT NIBBLE TO CHAR
        JMP     4$
3$      SUI     0A              /SUBTRACT 10
        ADI     'A'             /CONVERT NIBBLE TO CHAR
4$      CALL    PCHAR           /OUTPUT CHAR
        RET                     /RETURN
/
/VA REG
/ROUTINE TO OUTPUT CONTENTS OF REGISTER
/REG IS THE NAME OF THE REGISTER TO BE OUTPUT
/
VA      MVI     A,02            /GET 2 INTO A
        STA     ICHAR           /INIT CHAR INDEX
        CALL    GCHAR           /GET CHAR
        CPI     ' '             /CHECK FOR SPACE
        JZ      1$              /YES
        LXI     H,5$            /POINT TO MESSAGE
        CALL    PSTR            /OUTPUT STRING
        CALL    PLINE           /OUTPUT LINE
        JMP     4$              /EXIT
1$      CALL    HSW             /EVALUATE OPERAND
        CPI     0FF             /CHECK FOR ERROR
        JZ      4$              /NO
        MOV     A,B             /GET MS BYTE INTO A
        ORA     A               /CHECK FOR OVERFLOW
        JZ      2$              /NO
        LXI     H,6$            /YES. POINT TO MSG
        CALL    PSTR            /OUTPUT STRING
        CALL    PLINE           /OUTPUT LINE
        JMP     4$              /EXIT
2$      MOV     A.C             /GET OPERAND INTO A
        RAR                     /CHECK IF VALID REGISTER
        JNC     3$              /YES
        LXI     H.6$            /NO. POINT TO MSG
        CALL    PSTR            /OUTPUT STRING
        CALL    PLINE           /OUTPUT LINE
        JMP     4$              /EXIT
3$      LXI     H.REGS          /GET START OF REGISTER AREA
        DAD     B               /POINT TO REGISTER
        MOV     C,M             /GET LOW ORDER REGISTER
        INX     H                       /UPDATE REG POINTER
        MOV     B.M                     /GET HIGH ORDER REG
        CALL    WHS                     /CONVERT NUMBER AND OUTPUT
        MVI     A,20                    /GET SP CHAR INTO A
        CALL    PCHAR                   /OUTPUT CHAR
        MVI     A,2B                    /GET '+' CHAR
        CALL    PCHAR                   /OUTPUT CHAR
        CALL    WDS                     /CONVERT TO DECIMAL AND OUTPUT
        MVI     A,20                    /GET SP CHAAR AGAIN
        CALL    PCHAR                   /OUTPUT CHAR
        MVI     A.2D                    /GET '-' CHAR
        CALL    PCHAR                   /OUTPUT CHAR
        CALL    TCOMP                   /NEGATE
        CALL    WDS                     /CONVERT TO DECIMAL AND OUTPUT
        CALL    PLINE                   /OUTPUT LINE
4$      JMP     CMDPRS                  /RETURN TO COMMAND PROCESSOR
/MSG
5$      TXT     /(VA    ) INPUT FORMAT ERROR/
        DB      0
6$      TXT     /(VA    ) INVALID REGISTER/
        DB      0
/
/WHS
/CONVERTS WORD TO HEX STRING AND OUTPUTS
/B.C CONTAINS WORD
/ALL REGISTERS EXCEPT A PRESERVED
/
WHS     MOV     A,B                     /SWITCH B AND C
        MOV     B,C
        MOV     C,A
        CALL    BHS                     /CONVERT AND OUTPUT HIGH ORDER HALF
        MOV     A,B                     /SWITCH B AND C AGAIN
        MOV     B.C
        MOV     C,A
        CALL    BHS                     /CONVERT AND OUTPUT LOW ORDER HALF
        RET                             /RETURN
/
/LD REG VAL
/ROUTINE TO LOAD A REGISTER WITH A VALUE
/REG IS THE NAME OF THE REGISTER TO BE LOADED
/VAL IS THE VALUE TO BE LOADED
/
LD      MVI     A.02                    /GET 2 INTO A
        STA     ICHAR                   /INIT CHAR INDEX
        CALL    GCHAR                   /GET CHARACTER
        CPI     ' '                     /CHECK FOR SPACE
        JZ      1$                      /YES
        LXI     H.6$                    /POINT TO MSG
        CALL    PSTR                    /OUTPUT STRING
        CALL    PLINE                   /OUTPUT  LINE
        JMP     5$                      /EXIT
1$      CALL    HSW                     /EVALUATE REG OPERAND
        CPI     OFF                     /CHECK FOR ERROR
        JZ      5$                      /YES, EXIT
        MOV     A.B                     /GET HIGH ORDER OPERAND INTO A
        ORA     A                       /CHECK FOR OVERFLOW
        JZ      2$                      /NO
        LXI     H.7$                    /POINT TO MSG
        CALL    PSTR                    /OUTPUT STRING
        CALL    PLINE                   /OUTPUT LINE
        JMP     5$              /EXIT
2$      MOV     A,C             /GET LOW ORDER OPERAND INTO A
        RAR                     /CHECK IF VALID REGISTER
        JNC     3$              /YES
        LXI     H,7$            /POINT TO MSG
        CALL    PSTR            /OUTPUT STRING
        CALL    PLINE           /OUTPUT LINE
        JMP     5$              /EXIT
3$      LXI     H,REGS          /GET START OF REGISTER AREA
        DAD     B               /POINT TO REGISTER
        MVI     A,05            /GET 5 INTO A
        STA     ICHAR           /SAVE AT ICHAR
        CALL    GCHAR           /GET CHAR
        CPI     ' '             /CHECK FOR SPACE
        JZ      4$              /YES
        LXI     H,6$            /POINT TO MSG
        CALL    PSTR            /OUTPUT STRING
        CALL    PLINE           /OUTPUT LINE
        JMP     5$              /EXIT
4$      CALL    HSW             /EVALUATE VALUE
        CPI     OFF             /CHECK FOR ERROR
        JZ      5$              /EXIT
        MOV     M,C             /LOAD LOW ORDER REGISTER
        INX     H               /UPDATE REGISTER POINTER
        MOV     M,B             /LOAD HIGH ORDER REGISTER
5$      JMP     CMDPRS          /RETURN TO COMMAND PROCESSOR
/MSG
6$      TXT     /(LO   ) INPUT FORMAT ERROR/
        DB      0
7$      TXT     /(LO   ) INVALID REGISTER/
        DB      0
/
/GO LN
/STARTS PULSE PROGRAM EXECUTION AT A SPECIFIED LINE
/LN IS THE NUMBER OF THE SPECIFIED LINE
/
GO      LXI     H,12$           /POINT TO MESSAGE
        IN      PPS             /GET START STATUS
        ANI     SMPP            /CHECK FOR START STATUS
        JZ      6$              /OUTPUT MESSAGE
        LDA     PGMST           /GET PROGRAM AREA STATUS
        CPI     OFF             /CHECK FOR ZERO
        JNZ     1$              /NO
        LXI     H,8$            /POINT TO MSG
        JMP     6$              /ERROR EXIT
1$      MVI     A,02            /GET 2 INTO A
        STA     ICHAR           /INIT CHAR INDEX
        CALL    GCHAR           /GET CHAR
        CPI     ' '             /CHECK FOR SPACE
        JZ      2$              /YES
        LXI     H,9$            /POINT TO MSG
        JMP     6$              /ERROR EXIT
2$      CALL    HSW             /EVALUATE LINE NUMBER
        CPI     OFF             /CHECK FOR  ERROR
        JZ      7$              /YES, EXIT
        MOV     A,B             /CHECK FOR OVERFLOW
        ORA     A
        JZ      3$              /NO
        LXI     H,10$           /POINT TO MSG
        JMP     6$              /ERROR EXIT
```

```
3$      MOV     L,C             /GET LINE NUMBER INTO H,L
        MVI     H,00
        LXI     D,TLINE         /GET START OF LINE TABLE
        DAD     D               /POINT TO INDEX
4$      MOV     A,M             /GET LINE INDEX
        CPI     OFF             /CHECK FOR EMPTY
        JNZ     5$              /NO
        LXI     H,11$           /POINT TO MSG
        JMP     6$              /ERROR EXIT
5$      STA     LC              /SAVE INDEX AT LC
        JMP     PP              /START PULSE PROGRAMMER
6$      CALL    PSTR            /OUTPUT STRING
        CALL    PLINE           /OUTPUT LINE
7$      JMP     CMDPRS          /RETURN TO COMMAND PROCESSOR
/MSG
8$      TXT     /(GO    ) PROGRAM AREA EMPTY/
        DB      0
9$      TXT     /(GO    ) INPUT FORMAT ERROR/
        DB      0
10$     TXT     /(GO    ) INVALID LINE NUMBER/
        DB      0
11$     TXT     /(GO    ) LINE NUMBER OUT OF PROGRAM BOUNDS/
        DB      0
12$     TXT     /(GO    ) START PULSE PROGRAMMER/
        DB      0
/
/PP
/OBTAINS INSTRUCTIONS AND OPERANDS FROM PROGRAM
/CALLS HANDLER
/
PP      LDA     LC              /GET LOCATION COUNTER
        CPI     OFF             /CHECK FOR LAST INSTRUCTION
        JZ      3$              /EXIT
        MOV     B,A             /INIT LOOP COUNTER
        MOV     L,A             /SAVE LOCATION COUNTER IN H,L
        MVI     H,00
        LXI     D,TLINE         /GET START OF LINE TABLE
        DAD     D               /POINT TO NEXT LINE
1$      MOV     A,M             /CHECK INDEX FOR EMPTY
        CPI     OFF
        JNZ     2$              /NO. CONTINUE.
        INX     H               /UPDATE LINE POINTER
        INR     B               /UPDATE LOOP COUNTER
        MVI     A,OFF           /GET OFF INTO A
        CMP     B               /CHECK FOR LAST LINE
        JZ      3$              /EXIT
        JMP     1$              /TRY AGAIN
2$      STA     LC              /SAVE LOCATION COUNTER
        MOV     L,A             /SAVE INDEX IN H,L
        MVI     H,00
        DAD     H               /MPY BY 4 TO GIVE OFFSET
        DAD     H
        LXI     D,PGM           /GET START OF PROGRAM AREA
        DAD     D               /POINT TO INSTR ADDRESS
        MOV     A,M             /GET OPCODE
        STA     OPCODE          /SAVE OPCODE
        INX     H               /UPDATE POINTER AND SKIP NULL BYTE
        INX     H
        MOV     C,M             /GET FIRST OPERAND INTO B,C
        MVI     B,00
```

```
          INX       H                       /UPDATE POINTER
          MOV       E.M                     /GET SECOND OPERAND INTO D,E
          MVI       D.00
          LDA       LC                      /GET LOCATION COUNTER
          INR       A                       /UPDATE LOCATION COUNTER
          STA       LC                      /SAVE LOCATION COUNTER
          LDA       OPCODE                  /GET OPCODE AGAIN
          JMP       TJMP11                  /CALL HANDLER
3$        JMP       CMDPRS                  /RETURN
/
/HA
/HALTS PULSE PROGRAMMER. RETURNS CONTROL TO COMMAND PROCESSOR
/
HA        MVI       A,0FF                   /GET NUMBER OF INSTRUCTIONS
          STA       LC                      /SAVE AT LC
          JMP       PP                      /RETURN
/
/R1
/INITIALIZES ADDRESS COUNTER OF RAM 1
/
R1        MVI       H,SRAM1                 /GET START ADDRESS INTO H,L
          MVI       L,00
          SHLD      RAC1                    /SAVE START ADDRESS
          JMP       PP                      /RETURN
/
/R2
/INITIALIZES ADDRESS COUNTER OF RAM 2
/
R2        MVI       H,SRAM2                 /GET START ADDRESS INTO H,L
          MVI       L,00
          SHLD      RAC2                    /SAVE START ADDRESS
          JMP       PP                      /RETURN
/
/R3
/INITIALIZES ADDRESS COUNTER OF RAM 3
/
R3        MVI       H,SRAM3                 /GET START ADDRESS INTO H,L
          MVI       L,00
          SHLD      RAC3                    /SAVE START ADDRESS
          JMP       PP                      /RETURN
/
/SE REG1 REG2
/REGISTER 1 IS SET TO THE VALUE STORED AT
/REGISTER 2
/
SE        LXI       H.REGS                  /GET START OF REGISTER AREA
          DAD       D                       /POINT TO REG2
          MOV       E.M                     /GET LOW ORDER REG2
          INX       H                       /UPDATE REG2 POINTER
          MOV       D.M                     /GET HIGH ORDER REG2
          LXI       H.REGS                  /GET START OF REGISTER AREA
          DAD       B                       /POINT TO REG1
          MOV       M,E                     /SAVE LOW ORDER RESULT
          INX       H                       /UPDATE REG1 POINTER
          MOV       M.D                     /SAVE HIGH ORDER RESULT
          JMP       PP                      /RETURN
/
/IN REG1 REG2
/CONTENTS OF REG1 INCREMENTED BY CONTENTS OF REG2.
/RESULT LEFT IN REG1.
```

```
/
IN      LXI     H,REGS          /GET START OF REGISTER AREA
        DAD     D               /POINT TO REG2
        MOV     E,M             /GET LOW ORDER REG2
        INX     H               /UPDATE REG2 POINTER
        MOV     D,M             /GET HIGH ORDER REG2
        LXI     H,REGS          /GET START OF REGISTER AREA
        DAD     B               /POINT TO REG1
        MOV     A,M             /GET LOW ORDER REG1
        ADD     E               /ADD LOW ORDER REG2
        MOV     M.A             /SAVE LOW ORDER RESULT
        INX     H               /UPDATE REG1 POINTER
        MOV     A.M             /GET HIGH ORDER REG1
        ADC     D               /ADD HIGH ORDER REG2
        MOV     M,A             /SAVE HIGH ORDER RESULT
        JMP     PP              /RETURN
/
/DE REG1 REG2
/DECREMENT CONTENTS OF REGISTER 1 BY THE CONTENTS
/OF REGISTER 2. RESULTS STORED IN REGISTER 1.
/
DE      LXI     H,REGS          /GET START OF REGISTER AREA
        DAD     D               /POINT TO REG2
        MOV     E,M             /GET LOW ORDER REGISTER 2
        INX     H               /UPDATE REG2
        MOV     D,M             /GET HIGH ORDER REG2
        LXI     H,REGS          /GET START OF REG AREA
        DAD     B               /POINT TO REG1
        MOV     A,M             /GET LOW ORDER REG1
        SUB     E               /SUBTRACT LOW ORDER REG2
        MOV     M,A             /SAVE LOW ORDER RESULT
        INX     H               /UPDATE REG1 POINTER
        MOV     A,M             /GET HIGH ORDER REG1
        SBB     D               /SUBTRACT HIGH ORDER REG2
        MOV     M.A             /SAVE HIGH ORDER RESULT
        JMP     PP              /RETURN
/
/SB REG1 REG2
/DECREMENT CONTENTS OF REGISTER 1. IF RESULT IS NONZERO
/BRANCH TO SPECIFIED LINE NUMBER.
/LN IS STORED IN REGISTER 2.
/
SB      LXI     H.REGS          /GET START OF REGISTER AREA
        DAD     D               /POINT TO REG2
        MOV     E.M             /GET LINE NUMBER
        LXI     H,REGS          /GET START OF REGISTER AREA
        DAD     B               /POINT TO REG1
        MOV     C.M             /GET LOW ORDER REG1
        INX     H               /UPDATE REGISTER POINTER
        MOV     B,M             /GET HIGH ORDER REG1
        DCX     B               /DECREMENT B,C
        MOV     M,B             /SAVE HIGH ORDER REG1
        DCX     H               /UPDATE REGISTER POINTER
        MOV     M,C             /SAVE LOW ORDER REG1
        MOV     A.C             /CHECK FOR ZERO
        ORA     B
        JZ      2$              /YES. DONE
        LXI     H,TLINE         /GET START OF LINE TABLE
        DAD     D               /POINT TO INSTR INDEX
        MOV     A.M             /GET INSTR INDEX
```

```
          CPI       OFF                 /CHECK FOR EMPTY
          JZ        1$                  /ERROR
          STA       LC                  /SET LOCATION COUNTER
          JMP       2$                  /DONE
1$        CALL      ELINE               /OUTPUT LINE NUMBER
          LXI       H,3$                /POINT TO MSG
          CALL      PSTR                /OUTPUT STRING
          CALL      PLINE               /OUTPUT LINE
          JMP       HA                  /HALT PULSE PROGRAMMER
2$        JMP       PP                  /RETURN
/MSG
3$        TXT       /(SB    ) UNLINKED BRANCH/
          DB        0
/
/
/CO REG1 REG2
/COMPARES CONTENTS OF REG1 WITH CONTENTS
/OF REG2. SETS COMPARISON CODE.
/
CO        LXI       H,REGS              /GET START OF REGISTER AREA
          DAD       D                   /POINT TO REG2
          MOV       E,M                 /POINT TO LOW ORDER REG2
          INX       H                   /UPDATE REG2 POINTER
          MOV       D,M                 /GET HIGH ORDER REG2
          LXI       H.REGS              /GET START OF REGISTER AREA
          DAD       B                   /POINT TO REG1
          MOV       A,M                 /GET LOW ORDER REG1
          SUB       E                   /SUBTRACT LOW ORDER REG2
          MOV       C,A                 /SAVE LOW ORDER RESULT
          INX       H                   /UPDATE REG1 POINTER
          MOV       A,M                 /GET HIGH ORDER REG1
          SBB       D                   /SUBTRACT HIGH ORDER REG2
          MOV       B.A                 /SAVE HIGH ORDER RESULT
          ORA       C                   /CHECK FOR ZERO
          JNZ       1$                  /NOM
          MVI       A.01                /C(REG1) .EQ. C(REG2)
          STA       COMP                /SAVE CODE
          JMP       3$                  /DONE
1$        MOV       A.B                 /CHECK FOR NEGATIVE RESULT
          ORA       A
          JP        2$                  /NO
          MVI       A,02                /C(REG1) .LT. C(REG2)
          STA       COMP                /SAVE CODE
          JMP       3$                  /DONE
2$        MVI       A.04                /C(REG1) .GT. C(REG2)
          STA       COMP                /SAVE CODE
3$        JMP       PP                  /RETURN
/
/BR LN CODE
/BRANCH TO SPECIFIED LINE NUMBER IF
/(CODE.AND.COMP) .NE. 0
/
BR        LDA       COMP                /GET COMPARISON CODE
          ANA       E                   /.AND. CODE
          JZ        2$                  /NO BRANCH. DONE
          LXI       H,TLINE             /GET START OF LINE TABLE
          DAD       B                   /POINT TO INSTR INDEX
          MOV       A.M                 /GET INDEX
          CPI       OFF                 /CHECK FOR EMPTY
          JZ        1$                  /ERROR
```

```
        STA     LC              /SET LOCATION COUNTER
        JMP     2$              /DONE
1$      CALL    ELINE           /OUTPUT LINE NUMBER
        LXI     H,3$            /POINT TO MESSAGE
        CALL    PSTR            /OUTPUT STRING
        CALL    PLINE           /OUTPUT LINE
        JMP     HA              /HALT PULSE PROGRAMMER
2$      JMP     PP              /RETURN
/MSG
3$      TXT     /(BR    ) UNLINKED BRANCH/
        DB      0
/
/PA NIS
/PULSE PROGRAM SOURCE SET TO NIS
/00=FIFO, 01=RAM 1, 02=RAM 2, 03=RAM 3
/
PA      MOV     A,C             /GET NEXT INSTRUCTION SOURCE
        RRC                     /GET SOURCE BITS INTO MSB POSITIONS
        RRC
        ANI     0C0             /MASK OUT OTHER BITS
        STA     SOURCE          /SAVE SOURCE BITS
        JMP     PP              /RETURN
/
/0F REG1 REG2
/OUTPUT TIME,GATE TO FIFO
/2-COMPLEMENT OF TIME IS STORED AT REG1
/PULSE MASK IS STORED AT REG2
/
0F
        CALL    FETCH           /GET REG CONTENTS INTO B,C AND D,E
        MOV     A.B             /CHECK FOR ZERO
        ORA     C
        JZ      2$              /EXIT
        MVI     L.80            /GET FIFO ADDRESS INTO H,L
        MVI     H,0FF
1$      IN      PPS             /CHECK PP STATUS
        ANI     RMPP            /CHECK FOR READY
        JZ      1$              /NOT READY
        CALL    WPP             /OUTPUT CONTROL WORD TO FIFO
2$      JMP     PP              /RETURN
/
/01 REG1 REG2
/OUTPUT TIME GATE TO RAM1
/2-COMPLEMENT OF TIME STORED AT REG1
/PULSE MASK STORED AT REG2
/
01      CALL    FETCH           /GET REG CONTENTS INTO B,C D,E
        LHLD    RAC1            /GET RAM ADDRESS
        MVI     A,0F4           /GET HIGH ORDER MEMORY LIMIT
        CMP     H               /CHECK FOR OVERFLOW
        JZ      1$              /YES
        CALL    WPP             /WRITE TO RAM1
        LHLD    RAC1            /GET RAM ADDRESS AGAIN
        INX     H               /UPDATE RAM ADDRESS
        INX     H
        INX     H
        INX     H
        SHLD    RAC1            /STORE RAM ADDRESS
        JMP     2$              /DONE
1$      CALL    ELINE           /OUTPUT LINE NUMBER
```

```
        LXI     H,3$            /POINT TO MSG
        CALL    PSTR            /OUTPUT STRING
        CALL    PLINE           /OUTPUT LINE
        JMP     HA              /HALT PULSE PROGRAM
2$      JMP     PP              /RETURN
/MSG
3$      TXT     /(01    ) RAM ADDRESS OVERFLOW/
        DB      0
/
/02 REG1 REG2
/OUTPUT TIME,GATE TO RAM 2
/2-COMPLEMENT OF TIME STORED AT REG1
/GATE MASK STORED AT REG2
/
02      CALL    FETCH           /GET REG CONTENTS INTO B,C AND D,E
        LHLD    RAC2            /GET RAM ADDRESS
        MVI     A,0F8           /GET HIGH ORDER MEMORY LIMIT
        CMP     H               /CHECK FOR OVERFLOW
        JZ      1$              /YES
        CALL    WPP             /WRITE TO RAM 2
        LHLD    RAC2            /GET RAM ADDRESS AGAIN
        INX     H               /UPDATE RAM ADDRESS
        INX     H
        INX     H
        INX     H
        SHLD    RAC2            /STORE RAM ADDRESS
        JMP     2$              /DONE
1$      CALL    ELINE           /OUTPUT LINE NUMBER
        LXI     H,3$            /POINT TO MSG
        CALL    PSTR            /OUTPUT STRING
        CALL    PLINE           /OUTPUT LINE
        JMP     HA              /HALT PULSE PROGRAMMER
2$      JMP     PP              /RETURN
/MSG
3$      TXT     /(02    ) RAM ADDRESS OVERFLOW/
        DB      0
/
/03 REG1 REG2
/OUTPUT TIME.GATE TO RAM 3
/2-COMPLEMENT OF TIME IS STORED AT REG1
/PULSE MASK IS STORED AT REG2
/
03      CALL    FETCH           /GET REG CONTENTS INTO B,C AND D,E
        LHLD    RAC3            /GET RAM ADDRESS
        MVI     A,0FC           /GET HIGH ORDER MEMORY
        CMP     H               /CHECK FOR OVERFLOW
        JZ      1$              /YES
        CALL    WPP             /WRITE TO RAM 3
        LHLD    RAC3            /GET RAM ADDRESS AGAIN
        INX     H               /UPDATE RAM ADDRESS
        INX     H
        INX     H
        INX     H
        SHLD    RAC3            /STORE RAM ADDRESS
        JMP     2$              /DONE
1$      CALL    ELINE           /OUTPUT LINE NUMBER
        LXI     H.3$            /POINT TO MSG
        CALL    PSTR            /OUTPUT STRING
        CALL    PLINE           /OUTPUT LINE
        JMP     HA              /HALT PULSE PROGRAMMER
```

```
2$      JMP     PP              /RETURN
/MSG
3$      TXT     /(03    ) RAM ADDRESS OVERFLOW/
        DB      0
/
/WPP
/WRITES TIME, GATE SETTINGS TO PP MEMORY
/H,L CONTAINS PP ADDRESS
/B.C CONTAINS 2-COMPLEMENT OF TIME
/D.E CONTAINS PULSE MASK
/
WPP     MOV     M,C             /WRITE LOW ORDER TIME
        INX     H               /UPDATE PP ADDRESS
        MOV     A,B             /GET HIGH ORDER TIME
        ANI     3F              /MASK OUT SOURCE BITS
        MOV     B,A             /TEMP SAVE
        LDA     SOURCE          /GET SOURCE CODE
        ORA     B               /ADD IN HIGH ORDER TIME
        MOV     M,A             /WRITE HIGH ORDER TIME
        INX     H               /UPDATE PP ADDRESS
        MOV     M,E             /WRITE LOW ORDER GATE
        INX     H               /UPDATE PP ADDRESS
        MOV     M,D             /WRITE HIGH ORDER GATE
        RET                     /RETURN
/
/
/MS REG1 REG2
/OUTPUTS A TIME IN UNITS OF 1 MSEC TO THE FIFO
/REG1 CONTAINS THE TIME IN UNITS OF 1 MSEC
/REG2 CONTAINS THE PULSE MASK
/
MS      CALL    FETCH           /GET REG CONTENTS INTO B,C AND D,E
        MOV     A,C             /GET NUMBER OF 1 MSEC UNITS
        ORA     B               /CHECK FOR ZERO
        JZ      3$              /YES. EXIT
1$      PUSH    B               /TEMP STORAGE
        MVI     B,OD8           /GET 1 MSEC
        MVI     C,OF0
        MVI     H,OFF           /GET FIFO ADDRESS
        MVI     L,80
2$      IN      PPS             /GET PP STATUS
        ANI     RMPP            /CHECK FOR READY
        JZ      2$              /TRY AGAIN
        CALL    WPP             /OUTPUT TIME.GATE TO FIFO
        POP     B               /GET COUNTER AGAIN
        DCX     B               /UPDATE COUNTER AGAIN
        MOV     A,C             /GET REG C INTO A
        ORA     B               /CHECK FOR ZERO
        JNZ     1$              /BACK FOR MORE
3$      JMP     PP              /RETURN
/
/FETCH
/OBTAINS REGISTERS FROM INDICES IN B,C AND D,E
/ERROR CODE RETURNED IN A
/
FETCH   LXI     H,REGS          /GET START OF REGISTER AREA
        DAD     D               /POINT TO REG2
        MOV     E,M             /GET LOW ORDER REG2
        INX     H               /UPDATE REG2
        MOV     D.M             /GET HIGH ORDER REG2
        LXI     H.REGS          /GET START OF REGISTER AREA AGAIN
        DAD     B               /POINT TO REG1
        MOV     C,M             /GET LOW ORDER REG1
        INX     H               /UPDATE REG1
        MOV     B.M             /GET HIGH ORDER REG1
        RET                     /RETURN
/
/SC REG1 REG2
/OUTPUT A TIME IN UNITS OF 1 SECOND TO THE FIFO
/REG1 CONTAINS TIME IN SECONDS. 255 SECONDS MAXIMUM.
/REG2 CONTAINS PULSE MASK
/
SC      CALL    FETCH           /GET TIME,GATE MASKS
        MOV     A,C             /CHECK FOR ZERO
        ORA     B
        JZ      5$              /YES. DONE
        MOV     A.B             /CHECK FOR OVERFLOW
        ORA     B
        JZ      1$              /NO
        CALL    ELINE           /OUTPUT LINE NUMBER
        LXI     H.6$            /POINT TO MSG
        CALL    PSTR            /OUTPUT STRING
        CALL    PLINE           /OUTPUT LINE
        JMP     HA              /HALT PULSE PROGRAMMER
1$      MOV     A.C             /GET NUMBER OF SECONDS
2$      STA     NSEC            /SAVE NUMBER OF SECONDS
        LXI     B.03E8          /GET 1000 INTO B.C
3$      PUSH    B               /SAVE B.C
        MVI     B.0D8           /GET 1 MSEC
        MVI     C,0F0
        MVI     H,0FF           /GET FIFO ADDRESS
        MVI     L,80
4$      IN      PPS             /GET PP STATUS
        ANI     RMPP            /CHECK FOR READY
        JZ      4$              /TRY AGAIN
        CALL    WPP             /OUTPUT TO FIFO
        POP     B               /GET B,C AGAIN
        DCX     B               /UPDATE COUNTER
        MOV     A.C             /GET C INTO A
        ORA     B               /CHECK FOR ZERO
        JNZ     3$              /BACK FOR MORE
        LDA     NSEC            /GET NUMBER OF SECONDS
        DCR     A               /UPDATE NUMBER OF SECONDS
        JNZ     2$              /BACK FOR MORE
5$      JMP     PP              /RETURN
/MSG
6$      TXT     /(SC     ) TIME .GT. 255 SECONDS/
        DB      0
/
/T1 REG1 REG2
/OUTPUT SAMPLING TRAIN TO RAM 1
/REG1 CONTAINS NUMBER OF SAMPLING PULSES
/REG2 CONTAINS PULSE MASK
/REG D2 CONTAINS SAMPLING PERIOD
/
T1      CALL    FETCH           /GET REGISTER CONTENTS
        MOV     A.B             /CHECK FOR OVERFLOW
        ORA     B
        JZ      1$              /NO
        CALL    ELINE           /OUTPUT LINE NUMBER
        LXI     H,6$            /POINT TO MSG
        JMP     4$              /OUTPUT ERROR
1$      MOV     A.C             /GET NUMBER OF PULSES
        ANA     A               /CHECK FOR ZERO
        JZ      5$              /EXIT
        STA     NSAMPL          /SAVE COUNT
        LXI     H.REGS          /GET START OF REGISTER AREA
        LXI     B.00D2          /GET D2 INTO B,C
        DAD     B               /POINT TO D2
        MOV     C.M             /GET LOW ORDER SAMPLING TIME
        INX     H               /UPDATE REGISTER POINTER
        MOV     B,M             /GET HIGH ORDER SAMPLING TIME
        MOV     A.C             /CHECK FOR ZERO
        ORA     B
        JZ      5$              /EXIT
2$      LHLD    RAC1            /GET RAM ADDRESS COUNTER
        MVI     A.0F4           /GET HIGH ORDER MEMORY LIMIT
        CMP     H               /CHECK FOR OVERFLOW
        JZ      3$              /YES. ERROR
        CALL    WPP             /WRITE TO RAM 1
        LHLD    RAC1            /GET RAM ADDRESS AGAIN
        INX     H               /UPDATE RAM ADDRESS
        INX     H
        INX     H
        INX     H
        SHLD    RAC1            /STORE NEW RAM ADDRESS
        LDA     NSAMPL          /GET NUMBER OF SAMPLE PULSES
        DCR     A               /UPDATE
        STA     NSAMPL          /SAVE COUNT
        JNZ     2$              /BACK FOR MORE
        JMP     5$              /DONE
3$      CALL    ELINE           /OUTPUT LINE NUMBER
        LXI     H.7$            /POINT TO MSG
4$      CALL    PSTR            /OUTPUT STRING
        CALL    PLINE           /OUTPUT LINE
        JMP     HA              /HALT PULSE PROGRAMMER
5$      JMP     PP              /RETURN
/MSG
6$      TXT     /(T1     ) NUMBER OF SAMPLE PULSES .GT. 255/
        DB      0
7$      TXT     /(T1     ) RAM ADDRESS OVERFLOW/
        DB      0
/
/OD REG1 REG2
/OUTPUT DELAY TO THE FIFO. LENGTH OF DELAY
/IS C(FE)*C(REG1) IN UNITS OF 100 NSEC.
/REG1 CONTAINS UNIT TIME WHICH MAY NOT EXCEED 819.2 USEC.
/FE CONTAINS THE NUMBER OF UNITS TO BE OUTPUT.
/REG2 CONTAINS THE PULSE MASK.
/
OD      CALL    FETCH           /GET TIME,GATE MASKS
        MOV     L,E             /GET PULSE MASK INTO H,L
        MOV     H,D
        SHLD    MASK            /SAVE MASK
        MOV     A,B             /CHECK FOR ZERO
        ORA     C
        JZ      6$              /EXIT
        MVI     A.00            /CHECK FOR .LT. 8192
        SUB     C               /SUBTRACT LS BYTE
        MVI     A,20            /GET 20 INTO A
        SBB     B               /SUBTRACT MS BYTE
        JNC     1$              /NONZERO.
        LXI     H,7$            /POINT TO MSG
        CALL    ELINE           /OUTPUT LINE NUMBER
        CALL    PSTR            /OUTPUT STRING
        CALL    PLINE           /OUTPUT LINE
        JMP     HA              /HALT PULSE PROGRAMMER
1$      MOV     L.C             /GET UNIT TIME INTO H,L
        MOV     H,B
        SHLD    TIME            /SAVE UNIT TIME
        LXI     H,REGS          /GET START OF REG AREA INTO H,L
        LXI     D.00FE          /GET FE INTO D.E
        DAD     D               /POINT TO REGISTER FE
        MOV     E.M             /GET LOW ORDER BYTE
        INX     H               /UPDATE POINTER
        MOV     D,M             /GET HIGH ORDER BYTE
        MOV     A.D             /CHECK FOR ZERO
        ORA     E
        JZ      6$              /EXIT
        MOV     L.E             /GET COUNT INTO H,L
        MOV     H,D
        SHLD    COUNT           /SAVE COUNT
2$      LXI     H,0000          /INIT H,L
3$      DAD     B               /INCREMENT BY UNIT TIME
        MOV     E,L             /GET TIME INTO D,E
        MOV     D.H
        LHLD    COUNT           /GET COUNT INTO H,L
        DCX     H               /UPDATE COUNT
        MOV     A.L             /CHECK FOR ZERO
        ORA     H
        SHLD    COUNT           /SAVE COUNT
        MOV     L,E             /GET TIME BACK INTO H,L
        MOV     H.D
        JZ      4$              /DONE
        MVI     A,0FF           /CHECK FOR .LT. 8191
        SUB     L               /SUBTRACT LS BYTE
        MVI     A.1F            /GET 1F INTO A
        SBB     H               /SUBTRACT MS BYTE
        JNC     3$              /BACK FOR MORE
4$      MOV     C.L             /GET TIME INTO B,C
        MOV     B.H
        CALL    TCOMP           /NEGATE TIME
        LHLD    MASK            /GET PULSE MASK INTO H.L
        MOV     E.L             /GET MASK INTO D,E
        MOV     D,H
        MVI     L,80            /GET FIFO ADDRESS INTO H,L
        MVI     H.0FF
5$      IN      PPS             /GET PP STATUS
        ANI     RMPP            /CHECK FOR PP READY
        JZ      5$              /TRY AGAIN
        CALL    WPP             /OUTPUT TO PP
        LHLD    TIME            /GET UNIT TIME BACK INTO H,L
        MOV     C.L             /GET UNIT TIME INTO B.C
        MOV     B.H
        LHLD    COUNT           /GET COUNT INTO H,L AGAIN
        MOV     E,L             /GET COUNT INTO D,E
        MOV     D,H
        MOV     A,D             /CHECK FOR ZERO
        ORA     E
        JZ      6$              /EXIT
        JMP     2$                      /BACK FOR MORE
6$      JMP     PP                      /EXIT
/MSG
7$      TXT     /(OD     ) UNIT TIME .GT. 819.2 USEC/
        DB      0
/ELINE
/ROUTINE TO OUTPUT LINE NUMBER OF
/PULSE PROGRAM ERROR.
/
ELINE   LDA     LC                      /GET LOCATION COUNTER
        DCR     A                       /POINT TO LINE NUMBER
        MOV     C,A                     /GET LINE NUMBER INTO C
        CALL    BHS                     /CONVERT AND OUTPUT TO BUFFER
        MVI     A,20                    /GET SP CHAR INTO A
        CALL    PCHAR                   /OUTPUT SP CHAR TO BUFFER
        CALL    PLINE1                  /OUTPUT LINE
        RET                             /RETURN
/US
/ROUTINE TO OUTPUT DELAY IN UNITS OF USEC TO FIFO
/REG1 CONTAINS TIME IN UNITS OF USEC. 1000 USEC MAX.
/REG2 CONTAINS PULSE MASK
/
US      CALL    FETCH                   /GET REG CONTENTS INTO B,C AND D,E
        MOV     A,C                     /CHECK FOR ZERO
        ORA     B
        JZ      4$                      /EXIT
1$      MVI     A,0E8                   /CHECK FOR .LT. 1000
        SUB     C
        MVI     A,03
        SBB     B
        JNC     2$                      /.LT. 1000
        CALL    ELINE                   /OUTPUT LINE NUMBER
        LXI     H,5$                    /POINT TO MSG
        CALL    PSTR                    /OUTPUT STRING
        CALL    PLINE                   /OUTPUT LINE
        JMP     HA                      /HALT PULSE PROGRAMMER
2$      CALL    MPY10                   /MPY BY 10
        CALL    TCOMP                   /CONVERT TO TWO-COMPLEMENT
        MVI     L,80                    /GET FIFO ADDRSS INTO H,L
        MVI     H,0FF
3$      IN      PPS                     /GET PP STATUS
        ANI     RMPP                    /CHECK FOR PP READY
        JZ      3$                      /TRY AGAIN
        CALL    WPP                     /OUTPUT TO FIFO
4$      JMP     PP                      /RETURN
/MSG
5$      TXT     /(US     ) TIME .GT. 1000 USEC/
        DB      0
/
/HN
/ROUTINE TO OUTPUT TIME IN UNITS OF 100 NSEC TO FIFO
/REG1 CONTAINS TIME IN UNITS OF 100 NSEC
/REG2 CONTAINS PULSE MASK
HN      CALL    FETCH                   /GET REG CONTENTS INTO B,C AND D,E
        MOV     A,C                     /CHECK FOR ZERO
        ORA     B
        JZ      PP                      /EXIT
        CALL    TCOMP                   /CONVERT TIME TO TWO-COMPLEMENT
        MVI     L,80                    /GET FIFO ADDRESS INTO H,L
        MVI     H,0FF
```

```
1$      IN      PPS             /GET PP STATUS
        ANI     RMPP            /CHECK FOR PP READY
        JZ      1$              /TRY AGAIN
        CALL    WPP             /OUTPUT TO FIFO
        JMP     PP              /EXIT
/TCOMP
/PERFORMS TWO-COMPLEMENT OF DATA IN B,C
/RESULT RETURNED IN B,C
TCOMP   XRA     A               /CLEAR A
        SUB     C               /SUBTRACT LOW ORDER BYTE
        MOV     C.A             /SAVE LOW ORDER RESULT
        MVI     A,00            /CLEAR A AGAIN
        SBB     B               /SUBTRACT HIGH ORDER BYTE
        MOV     B.A             /SAVE HIGH ORDER RESULT
        RET                     /RETURN
/
/MPY10
/MULTIPLIES CONTENTS OF B,C BY 10
/RESULT RETURNED IN B,C
MPY10   PUSH    H               /SAVE H,L
        MOV     L,C             /GET MULTIPLICAND INTO H,L
        MOV     H,B
        DAD     H               /MULTIPLY BY 10
        DAD     H
        DAD     H
        DAD     B
        DAD     B
        MOV     C,L             /GET RESULT INTO B,C
        MOV     B.H
        POP     H               /GET H,L AGAIN
        RET                     /RETURN
/
/SYSTEM TABLES
/
TOPSO   TXT     /CL/
        TXT     /ED/
        TXT     /LI/
        TXT     /EC/
        TXT     /VA/
        TXT     /LO/
        TXT     /GO/
        TXT     /DF/
        DB      0
TJMPO   CPI     00
        JZ      CL
        CPI     01
        JZ      ED
        CPI     02
        JZ      LI
        CPI     03
        JZ      EC
        CPI     04
        JZ      VA
        CPI     05
        JZ      LO
        CPI     06
        JZ      GO
        CPI     07
        JZ      DF
        JMP     CMDPRS
```

```
/
TOPS11  TXT     /BR/
        TXT     /OF/
        TXT     /01/
        TXT     /02/
        TXT     /03/
        TXT     /R1/
        TXT     /R2/
        TXT     /R3/
        TXT     /IN/
        TXT     /DE/
        TXT     /SE/
        TXT     /CO/
        TXT     /PA/
        TXT     /MS/
        TXT     /SC/
        TXT     /HA/
        TXT     /HN/
        TXT     /SB/
        TXT     /T1/
        TXT     /OD/
        TXT     /RE/
        TXT     /US/
        DB      0
TJMP11  CPI     00
        JZ      BR
        CPI     01
        JZ      OF
        CPI     02
        JZ      01
        CPI     03
        JZ      02
        CPI     04
        JZ      03
        CPI     05
        JZ      R1
        CPI     06
        JZ      R2
        CPI     07
        JZ      R3
        CPI     08
        JZ      IN
        CPI     09
        JZ      DE
        CPI     0A
        JZ      SE
        CPI     0B
        JZ      CO
        CPI     0C
        JZ      PA
        CPI     0D
        JZ      MS
        CPI     0E
        JZ      SC
        CPI     0F
        JZ      HA
        CPI     10
        JZ      HN
        CPI     11
        JZ      SB
```

```
            CPI     12
            JZ      T1
            CPI     13
            JZ      OD
            CPI     14
            JZ      RE
            CPI     15
            JZ      US
            JMP     CMDPRS
/
/SYSTEM DEVICE REGISTERS
/
PPS         EQU     80
RMPP        EQU     80
SMPP        EQU     40
TTO         EQU     00
TTI         EQU     00
TTS         EQU     01
RMTTI       EQU     02
RMTTO       EQU     01
SRAM1       EQU     0F0
SRAM2       EQU     0F4
SRAM3       EQU     0F8
/
/THE FOLLOWING MUST BE IN RAM
/
/SYSTEM PARAMETERS AND BUFFERS
/
CHAR        DS      1
SIGN        DS      1
NICHAR      DS      1
ICHAR       DS      1
NIBUF       EQU     50
IBUF        DS      NIBUF
OCHAR       DS      1
NOBUF       EQU     50
OBUF        DS      NOBUF
/
COMP        DS      1
RCYCLE      DS      1
ECHO        DS      1
SOURCE      DS      1
LN          DS      1
OPCODE      DS      1
OP1         DS      1
OP2         DS      1
OFF         EQU     0FF
LC          DS      1
PGMST       DS      1
NSEC        DS      1
NSAMPL      DS      1
MASK        DS      2
COUNT       DS      2
TIME        DS      2
RAC1        DS      2
RAC2        DS      2
RAC3        DS      2
NIMAX       EQU     0FF
REGS        DS      100
TLINE       DS      100
```

```
PGM      DS       NIMAX*3
/
LAST     EQU      .
SIZE     EQU      LAST-FIRST
/
         END
```

REFERENCES

1) Rose M., Elementary Theory of Angular Momentum, New York (1957)

2) Edmonds A., Angular Momentum and Quantum Mechanics, Princeton (1968)

3) Tinkham M., Group Theory and Quantum Mechanics, New York (1964)

4) Brink D. and Satchler G., Angular Momentum, Oxford (1968)

5) Silver B., Irreducible Tensor Methods, New York (1976)

6) Abragam A., Principles of Nuclear Magnetism, Oxford (1961)

7) Slichter C., Principles of Magnetic Resonance, New York (1978)

8) Goldman M., Spin Temperature and NMR in Solids, New York (1970)

9) Abragam A., Principles of Nuclear Magnetism Ch. 4, Oxford (1961)

10) Bloch F., Phys. Rev. 69, 127 (1946)

11) Mehring M., High Resolution NMR in Solids, New York (1976)

12) Haeberlin U., High Resolution NMR in Solids, Selective Averaging, New York (1976)

13) Racah G., Phys. Rev. 61, 186 (1942)

14) Stephen M. and Straley J., Rev. Mod. Phys. 46, 617 (1974)

15) deGenne, Physics of Liquid Crystals, Clarendon Press (1974)

16) Priestley E. (ed.), Introduction to Liquid Crystals, Plenum Press (1975)

17) Chandrasekhar, Liquid Crystals, Cambridge University Press (1977)

18) Johnson J. and Porter R., Liquid Crystals and Ordered Fluids, New York (1974)

19) Gray G. and Luckhurst G., Molecular Physics of Liquid Crystals New York (1979)

20) Gray G. and Winsor P., Liquid Crystals and Plastic Crystals, New York (1976)

21) Gray G., Molecular Structure and Properties of Liquid Crystals,

Academic Press, London (1962)

22) Maier W. and Saupe A., Z. Naturf. A13, 564 (1958)

23) De Vries A., Molecular Crystals and Liquid Crystals 11, 361 (1970)

24) De Vries A., Molecular Crystals and Liquid Crystals 20, 119 (1973)

25) Madhusudana N. et al, Molecular Crystals and Liquid Crystals 13, 61 (1971)

26) Diele S. et al, Molecular Crystals and Liquid Crystals 16, 105 (1972)

27) De Jeu W. and De Poorter J., Physics Letters 61A, 114 (1977)

28) Taylor T. et al, Phys. Rev. Lett. 24, 359 (1970)

29) Doucet J. and Levelut A., J. de Physique 38, 1163 (1977)

30) Taylor T., Phys. Rev. Lett. 25, 722 (1970)

31) De Vries A. and Fishel D., Molecular Crystals and Liquid Crystals 16, 311 (1972)

32) De Vries A., J. Chem. Phys. 61, 2367 (1974)

33) Doucet J. et al, Phys. Rev. Lett. 32, 301 (1974)

34) Descamps M. and Coulon G., Solid State Communications 20, 379 (1976)

35) Pines A. and Chang J., Phys. Rev. A 10, 946 (1974)

36) Pines A., Ruben D., and Allison S., Phys. Rev. Lett. 33, 1002 (1974)

37) Allison S., M.S. Thesis, Dept. of Chemistry, University of Calif. Berkeley (1975)

38) Rowell J. et al, J. Chem. Phys. 43, 3442 (1965)

39) Charvolin J. and Deloche B., Second Specialized Colloque, Ampere, Budapest, Hungary (1975)

40) Wise R. et al, Phys. Rev. A 7, 1366 (1973)

41) Luz Z. and Meiboom S., J. Chem. Phys. 59, 275 (1973)

42) Luz Z., Hewitt R., and Meiboom S., J. Chem. Phys. 61, 1758 (1974)

43) Wulf A., J. Chem. Phys. 63, 1564 (1975)

44) Deloche B. et al, J. de Physique 36, C1-21 (1975)

45) Bos P. et al, Molecular Crystals and Liquid Crystals 40, 59 (1977)

46) Bos P. and Doane J., Phys. Rev. Lett. 40, 1030 (1978)

47) Hsi S., Zimmerman H., and Luz Z., J. Chem. Phys. 69, 4126 (1978)

48) Deloche B. and Charvolin J., J. de Physique 61, L39 (1980)

49) Hayamizu K. and Yamamoto O., J. Mag. Res. 41, 94 (1980)

50) Dong R. et al, J. Chem. Phys. 74, 633 (1981)

51) Luz Z. and Samulski E., J. Chem. Phys. 73, 142 (1980)

52) Seliger J. et al, Phys. Rev. Lett. 38, 411 (1977)

53) Allender D. and Doane J., Phys. Rev. A 17, 1177 (1978)

54) Cheng C. and Brown T., J. Chem. Phys. 67, 797 (1977)

55) Vega S., J. Chem. Phys. 63, 3769 (1975)

56) Vega S. and Pines A., J. Chem. Phys. 66, 5624 (1977)

57) Shattuck T., PhD Thesis, Dept. of Chemistry, University of Calif., Berkeley (1976)

58) Wemmer D., PhD Thesis, Dept. of Chemistry, University of California, Berkeley (1978)

59) Allison S., M.S. Thesis, Dept. of Chemistry, University of Calif., Berkeley (1975)

60) Luckhurst G., Ptak M., and Sanson A., J. Chem. Soc., Faraday Trans. II 69, 1752 (1973)

61) Hornreich R. and Shtrikman S., Solid State Comm. 17, 1141 (1975)

62) Smith G. and Garlund Z., J. Chem. Phys. 59, 3214 (1973)

63) Tadras W., Ekladius L., and Salka A., J. Chem. Soc. 2351 (1954)

64) Partch R., Tet. Lett. 3071 (1964)

65) Sterna L., PhD Thesis, Dept. of Chemistry, University of

Calif., Berkeley (1981)

66) Onsager, Ann. N.Y. Acad. Sci. 51, 627 (1949)

67) Maier W. and Saupe A., Z. Naturf. A13, 564 (1958)

68) deGenne P.G., C.R. Acad. Sc. Paris t. 274 B-758 (1972)

69) McMillian W., Phys. Rev. A 8, 1921 (1973)

70) McMillian W. and Meyer R., Phys. Rev. A 9, 899 (1974)

71) Wulf A., Phys. Rev. A 11, 365 (1975)

72) Priest R., J. de Physique 36, 437 (1975)

73) Cabib D., J. de Physique 38, 419 (1977)

74) Doucet J. and Levelut A., J. de Physique 38, 71 (1977)

75) Hardouin F., Mol. Cryst. Liq. Cryst. 39, 241 (1977)

76) Hevret H., Phys. Rev. Lett. 34, 451 (1975)

77) Dianoux A., Hevret H., and Volino F., J. de Physique 38, 809 (1977)

78) Wokaun A. and Ernst R., J. Chem. Phys. 67, 1752 (1977)

79) Vega S., J. Chem. Phys. 68, 5518 (1978)

80) Aue W., Bartholdi E., and Ernst R., J. Chem. Phys. 64, 2229 (1976)

81) Jeener J., Meier B., Bachmann P., and Ernst R., J. Chem. Phys. 71, 4546 (1979)

82) Murdoch J., PhD Thesis, Dept. of Chemistry, University of Calif., Berkeley (1983)

83) Pines A., Wemmer D., Tang J., and Sinton S., Bull. Am. Phys. Soc. 21, 23 (1978)

84) Drobny G., Pines A., Sinton S., Weitekamp D., and Wemmer D., Faraday Division of the Chemical Society, Symposium 13, 49 (1979)

85) Hahn E., Phys. Rev. 80, 580 (1950)

86) Wokaun A. and Ernst R., Chem. Phys. Lett. 52, 407 (1977)

87) Bodenhausen G., Vold R.R., and Vold R.L., J. Mag. Res. 37, 93 (1980)

88) Sinton S., PhD Thesis, Dept. of Chemistry, University of Calif., Berkeley (1981)

89) Emsley J. and Lindon J., NMR Spectroscopy Using Liqiud Crystal Solvents, Oxford (1975)

90) Diehl P. and Khetrapal C., Canadian J. Chem. 47, 1411 (1969)

91) Warren W., PhD Thesis, Dept. of Chemistry, University of Calif., Berkeley (1980)

92) Wemmer D., Drobny G., Pines A., Sinton S., Weitekamp D., Ramis-79 Plenary Lecture

93) Snyder L., J. Chem. Phys. 43, 4041 (1965)

94) The literature on this subject (up to 1975) is reviewed in reference 89

95) Hohener A., Muller L., and Ernst R., Mol. Phys. 38, 910 (1979)

96) Sinton S. and Pines A., Chem. Phys. Lett. 76, 263 (1980)

97) Tang J. and Pines A., J. Chem. Phys. 72, 3290 (1980)

98) Tang J. and Pines A., J. Chem. Phys. 73, 2512 (1980)

99) Longuet-Higgins H., Mol. Phys. 6, 445 (1963)

100) Flory P., Statistical Mechanics of Chain Molecules, New York (1969)

101) a.Emsley J., Luckhurst G., and Stockley C., Mol. Phys. 38, 1687 (1979)
b.Chavolin J. and Deloche B., J. Phys. 37, c3-67 (
c.Emsley J., Luckhurst G., Gray G., and Mosley A., Mol. Phys. 35, 1499 (1978)

102) a.Emsley J. and Luckhurst G., Mol. Phys. 41, 19 (1980)
b.Emsley J., Khoo S., and Luckhurst G., Mol. Phys. 37, 959 (1979)
c.Burnell E. and DeLange C., J. Mag. Res. 39, 461 (1980)

103) Huang T., Skarkune R., Wittebort R., Griffin R., and Oldfield G.,

J. Amer. Chem. Soc. 102, 7377 (1981)

104) Gilman H., Zoellner E., and Selby W., J. Amer. Chem. Soc. 89, 3911 (196

105) Gilman H., Jones R., and Woods L., J. Org. Chem. 17, 1630 (1952)

106) Cross V., Hester R., and Waugh J., Rev. Sci. Instr. 47, 1446 (1976)

107) Data General Corporation, How to Use Nova Computers, DGC (1969)

108) Osborne A. and Kane J., Introduction to Microprocessors V2, Berkeley (1978)